Macroautophagy, alpha-synuclein and dopamine neurotransmission: implications for Parkinson's disease



Benjamin Hunn

Lincoln College

Department of Physiology, Anatomy and Genetics

University of Oxford

Trinity Term, 2017

A thesis submitted towards the degree of Doctor of Philosophy

Macroautophagy, alpha-synuclein and dopamine neurotransmission: implications for Parkinson's disease

A thesis submitted for the degree of Doctor of Philosophy, Trinity Term, 2017

Benjamin Hunn, Lincoln College, University of Oxford

Abstract

Parkinson's disease (PD) is an incurable neurological disease characterised by impairment of motor function, death of substantia nigra pars compacta (SNc) dopamine (DA) neurons and accumulation of the protein α-synuclein. Macroautophagy, a major process by which deleterious cellular contents are degraded, is implicated in both sporadic and genetic PD, and macroautophagy inducers are currently in PD clinical trials. However, little is known about the interaction between α-synuclein and macroautophagy *in vivo*.

In this thesis, the interaction between impaired macroautophagy in DA neurons and α-synuclein was studied by generating novel transgenic mice. Mice were bred featuring conditional knockout of *ATG7*, a gene essential for macroautophagy, in DA neurons (*ATG7*cKO$^{DAT\text{-IRES-cre}}$), and expressing the full-length human α-synuclein gene (h*SNCA*). Mice carrying the *ATG7*cKO$^{DAT\text{-IRES-cre}}$ genotype developed key features of PD, including loss of SNc DA neurons, reductions in caudate-putamen DA and the development of protein aggregates in DA neurons. Presence of the h*SNCA* gene had minimal effect on histological phenotypes. Paradoxically, *ATG7*cKO$^{DAT\text{-IRES-cre}}$ mice displayed improvements in some elements of motor function, including increased locomotion, increased gait swing speed and improved motor coordination in old age. There was no effect of the h*SNCA* gene on behavioural phenotypes.

In order to determine a physiological basis for the discrepancy between the neuropathological and motor phenotypes associated with the *ATG7*cKO$^{DAT\text{-IRES-cre}}$ genotype, DA neurotransmission was examined using fast-scan cyclic voltammetry (FCV). FCV demonstrated that the *ATG7*cKO$^{DAT\text{-IRES-cre}}$ genotype increased evoked DA levels, reduced the rate of DA reuptake, and increased evoked DA in response to repeated stimuli. The finding that impaired macroautophagy in DA neurons enhances DA neurotransmission was confirmed in a second transgenic mouse model. These data demonstrating that impaired macroautophagy enhances dopamine neurotransmission, thus improving behavioural phenotypes while worsening some pathological phenotypes, has direct implications for PD pathogenesis, drug discovery and clinical trials.

Acknowledgements

I would like to thank my supervisors, Richard Wade-Martins and Stephanie Cragg, for allowing me to be their student. To Richard, for his optimism, wisdom, generosity, and constant support. To Steph, for her scholarship and good humour, and teaching me rigour in experimental design and scientific language. To both of you, I hope your faith in me has been validated. I am grateful also to the Rhodes Trust, the Guarantors of Brain and the University of Oxford for supporting my doctoral studies.

Thank you to Sarah Threlfell, a brilliant scientist and even better person who has been an unerring font of knowledge, support and grace, even in the most trying of times. This project would not have been possible without the smiling presence, expertise and hard work of Milena Cioroch, to whom I am extremely grateful. Thanks go also to Thierry Deltheil for helping me find my feet with mouse experiments, and Natalie Doig for teaching me stereology and being an excellent person to have beer with in Mexico. I am grateful to Nora Bengoa-Vergniory, for indulging my many cries for help and bad jokes with a smile and compassion. I am very appreciative to Siv Vingill for her insight and stepping up to help out with this project at the end. Thanks also to Katie Hewitt, who was always superbly helpful. Alexei Bygrave was a star in teaching me the Y-maze, and for advice on thesis formatting. The Biomedical Services staff also deserve a large share of the credit for the work in this thesis, as do the mice.

I would like to thank current and former members of the Wade-Martins lab for mateship, collaborations, and making days in the lab fun: Rozzy, Kathie, Brent, Hugo, Natalie, Dayne, Mel, Heike, Max, Fede, Brian, Beccy, Marika, Charmaine, Alastair, Heather, Sarah, Tara, Gabby, Emma, and that brilliant man, gone too soon, Paul. Likewise, members of the Cragg lab, Katherine, Yan Feng, Mark, Emmanuel, Bradley and Richard have been smiling presences behind the FCV rigs day after day.

To those friends who have made these four years in Oxford some the best of my life, I have only love: Flounder, Geoff, Mandy, Slow-Mo, Shrike, Fist, Hayriye, Pig, Clag, Kirbs, CP, Moizza, MD, Pat, Dave, Genevieve, der Hund, Robbie, Liz, James, Ayo and Freya (definitely not in order of importance).

To Alex and Nick, thanks for the sort of sibling love that keeps you grounded. Thank you to my grandparents for unshakeable faith and pride in me, and to Mum and Dad, whose love and support has been unwavering, and whose sacrifice made it possible to get here, thank you. Most of all, this is for Katie Rose Stone, with all my love.

Declaration

This thesis contains no material that has been accepted for the award of any other degree or diploma in any University or other institution. To the best of my knowledge, the thesis contains no copy or paraphrase of material previously published by another person except where due reference is made in the text. All data presented are the result of my own work unless otherwise specified.

Benjamin Hunn

This thesis contains 41 688 words.

Publications and conference presentations

Publications:

Doucet M, El-Turabi A, Zabel F, **Hunn BHM**, Bengoa-Vergniory N, Cioroch M, Ramm M, Smith AM, Gomes AC, Cabral de Miranda G, Wade-Martins R, Bachmann MF. Preclinical development of a vaccine against oligomeric alpha-synuclein based on virus-like particles. *PLoS ONE* 2017;12:e0181844.

Hunn BHM, Cragg SJ, Bolam JP, Spillantini M-G, Wade-Martins R. Impaired intracellular trafficking defines early Parkinson's disease. *Trends in Neurosciences* 2015;38:178–88.

Conference presentations:

Hunn BHM, Threlfell S, Alegre-Abarrategui J, Deltheil T, Bengoa-Vergniory N, Oliver PL, Cioroch M, Doig N, Bannerman DM, Cragg SJ, Wade-Martins R. Impairment of macroautophagy enhances dopamine neurotransmission and rescues motor deficits despite worsened neuropathology in a mouse model of Parkinson's disease. Selected poster presentation. International Basal Ganglia Society Conference; Merida, Mexico, 2017.

Hunn, BHM, Deltheil, T, Alegre-Abarrategui, J, Threlfell, S, Cioroch, M, Cragg, SJ, Wade-Martins, R. A multi-hit model of Parkinson's disease: interplay of α-synuclein and autophagy. Selected poster presentation. Parkinson's UK Research Conference; York, United Kingdom, 2014.

Table of contents

Abstract ..... **i**

Acknowledgements ..... **ii**

Declaration ..... **iii**

Publications and conference presentations ..... **iv**

Table of contents ..... **v**

List of figures ..... **x**

List of tables ..... **xiii**

Abbreviations ..... **xiv**

1 Introduction **2**

1.1 Parkinson's disease **2**

1.1.1 Clinical features of Parkinson's disease 2

1.1.1.1 Motor symptoms 2

1.1.1.1.1 Non-motor symptoms 4

1.1.2 Pathological hallmarks of Parkinson's disease 6

1.1.3 Pathophysiology of Parkinson's disease 8

1.1.4 Treatment of Parkinson's disease 10

1.1.5 Risk factors for the development of Parkinson's disease 11

1.1.5.1 Genetic risk factors for Parkinson's disease 11

1.1.5.1.1 Familial genetic mutations that cause Parkinson's disease 11

1.1.5.1.2 Genetic factors conferring risk for sporadic Parkinson's disease 16

1.1.5.2 Environmental risk factors for sporadic Parkinson's disease 18

1.2 α-Synuclein **21**

1.2.1 The physiological localisation and function of α-synuclein 21

1.2.2 The role of α-synuclein in Parkinson's disease 24

1.2.2.1 α-Synuclein aggregation and impaired protein clearance 25

1.2.2.2 Mitochondrial dysfunction, oxidative stress and calcium handling 26

1.2.2.3 Prion-like propagation of α-synuclein 28

1.3 Autophagy **30**

1.3.1 Macroautophagy 32

1.3.2 Chaperone-mediated autophagy 37

1.3.3 Microautophagy 38

1.3.4 The potential role of macroautophagy in Parkinson's disease 39

1.3.4.1 Pathological evidence for a role of macroautophagy in Parkinson's disease 39

1.3.4.2 Genetic evidence for a role of macroautophagy in Parkinson's disease 39

1.3.4.3 Interactions between α-synuclein and macroautophagy: evidence of a role for macroautophagy manipulation in treating Parkinson's disease 41

1.4 α-Synuclein rodent models of Parkinson's disease **43**

1.5 Rodent models of macroautophagy impairment **48**

1.6 Aims of thesis **53**

2 Materials and Methods **55**

2.1 Ethical declaration 55
2.2 Biochemical methods 55
2.2.1 Genotyping of mice 55
2.2.1.1 Lysis of ear clips 55
2.2.1.2 Polymerase chain reaction 56
2.2.1.3 Agarose gel electrophoresis of PCR products 56
2.2.2 Immunohistochemistry 59
2.2.2.1 Transcardiac perfusion 59
2.2.2.2 3,3'-diaminobenzidine immunohistochemistry of free-floating slices 59
2.2.2.3 Immunohistochemistry of paraffin-embedded slices 60
2.2.2.3.1 Tissue preparation of paraffin-embedded slices 60
2.2.2.3.2 Immunofluorescent immunohistochemistry of paraffin-embedded slices 61
2.2.2.3.3 3,3'-diaminobenzidine immunohistochemistry of paraffin-embedded slices 62
2.2.3 Stereology 63
2.2.4 Sodium dodecyl sulfate polyacrylamide gel electrophoresis and immunoblotting 64
2.2.4.1 Tissue preparation for protein electrophoresis 64
2.2.5 Fast-scan cyclic voltammetry 65
2.2.5.1 Preparation of recording electrodes for fast-scan cyclic voltammetry 65
2.2.5.2 Preparation of acute striatal slices for fast-scan cyclic voltammetry . 66
2.2.5.3 Dopamine recordings with fast-scan cyclic voltammetry 66
2.2.5.4 Dopamine recording sites 68
2.2.5.5 Analysis of cyclic voltammograms 68
2.2.6 High-performance liquid chromatography with electrochemical detection 70
2.2.6.1 Preparation of samples for high-performance liquid chromatography 70
2.2.6.2 Electrochemical detection and measurement during high-performance liquid chromatography 71
2.3 Behavioural testing 72
2.3.1 Locomotor activity 72
2.3.2 Digital gait analysis 72
2.3.3 Rotarod 73
2.3.4 Inverted screen 73
2.3.5 Stool collection 74
2.3.6 Spontaneous alternation in a T-maze 74
2.3.7 Spatial novelty preference in a Y-maze 75
2.3.8 Tail suspension 75
2.3.9 Elevated plus-maze 76
2.3.10 Olfactory testing 76
2.4 Statistical analysis 77

3 Generation and histological characterisation of a mouse model to examine the interaction between human alpha-synuclein and impaired macroautophagy in dopamine neurons 80
3.1 Overview 80
3.2 Aims of Chapter 3 81

3.3 Introduction 81
3.3.1 Choice of model species 81
3.3.2 Methods of impairing macroautophagy *in vivo* 82
3.3.3 Method of expressing human α-synuclein 85
3.4 Results 86
3.4.1 Generation of transgenic mouse lines 86
3.4.2 Confirmation of Mendelian inheritance of genetic modifications in experimental mouse cohorts 88
3.4.3 Confirmation of functionally impaired macroautophagy as a result of *ATG7* knockout in dopamine neurons 89
3.4.4 Confirmation of human α-synuclein expression in mice carrying the h*SNCA* transgene 91
3.4.5 The *ATG7*cKO$^{DAT\text{-IRES-cre}}$ genotype is associated with selective loss of substantia nigra dopamine neurons 92
3.4.6 Complex effects of h*SNCA* and *ATG7*cKO$^{DAT\text{-IRES-cre}}$ on caudate-putamen dopamine content 94
3.4.7 Absence of Lewy pathology in h*SNCA*:*ATG7*cKO$^{DAT\text{-IRES-cre}}$ mice aged 20 to 24 months 96
3.4.8 The *ATG7*cKO$^{DAT\text{-IRES-cre}}$ genotype causes the accumulation of macroautophagic substrates in substantia nigra neurons, resembling some aspects of Parkinson's disease 101
3.4.9 Characterisation of macroautophagic substrates in dopamine neurons neurons of mice aged 20 to 24 months using immunofluorescent immunohistochemistry 103
3.5 Discussion 107
3.5.1 Data from collaborative experiments on hSNCA:*ATG7*cKO$^{DAT\text{-IRES-cre}}$ mice 107
3.5.2 Degeneration of the nigrostriatal system 107
3.5.3 Histological features of Parkinson's disease neuropathology 109
3.5.4 Absence of interaction between impaired macroautophagy and human α-synuclein 109
3.5.5 Limitations of the model system 110
3.5.6 Summary of findings from this chapter 112

4 Behavioural characterisation of a mouse model to examine the interaction between human alpha-synuclein and impaired macroautophagy in dopamine neurons 114
4.1 Overview 114
4.2 Aims of Chapter 4 115
4.3 Results 116
4.3.1 General health and characteristics of experimental mice 116
4.3.2 Assessment of the effects of impaired macroautophagy in dopamine neurons and human α-synuclein expression on motor function in transgenic mice 118
4.3.2.1 Older mice have reduced muscle strength 118
4.3.2.2 The *ATG7*cKO$^{DAT\text{-IRES-cre}}$ genotype is associated with hyperlocomotion 119
4.3.2.3 Improved rotarod performance in aged mice with the *ATG7*cKO$^{DAT\text{-IRES-cre}}$ genotype 120

4.3.2.4 The *ATG7*cKO$^{DAT\text{-IRES-cre}}$ genotype is associated with increases in forefoot swing speed and gait cadence 123
4.3.3 The effects of impaired macroautophagy in dopamine neurons and human α-synuclein expression on parkinsonian non-motor phenotypes in transgenic mice 126
4.3.3.1 The *ATG7*cKO$^{DAT\text{-IRES-cre}}$ genotype is associated with reduced successful spontaneous alternation in the T-maze, but no deficits were found in a Y-maze spatial novelty preference task 126
4.3.3.2 No association between genotype and measures of gastrointestinal function 129
4.3.3.3 No association between genotype and depression- or anxiety-like phenotypes 131
4.3.3.4 No association between genotype and olfactory function in aged mice 133
4.4 Discussion 135
4.4.1 Association of *ATG7*cKO$^{DAT\text{-IRES-cre}}$ genotype with improved motor function 135
4.4.2 *ATG7*cKO$^{DAT\text{-IRES-cre}}$ and measures of memory 136
4.4.3 Absence of association between h*SNCA* and parkinsonian phenotypes 137
4.5 Chapter summary 138
5 Characterisation of dopamine neurotransmission in a mouse model examining the interaction between human alpha-synuclein and impaired macroautophagy in dopamine neurons 140
5.1 Introduction 140
5.2 Aims of Chapter 5: 142
5.3 The electrochemical basis of fast-scan cyclic voltammetry 142
5.4 Results 144
5.4.1 The *ATG7*cKO$^{DAT\text{-IRES-cre}}$ genotype is associated with increased peak evoked $[DA]_o$ in the caudate-putamen at 1 month, but lower peak release at 6 and 20 to 24 months. 144
5.4.2 Impairment of macroautophagy in dopamine neurons is associated with reduced rates of dopamine reuptake independent of age, in both the caudate-putamen and nucleus accumbens 147
5.4.3 Assessment of dopamine release probability 150
5.4.4 Evoked dopamine levels in response to stimuli of different frequencies 153
5.4.5 The ability to respond to repeated stimuli: paired-pulse depression 155
5.5 Discussion 163
5.5.1 Impaired macroautophagy in dopamine neurons increases evoked dopamine concentrations 163
5.5.2 Dopamine reuptake is impaired when macroautophagy is impaired 165
5.5.3 In most contexts, impaired macroautophagy in dopamine neurons reduces paired-pulse depression, whereas human α-synuclein increases paired-pulse depression 167
5.5.4 Dopamine neurotransmission and tests of motor function: correlation does not equal causation 168
5.5.5 Strengths and limitations of examining dopamine neurotransmission using fast-scan cyclic voltammetry 168
5.5.6 Chapter summary 170

6 Examination of dopamine neurotransmission when macroautophagy is impaired in dopamine neurons, using a *TH*-IRES-cre driver line 172
6.1 Introduction 172
6.2 Chapter aims 174
6.3 Results 175
6.3.1 Generation of *ATG7*cKO$^{TH\text{-IRES-cre}}$ mice 175
6.3.2 Peak dopamine release is increased in mice with impaired macroautophagy in dopamine neurons using an *ATG7*cKO$^{TH\text{-IRES-cre}}$ model 177
6.3.3 The rate of dopamine reuptake is reduced in the caudate-putamen, but not the nucleus accumbens, in mice with impaired macroautophagy in dopamine neurons, using an *ATG7*cKO$^{TH\text{-IRES-cre}}$ model..... 179
6.3.4 Dopamine release probability is unchanged in mice with impaired macroautophagy in dopamine neurons using an *ATG7*cKO$^{TH\text{-IRES-cre}}$ model 181
6.3.5 Impairment of macroautophagy in dopamine neurons does not change frequency responsiveness of evoked $[DA]_o$ in an *ATG7*cKO$^{TH\text{-IRES-cre}}$ model 183
6.3.6 Impairment of macroautophagy in dopamine neurons is associated with reduced paired-pulse depression in an *ATG7*cKO$^{TH\text{-IRES-cre}}$ model..... 185
6.3.7 No effect of macroautophagy impairment on dopamine content in the caudate-putamen or nucleus accumbens in an *ATG7*cKO$^{TH\text{-IRES-cre}}$ model 188
6.4 Discussion 189
6.4.1 The effect of macroautophagy impairment in dopamine neurons on neurotransmission is similar between *ATG7*cKO$^{TH\text{-IRES-cre}}$ and *ATG7*cKO$^{DAT\text{-IRES-cre}}$ mice..... 189
6.4.2 Differences in dopamine neurotransmission between *ATG7*cKO$^{DAT\text{-IRES-cre}}$ and *ATG7*cKO$^{TH\text{-IRES-cre}}$ mice 190
6.4.3 Limitations of examining dopamine neurotransmission using the *TH*-IRES-cre system 192
6.4.4 Chapter summary..... 194

7 Discussion..... 196
7.1 Overview 196
7.2 Impaired macroautophagy in dopamine neurons has divergent effects on parkinsonian phenotypes, worsening neuropathology but improving behavioural measures 196
7.3 Why don't h*SNCA*:*ATG7*cKO$^{DAT\text{-IRES-cre}}$ mice form Lewy bodies?..... 199
7.4 Lack of pathological and motor phenotypes associated with the h*SNCA* gene 200
7.5 Absence of interactions between h*SNCA*:*ATG7*cKO$^{DAT\text{-IRES-cre}}$ and h*SNCA* 201
7.6 Macroautophagy may be a novel direct or indirect regulator of the dopamine transporter 202
7.7 Impaired macroautophagy in dopamine neurons is associated with improved motor function: implications for clinical trials 204

Appendix: midbrain dopamine neuron counts 205

References..... 207

List of figures

Figure 1.1. Basal ganglia in health and Parkinson's disease.....9

Figure 1.2. Structure of α-synuclein. 21

Figure 1.3. Autophagic pathways within the cell. 31

Figure 2.1. Sampling sites used for fast-scan cyclic voltammetry in Chapters 5 and 6. 69

Figure 3.1. In-situ hybridisation studies in experimental mice demonstrate reduced *ATG7* expression in the midbrain of *ATG7*cKO$^{DAT\text{-IRES-cre}}$ mice.....84

Figure 3.2. Generation of experimental genotypes.....87

Figure 3.3. Experimental genotypes are inherited in Mendelian ratios. 88

Figure 3.4. Increased P62 in the midbrain of 6 month-old *ATG7*cKO$^{DAT\text{-IRES-cre}}$ mice. 90

Figure 3.5 Expression of human α-synuclein in 6 month-old transgenic mice. 91

Figure 3.6. The *ATG7*cKO$^{DAT\text{-IRES-cre}}$ genotype is associated with dopamine neuron loss in the substantia nigra pars compacta, but not the ventral tegmental area. 93

Figure 3.7. The *ATG7*cKO$^{DAT\text{-IRES-cre}}$ genotype is associated with reduced dopamine content in the caudate-putamen, and there are age-related changes in dopamine content associated with the h*SNCA* transgene. 95

Figure 3.8. Immunohistochemical analysis of α-synuclein expression in the striatum and substantia nigra pars compacta of experimental mice aged 20 to 24 months.....97

Figure 3.9. Immunohistochemical analysis of α-synuclein expression in the cortex and hippocampus of experimental mice aged 20 to 24 months. 98

Figure 3.10. Immunohistochemical analysis of human α-synuclein expression in the striatum and substantia nigra pars compacta of experimental mice aged 20 to 24 months. 99

Figure 3.11. Immunohistochemical analysis of human α-synuclein expression in the cortex and hippocampus of experimental mice aged 20 to 24 months.....100

Figure 3.12. High-magnification comparison of human α-synuclein, ubiquitin and P62 staining in the substantia nigra of experimental mice and human Parkinson's disease controls. 102

Figure 3.13. P62 aggregates develop in the substantia nigra pars compacta of 20 to 24 month-old mice when macroautophagy is impaired in DAT-positive neurons.....104

Figure 3.14. P62 aggregates in the ventral tegmental area of 20 to 24 month-old mice when macroautophagy is impaired in DAT-positive neurons. 105

Figure 3.15. Occasional ubiquitin aggregates develop in substantia nigra dopamine neurons of 20 to 24 month-old mice when macroautophagy is impaired in DAT-positive neurons. 106

Figure 4.1. Weight does not differ between experimental genotypes. 117

Figure 4.2. Muscle strength does not differ between experimental genotypes. 118

Figure 4.3. Impaired macroautophagy in dopamine neurons is associated with increased locomotor activity in the open-field. 119

Figure 4.4. Impaired macroautophagy in dopamine neurons is associated with improved rotarod performance in old but not young mice. 121

Figure 4.5. Impaired macroautophagy in dopamine neurons is associated with improved performance during rotarod training in 21 month-old mice. 122

Figure 4.6. No effect of genotype on performance during rotarod training in 3 month-old mice. 122

Figure 4.7. *ATG7*cKO$^{DAT\text{-IRES-cre}}$ mice have increased forefoot swing speed, but no changes in stride length. 124

Figure 4.8. *ATG7*cKO$^{DAT\text{-IRES-cre}}$ mice have increased gait cadence, but no changes in gait velocity. 125

Figure 4.9. Impaired macroautophagy in dopamine neurons is associated with a reduced rate of spontaneous alternation in the T-maze. 128

Figure 4.10. No deficit associated with experimental genotypes in 21 month-old mice tested using a spatial novelty preference test in a Y-maze. 128

Figure 4.11. No effect of impaired dopamine neuron macroautophagy or human α-synuclein expression on gastrointestinal function. 130

Figure 4.12. Absence of depression- or anxiety-like phenotypes associated with experimental genotypes. 132

Figure 4.13. No evidence of olfactory deficit associated with experimental genotypes in 21 month-old mice. 134

Figure 5.1. The *ATG7*cKO$^{DAT\text{-IRES-cre}}$ genotype is associated with increased peak evoked $[DA]_o$ in the caudate-putamen at 1 month, but lower peak release at 6 and 20 to 24 months. The h*SNCA* gene is associated with reduced evoked $[DA]_o$ at 20 to 24 months. 145

Figure 5.2. *ATG7*cKO$^{DAT\text{-IRES-cre}}$ is associated with increased peak evoked $[DA]_o$ in the nucleus accumbens, independent of age. 146

Figure 5.3. *ATG7*cKO$^{DAT\text{-IRES-cre}}$ is associated with a reduced rate of caudate-putamen dopamine reuptake, independent of age. 148

Figure 5.4. Both *ATG7*cKO$^{DAT\text{-IRES-cre}}$ and h*SNCA* reduce dopamine reuptake rate in the nucleus accumbens, independent of age. 149

Figure 5.5. *ATG7*cKO$^{DAT\text{-IRES-cre}}$ is associated with increased quadruple pulse to single pulse ratio in the caudate-putamen in 1 month-old mice, but not in older mice, or in the nucleus accumbens. 152

Figure 5.6. In striatal slices from 1 month-old mice, *ATG7*cKO$^{DAT\text{-IRES-cre}}$ is associated with increased dopamine release in the nucleus accumbens across all frequencies, but not in the caudate putamen. 154

Figure 5.7. Paired-pulse depression in a paired single pulse protocol in the caudate-putamen is reduced by *ATG7*cKO$^{DAT\text{-IRES-cre}}$ and increased by h*SNCA*. 157

Figure 5.8. Paired-pulse depression in a paired quadruple pulse protocol in the caudate-putamen is reduced by *ATG7*cKO$^{DAT\text{-IRES-cre}}$ and increased by h*SNCA*. 158

Figure 5.9. Paired-pulse depression in a single pulse-quadruple pulse protocol in the caudate-putamen is reduced by *ATG7*cKO$^{DAT\text{-IRES-cre}}$ independent of age and increased by h*SNCA* in 20 to 24 month-old mice. 159

Figure 5.10. Paired-pulse depression in a paired single pulse protocol in the nucleus accumbens is reduced by *ATG7*cKO$^{DAT\text{-IRES-cre}}$. 160

Figure 5.11. Paired-pulse depression in a paired quadruple pulse protocol in the nucleus accumbens is decreased by *ATG7*cKO$^{DAT\text{-IRES-cre}}$. 161

Figure 5.12. Age-dependent increase in paired-pulse depression of dopamine release associated with h*SNCA* in a single pulse-quadruple pulse protocol in the nucleus accumbens. 162

Figure 6.1. Generation of experimental genotypes.....176

Figure 6.2. Increased evoked $[DA]_o$ release in response to a single stimulus in the caudate-putamen and nucleus accumbens in striatal slices from 1 month-old *ATG7*cKO$^{TH\text{-IRES-cre}}$ mice. 178

Figure 6.3. The *ATG7*cKO$^{TH\text{-IRES-cre}}$ genotype is associated with a reduced rate of dopamine reuptake in the caudate-putamen, but not the nucleus accumbens. 180

Figure 6.4. Dopamine release probability is unchanged by impaired macroautophagy in dopamine neurons in an *ATG7*cKO$^{TH\text{-IRES-cre}}$ model.....182

Figure 6.5. Magnitude of evoked $[DA]_o$ in response to physiologically-relevant stimulation frequencies is unchanged by the *ATG7*cKO$^{TH\text{-IRES-cre}}$ genotype in the caudate-putamen and nucleus accumbens. 184

Figure 6.6. Macroautophagy impairment in dopamine neurons reduces paired-pulse depression of evoked $[DA]_o$ in the caudate-putamen in a *ATG7*cKO$^{TH\text{-IRES-cre}}$ model. 186

Figure 6.7. Macroautophagy impairment in dopamine neurons reduces paired-pulse depression of evoked $[DA]_o$ in the nucleus accumbens in some contexts in a *ATG7*cKO$^{TH\text{-IRES-cre}}$ model. 187

Figure 6.8. No effect of macroautophagy impairment on dopamine content in the caudate-putamen or nucleus accumbens. 188

Figure 7.1. Divergent effects of impaired macroautophagy in dopamine neurons on parkinsonian phenotypes: a suggested framework. 198

List of tables

Table 1.1. An overview of PARK loci 12

Table 1.2. Genes reaching genome-wide significance for association with sporadic Parkinson's disease 17

Table 1.3. ATG proteins and their functions 36

Table 1.4. α-Synuclein BAC transgenic mouse models of Parkinson's disease 48

Table 1.5. Mouse models of conditional *ATG7* deletion in dopamine neurons 52

Table 2.1. PCR reaction components 58

Table 2.2. Primer sequences for genotyping transgenic mice 58

Table 2.3. Primary antibodies for immunohistochemistry 63

Table 3.1. Summary of neuropathological effects of *ATG7*cKO$^{DAT\text{-IRES-cre}}$ and h*SNCA* genotypes in experimental mice 112

Table 4.1. Summary of behavioural assays used to phenotype experimental mice 115

Table 4.2. Summary of behavioural effects of *ATG7*cKO$^{DAT\text{-IRES-cre}}$ and h*SNCA* genotypes 138

Table 5.1. Summary of effects of *ATG7*cKO$^{DAT\text{-IRES-cre}}$ and hSNCA on paired-pulse depression 156

Table 5.2. Dopamine neurotransmission phenotypes associated with *ATG7*cKO$^{DAT\text{-IRES-cre}}$ and h*SNCA* genotypes in experimental mice 170

Table 6.1. Summary of effects of *ATG7*cKO$^{TH\text{-IRES-cre}}$ paired-pulse depression 185

Table 6.2. Comparison of the effects of the *ATG7*cKO$^{TH\text{-IRES-cre}}$ and *ATG7*cKO$^{DAT\text{-IRES-cre}}$ genotypes on dopamine neurotransmission in acute striatal slices from 1 month-old mice 190

Table 7.1. Summary of the effects of ATG7cKO and hSNCA genotypes in experimental mice 196

Appendix Table 1. Substantia nigra dopamine neuron counts with gene effects analysed using two-way ANOVA in each age group 205

Appendix Table 2. Ventral tegmental area dopamine neuron counts with gene effects analysed using two-way ANOVA in each age group 206

Abbreviations

$[DA]_o$	Extracellular dopamine
5-HIAA	5-hydroxyindoleacetic acid
6-OHDA	6-hydroxydopamine
A30P	Ala30Pro mutation in *SNCA*
A53T	Ala53Thr mutation in *SNCA*
AAV	Adeno-associated virus
ABC	Avidin-biotin complex
aCSF	Artificial cerebrospinal fluid
AD	Alzheimer's disease
AMBRA1	Activating molecule in Beclin-1-regulated autophagy protein 1
AMPK	Adenosine monophosphate-activated protein kinase
ANOVA	Analysis of variance
Atg	Autophagy-related gene (yeast)
ATG	Autophagy-related gene (mammals)
*ATG5*cKO	Conditional knockout of *ATG5*
*ATG7*cKO	Conditional knockout of *ATG7*
ATG16L1	ATG16-like 1
ATPase	Adenosine triphosphatase
BAC	Bacterial Artificial Chromosome
Barkor	Beclin 1-associated autophagy-regulated key regulator
cDNA	Complementary DNA
CFM	Carbon-fibre microelectrodes
cKO	Conditional knockout
cm	Centimetre
CMA	Chaperone-mediated autophagy

CPu	Caudate-putamen
CSPα	Cysteine string protein-α
DA	Dopamine
DAB	Diaminobenzidine
DAPI	Diamidino-2-phenylindole
DAT	Dopamine transporter
DNA	Deoxyribonucleic acid
dNTP	Deoxynucleotide triphosphate
DOPAC	4-dihydroxyphenylacetic acid
EDTA	Ethylenediaminetetraacetic acid
EOPD	Early onset Parkinson's disease
FAK	Family kinase-interacting protein of 200 kDa
FCV	Fast-scan cyclic voltammetry
GAK	Cyclin-G-associated kinase
GBA	Gene encoding glucocerebrocidase
GPe	External globus pallidus
GPi	Internal globus pallidus
GTPase	Guanosine triphosphatase
GWAS	Genome-wide association studies
HEPES	4-(2-hydroxyethyl)-1-piperazineethanesulfonic acid
HPLC	High-performance liquid chromatograph
h*SNCA*	Human wild-type *SNCA* locus
HVA	Homovanillic acid
IBA1	Ionized calcium-binding adapter molecule 1
IRES	Internal ribosome entry sequence
ISH	In-situ hybridisation
kDa	Kilodaltons
L-DOPA	L-3,4-dihydroxyphenylalanine

LAMP-2A	Lysosome-associated membrane protein 2A
LC3	Microtubule-associated protein 1A/1B-light chain 3
LRRK2	Leucine-rich repeat kinase 2
MPP+	1-methyl-4-phenyl-2,3-dihydropyridium
MPPP	1-methyl-4-phenyl-propion-oxypiperidine
MPTP	1-methyl-4-phenyl-1,2,3,6-tetrahydropyridine
m*SNCA*	Mouse wild-type *SNCA* locus
mTOR	Mammalian target of rapamycin
NA	Noradrenaline
NAC	Non-amyloid-β component of Alzheimer's disease amyloid
NAcC	Core of the nucleus accumbens
NAcS	Shell of the nucleus accumbens
PBS	Phosphate-buffered saline
PCR	Polymerase chain reaction
PD-MCI	Parkinson’s disease - mild cognitive impairment
PD	Parkinson’s disease
PDD	Parkinson’s disease dementia
PE	Phosphatidylethanolamine
PET	Positron emission tomography
PFA	Paraformaldehyde
PI3P	Phosphatidylinositol 3-phosphate
PINK1	PTEN-induced kinase 1
PLA	Proximity ligation assay
PPD	Paired-pulse depression
PSP	Progressive supranuclear palsy
RAB7L1	Rab-7-like protein 1
RIPA	Radioimmunoprecipitation assay
RNA	Ribonucleic acid

RNase	Ribonuclease
ROS	Reactive oxygen species
SDS-PAGE	Sodium dodecyl sulfate polyacrylamide gel electrophoresis
SEM	Standard error of the mean
SERT	Serotonin transporter
siRNA	Short inhibitory ribonucleic acid
SNARE	Soluble N-ethylmaleimide-sensitive factor attachment protein receptor
SNc	Substantia nigra pars compacta
SNCA	Gene encoding α-synuclein
SNCA-OVX	BAC-based α-synuclein overexpressing mouse
SNPs	Single-nucleotide polymorphisms
SNr	Substantia nigra pars reticulata
STN	Subthalamic nucleus
TAE	Tris-acetate-ethylenediamine tetraacetic acid
TBI	Traumatic brain injury
TBS	Tris-buffered saline
TBST	Triton X-100
TFEB	Transcription factor EB
TH	Tyrosine hydroxylase
Thal	Thalamus
UKL1	Unc-51-like kinase 1
UPS	Ubiquitin-proteasome system
UTR	Untranslated region
VPS35	Vacuolar protein sorting-associated protein 35
VTA	Ventral tegmental area
WT	Wild-type

Chapter 1: Introduction

1 Introduction

1.1 Parkinson's disease

Parkinson's disease (PD) is a common neurodegenerative disease characterised by insidious deterioration of motor control, and often associated with mood, sleep and cognitive disturbances (Parkinson 1817; Emre 2003; Lees *et al.* 2009). Over 1% of all people over the age of 65 suffer from PD (de Rijk *et al.* 1995). Similar to other neurodegenerative diseases, age is a key risk factor for the development of PD. By 2030, an estimated 130,000 Britons will be living with PD (Dorsey *et al.* 2007). PD carries a significant economic cost, including direct and indirect health care costs, and lost productivity (Clarke *et al.* 1995; Dodel *et al.* 1998; Berger *et al.* 2000). In the United Kingdom, the direct economic cost of PD can be estimated at five hundred million pounds per year (Findley *et al.* 2003; Dorsey *et al.* 2007). Currently, PD is incurable, irreversible, and treatment is limited to the management of symptoms. Further knowledge of the molecular pathways that contribute to the pathogenesis of PD is integral to the development of new therapies for this disease.

1.1.1 Clinical features of Parkinson's disease

1.1.1.1 Motor symptoms

Clinically, the motor symptoms of PD are characterised by resting tremor, rigidity, bradykinesia, and postural instability (Parkinson 1817; Jankovic 2008). The term parkinsonism is used to describe this symptom complex, and although PD is the most common cause of parkinsonism, other diseases and drugs are secondary causes (Caslake *et*

al. 2008; Munhoz *et al.* 2010). In PD these characteristics are not universal; patients with PD display temporally and anatomically heterogeneous symptoms. Other motor features that occur frequently in PD include development of a shuffling gait and freezing of gait (Jankovic 2008).

The resting tremor exhibited in PD is coarse, with a frequency of four to six cycles per second, and is present in approximately 70% of patients (Hughes *et al.* 2001; Connolly and Lang 2014). The distal parts of the limbs are predominately affected, commonly the fingers, giving rise to the classical "pill rolling" tremor of PD. Asymmetry of tremor is frequent in PD, and may help distinguish organic disease from drug-induced parkinsonism (Hughes *et al.* 2001).

Rigidity of the limbs is classically observed in PD, although rigidity affecting the neck and the trunk can also be seen. PD patients develop increased resistance to passive movement of the joints, and this rigidity is often accompanied by a "cogwheel" phenomenon, which some authors propose to be due to an interaction between tremor and rigidity (Findley *et al.* 1981). The presence of bradykinesia, or slowness of movement, can be observed in gross and fine motor movements, and is associated with a progressive reduction in speed and amplitude of sequential motor tasks (Jankovic 2008).

Postural instability typically manifests as impaired balance, and is associated with greater fall risk (Ashburn *et al.* 2001). In combination with bradykinesia, balance problems are likely to contribute to the development of the shuffling gait commonly observed in PD.

Postural instability occurs in approximately half of PD patients within five years of diagnosis (DeMaagd and Philip 2015).

Motor symptoms are the most common presenting symptom in PD, and are the major factor leading to initiation of medication (Connolly and Lang 2014). Modelling PD pathogenesis in laboratory animals should therefore include a rigorous evaluation of as many motor symptom correlates as possible.

1.1.1.1.1 Non-motor symptoms

Several non-motor symptoms are commonly associated with PD; recent research has demonstrated that these symptoms can cause the greatest impact on quality of life for PD patients (Alvarado-Bolanos *et al.* 2015). Common non-motor symptoms include cognitive dysfunction, mood disorders such as anxiety and depression, autonomic disturbances, olfactory deficits and sleep perturbations.

There is a broad spectrum of cognitive dysfunction in PD, from unaffected individuals to those with mild cognitive impairment (PD-MCI) and patients with frank dementia (Parkinson's disease dementia, PDD). Longitudinal cohort studies have demonstrated that 50% of PD patients that survive for 10 years or longer will develop PDD, increasing to 80% of patients who survive for 20 or more years (Hely *et al.* 2008). There is an association with PDD and falls, which, along with pneumonia, are the most common reasons for PD patients to be admitted to hospital.

Mood disorders, especially anxiety and depression, are more frequent in PD patients than in the general population. Anxiety disorders are present in 40% of PD patients, and may represent a preclinical risk factor; most commonly patients suffer from general anxiety disorder (Chen *et al.* 2015). Depression is present in approximately 36% of PD patients, on average, and some evidence exists that there is biological, rather than a purely reactive basis for the association of this disorder with PD (Chen *et al.* 2015). For example, studies have demonstrated deficits in serotonergic circuits in PD patients with depression, compared to those without depression (Boileau *et al.* 2008; Politis *et al.* 2010).

Autonomic disturbances, such as constipation, hyperhidrosis, orthostatic dizziness and urinary and erectile dysfunction, contribute significantly to the morbidity associated with PD. Constipation is present in 50% of patients with established PD, and precedes development of the disease in 20% of cases (Chen *et al.* 2015). Constipated adults are more than twice as likely to develop PD than those without constipation (Adams-Carr *et al.* 2016).

Hyposmia (reduced ability to detect odours) is present in approximately three-quarters of all PD patients, and has been promulgated as a preclinical marker of PD (Montgomery *et al.* 1999; Ponsen *et al.* 2004; Chen *et al.* 2015). In a study by Montgomery and colleagues, 10% of asymptomatic first-degree relatives of PD patients who suffered hyposmia were diagnosed with PD over a two year period; no relatives with normal olfaction were diagnosed with PD in that time (Montgomery *et al.* 1999).

In summary, non-motor features of PD contribute significantly to the suffering of patients, and it is therefore important that any efforts to understand the molecular mechanisms of PD also encompass these symptoms.

1.1.2 Pathological hallmarks of Parkinson's disease

Although PD is increasingly recognized as a global nervous system disorder, the pathological hallmark of PD remains neuron loss in the substantia nigra pars compacta (SNc). The SNc is a region of the midbrain containing a large number of pigmented dopamine (DA)-producing neurons. Gross examination of brains from patients with PD demonstrates pallor of the SNc. On microscopy, loss of neuromelanin-containing catecholaminergic neurons in the SNc is seen (Pakkenberg and Brody 1965). Typically, investigators use tyrosine hydroxylase (TH), the rate-limiting enzyme in DA synthesis, to identify and count SNc neurons (Rudow *et al.* 2008). In PD, 70 to 90% of SNc DA neurons are lost (Rudow *et al.* 2008). A key feature of PD is the selective loss of SNc DA neurons compared to the neighbouring ventral tegmental area (VTA) (Hirsch *et al.* 1988). VTA DA neurons synapse in the nucleus accumbens, in addition to the amygdala, hippocampus and different areas of cortex. Loss of DA neurons in the SNc is accompanied by the loss of their projections, most of which terminate in the caudate-putamen. Accordingly, dopamine concentrations are significantly reduced in the caudate-putamen of PD patients (Ehringer and Hornykiewicz 1960; Bernheimer *et al.* 1973).

In most cases of PD, loss of DA neurons in the SNc is accompanied by neuronal collections called Lewy bodies, and elongated neuronal processes known as Lewy neurites

(Lewy 1912; Braak *et al.* 2006). Lewy bodies and Lewy neurites are thought to be predominantly composed of fibrillar aggregates of α-synuclein (Spillantini *et al.* 1997; Bisaglia *et al.* 2009). Two types of Lewy bodies are commonly cited: a classical brainstem type, consisting of an acidophilic core and a pale halo, and a cortical type without a halo (Spillantini *et al.* 1997; Braak and Del Tredici 2008). The core of both types is rich in ubiquitin, and both contain α-synuclein, which in the brainstem type is mostly located in the halo (Kuzuhara *et al.* 1988).

Pale bodies often accompany Lewy pathology, and are thought to be precursors of Lewy bodies (Braak *et al.* 2005). Pale bodies are smoothly contoured, pale-staining structures that predominantly occur in DA neurons of the SNc. Lewy plaques are a less frequent accompaniment, and are extracellular spherical complexes that have a core of amyloid-β, a protein that constitutes a significant component of the extracellular plaques of Alzheimer's disease (AD). Lewy plaques are typically surrounded by dystrophic Lewy neurites that contain α-synuclein.

Lewy pathology is observed in brain regions other than the SNc, and the presence of Lewy pathology and associated neurodegeneration is thought to be responsible for some of the clinical manifestations in PD. Furthermore, it has been proposed by Braak and others that Lewy pathology affects interconnected brain regions in a predictable sequence (Braak *et al.* 2006). In this hypothesis, Lewy pathology starts in two sites: the olfactory neurons and nuclei, and the medulla. From these two sites, pathology progresses through the midbrain and amygdala, although initially there is no neuron loss in the SNc. Subsequently,

midbrain degeneration progresses, and Lewy pathology spreads to the cortex, beginning in the temporal lobe. In the final stages, the SNc has lost almost all DA neurons, and the cortex becomes more fully involved, particularly the insular and cingulate cortex, but also association areas and in some cases primary cortex.

1.1.3 Pathophysiology of Parkinson's disease

The SNc is a region of the midbrain that is responsible for regulating movement via its effects on the direct and indirect basal ganglia motor pathways (Figure 1.1) (DeLong and Wichmann 2007). SNc neurons project to the striatum, where they release DA onto medium spiny neurons. The effect of DA on the medium spiny neurons is dependent on the type of dopamine receptor expressed on the cell surface; D1 receptors are excitatory, whereas D2 receptors are inhibitory. SNc dopaminergic pathways are responsible for facilitating the firing of the direct motor pathway, and inhibiting the action of the indirect motor pathway (DeLong and Wichmann 2007). The direct and indirect pathways have opposing actions: the direct pathway promotes movement, whereas the indirect pathway acts as a brake on movement. Accordingly, loss of SNc regulation of the direct and indirect pathways, as occurs in PD, results in the symptom of bradykinesia. It has been further suggested that death of SNc dopaminergic neurons results in the classical resting tremor of PD, through the precipitation of an oscillatory firing pattern within the subthalamopallidal circuit (Bevan *et al.* 2002; Terman *et al.* 2002). There are numerous other pathways which are involved in PD, and which may be responsible for the remaining manifestations of disease. For example, alterations in the dopaminergic aspects of the mesocortical circuit may underlie cognitive dysfunction in PD; similarly mesolimbic disturbance may produce abnormal reward-seeking behaviour (Mattay *et al.* 2002;

Bosboom *et al.* 2004; Schott *et al.* 2007). Degeneration of medullary nuclei, which exert control of the sympathetic nervous system, may cause some of the autonomic disturbances previously discussed.

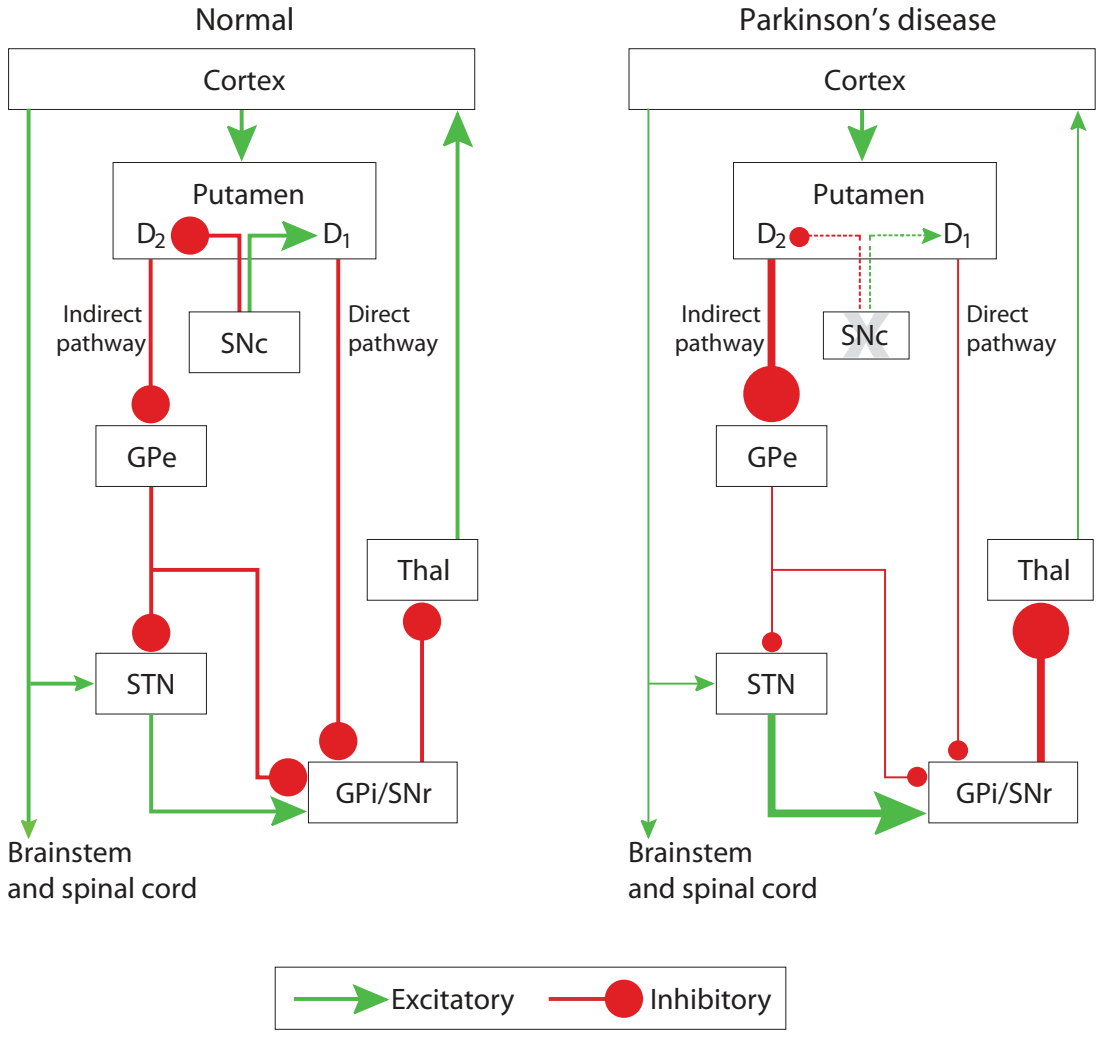


Figure 1.1. Basal ganglia in health and Parkinson's disease.
Dopaminergic output from the SNc facilitates movement by acting to inhibit the indirect pathway and facilitate the direct pathway. Loss of SNc DA neurons, as occurs in PD, reduces this effect, and gives rise to some of the motor manifestations of PD. Thickness of lines denotes strength of connections. GPe, external globus pallidus, GPi, internal globus pallidus; SNc, substantia nigra pars compacta; SNr, substantia nigra pars reticulata; STN, subthalamic nucleus; Thal, thalamus. Adapted from Miocinovic et al. (2013).

1.1.4 Treatment of Parkinson's disease

There are no established medications that improve or stabilise neurodegeneration in PD. Treatment is limited to managing the symptoms of PD, and focuses on increasing DA supply to striatal medium spiny neurons. Medication is commenced when patients experience functional impairment or other harms as a result of PD; in general, initiation of medication is associated with an improvement in quality of life (Korczyn *et al.* 1999; Fahn *et al.* 2004; PD MED Collaborative Group 2014). The mainstay of PD treatment is oral L-DOPA (L-3,4-dihydroxyphenylalanine), which is produced endogenously from L-tyrosine by TH. Oral administration of L-DOPA precludes the need for TH to produce it, and as TH is the rate-limiting enzyme in DA synthesis, this increases the supply of DA. L-DOPA is typically administered with a peripheral decarboxylase inhibitor, such as carbidopa, to prevent its metabolism in peripheral tissues. Unfortunately, L-DOPA therapy is associated with the development of dyskinesia. A second major drug class in PD are the dopamine receptor agonists, the most used of which are pramipexole and ropinirole. A randomized controlled trial comparing L-DOPA and ropinirole demonstrated that the development of dyskinesia was significantly reduced in the ropinirole group (Rascol *et al.* 2000). However, dopamine receptor agonists are associated with an increased frequency of other adverse effects, such as hallucinations and problems with impulse control, especially in the elderly. For this reason, contemporary guidelines suggest starting younger patients on a dopamine agonist, whereas older patients should be started on L-DOPA (Connolly and Lang 2014). A number of other medications are used to address various other facets of PD; meta-analyses have demonstrated a small symptomatic benefit of monoamine oxidase inhibitors, and anticholinergic agents and β-blockers have been used to treat tremor (Connolly and Lang 2014). Recent data from Mittal and colleagues (2017) has shown that

β-adrenergic agonists such as salbutamol regulate α-synuclein production, and use of β-adrenergic agonists are protective against PD in a large Norwegian cohort.

1.1.5 Risk factors for the development of Parkinson's disease

1.1.5.1 Genetic risk factors for Parkinson's disease

Genetic risk factors can be divided into familial genetic mutations that inevitably cause PD, and genetic factors that confer increased risk in the sporadic form of PD. It should be noted that familial forms of PD account for approximately five percent of prevalent cases; their major importance in the context of this analysis is as an indicator of the molecular pathogenesis of PD (Klein and Westenberger 2012).

1.1.5.1.1 Familial genetic mutations that cause Parkinson's disease

Genetic mutations that cause familial PD are designated as "PARK" loci (Table 1.1). Mutations in three genes cause autosomal dominant PD: *SNCA* (PARK1), *LRRK2* (PARK8) and *VPS35* (PARK17). *SNCA* is the gene that encodes α-synuclein, the predominant component of two pathological hallmarks of PD, Lewy bodies and Lewy neurites. In 1997, the first genetic studies to elucidate causal genetic lesions in PD found a dominantly inherited substitution in *SNCA* – the Ala53Thr (A53T) mutation – in a large Italian family (Polymeropoulos *et al.* 1997). Four mutations in SNCA that cause PD have since been identified: Ala30Pro (A30P), Glu46Lys, His50Gln and Gly51Asp (Polymeropoulos *et al.* 1997; Krüger *et al.* 1998; Zarranz *et al.* 2004; Appel Cresswell *et al.* 2013; Lesage *et al.* 2013; Proukakis *et al.* 2013). Further linkage analyses demonstrated a causal, autosomal-dominant association between *SNCA* duplications and triplications and

the development of late-onset PD in several pedigrees (Singleton *et al.* 2003; Fuchs *et al.* 2007). The clinical presentation of patients with PD associated with single-point *SNCA* mutations is largely analogous to sporadic PD, and these patients are generally L-DOPA responsive. Patients who suffer PD secondary to *SNCA* duplication or triplications display more prominent non-motor symptoms of autonomic dysfunction and cognitive impairment. Progression is more rapid in patients with *SNCA* triplications compared to those with *SNCA* duplications.

Table 1.1. An overview of PARK loci

Designation	Locus	Gene	Disease type	Inheritance	Discovery method
PARK1/4	4q21-22	*SNCA*	EOPD	D	Linkage analysis
PARK2	6q25.2-q27	*Parkin*	EOPD	AR	Linkage analysis
PARK3	2p13	*Unknown*	Classical PD	AD	Linkage analysis
PARK5	4p13	*UCHL1*	Classical PD	AD	Candidate gene approach
PARK6	1p35-p36	*PINK1*	EOPD	AR	Linkage analysis
PARK7	1p36	*DJ-1*	EOPD	AR	Linkage analysis
PARK8	12q12	*LRRK2*	Classical PD	AD	Linkage analysis
PARK9	1p36	*ATP13A2*	Kufor-Rakeb syndrome	AR	Linkage analysis
PARK10	1p362	*Unknown*	Classical PD	Risk factor	Linkage analysis
PARK11	2q36-27	*Unknown*	Late-onset PD	AD	Linkage analysis
PARK12	Xq21-q25	*Unknown*	Classical PD	Risk factor	Linkage analysis
PARK13	2p12	*HTRA2*	Classical PD	AD or risk factor	Candidate gene approach
PARK14	22q13.1	*PLA2G6*	Parkinsonism with dystonia	AR	Linkage analysis
PARK15	22q12-q13	*FBX07*	Juvenile parkinson-pyramidal syndrome	AR	Linkage analysis
PARK16	1q32	*Unknown*	Classical PD	Risk factor	GWAS
PARK17	16q11.2		Classical PD	AD	Exome sequencing
PARK18	3q27.1	*EIF4G1*	Classical PD	AD	Linkage analysis
PARK19	1p31.3	*DNAJC6*	EOPD	AR	Exome sequencing

AD, autosomal dominant; AR, autosomal recessive; EOPD, early onset Parkinson's disease; GWAS, genome-wide association study. Adapted from Hernandez *et al.* (2016) and Klein & Westenberger (2012).

Dominantly inherited genetic disruptions were later identified in *LRRK2*, the gene encoding leucine-rich repeat kinase 2 (LRRK2), a guanosine triphosphatase and kinase that has multiple roles in striatal neurotransmission, neuronal homeostasis, autophagy and immunity (Paisan-Ruiz *et al.* 2004; Zimprich *et al.* 2004; Kachergus *et al.* 2005; Lesage *et al.* 2005; Alegre-Abarrategui *et al.* 2009; Ozelius *et al.* 2009; Aasly *et al.* 2010). Patients

with *LRRK2* mutations present with a variable clinical and neuropathological phenotype, with features that span those of sporadic PD, and associated syndromes such as progressive supranuclear palsy (PSP) and simple nigral degeneration (Zimprich *et al.* 2004).

The most recently identified autosomal dominant genetic lesion that causes PD is an aspartate to asparagine mutation at amino acid 620 of the vacuolar protein sorting-associated protein 35 (VPS35), which was described in Swiss and Austrian pedigrees with late-onset PD, and later in Japanese and French families (Vilarino-Gueell *et al.* 2011; Zimprich *et al.* 2011; Ando *et al.* 2012; Lesage *et al.* 2012). VPS35 is the largest subunit of a large multimeric complex, termed retromer, that is responsible for retrograde transport of proteins from endosomes to the Golgi complex in mammalian cells (Reddy and Seaman 2001; Hierro *et al.* 2007). Retromer has been implicated in the development of other neurodegenerative diseases, most notably AD, where it has been shown in animal models that loss of retromer increases the amount of the suspected pathogenic protein in AD, amyloid-β (Muhammad *et al.* 2008).

A further six PD-causing gene mutations have been identified in families displaying an autosomal recessive pattern of disease inheritance. The first to be described were missense mutations in the gene encoding Parkin (*PARK2*). *PARK2* deletions were found to be causally associated with autosomal recessive juvenile PD in Japanese patients, a finding replicated in large European cohorts (Kitada *et al.* 1998; Abbas *et al.* 1999; Lucking *et al.* 2000). It is important to note that these patients with autosomal recessive juvenile PD

typically tend not to demonstrate Lewy body pathology (Yamamura *et al.* 1998; Mori *et al.* 1998; Shimura *et al.* 1999; Hayashi *et al.* 2000; van de Warrenburg *et al.* 2001; Farrer *et al.* 2001; Gouider-Khouja *et al.* 2003; Sasaki *et al.* 2004; Pramstaller *et al.* 2005; Cornejo-Olivas *et al.* 2015). Following the discovery of the association between *PARK2* and PD, functional studies revealed a role of Parkin as a ubiquitin-protein ligase that is responsible for ubiquitination of the α-synuclein interacting protein synphilin-1 (Chung *et al.* 2001; Shimura *et al.* 2001).

In 2003, Bonifati and his colleagues described mutations in *DJ-1* as responsible for an autosomal recessive form of PD in separate Dutch and Italian families; specifically they found exon deletions and loss-of-function mutations respectively (Bonifati *et al.* 2003). Furthermore, *DJ-1* mutation homozygosity is also thought to explain the development of a complex of parkinsonism, dementia and amyotrophic lateral sclerosis that is present in an Italian family (Annesi *et al.* 2005). DJ-1 is a protein that localises to mitochondria and experimental evidence suggests that it is protective against oxidative stress in dopaminergic neurons; DJ-1 mutations found in PD patients are likely to increase neuronal susceptibility to oxidative stress (Taira *et al.* 2004; Moore *et al.* 2005; Zhang *et al.* 2005; Guzman *et al.* 2010). Olzmann *et al.* (2007) have demonstrated that Parkin can ubiquitinate DJ-1, indicating that mutations in these genes may cause disease via the same or similar pathways.

PTEN-induced kinase 1 (PINK1) is an outer mitochondrial membrane protein that interacts with Parkin to mediate mitophagy, and is required for normal mitochondrial

function (a subtype of autophagy, a cellular process for protein degradation that is discussed later in this thesis) (Park *et al.* 2006; Exner *et al.* 2007; Poole *et al.* 2008; Geisler *et al.* 2010; Matsuda *et al.* 2010; Narendra *et al.* 2010; Vives-Bauza *et al.* 2010). Multiple missense mutations have been identified in *PINK1* that are associated with autosomal recessive inheritance of early-onset PD phenotypes in Italian and Spanish families (Valente *et al.* 2004).

ATP13A2 mutations have been identified as causative in the development of Kufor-Rakeb syndrome, a rare autosomal dominant-inherited disease that features juvenile parkinsonism, pallido-pyramidal degeneration and supranuclear upgaze palsy (Ramirez *et al.* 2006). *ATP13A2* encodes for a lysosomal type 5 adenosine triphosphatase (ATPase) that plays a role in some pathways relevant to Parkinson's disease, including the autophagy pathway and mitochondrial health (Dehay *et al.* 2012; Usenovic *et al.* 2012; Grünewald *et al.* 2012; Gusdon *et al.* 2012).

More recently, causative genetic disruptions in the genes *PLA2G6* and *FBXO7* have been reported. Mutations in *PLA2G6* cause levodopa-responsive parkinsonism with dystonia, and fibroblasts taken from these patients show impaired mitochondrial function (Kinghorn *et al.* 2015). *PLA2G6* encodes a phospholipase that hydrolysed glycerophospholipids to produce free fatty acids (Balsinde and Balboa 2005). Individuals who are homozygous for *FBXO7* mutations develop a parkinsonian-pyramidal syndrome beginning in childhood (Shojaee *et al.* 2008). Knockout of *FBXO7* in the brains of mice causes impaired proteasomal function (Vingill *et al.* 2016).

Another significant inherited genetic risk factor that does not have a PARK designation, but is worthy of note, are mutations in the *GBA* gene (Sidransky *et al.* 2009). *GBA* encodes for glucocerebrocidase, which is a lysosomal hydrolase. Individuals who are homozygous for *GBA* mutations develop Gaucher's disease, the most common lysosomal storage disorder. Those who are heterozygous for *GBA* mutations have substantially increased risk of PD, over five times that of non-carriers (Sidransky *et al.* 2009). The estimated prevalence of *GBA* mutations in PD patients is 5 to 10% (Migdalska Richards and Schapira 2016).

1.1.5.1.2 Genetic factors conferring risk for sporadic Parkinson's disease

Variation in individual genes confers modest risk for sporadic PD. Recently, Nalls *et al.* performed a meta-analysis of genome-wide association studies (GWAS) that delineated common single-nucleotide polymorphisms (SNPs) that are associated with sporadic PD (Nalls *et al.* 2014). This study identified common SNPs in 24 genes as contributors to PD risk in large Japanese and European populations. While an in-depth discussion of all of these genes is beyond the scope of this thesis, a summary of the meta-analysis results is provided in Table 1.2. Of these genes, *SNCA, LRRK2* and *GBA* are also associated with inherited PD.

Table 1.2. Genes reaching genome-wide significance for association with sporadic Parkinson's disease			
Gene	**P value**	**Odds ratio**	**Gene product and function**
SNCA	4.16×10^{-73}	0.76	Encodes α-synuclein. Pre-synaptically enriched with roles in synaptic vesicle exocytosis (Abeliovich *et al.* 2000).
MAPT	2.37×10^{-48}	0.769	Encodes microtubule-associated protein tau. Stabilises microtubules (Cleveland *et al.* 1977).
TMEM175	1.02×10^{-43}	0.786	Encodes transmembrane protein 175. Potassium channel that regulates lysosomal function (Cang *et al.* 2015).
GBA	1.37×10^{-29}	1.824	Encodes glucocerebrocidase. Lysosomal enzyme (Sidransky *et al.* 2009).
MCCC1	2.14×10^{-21}	0.842	Encodes methylcrotonoyl-CoA carboxylase 1. Mitochondrial enzyme (Morscher *et al.* 2012).
STK39	1.15×10^{-20}	1.214	Encodes serine/threonine kinase 39. Upstream activator of MAPK pathways (Dan *et al.* 2001).
ACMSD	9.13×10^{-20}	0.875	Encodes aminocarboxymuconate semialdehyde decarboxylase. Processes quinolinate, a neuronal excitotoxin (Fukuoka *et al.* 2002).
BST1	9.44×10^{-18}	1.126	Encodes bone marrow stromal cell antigen 1. Role in B-cell growth (Kaisho *et al.* 1994).
RAB7L1	1.66×10^{-16}	1.122	Encodes rab-7-like protein 1. Interacts with LRRK2 in and functions in the retromer and lysomal pathways (MacLeod *et al.* 2013).
LRRK2	5.24×10^{-14}	1.155	Encodes leucine-rich repeat kinase 2. Has GTPase and kinase domains, roles in striatal neurotransmission, immune function and autophagy (see previous section).
TMEM229B	6.63×10^{-14}	0.897	Encodes transmembrane protein 229b. Unknown function.
INPP5F	4.34×10^{-13}	1.624	Encodes inositol polyphosphate-5-phosphatase F. Functions in the endocytic pathway (Nakatsu *et al.* 2015).
GPNMB	1.18×10^{-12}	1.11	Encodes transmembrane glycoprotein NMB. Associated with lysosomal storage disease (Marques *et al.* 2016).
HLA-DQB1	1.19×10^{-12}	0.826	Encodes major histocompatibility complex, class II, DQ beta 1. Essential immune functions (Olerup *et al.* 1992).
BCKDK	2.43×10^{-12}	1.103	Encodes branched chain ketoacid dehydrogenase kinase. Inactivates an enzyme complex that converts branched-chain amino acids to ketoacids (Novarino *et al.* 2012).
CCDC62	6.02×10^{-12}	1.105	Encodes coiled-coil domain containing 62. Role in myeloid cells (Chan *et al.* 2016).
RIT2	7.74×10^{-12}	0.904	Ras Like Without CAAX 2. Interferon signaling protein (Liscovitch and French 2014).
MIR4697	9.83×10^{-12}	1.105	MicroRNA 4697. Unknown function.
VPS13C	1.23×10^{-11}	1.113	Encodes Vacuolar Protein Sorting 13 Homolog C. Associated with mitochondria (Lesage *et al.* 2005).
DDRGK1	3.04×10^{-11}	1.111	Encodes DDRGK domain containing 1. Part of the ubiquitin fold modifier complex, involved in endoplasmic reticulum homeostasis (Liu *et al.* 2017).
GCH1	5.85×10^{-11}	0.904	Encodes GTP cyclohydrolase 1. Involved in dopamine homeostasis; loss causes dopamine-responsive dystonia (Ichinose *et al.* 1994).
SIPA1L2	4.87×10^{-10}	1.131	Encodes Signal Induced Proliferation Associated 1 Like 2. A GTPase.
DLG2	3.96×10^{-7}	0.929	Encodes disks large homolog 2. Post-synaptic protein that acts as a receptor scaffold (Kim *et al.* 1996).
SPPL2B	5.57×10^{-7}	1.097	Signal peptide peptidase-like 2B. Role in B cell development (Schneppenheim *et al.* 2014).
GTPase, guanosine triphosphatase. MAPK, mitogen-associated protein kinase. NMB, neuromedin B. Data from Nalls *et al.* (2014).			

1.1.5.2 Environmental risk factors for sporadic Parkinson's disease

A number of environmental risk factors have been described that associate with PD, and those that carry the most evidence are described in this section. Factors that are associated with increased PD risk include age, sex, pesticide exposure and traumatic brain injury (TBI). Exposures that have an inverse relationship with PD diagnoses include tobacco and caffeine.

Like many neurodegenerative diseases, there is a strong relationship between age and the development of clinical PD. A recent meta-analysis of age-specific PD prevalence found that there are 41 PD sufferers per 100,000 individuals in the fifth decade of life, rising to 1,903 individuals per 100,000 in the ninth decade and above (Pringsheim *et al.* 2014). Although the association between age and PD risk is robust, the mechanisms by which age mediates increased risk are unclear; possible explanations include age-related protein accumulation, mitochondrial dysfunction, impaired calcium handling, altered iron homeostasis, or, more likely, a combination of multiple mechanisms (Reeve *et al.* 2014).

Men have a higher incidence of PD than women. Most studies describe a 3:2 male to female ratio for PD incidence, although this ratio may be higher in elderly subgroups, and lower in Asian populations (Wooten *et al.* 2004; Taylor *et al.* 2007). A number of explanations for the male preponderance in PD diagnoses have been put forward. Some of the most reductive hypotheses are that oestrogen is protective against PD, testosterone is harmful, or both. Some epidemiologic evidence supports these concepts; a higher number of women that have undergone hysterectomy or oophorectomy develop PD (Benedetti *et*

al. 2001; Rocca *et al.* 2008). Additionally, slower progression of PD has been described in female patients (Haaxma *et al.* 2007). Alternative explanations for greater PD risk in males include the presence of a recessive susceptibility gene on chromosome X, or a predisposition to other risk factors that is conferred by the male lifestyle (Kieburtz and Wunderle 2013).

Pesticide exposure as a risk factor for PD has received considerable attention, and work in laboratory animals has suggested that pesticide exposure can invoke a parkinsonian syndrome (Betarbet *et al.* 2000). The largest meta-analysis assessing pesticide exposure and risk of PD reported an adjusted odds ratio of 1.39 for those exposed compared with unexposed individuals (Pezzoli and Cereda 2013). In particular, exposure to paraquat and maneb or manxozeb pesticides was identified as carrying the highest risk for PD development. *In vivo* experiments have demonstrated the combination of both pesticides, which are frequently used in geographic proximity, is more potent that either alone (Thiruchelvam *et al.* 2000).

More recently, investigators have directed their attention to the relationship between TBI and the development of PD. A recent meta-analysis demonstrated that individuals suffering TBI had 57% higher risk of developing PD (Jafari *et al.* 2013). Lee and her colleagues extended this analysis to prospectively identify an interaction between paraquat exposure and TBI that was more than the additive risk of each exposure individually (Lee *et al.* 2012). This epidemiological finding mirrored the results of earlier *in vivo* experiments conducted in rats by Hutson *et al.* (2011).

Multiple studies have found that tobacco use is associated with a reduced risk of PD (Hernán *et al.* 2002; Ritz *et al.* 2007). A pooled analysis conducted by Ritz and her colleagues (2007) found a dose-dependent association between smoking and PD; in cohort studies the odds ratio for developing PD was as low as 0.23 for current smokers when compared with those who never smoked. Other tobacco exposures, such as pipe or cigar smoking, also had an inverse association with PD risk. The reasons for the inverse association between tobacco exposure and PD have not been determined. One explanation is that nicotine exposure promotes DA neuron survival. Noncausal explanations include that nicotine masks parkinsonian symptoms, thus delaying diagnosis. Alternatively, increased mortality associated with smoking may reduce age-specific PD incidence.

Similar to tobacco, caffeine exposure is associated with decreased PD risk (Hernán *et al.* 2002; Costa *et al.* 2010; Liu *et al.* 2012). In a recent meta-analysis, the relative risk of PD was 0.75 for those routinely exposed to caffeine when compared to those who did not have a regular caffeine intake (Costa *et al.* 2010). Although caffeine and tobacco intake are correlated behaviours, the protective effect of caffeine persists in subgroup analyses of never smokers, or when data is adjusted for tobacco exposure (Hernán *et al.* 2002; Costa *et al.* 2010; Liu *et al.* 2012). The protective association between caffeine and PD has led to small clinical trials. A recent randomised trial of 61 PD patients, conducted by Postuma and his co-workers (2012), demonstrated a positive effect of caffeine on the motor symptoms of PD.

1.2 α-Synuclein

1.2.1 The physiological localisation and function of α-synuclein

α-Synuclein was named after its localization to presynaptic vesicles (Iwai *et al.* 1995; Jakes *et al.* 2001). Subsequently, β-synuclein and γ-synuclein were identified. The three synucleins are highly homologous. α-Synuclein is expressed ubiquitously throughout the brain, especially in the striatum, cortex, hippocampus, thalamus, cerebellum and olfactory bulb (Jakes *et al.* 2001; Mori *et al.* 2002; Totterdell *et al.* 2004). α-Synuclein consists of 140 amino acids, and can be divided into three parts: the amphipathic region, the NAC domain, and the C-terminal acidic tail (Figure 1.3). Historically, α-synuclein has been described as an intrinsically disordered monomer of approximately 14 kilodaltons (kDA). However, more recently, there has been debate as to whether the physiological species of α-synuclein is a tetramer (Bartels *et al.* 2011; Burré *et al.* 2013). At the time of writing there was no consensus in the literature regarding the predominant physiological form of α-synuclein (Fauvet *et al.* 2012; Dettmer *et al.* 2013; Araki *et al.* 2016).

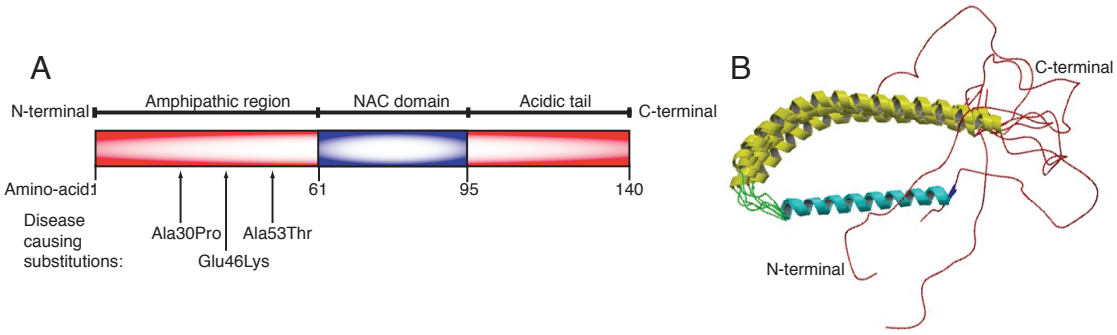


Figure 1.2. Structure of α-synuclein.
(A) The α-synuclein protein, in schematic form. It is divided into three domains, the amphipathic region, the non-amyloid-β component of Alzheimer's disease amyloid (NAC) domain, and the C-terminal acidic tail. (B) The micelle-bound structure of α-synuclein solved using nuclear magnetic and electron paramagnetic resonance (taken from the Protein Databank, ID: 1XQ8). Adapted from Hunn et al. (2015).

Evidence suggests that a key physiological role of α-synuclein is to regulate exocytosis of neurotransmitters at the synapse. α-Synuclein knockout mice have normal survival and brain architecture, but exhibit increased DA release with paired stimuli, have reduced striatal DA content with age and a diminished locomotor response to amphetamine (Abeliovich *et al.* 2000; Al-Wandi *et al.* 2010; Connor-Robson *et al.* 2016). Conversely, α-synuclein overexpression significantly inhibits DA release both *in vitro* and *in vivo* (Nemani *et al.* 2010; Janezic *et al.* 2013). These data are consistent with findings in combinatorial α-β-γ-synuclein knockout mice, which demonstrate increased striatal DA release (Anwar *et al.* 2011). α-β-γ-Synuclein knockout mice also exhibit structural changes, with smaller synapses (Vargas *et al.* 2017). Concordant with a role of α-synuclein in regulating synaptic exocytosis are reports that α-synuclein regulates vesicle clustering in yeast, neurons, and transgenic mice (Gitler *et al.* 2008; Soper *et al.* 2008; Janezic *et al.* 2013; Burré *et al.* 2014; Wang *et al.* 2014). The clustering effect mediated by α-synuclein has been shown to restrict synaptic vesicle motility (Wang *et al.* 2014).

The mechanism by which α-synuclein regulates neurotransmitter release may be through its association with soluble N-ethylmaleimide-sensitive factor attachment protein receptor (SNARE) complexes. SNARE complexes mediate membrane fusion to allow synaptic vesicle exocytosis, after which they rapidly disassociate to an unfolded state. Disassociated SNARE proteins are prone to misfolding and non-specific interactions, and thus there are four chaperone proteins to safeguard SNARE proteins at the synapse: cysteine string protein-α (CSPα) and the synucleins (Chandra *et al.* 2005; Burré *et al.* 2014). Knockout of CSPα is neurotoxic, but can be rescued by α-synuclein overexpression, suggesting a similar role in preventing synaptic degeneration (Chandra *et al.* 2005). Diao *et al.* (2013) have provided data suggesting that the effect of α-synuclein on vesicle clustering is

mediated via SNARE complexes. Although most work on the function of SNARE complexes has been focused on the synapse, there is increasing recognition that many essential intracellular trafficking functions are governed by SNARE complexes, including macroautophagy, providing a potential mechanism for α-synuclein to regulate these processes (Nair *et al.* 2011). Other physiological roles for α-synuclein are also being explored: emerging evidence suggest that a α-synuclein may regulate mitochondrial bioenergetics (Ludtmann *et al.* 2016).

β-Synuclein is a 134 amino-acid protein that has an overlapping expression pattern with α-synuclein, and shares its synaptic localisation. β-synuclein shares most homology with α-synuclein (61%), although crucially it lacks the 11 amino acid NAC region (Spillantini *et al.* 1995; Jakes *et al.* 2001; Sung and Eliezer 2007). In comparison with α- and γ-synuclein, β-synuclein resists aggregation, probably due to the absence of the NAC domain (Biere *et al.* 2000). Some authors have suggested that β-synuclein acts as a natural inhibitor to α-synuclein toxicity, and there is little association between β-synuclein and disease (Hashimoto *et al.* 2001). Recent studies in combinatorial knockout mice suggest that β-synuclein is required for maintaining motor performance into old age (Connor-Robson *et al.* 2016).

γ-Synuclein, also known as persyn, was the last of the three synucleins to be identified (Ninkina *et al.* 1998; Buchman *et al.* 1998). In mice, γ-synuclein is predominantly expressed in primary sensory neurons, sympathetic neurons and motor neurons. Unlike α- and β-synuclein, which are largely synaptic proteins, γ-synuclein appears to be primarily located in the soma, and in axons. Additionally, γ-synuclein also has roles in adipocyte

lipolysis (Millership *et al.* 2012). Expression of γ-synuclein is unable to rescue CSPα knockout, suggesting its function does not overlap with α-synuclein, at least at the synapse (Ninkina *et al.* 2012). The physiological localisation of γ-synuclein in the spinal cord is correlated with pathological phenotypes associated with overexpression, which include loss of 40% of lower motor neurons (Ninkina *et al.* 2009). Consistent with this phenotype, γ-synuclein aggregates can be observed in some cases of amyotrophic lateral sclerosis (Peters *et al.* 2015).

1.2.2 The role of α-synuclein in Parkinson's disease

Multiple independent avenues of research discussed earlier in this chapter have implicated α-synuclein in the pathogenesis of PD, including the presence of α-synuclein in Lewy bodies, inherited cases of PD caused by mutations or multiplications of the gene encoding α-synuclein (*SNCA*), and genome-wide association studies linking sporadic PD and *SNCA*. For these reasons, the pathogenic potential of α-synuclein has been intensively investigated, and several interrelated toxic effects of α-synuclein have been evidenced. Some of the major areas of study are summarised on the following pages.

1.2.2.1 α-Synuclein aggregation and impaired protein clearance

The potential for aggregation of α-synuclein to serve as a causative factor in PD has intuitive appeal, as Lewy bodies and neurites are partly composed of α-synuclein aggregated into amyloid-like fibrils (Spillantini *et al.* 1997). Additionally, there is significant experimental evidence to support the toxicity of aggregated α-synuclein. Wild-type α-synuclein forms amyloid-like fibrils when incubated in solution, and mutations in α-synuclein that cause PD have a more rapid aggregation profile (Conway *et al.* 1998; Lashuel *et al.* 2002). Aggregated forms of α-synuclein are deleterious to neurons both *in vivo* and *in vitro* (Masliah *et al.* 2000; Saha *et al.* 2000). In contrast, related proteins that do not aggregate, such as β-synuclein, or α-synuclein with the NAC region removed, do not demonstrate toxicity (Periquet *et al.* 2007). Although these observed links between α-synuclein aggregation and neurotoxicity exist, there is no correlation between clinical PD severity and Lewy body number (Parkkinen *et al.* 2011). The absence of correlation between Lewy pathology and disease may be explained, in part, by observations that oligomers of α-synuclein, rather than fully-formed fibrils, are the most toxic α-synuclein species (Winner *et al.* 2011).

In eukaryotic cells there are two major degradation systems: the ubiquitin-proteasome system (UPS) and autophagy (discussed in Section 1.8). The UPS is responsible for the degradation of most cytosolic and nuclear proteins in mammalian cells, including short-lived regulatory and misfolded proteins, as well as longer-lived proteins, which represent the bulk of cell components (Periquet *et al.* 2007). In the UPS, proteins are targeted for degradation through a series of enzymatic reactions that label them with ubiquitin (Winner

et al. 2011). These proteins, now "ubiquitinated," are then degraded by a proteolytic organelle called the proteasome.

The UPS has been linked to PD. Lewy bodies are immunoreactive for components of the proteasome (McNaught *et al.* 2002). Post-mortem nigral tissue from PD patients has lower proteasomal activity than control tissue (McNaught and Jenner 2001). In agreement, the transcription of genes encoding for UPS proteins is reduced in SNc lysates from PD patients (Grünblatt *et al.* 2004). α-Synuclein is degraded through both the UPS and autophagic pathways (Webb *et al.* 2003; Ebrahimi-Fakhari *et al.* 2011). However, aggregated α-synuclein and PD-associated mutant α-synuclein are resistant to degradation by the UPS, and also inhibit the function of the UPS (Stefanis *et al.* 2001; Snyder *et al.* 2003; Lindersson *et al.* 2004). It has been shown that familial PD can be caused by autosomal-recessive mutations in Parkin, a ubiquitin E3-ligase that tags proteins with ubiquitin as a signal for UPS degradation (Xiong *et al.* 2009). These patients are thought to lack a functional ubiquitination pathway, and this may explain the absence of Lewy bodies on post-mortem examination in most cases (Yamamura *et al.* 1998; Mori *et al.* 1998; Hayashi *et al.* 2000; van de Warrenburg *et al.* 2001; Farrer *et al.* 2001; Gouider-Khouja *et al.* 2003; Sasaki *et al.* 2004; Pramstaller *et al.* 2005; Cornejo-Olivas *et al.* 2015).

1.2.2.2 Mitochondrial dysfunction, oxidative stress and calcium handling

Dysfunction of mitochondria, and the associated production of free radicals causing oxidative stress has been an area of significant attention in PD. One of the earliest suggestions that mitochondrial dysfunction may be significant in PD was the discovery of

the potent neurotoxin MPTP (1-methyl-4-phenyl-1,2,3,6-tetrahydropyridine). MPTP is a synthetic analogue of the narcotic meperidine, and its neurotoxic properties were accidentally discovered when drug addicts developed parkinsonism following injection of a "synthetic heroin" (1-methyl-4-phenyl-propion-oxypiperidine (MPPP)). It was found that preparations of MPPP had been contaminated with MPTP (Langston *et al.* 1999). The toxic end-product of MPTP metabolism, 1-methyl-4-phenyl-2,3-dihydropyridium (MPP+), was identified as responsible for midbrain dopamine neuron death (Langston *et al.* 1984). Later investigations found that selectivity of MPP+ for dopamine neurons was conferred by selective uptake through the dopamine transporter (DAT) and other monoamine transporters (Javitch *et al.* 1985). MPP+ inhibits mitochondrial complex I, ultimately leading to neuron death (Vyas *et al.* 1986).

The discovery of the mechanism of MPTP toxicity spurred subsequent investigations into mitochondria in PD patients. Schapira and his colleagues observed reduced mitochondrial activity in the SNc of PD patients (Schapira *et al.* 1990). Similarly, mitochondrial activity is lower in cell lines that contain mitochondrial deoxyribonucleic acid (DNA) from PD patients; it is unclear if these defects in mitochondrial DNA are inherited or arise somatically (Gu *et al.* 1998). Dysfunction of mitochondria is thought to cause the production of reactive oxygen species (ROS), precipitating oxidative stress. Oxidative damage to DNA and ribonucleic acid (RNA) has been shown in the SNc of PD patients (Zhang *et al.* 1999). Other sequelae of oxidative stress have also been observed in the brains of PD patients, including increased lipid peroxidation and superoxide dismutase activity (Saggu *et al.* 1989; Dexter *et al.* 1989).

There is a two-way relationship between α-synuclein and mitochondrial dysfunction. Inhibitors of mitochondrial complex-I, including MPTP, lead to the accumulation of α-synuclein *in vitro* and *in vivo* (Kowall *et al.* 2000; Vila *et al.* 2000; Sherer *et al.* 2003; Fountaine and Wade-Martins 2007; Fountaine *et al.* 2008). Similarly, increased levels of ROS increase α-synuclein aggregation. Consistent with a toxic mechanism by which ROS acts via α-synuclein, α-synuclein knockout mice and cells are resistant to MPTP intoxication; conversely, mice overexpressing α-synuclein are more susceptible to the neurotoxic effects of MPTP (Dauer *et al.* 2002; Robertson *et al.* 2004; Nieto *et al.* 2006). However, it has also been shown that overexpression or aggregation of α-synuclein can cause mitochondrial dysfunction and increase ROS production (Hsu *et al.* 2000; Parihar *et al.* 2008).

A relationship between calcium handling in SNc DA neurons and oxidative stress has also been described. SNc DA neurons are autonomous pacemaking cells, and are unusual in that the calcium channels that they express feature $Ca_v1.3$ α-subunits, rather than the more typical $Ca_v1.2$ α-subunit (Chan *et al.* 2007). These $Ca_v1.3$-positive channels allow large influxes of calcium, and it is proposed that, over time, large calcium currents induce mitochondrial depolarization and dysfunction, and production of ROS (Chan *et al.* 2007; Guzman *et al.* 2010). The use of anti-hypertensive agents that antagonize Ca_v channels is associated with reduced risk of PD, prompting recent clinical trials that repurpose such agents to attempt to slow PD progression (Simon *et al.* 2010; Ritz *et al.* 2010; Simuni *et al.* 2010; Parkinson Study Group 2013; Gudala *et al.* 2015).

1.2.2.3 Prion-like propagation of α-synuclein

Prions are protein aggregates that lack nucleic acid and can be transmitted from neuron-to-neuron, with the prion acting as a template for further production of misfolded proteins in healthy neurons. Disease can thus be propagated throughout the nervous system. There are several relatively rare human prion diseases, including Creutzfeldt–Jakob disease, fatal familial insomnia, and kuru. Prion-like spread is consistent with the stepwise progression of PD pathology throughout the brain proposed by Braak *et al.* (2006) – from the olfactory bulb or medulla, through the midbrain, to the cortex. A series of clinical and laboratory findings have provided support for the hypothesis that PD represents a prion-like disorder. A key discovery was the post-mortem finding in three PD patients that Lewy bodies developed in foetal neural grafts 11 to 16 years after transplantation (Li *et al.* 2008; Kordower *et al.* 2008a; 2008b). This contrasted with an earlier report of an autopsy of a similar patient performed 18 months following transplantation of foetal tissue, where survival of transplanted neurons and dense innervation of the striatum occurred but with no overt pathology (Kordower *et al.* 1995). These findings prompted several experiments in rodents to elucidate the nature of spreading α-synuclein pathology. Luk and colleagues (2012a) showed that injection of synthetic α-synuclein into the dorsal striatum of wild type mice led to spreading Lewy-like pathology, including to the substantia nigra, and associated motor deficits. α-Synuclein transfer to cultured dopaminergic neurons grafted into α-synuclein transgenic mice has also been observed, recapitulating the clinical findings (Desplats *et al.* 2009; Hansen *et al.* 2011).

1.3 Autophagy

Autophagy (auto – self, phagy – to eat) describes an evolutionarily-conserved controlled cellular process by which organelles, toxic aggregated proteins, and invading microorganisms undergo sequestration and regulated degradation. In eukaryotic cells autophagy is stimulated by multiple environmental stressors, including development, nutrient deprivation, intracellular clearance, tumour suppression, immunity, and ageing. Autophagy results in the release of amino acids, lipids and carbohydrates to the cytosol to participate in further biosynthetic processes.

Most investigators refer to three different types of autophagy: macroautophagy, microautophagy and chaperone-mediated autophagy (CMA) (Figure 1.3). All types of autophagy have a final common pathway by which cellular material is degraded in vesicles that contain digestive enzymes, known as lysosomes. Macroautophagy is considered the major pathway through which most degradation of cellular contents proceeds; it involves the engulfment of cytoplasmic contents in a double-walled membrane, termed the phagophore. CMA is a mechanism by which proteins are targeted from the cytosol to the lysosomal membrane, and are then translocated directly across the lysosomal membrane. Microautophagy defines a process where direct lysosomal uptake of cellular contents occurs by invagination of the lysosomal membrane. Macroautophagy is the major focus of this thesis, and therefore the most attention is devoted to it in the following sections.

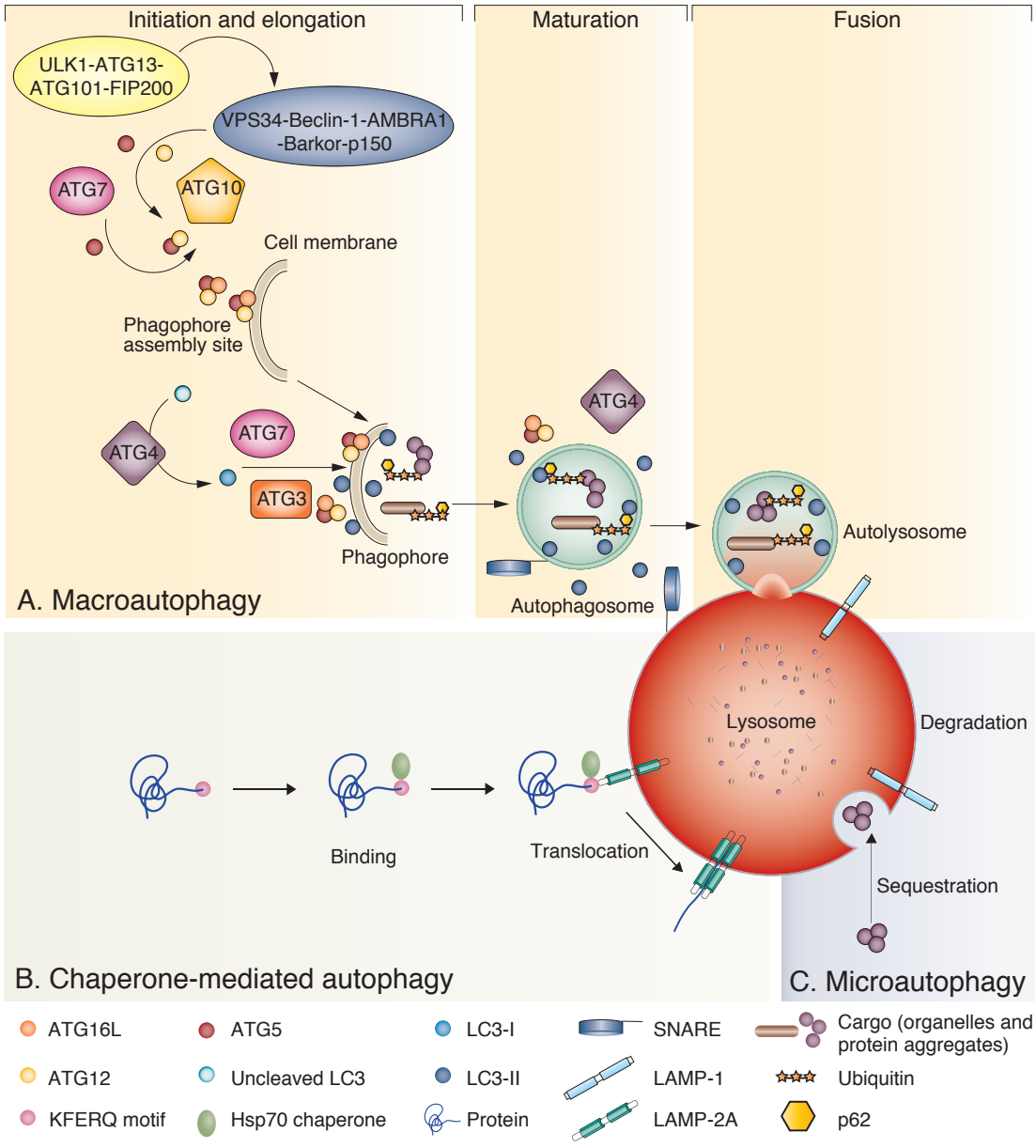


Figure 1.3. Autophagic pathways within the cell.
(A) Macroautophagy. Briefly, the ULK1 complex activates the VPS34 complex, which initiates phagophore formation through the actions of ATG7, ATG10, ATG3 and ATG4. The phagophore engulfs P62 and ubiquitin labelled cargo, which matures and then fuses with the lysosome. (B) Chaperone-mediated autophagy. Hsp70 chaperone proteins can attach to proteins featuring a KFERQ motif. Hsp70 then attaches to LAMP-2A. LAMP-2A forms a multimer which mediates translocation of the protein into the lysosome. (C) Microautophagy. The lysosomal membrane invaginates to sequester cargo from the cytoplasm, which is then degraded. Adapted from Harris and Rubinsztein (2012) and Boya *et al.* (2013).

1.3.1 Macroautophagy

A major advance in the study of autophagy was the discovery of the autophagy-related (*Atg)* gene family in budding yeast. The *Atg* genes were found to be essential for autophagy in yeast, a finding replicated in mice and likely to be true in *Homo sapiens*, given the presence of human homologues (the mammalian versions are capitalised – *ATG* – and summarised in Table 1.3). These genes, and the proteins they encode, provide a useful framework for discussing the process of macroautophagy, and some of these proteins also have roles in CMA and microautophagy. Macroautophagy can be divided into four stages: initiation of phagophore formation, elongation of the phagophore, maturation of the phagophore into the autophagosome, and fusion of the autophagosome with the lysosome to form the autolysosome (Figure 1.3A).

Initiation of macroautophagy is triggered by activation of a complex comprising of unc-51-like kinase 1 (ULK1, a mammalian homologue of Atg1), ATG13, ATG101 and FIP200 (FAK family kinase-interacting protein of 200 kDa) (Luk *et al.* 2012a). This complex begins phagophore formation at what some authors have termed the "phagophore assembly site" (Desplats *et al.* 2009; Hansen *et al.* 2011). ULK2 is a paralog of ULK1, and can act as a functional substitute in this complex (Jung *et al.* 2009; Hosokawa *et al.* 2009). ULK1/2 kinase activity recruits VPS34 to the phagophore (Feng *et al.* 2016). VPS34 (a class III PI3 kinase) and the protein Beclin 1 then form a complex. VPS34 may also complex with other proteins, such as AMBRA1 (activating molecule in Beclin-1-regulated autophagy protein 1). Barkor (Beclin 1-associated autophagy-regulated key regulator, a mammalian homologue of Atg14) and p150 are also thought to be important in the function of the VPS34 complex (McAlpine *et al.* 2013). The activated VPS34 complex switches on ATG

proteins and produces phosphatidylinositol 3-phosphate (PI3P), which is a lipid component of the autophagosome.

Following the initiation of phagophore formation, the phagophore elongates. Two ubiquitin-like conjugation systems are part of the phagophore elongation process. The first system involves the covalent conjugation of ATG5 to ATG12, a process for which both ATG7 and ATG10 are essential (Itakura and Mizushima 2010). The ATG5-ATG12 complex then interacts with ATG16-like 1 (ATG16L1) (Panaretou *et al.* 1997; Sun *et al.* 2008); this complex may assist in the second conjugation reaction. The second conjugation system involves microtubule-associated protein 1A/1B-light chain 3 (LC3). LC3-I is converted to LC3-II by the addition of phosphatidylethanolamine (PE); this is achieved through sequential processing by the protease ATG4, followed by ATG7 and finally ATG3 (Mizushima *et al.* 1998). Other proteins have important roles in phagophore elongation, including ATG9, which is thought to shuttle membrane between the elongating phagophore and the membrane donor. The origins of phagophore membranes are not well understood, and could include the endoplasmic reticulum, mitochondria, Golgi complex, or other intracellular vesicles (Hamasaki *et al.* 2013a; 2013b; Biazik *et al.* 2015).

LC3-II has a function in phagophore elongation, but also in cargo recognition, where it binds to P62, a protein that helps to mark organelles and cytosolic proteins for degradation by interacting with ubiquitin (Mizushima *et al.* 1999). Ubiquitin is a molecule that targets waste proteins to the proteosome for degradation. However, once proteins have aggregated, they are not degraded efficiently by the proteosome and therefore may become targets for

macroautophagy via P62 binding. Phagophores become tethered to macroautophagic cargo through the interaction of P62 and LC3-II. Closure of phagophores is achieved by ATG2A and ATG2B; knockdown of these proteins causes the accumulation of unclosed phagophores (Kirisako *et al.* 2000; Ichimura *et al.* 2000).

Autophagosome maturation is characterized by the removal of ATG proteins and PI3P from the membrane surface, and is likely to be a prerequisite for fusion to the lysosome (Pankiv *et al.* 2007). Proteins that are associated with the phagophore, such as ULK1 and ATG16L1, are absent from mature autophagosomes. In yeast, Atg8, equivalent to human LC3, is also absent from the outer surface of mature autophagosomes, but it is unclear if this remains true in mammalian cells (Velikkakath *et al.* 2012). Clearance of ATG proteins and PI3P from the surface of the autophagosome is likely accomplished by ATG4 and PI3P phosphatases (Reggiori and Ungermann 2017).

The final event in the process of macroautophagy is the fusion of the autophagosome with the lysosome to form the autolysosome. In the autolysosome, the cargo and inner membrane of the autophagosome are degraded by lysosomal enzymes. Fusion of the autophagosome with the lysosome is governed by SNARE proteins such as Sso1/2 and Sec9 (Moreau *et al.* 2011). Autophagosome formation can occur randomly in the cytoplasm, however to increase the likelihood of fusion, autophagosomes are transported along microtubules to the microtubule-organising centre, where lysosomes are abundant.

Specialised types of macroautophagy have also been described, usually targeting specific cellular organelles for degradation (Klionsky *et al.* 2007). Perhaps the most commonly cited, and most relevant to PD, is mitophagy – the selective degradation of mitochondria. Both PINK1 and Parkin have roles in mitophagy where they participate in a molecular pathway where PINK1 phosphorylates both Parkin and ubiquitin in response to mitochondrial depolarisation (Koyano *et al.* 2014). Other selective autophagy pathways include reticulophagy (the endoplasmic reticulum) and ribophagy (ribosomes). It should also be noted that an ATG5/ATG7-independent pathway of macroautophagy has been reported, however it has only been observed under specific starvation conditions, and its relevance in normal conditions is uncertain (Nishida *et al.* 2009).

Regulation of macroautophagy is complex and not fully understood, however some fundamental signaling pathways are well resolved. The mammalian target of rapamycin (mTOR) is a serine-threonine kinase that acts as a master negative regulator of macroautophagy. mTOR blocks the activity of the ULK1 kinase complex by phosphorylating and therefore inactivating ULK1 and ATG13, thus preventing phagophore biogenesis. mTOR also negatively regulates transcription factor EB (TFEB), which controls lysosome biogenesis (Betin *et al.* 2013; Wu *et al.* 2014). By this mechanism mTOR regulates lysosome number, and therefore manipulates the likelihood of fusion events between autophagosomes and lysosomes. mTOR-independent regulatory pathways also exist; Bcl-2 is able to regulate Beclin-1, 5'-activated-AMP-activated protein kinase (AMPK) is able to regulate ULK1 and intracytosolic calcium levels are able to regulate autophagy through proteins known as calpains (Yousefi *et al.* 2006; Wei *et al.* 2008; Cárdenas *et al.* 2010).

Table 1.3. ATG proteins and their functions

Yeast	Mammals	Function
Atg1	ULK1, 2	Kinase part of the ULK-ATG13-ATG101-FIP200 complex.
Atg2	ATG2A, B	Essential for closure of phagophores and important for ATG9 recruitment to expanding autophagosomes.
Atg3	ATG3	E2-like enzyme in LC3 lipidation.
Atg4	ATG4A, B, C, D	Cysteine protease involved in LC3 activation and delipidation.
Atg5	ATG5	Part of the ATG12-ATG5 complex, acting as an E3-like enzyme in LC3 lipidation.
Atg6	Beclin 1	Part of the VPS34 PI3K complex.
Atg7	ATG7	E1-like enzyme in LC3 and ATG12 conjugation.
Atg8	LC3A, B, C; GABARAPs, GATE16	Ubiquitin-like proteins that conjugate to PE and are used as autophagosome markers.
Atg9	mATG9	Transmembrane protein postulated to be a carrier for membranes during phagophore expansion.
Atg10	ATG10	E2-like enzyme in ATG12 conjugation.
Atg12	ATG12	Ubiquitin-like protein that conjugates to ATG5.
Atg13	ATG13	Part of the ULK-ATG13-ATG101-FIP200 complex and target of the mTOR signaling pathway.
Atg14	ATG14L	Part of the VPS34-PI3K complex.
Atg16	ATG16L1, 2	Binds to ATG5-ATG12 and is postulated to specify LC3 lipidation sites in autophagic membranes.
Atg17	FIP200	Part of the ULK-ATG13-ATG101-FIP200 complex.
Atg18	WIPI-1, 2, 3, 4	Part of the ATG2-WIPI complex important for ATG9 recruitment to autophagosome.
Atg29	No data	Forms a complex with Atg17 and Atg31 in yeast.
Atg31	No data	Forms a complex with Atg17 and Atg29 in yeast.
No data	ATG101	Part of the ULK-ATG13-ATG101-FIP200 complex.

Atg/ATG, autophagy-related gene; FIP200, FAK family kinase-interacting protein of 200 kDa; LC3, microtubule-associated protein 1A/1B-light chain 3; PE, phosphatidylethanolamine. Adapted from Bento *et al.* (2016).

1.3.2 Chaperone-mediated autophagy

CMA is a type of selective protein degradation that has only been observed in mammalian cells. All proteins that can be degraded by CMA feature a pentapeptide amino acid sequence, KFERQ or a similar sequence, that is necessary and sufficient for targeting the protein substrate to lysosomes (Dice 1990; Nair *et al.* 2011). Indeed, if a KFERQ motif is inserted into a protein that previously lacked such a sequence, it is then able to be degraded via CMA (Settembre *et al.* 2011; Llopis *et al.* 2011; Settembre *et al.* 2012). Proteins degraded by CMA are identified individually by a cystosolic chaperone, heat-shock protein 70 (Hsp70), that directs the protein to the lysosome by binding to the KFERQ or KFERQ-like sequence (Dice *et al.* 1986; Terlecky and Dice 1993). Once at the lysosome, Hsp70 facilitates binding of the substrate protein to a lysosomal transmembrane protein, lysosome-associated membrane protein 2A (LAMP-2A) (Koga *et al.* 2011). LAMP-2A then multimerises in the lysosomal membrane, a step which is essential for the translocation of the substrate into the lysosome (Chiang *et al.* 1989). Once the protein enters the lysosomal lumen, it is degraded to its constituent parts by lysosomal enzymes.

CMA is of potential importance in PD, as wild-type α-synuclein can be degraded via CMA due to the presence of a KFERQ-like sequqence, VKKDQ (Cuervo *et al.* 2004). The binding of DA to α-synuclein inhibits this process, suggesting a mechanism for selective degeneration of SNc neurons (Cuervo *et al.* 2004). Furthermore, pathogenic mutations in α-synuclein that cause PD, such as A30P and A53T, result in α-synuclein that binds to LAMP-2A but is unable to be translocated, effectively blocking the degradation of α-synuclein and other proteins via CMA (Bandyopadhyay *et al.* 2008). While a more extensive discussion of the potential involvement of CMA in PD pathogenesis is beyond

the scope of this thesis, it is important to note that this area is a fruitful and ongoing area of research.

1.3.3 Microautophagy

Microautophagy is the least studied of the autophagy subtypes; much of the current understanding of microautophagy comes from studies in yeast, although it has been observed in mammalian cells (Ahlberg *et al.* 1982; Ahlberg and Glaumann 1985; Sakai *et al.* 1989; Roberts *et al.* 2003; Priault *et al.* 2005; Martinez-Vicente *et al.* 2008). In broad terms, microautophagy consists of engulfment of small portions of the cytoplasm by the lysosome, and can be selective, for example targeting mitochondria ("micromitophagy") or the nucleus ("micronucleophagy") (Cuervo *et al.* 2004). Regulation of microautophagy in mammalian cells, and the involvement of microautophagy in disease are fields ripe for investigation and elucidation.

1.3.4 The potential role of macroautophagy in Parkinson's disease

1.3.4.1 Pathological evidence for a role of macroautophagy in Parkinson's disease

Several pathological observations implicate defective macroautophagy in the pathogenesis of PD. Accumulation of autophagic vacuoles in SNc neurons of PD patients was first described by Anglade and colleagues (1997). Later data showed a reduction in the level of Lamp1, a lysosomal marker, and increased levels of LC3-II in PD SNc (Dehay *et al.* 2010; Ferrer *et al.* 2011). Similarly, Chu and colleagues (2009) found that Lamp1 was reduced in PD brain, and that remaining Lamp1 colocalised with α-synuclein in Lewy bodies. In pathological studies, both P62 and ubiquitin are associated with Lewy bodies (Zatloukal *et al.* 2002). More recently, Miki *et al.* investigated the expression levels of proteins involved in autophagosome initiation in the SNc from PD patients, finding increased levels of ULK1, ULK2, Beclin-1, VPS34 and AMBRA1 (Miki *et al.* 2016). In addition to histopathological and proteomic evidence, trancriptomic studies from PD brain suggest that the autophagic system is dysregulated. Specifically, two independent pathway transcriptomic analyses have included the mTOR pathway amongst those dysregulated in the SNc of human PD cases (Miki *et al.* 2016).

1.3.4.2 Genetic evidence for a role of macroautophagy in Parkinson's disease

There is some genetic evidence that implicates macroautophagy in PD pathogenesis. *SNCA*, encoding α-synuclein, was the first familial PD gene to be identified, and is the gene most significantly associated with sporadic disease. α-Synuclein impairs macroautophagy, an effect that may be mediated by the need for SNARE complexes in order for macroautophagy to occur (Nair *et al.* 2011).

Other genes causing PD also have roles in macroautophagy. Several researchers have reported that LRRK2 is a regulator of macroautophagic activity (Alegre-Abarrategui *et al.* 2009; Ramonet *et al.* 2011; Pedro *et al.* 2013; Schapansky *et al.* 2014). Recent evidence from an unbiased protein-protein interaction study has demonstrated that LRRK2 interacts with proteins encoded by two other candidate genes for sporadic PD susceptibility: rab-7-like protein 1 (RAB7L1/RAB29) and cyclin-G-associated kinase (GAK) (Beilina *et al.* 2014). This confirms previous work that identified Rab7L1 as a LRRK2 binding partner (MacLeod *et al.* 2013). The LRRK2–Rab7L1–GAK complex promotes clearance of Golgi-derived vesicles through the autophagy–lysosome pathway (Beilina and Cookson 2016). Notably, the RAB7L1 locus modifies LRRK2-associated risk in four GWAS cohorts, underscoring the potential therapeutic importance of LRRK2–Rab7L1 interactions (MacLeod *et al.* 2013). Manzoni and co-workers have determined that the regulatory action of LRRK2 on macroautophagy may be mediated by its kinase domain (Manzoni *et al.* 2013). As discussed previously, the products of *Parkin* and *PINK1* both have important roles in mitophagy (Koyano *et al.* 2014).

Additionally, a number of genes associated with inherited PD impact the function of the lysosome. Glucocerebrocidase, encoded by *GBA,* is a lysosomal enzyme. Mazzulli *et al.* have shown in human Gaucher's disease stem cells and a-synuclein mouse-model neurons that glucocerebrosidase mediates lysosomal breakdown of α-synuclein (Mazzulli *et al.* 2011). Subsequent α-synuclein aggregation, in turn, caused reduced glucocerebrosidase activity, forming a possible positive-feedback loop in PD pathogenesis. These findings also have relevance for PD that is unrelated to *GBA* mutations; reduction of glucocerebrocidase activity in PD brains is associated with increased α-synuclein expression (Murphy *et al.*

2014). Similarly, pathogenic mutations in *ATP13A2*, which encodes a lyosomal ATPase, cause lysosomal dysfunction and toxic accumulation of α-synuclein (Usenovic *et al.* 2012). Genes associated only with sporadic PD in GWAS have roles in the lysosome. LAMP3, a lysosomal protein, has been shown to regulate autophagy in breast cancer cells, but this has not been examined in neurons (Nagelkerke *et al.* 2014).

Examination of genetic evidence for a role of *ATG* genes in determining PD susceptibility has not been thoroughly conducted at a population level. In part, this is due to limitations on GWAS data that reduce its public availability (Nalls *et al.* 2014). However, in a small study, Chen and his colleagues determined that variation in the *ATG7* promoter region, decreasing *ATG7* expression, implied risk for sporadic PD in a Chinese population (Chen *et al.* 2013). Likewise, polymorphisms in *ATG7* modify the age of onset in Huntington's disease, a neurodegenerative disease affecting the striatum (Metzger *et al.* 2013).

1.3.4.3 Interactions between α-synuclein and macroautophagy: evidence of a role for macroautophagy manipulation in treating Parkinson's disease

Several *in vitro* analyses have demonstrated that α-synuclein is degraded both by the UPS and macroautophagy, and that α-synuclein aggregates are predominantly tackled by macroautophagy (Webb *et al.* 2003; Vogiatzi *et al.* 2008). Similarly, it has been shown that when autophagy is inhibited in cells, concentrations of α-synuclein are increased, and α-synuclein is released into culture media (Lee *et al.* 2013). Additionally, α-synuclein itself has been shown to inhibit macroautophagy, a phenomenon that may be mediated by

SNARE proteins that participate in the macroautophagic process (Winslow *et al.* 2010; Nair *et al.* 2011; Tanik *et al.* 2013).

Based on the pathological analyses, genetic evidence, and experiments described above, experiments have been conducted in yeast, cell lines, *Caenorhabditis*, *Drosophila*, mice, rats and humans in order to investigate the utility of macroautophagy manipulation to clear α-synuclein and therefore treat PD. The first of these studies used rapamycin to inhibit the action of mTOR and therefore stimulate macroautophagy in cells, mice and rats (Webb *et al.* 2003; Crews *et al.* 2010; Decressac *et al.* 2013; Bai *et al.* 2015). In all of these studies, α-synuclein aggregates were reduced, and neurodegeneration was rescued. In addition, Bai and colleagues showed that motor deficits associated with α-synuclein overexpression could be rescued (Bai *et al.* 2015). Trehalose is a compound that promotes autophagy through an mTOR-independent pathway, and has been shown to increase degradation of α-synuclein in cells and transgenic rodent models of PD (Sarkar *et al.* 2007; He *et al.* 2016). A number of viral constructs that stimulate autophagy have also been shown to clear α-synuclein. For example, expression of Beclin 1 via lentiviral vector has been shown to ameliorate aggregation and toxicity of α-synuclein (Spencer *et al.* 2009). Finally, Hebron *et al.* (2013) have shown that nilotinib, a putative autophagy stimulator that is used to treat chronic myelogenous leukaemia, can reduce α-synuclein levels and ameliorate behavioural phenotypes in rodent α-synuclein PD models. Similarly, a study in mice has demonstrated that nilotinib protects against MPTP toxicity (Karuppagounder *et al.* 2014). On the strength of these results, nilotinib has progressed into the clinic and completed Phase I studies; randomised, double-blind trials are in progress (Pagan *et al.* 2016).

It should be noted that some of the PD models that have been used to test the utility of autophagic compounds have innate limitations, and these will be discussed in the following section. In addition, the interaction of impaired macroautophagy and α-synuclein on pathology and behaviour *in vivo* has not been determined. In this thesis, the question of the effect of the interaction between impaired macroautophagy and α-synuclein on neuropathology will be examined in Chapter 3, and the effect on behaviour in Chapter 4. Aspects of DA neurotransmission that likely underlie behaviour will be described in Chapters 5 and 6. All of these questions will be examined using mouse models, which will be discussed in the subsequent sections.

1.4 α-Synuclein rodent models of Parkinson's disease

In order to gain insights into the pathogenesis of PD, and to aid the development of disease-modifying agents, numerous models of PD in non-human species have been developed. Dawson *et al.* highlighted some key aspects of PD that a sound model should possess: age-dependent progressive loss of DA neurons; motor symptoms such as slowness of movement, rigidity, tremor, and postural instability; L-DOPA responsiveness; and the presence of Lewy bodies and neurites that contain α-synuclein and ubiquitin. To date, no model of PD has fulfilled all of these criteria (Dawson *et al.* 2010).

PD models have been developed in non-human primates, rats, mice, *Drosophila*, *Caenorhabditis* and fish (Feany and Bender 2000; Kordower *et al.* 2000; Braungart *et al.* 2004; Matsui *et al.* 2012; Janezic *et al.* 2013; Sloan *et al.* 2016). In order to cause a PD-like phenotype in these animals, different toxins, direct injection of viruses or proteins, and

the introduction of genetic modifications have been utilised. Among the common toxins used are MPTP, 6-hydroxydopamine (6-OHDA), paraquat and rotenone (Arai *et al.* 1990; Przedbroski *et al.* 1995; Betarbet *et al.* 2000; Jackson-Lewis and Przedborski 2007). Viruses expressing LRRK2 and α-synuclein have been inoculated into midbrain structures (Kirik *et al.* 2002; Dusonchet *et al.* 2011). Likewise, α-synuclein aggregates have been directly injected into the striata of rodents and non-human primates (Luk *et al.* 2012a). A number of transgenic models of PD have been developed, which aim to endogenously recapitulate features of PD by overexpressing, substituting, suppressing or abolishing expression of a particular PD related gene. These are typically rodents that feature expression of α-synuclein or LRRK2, or knockout of genes that cause autosomal recessive PD, such as *PINK1*, *PARK2* (Parkin), *DJ-1* and *ATP13A2* (Goldberg *et al.* 2003; 2005; Gautier *et al.* 2008; Janezic *et al.* 2013; Schultheis *et al.* 2013; Sloan *et al.* 2016). All of the models mentioned above have strengths and weaknesses. The following discussion will focus on rodent models that utilise α-synuclein to model PD.

Investigators have utilized direct stereotactic injections of viruses that then induce overexpression or knockdown of disease-related proteins in infected cells. A typical example would involve inoculating the striatum, VTA or SNc with adeno-associated virus (AAV) expressing wild-type or mutant human α-synuclein (Oliveras-Salvá *et al.* 2013). These techniques were first developed in rats and then introduced to mice (Kirik *et al.* 2002; Bianco *et al.* 2002; Klein *et al.* 2002; Yamada *et al.* 2004; Oliveras-Salvá *et al.* 2013). Such injections cause a rapidly progressive neurodegenerative phenotype, such that in some studies fewer than 20% of DA neurons are present at eight weeks (Klein *et al.* 2002; Kirik *et al.* 2002; Yamada *et al.* 2004; Oliveras-Salvá *et al.* 2013). Some investigators report associated reductions in motor function (Kirik *et al.* 2002).

Interestingly, Hall *et al.* reported that when they targeted the VTA and the diagonal band of Broca with AAV expressing wild-type human α-synuclein, rats showed spatial learning deficits (Hall *et al.* 2013). Criticisms similar to those made of toxin-based PD models can be made of viral models; they are rapidly progressive and directed solely towards the dopaminergic system. In addition, researchers rarely control for the effect of protein overexpression by introducing viruses expressing scrambled α-synuclein or another protein.

More recently, models have been developed that use pre-formed fibrils of α-synuclein injected directly into the striata of mice. This strategy results in the spread of α-synuclein inclusions throughout the brain, analogous to the proposed prion-like spread of human disease. Initial studies utilising these protocols were conducted in mice expressing human A53T α-synuclein, and these mice developed a rapidly progressive and ultimately lethal neurodegenerative phenotype (Mougenot *et al.* 2012; Luk *et al.* 2012b). Subsequent experiments found a similar phenomenon in wild-type mice, but with a less severe behavioural phenotype and lower mortality (Luk *et al.* 2012a). Mice inoculated with α-synuclein are useful to map the spread of α-synuclein aggregates through the brain, and to and from the periphery. By the same token, therapeutic agents that target the prion-like spread of α-synuclein can be trialled in these models, and these trials can be conducted relatively quickly due to a rapidly-developing phenotype. The obvious criticism of this model is that it requires exogenous inoculation with α-synuclein, a phenomenon that is not likely to occur in PD.

The first transgenic PD mouse models to be developed utilised complementary DNA (cDNA) cloning to express α-synuclein driven by a heterologous promoter. These mice express human wild-type, A53T or A30P α-synuclein from the mouse PDGF-β, Thy-1, rat TH, and mouse and hamster prion promoters (Masliah *et al.* 2000; Kahle *et al.* 2000; van der Putten *et al.* 2000; Matsuoka *et al.* 2001; Lee *et al.* 2002; Gómez-Isla *et al.* 2003). Such mice have provided a further useful tool to study the effects of α-synuclein *in vivo*, and to trial treatments targeting α-synuclein. Typically, the phenotype of these mice depends on the promoter used to drive expression of the *SNCA* transgene; expression of α-synuclein varies from half of the endogenous mouse α-synuclein level to over ten times the endogenous level. Additionally, depending on the promoter used, α-synuclein can be expressed in high levels in tissues where this is not normally seen, and that are unaffected in PD. Of note are high-levels of α-synuclein expression and motor neuron toxicity in the spinal cord, particularly when using the Thy-1 promoter, which can give rise to motor impairment and reduced survival without degeneration of the dopaminergic system. In general, cDNA models develop age-related motor impairment and some features of neurodegeneration, but do not develop Lewy bodies or neurites. Only in a few models is DA neuron loss observed (Javier Blesa 2014; Hatami and Chesselet 2015). One aspect relevant for this thesis that can be gleaned from analysis of cDNA transgenic mice is that the presence of mouse endogenous α-synuclein may be important in determining neurotoxicity. Cabin *et al.* developed mice that expressed human A53T α-synuclein in mice with and without endogenous mouse α-synuclein; only the mice that lacked endogenous mouse α-synuclein lost DA neurons (Cabin *et al.* 2005).

The development of the Bacterial Artificial Chromosome (BAC), a high-capacity genetic vector, allowed the generation of transgenic mice that expressed α-synuclein from the

endogenous human locus under the control of its native promoter (Johnson and Wade-Martins 2011; Janezic *et al.* 2013). A key advantage of BAC mice is that, because the gene of interest is expressed from its endogenous promoter, the physiological spatiotemporal expression profile of the gene is preserved. A small number of BAC *SNCA* mice have been described, and these are summarised in Table 1.4 (Taylor *et al.* 2010; Yamakado *et al.* 2012; Hansen *et al.* 2013; Janezic *et al.* 2013). The Wade-Martins laboratory has previously characterised a BAC-based α-synuclein overexpressing mouse, termed the *SNCA*-OVX mouse. This mouse expresses the full-length human *SNCA* gene on a mouse wild-type α-synuclein null background (Janezic *et al.* 2013). The expression of human α-synuclein in the *SNCA*-OVX mouse is approximately twice that of endogenous mouse α-synuclein, and this is associated with a loss of approximately 30% of SNc DA neurons in mice at 18 months of age. Age-related reductions in stride length and rotarod performance were observed, in addition to an age-independent constipation-like phenotype.

DA neurotransmission was also examined in the *SNCA*-OVX mouse, using fast-scan cyclic voltammetry (FCV). FCV is an electrochemical technique used to detect DA in real-time in living tissues; it is used in Chapters 5 and 6 of this thesis, and the method is described in detail in Chapter 2. Briefly, FCV involves providing a stimulus, which can be behavioural in the case of *in vivo* FCV, or chemical or electrical, in the case of *ex vivo* FCV, and then measuring evoked extracellular dopamine. Typically the level of extracellular dopamine is referred to by the annotation $[DA]_o$, and this term will be used in the remainder of this thesis. In the SNCA-OVX mouse, there was a reduction in peak evoked $[DA]_o$ beginning at 3 to 4 months of age. The reduction in peak $[DA]_o$ preceded neuron loss, consistent either with a role of α-synuclein as a negative regulator of vesicle exocytosis, or with early neurotoxicity.

Table 1.4. α-Synuclein BAC transgenic mouse models of Parkinson's disease

Reference	α-Synuclein variant	α-Synuclein level (%WT)	Oldest age (months)	Neuropathology	Behaviour	Dopamine neurotransmission
Yamakado *et al.* 2012	WT	270	24	Increased striatal DAT; Increased cortical SERT	Hyperlocomotor; Decreased anxiety-like behaviour	Not examined
Hansen *et al.* 2013	WT fused to GFP	-5	15	Phosphorylated α-synuclein; No DA cell loss	Reduce locomotor activity with amphetamine; Reduced rotarod fall latency; Reduced olfaction	Reduced DA release; Reduced DA reuptake at 3 months
Janezic *et al.* 2013	WT	190	18	30% DA neuron loss	Reduced stride length; Reduced rotarod fall latency.	Reduced DA release; Normal DA reuptake
Taylor *et al.* 2010	WT or A30P	10	23	No DA neuron loss	Decreased anxiety-like behavior at 6 months	Reduced DA release; Normal DA reuptake

A30P, Ala30Pro; BAC, Bacterial artificial chromosome; DA, dopamine; DAT, dopamine transporter; SERT, serotonin transporter; WT, wild-type. Adapted from Hatami and Chesselet (2015).

1.5 Rodent models of macroautophagy impairment

Mice lacking the autophagy-essential gene *Beclin1* (*ATG6*) are unable to develop beyond the eighth embryonic day (Yue *et al.* 2003). Mice that lack other autophagy-essential genes, such as *ATG5* or *ATG7*, appear essentially normal at birth, but die within the first day of life (Kuma *et al.* 2004; Komatsu *et al.* 2005). The cause of death in autophagy-deficient mice may be related to an inability to liberate energy from hepatic and adipocytic stores (Yue *et al.* 2003). General examination of organs from *ATG5* and *ATG7* deficient mice did not demonstrate any architectural abnormalities. Mice that are heterozygous for *ATG5* or *ATG7* have normal survival to at least 16 months of age (Kuma *et al.* 2004; Komatsu *et al.* 2005).

Genetic models have been developed that utilize conditional deletion of autophagy-essential genes in neurons to impair macroautophagy using the cre-lox system (Betz *et al.*

1996). In these mice, *ATG5* or *ATG7* is flanked by two loxP sites ("floxed"), and is excised by cre recombinase, which is expressed under the transcriptional control of a neuronal gene. For example, in mice that are homozygous for the floxed *ATG7* allele, no *ATG7* is expressed in cells expressing the cre recombinase, and therefore macroautophagy is significantly impaired. The ability to use conditional deletion systems has helped evade the early mortality associated with impairment of macroautophagy in the whole organism.

The effect of impairing macroautophagy in all neurons was demonstrated by two mouse models featuring conditional knockout (cKO) of *ATG5* or *ATG7* (Komatsu *et al.* 2006; Hara *et al.* 2006). Both mouse models used the *Nestin* promoter to express cre recombinase (*Nestin*-cre), thus conferring neuronal selectivity; the cre recombinase excised floxed alleles of *ATG5* or *ATG7* (*ATG5*cKO$^{Nestin\text{-cre}}$ and *ATG7*cKO$^{Nestin\text{-cre}}$). In both mice widespread neurodegeneration was observed, accompanied by gross locomotor impairment, including a limb-clasping phenotype and abnormal gait. Survival was significantly attenuated, such that no *ATG7*cKO$^{Nestin\text{-cre}}$ mice survived beyond 28 weeks (Komatsu *et al.* 2006; Hara *et al.* 2006). Loss of neurons was demonstrated in the cerebellum, and there was an increased number of dying neurons in the cerebral cortex. Ubiquitin-positive inclusions were found in surviving neurons (Komatsu *et al.* 2006).

Subsequently, investigators began to restrict cre recombinase expression, and therefore macroautophagy impairment, to DA neurons (Table 1.5). This was accomplished by using transgenic cre-driver mouse lines under the control of the *DAT* or *TH* genetic loci. In this thesis, all mice described have the genetic sequences for the cre recombinase 'knocked-in' to *DAT* or *TH*.

A number of different *DAT* and *TH* cre-driver lines are available, and each has advantages and shortcomings. A key consideration appears to be whether the *DAT* or *TH* locus is used to drive cre expression. An analysis by Lammel and colleagues (2015) found that lines employing the *TH* promoter exhibit substantial transgene expression in non-DA neurons, with unintentionally targeted cells reaching 50 to 60% of the total. In contrast, a line using *DAT* as the cre driver had only 4% off-target expression.

A second consideration is expression of the driver gene in non-neuronal tissues. While *DAT* expression is relatively confined to midbrain structures; *TH* driver lines show expression in the adrenal medulla and the sympathetic ganglia of the spinal cord (Gelman *et al.* 2003). Impaired cell function in these sites has the potential to impact on behavioural studies. In particular, the adrenal medulla is responsible for synthesising circulating adrenaline and noradrenaline, and thus any disruption is likely to have significant effects on behaviour. A final aspect impacting the utility of cre-driver lines is how the endogenous gene drives expression of the cre recombinase. Cre can either be expressed close to a gene start codon, thus entirely disrupting transcription of one copy of the gene. Alternatively, the cre can be inserted into an internal ribosome entry sequence (IRES), theoretically allowing transcription of both copies of the gene. In the remainder of this thesis, driver lines are of the first type unless the IRES notation is used, for example *TH*-cre is used to describe a conventional cre knockin mouse, whereas a *TH*-IRES-cre has cre knocked into an IRES in the *TH* locus. Note that only conditional deletion of *ATG7* has been used in conjunction with *TH* and *DAT* cre-driver lines; *ATG5* has not been utilised. The Mouse Genome Database nomenclature for the *DAT*-IRES-cre driver line used in this thesis is Slc6a3$^{tm1.1(cre)Bkmn}$ and for the *TH*-IRES-cre line it is Th$^{tm1(cre)Te}$.

Hernandez *et al.* (2012) were the first to generate mice with impaired DA neuron autophagy. They examined dopaminergic neurotransmission in an *ATG7*cKO$^{DAT\text{-cre}}$ model using FCV. *Ex vivo* FCV conducted on eight to ten week old mice found increased peak $[DA]_o$ in the dorsal striatum. Paired-pulse depression (PPD) describes an effect where, when two stimuli are given at short intervals, the second stimulus will result in lower $[DA]_o$ than the first stimulus. Examining PPD in *ATG7*cKO$^{DAT\text{-cre}}$ mice, Hernandez and colleagues found a reduction in PPD compared to control animals. Additionally, DA half-life was examined: there was no difference between genotypes, which was cited as evidence of normal DAT function. Behavioural tests conducted on a small cohort (4 per genotype) found no differences between mice with preserved macroautophagy and those with impaired macroautophagy in DA neurons. As yet, there are no data confirming these effects of macroautophagy impairment on DA neurotransmission in the same model, or in a model that does not manipulate *DAT,* such as a *TH*-cre or *TH*-IRES-cre model. Experiments to confirm these findings are presented as part of Chapter 5, while DA neurotransmission in a *TH*-IRES-cre model is considered in Chapter 6.

Friedman and her coworkers (2012) further characterised the effect of macroautophagy impairment in DA neurons using an *ATG7*cKO$^{TH\text{-IRES-cre}}$ line. They found approximately 40% loss of SNc neurons at nine months of age, and the development of ubiquitin and P62 inclusions in DA neurons. Similar analyses were provided in later studies by Ahmed *et al.* (2012) and Inoue and coworkers (2012), both utilising a *DAT*-cre system. Paradoxically, Ahmed and colleagues found that the *ATG7*cKO$^{DAT\text{-cre}}$ model had a hyperlocomotor

phenotype at a young age, but this finding was not further explored. Studies were then conducted in *ATG7*cKO$^{TH\text{-cre}}$ mice to determine the effect of MPTP intoxication when DA neuron macroautophagy was impaired. Niu and colleagues found that *ATG7*cKO$^{TH\text{-cre}}$ mice had fewer DA neurons, and the remaining neurons were less susceptible to MPTP intoxication (Niu *et al.* 2016).

Table 1.5. Mouse models of conditional *ATG7* deletion in dopamine neurons

Reference	Cre system	Oldest age (months)	Neuropathology	Behaviour	Dopamine neurotransmission
Hernandez *et al.* 2012	*DAT*-cre (Zhuang *et al.* 2005)	3	Increased TH axon profile area in the striatum	No differences (n=4)	Increased striatal DA release Improved recovery of DA release Normal DA reuptake
Inoue *et al.* 2012	*DAT*-cre (Zhuang *et al.* 2005)	12	50% DA neuron loss at 12 months of age; Ubiquitin, P62, tau inclusions	Not examined	Not examined
Friedman *et al.* 2012	*TH*-IRES-cre (Lindeberg *et al.* 2004)	20	40% DA neuron loss at 9 months of age; Ubiquitin, P62 inclusions; Reduced striatal DA	Reduced locomotor activity at 9 months; Increased step error on beam traverse	Not examined
Ahmed *et al.* 2012	*DAT*-cre (Zhuang *et al.* 2005)	12	40% DA neuron loss at 9 months of age; Ubiquitin, P62 inclusions; Reduced striatal DA	Hyperlocomotor at 7 months of age	Not examined
Niu *et al.* 2016	*TH*-cre (Gelman *et al.* 2003)	12	40% DA neuron loss at 12 months of age; Ubiquitin, P62 inclusions; Reduced striatal TH; Reduced susceptibility to MPTP	Reduced effect of MPTP on gait overlap asymmetry at 5 months, but not 12 months	Not examined

DA, dopamine; DAT, dopamine transporter; MPTP, 1-methyl-4-phenyl-1,2,3,6-tetrahydropyridine; TH, tyrosine hydroxylase.

1.6 Aims of thesis

The potential for interaction between α-synuclein and impaired macroautophagy in DA neurons on pathology, behaviour and DA neurotransmission *in vivo* has not been determined. This thesis will examine the hypothesis that α-synuclein and impaired macroautophagy will interact to produce parkinsonian phenotypes.

The aims of this thesis will be addressed in four chapters:

Chapter 3: Generation and initial pathological characterisation of aged mice featuring:

a. Overexpression of a human α-synuclein transgene from the complete human wild-type *SNCA* genomic locus (h*SNCA*);
b. Impairment of macroautophagy in DA neurons (*ATG7*cKO$^{DAT\text{-IRES-cre}}$);
c. Both impairment of macroautophagy in DA neurons and overexpression of a BAC human α-synuclein transgene from the complete human wild-type *SNCA* genomic locus (h*SNCA*:*ATG7*cKO$^{DAT\text{-IRES-cre}}$); or
d. Neither genetic lesion (control).

Chapter 4: Use of a longitudinal behavioural testing battery to characterise the motor and non-motor phenotypes of transgenic mice generated in Chapter 3.

Chapter 5: Examination of dopamine neurotransmission using fast-scan cyclic voltammetry in a large longitudinal study of mice generated in Chapter 3.

Chapter 6: Generation of a second transgenic line featuring conditional deletion of *ATG7* in dopamine neurons (ATG7cKO$^{TH\text{-IRES-cre}}$), examination of dopamine neurotransmission using fast-scan cyclic voltammetry, and analysis of dopamine content in the striatum.

Chapter 2: Materials and Methods

2 Materials and Methods

2.1 Ethical declaration

All experiments and procedures conducted on animals were carried out in accordance with United Kingdom Home Office regulations under the *Animal (Scientific Procedures) Act* (1986), and were approved by the local ethical review board at the University of Oxford. All mice were housed in the University of Oxford Biomedical Services Building. Mice had access to standard food and water *ad libitum*. Mouse holding rooms were maintained at 22˚C and 60 to 70% humidity on a 12 hour light-dark cycle. All mice were bred on a C57/BL6 background. For all experiments, animals of both sexes were used unless indicated otherwise.

2.2 Biochemical methods

Investigators were blinded to mouse genotype when experiments were performed. Unless otherwise specified, all chemicals were obtained from Sigma-Aldrich (Missouri, United States of America).

2.2.1 Genotyping of mice

2.2.1.1 Lysis of ear clips

After weaning, mice were ear-clipped for identification, and to obtain tissue for genotyping. Ear clips were lysed in a 225 μL of lysis buffer (50mM KCl, 1.5 mM $MgCl_2$, 10 mM Tri pH 8.5, 0.45% CA-630 (Igepal), 0.45% ®-20, 225 ng Proteinase K) for 150

minutes at 55˚C, followed by 20 minutes at 95˚C to denature proteinase K. Lysates were stored at -20˚C.

2.2.1.2 Polymerase chain reaction

Polymerase chain reaction (PCR) was performed on ear clip lysates to determine mouse genotypes. PCR reactions were prepared according to the quantities described in Table 2.1, with the relevant primers included (Table 2.2). PCR reactions were plated in 96-well plates, and run on a DNA Engine Tetrad 2 Peltier Thermal Cycler (Bio-Rad, California, United States of America), using the PCR programme below.

PCR conditions:

1. 95˚C for 15 minutes.
2. 95˚C for 30 seconds.
3. 55˚C for 30 seconds.
4. 72˚C for 60 seconds.
5. Go to step 2. Repeat for 34 cycles.
6. 72˚C for 3 minutes.
7. 15˚C forever.

2.2.1.3 Agarose gel electrophoresis of PCR products

2% agarose gels were prepared by combining 10 mL of 50x Tris-acetate-ethylenediamine tetraacetic acid (TAE) buffer, 10 g of agarose and 490 mL of Milli-Q® water. Agarose was dissolved by heating the solution to boiling, and mixing gently. The solution was cooled to

approximately 55˚C and 15 µL of ethidium bromide was added. The solution was poured into a Mini-Gel Caster (Bio-Rad, California, United States of America), and 30-well combs inserted. The gel was allowed to set for 1 hour. The gel was placed in a Mini-Sub electrophoresis cell (Bio-Rad, California, United States of America), and submerged in TAE buffer. 10 µL of PCR product was placed into each well, alongside 5 µL of Gene Ruler 1KB+ DNA ladder (Thermo Fisher Scientific, Massachusetts, United States of America) as a molecular weight marker. A current was applied to the gel at 80 volts for 70 minutes, and the gel subsequently placed in a Gel Doc XR (Bio-Rad, California, United States of America) and imaged using ultraviolet light. Images were captured using the Quantity One® software program (Bio-Rad, California, United States of America). Agarose gel images were presented using Adobe® Illustrator® (Adobe, California, United States of America).

Table 2.1. PCR reaction components

Component	Supplier	Amount per reaction (µL)
RNase free water	Life Technologies, California, United States of America	6.15
Q solution	Qiagen, Venlo, the Netherlands	3.00
PCR buffer (10x)	Applied Biosystems, California, United States of America	1.50
Ear clip lysate	N/A	1.00
$MgCl_{2\,(aq)}$	Applied Biosystems, California, United States of America	0.90
dNTP mix	Sigma Aldrich, Missouri, United States of America	0.75
Forward primer	Primers supplied by Integrated DNA Technologies, Leuven, Belgium or Sigma Aldrich, Missouri, United States of America	0.75
Reverse primer		0.75
AmpliTaq Gold™ polymerase	Applied Biosystems, California, United States of America	0.20

DNA, deoxyribose nucleic acid; dNTP, deoxynucleotide triphosphate; N/A, not applicable; RNase, ribonuclease.

Table 2.2. Primer sequences for genotyping transgenic mice

Gene name	Forward primer (5' to 3')	Reverse primer (5' to 3')	Product size
ATG7 (wild-type allele)	TCCAAGCAGCTCTTGACTACT	GGCTGCTACTTCTGCAATGATG	560
ATG7 (floxed allele)	TGGCTGCTACTTCTGCAATGATGT	CAGGACAGAGACCATCAGCTCCAC	585
DAT (wild-type allele)	TGGCTGTTGGTGTAAAGTGG	GGACAGGGACATGGTTGACT	264
DAT (Cre allele)	GGCGCGGCAACACCATTTTT	CCGGGCTGCCACGACCAA	446
h*SNCA* (3' junction)	GGCCTCTGTCGTTTCCTTTCTCTG	ACGTGCATAGGCAGAGCTAAAACCT	450
h*SNCA* (5' junction)	CACTGAGTATTGTTCTGGTAAC	TCAAACATGAGAATTGGTCG	450
m*SNCA* (wild-type)	CAGCTCAAGTTCAGCCACGA	AAGGAAAGCCGAGTGATGTAC	550
TH (wild-type allele)	CATCGCATAAACTGGGTGTG	TGAATCCCAAAGCCATCTAGG	190
TH (Cre allele)	GCATAACCAGTGAAACAGCATTGCTG	GGACATGTTCAGGGATCGCCAGGCG	250

ATG7, autophagy-related gene 7; *DAT*, dopamine transporter; h*SNCA*, human gene encoding α-synuclein; m*SNCA*, mouse gene encoding α-synuclein; *TH*, tyrosine hydroxylase.

2.2.2 Immunohistochemistry

2.2.2.1 Transcardiac perfusion

Mice were anaesthetised using 150 μL of pentobarbitone delivered via intraperitoneal injection. Following the cessation of toe pinch and palpebral reflexes, the thoracic cavity was opened and transcardiac perfusion performed with 25 mL of phosphate-buffered saline (PBS), followed by 25 mL of 4% paraformaldehyde (PFA) diluted in PBS. Brains were removed and fixed overnight in 4% PFA. For free-floating sections, brains were then cryoprotected in 30% sucrose for 3 days prior to sectioning. For paraffin sectioning, brains were kept in PFA for 14 days.

2.2.2.2 3,3'-diaminobenzidine immunohistochemistry of free-floating slices

Brains were immersed in dry ice and then sectioned in the coronal plane in 50 μm slices using a SM 2000R sliding microtome (Leica Microsystems, Wetzlar, Germany) with a cooled stage. Following sectioning, slices were stored in cryoprotectant at -20˚C. On the day of staining, free floating sections were washed 3 times in tris-buffered saline (TBS; (TBS; 50 mM Tris, 150 mM NaCl, 2 mM KCl, pH 8), and then incubated in 3% H_2O_2 to quench endogenous peroxidases. Sections were then washed a further 3 times and then blocked for 1 hour in PBS with 10% goat serum. Sections were incubated in the blocking medium with the primary antibody (see table 2.3.) overnight at 4˚C. The following day sections were washed 3 times in TBS, and then incubated with a species-appropriate appropriate biotinylated secondary antibody (all manufactured by Vector Laboratories, Peterborough, United Kingdom) diluted 1 in 200 in TBS with 0.1% Triton X-100 (TBST) for 1 hour. Following secondary antibody incubation, brain sections were washed 3 times in TBS. Subsequently, sections were incubated in an avidin-biotin complex (ABC) solution

(Vectastain® Elite® ABC Kit, manufactured by Vector Laboratories, Peterborough, United Kingdom) for 1 hour. Sections were then washed 3 times in TBS. Finally, sections were exposed to a solution consisting of 3,3'-diaminobenzidine (DAB) and urea hydrogen peroxide (SIGMAFAST™ kit, prepared as per the manufacturer's instructions). Following DAB exposure, sections were again washed 3 times in TBS. DAB-stained sections were transferred to microscopy slides (Superfrost™ Plus, VWR, Pennsylvania, United States of America), and slides were dried for 48 hours. Sections were then counterstained with haematoxylin (Gill's formula, Vector Laboratories, Peterborough, United Kingdom), then rinsed in Milli-Q® water, and dehydrated with sequential submersion in 50% ethanol, 75% ethanol, 95% ethanol, 100% ethanol, 50% xylenes with 50% ethanol, and finally 100% xylenes. Coverslips were mounted on slides using DPX mounting medium and imaged using an Evos FL Auto microscope (Life Technologies, California, United States of America). Brightness and contrast were adjusted uniformly across genotypes.

2.2.2.3 Immunohistochemistry of paraffin-embedded slices

2.2.2.3.1 Tissue preparation of paraffin-embedded slices

PFA-fixed brains were paraffin-embedded using a Shandon Excelsior (Thermo Fisher Scientific, Massachusetts, United States of America) by Richard Stillion at the Dunn School of Pathology, University of Oxford. Brains were placed in the following solutions in a stepwise fashion, under vacuum conditions: 70% ethanol (90 minutes), 80% ethanol (90 minutes), 90% ethanol (90 minutes), 100% ethanol (3 steps of 90 minutes each), Histoclear (Thermo Fisher Scientific, Massachusetts, United States of America; two steps of 90 minutes each, and 1 step of 120 minutes), and finally paraffin wax (2 steps of 60

minutes and 1 step of 120 minutes). Paraffin blocks were sectioned at 4 μM using a Leica microtome (Leica Microsystems, Wetzlar, Germany), and sections mounted on slides.

2.2.2.3.2 Immunofluorescent immunohistochemistry of paraffin-embedded slices

Slides mounted with paraffin-embedded tissue were heated to 55˚C to melt paraffin, and then rehydrated through sequential placement in xylenes, Histo-Clear (National Diagnostics, Georgia, United States of America), 100% ethanol, 95% ethanol, 70% ethanol and Milli-Q® water. Slides were then immersed in 10% H_2O_2 for 30 minutes to quench endogenous peroxidases, and then rinsed in Milli-Q® water. In order to retrieve antigens masked during PFA fixation, slides were placed in citric acid buffer (Abcam, Cambridgeshire, United Kingdom) and microwaved for 10 minutes in total. Slides were washed 3 times with TBS and 0.05% ® 20, and then incubated with a blocking solution consisting of 1 M glycine and 10% goat serum in TBST for 1 hour. Slides were then incubated with a primary antibody (Table 2.3) in the blocking solution for 1 hour. Slides were then washed 3 times with TBS and 0.05% TWEEN® 20, and then incubated for 1 hour with secondary antibodies (Alexa Fluor® 488 and 594, Life Technologies, California, United States of America) diluted 1:200 in the blocking solution. Slides were then incubated in a TBS and 0.05% TWEEN® 20 solution containing a 1:1000 dilution of 4',6-diamidino-2-phenylindole (DAPI) for 5 minutes. Slides were washed 3 times with TBS and 0.05% TWEEN® 20, and then coverslips mounted using FluorSave™ mounting medium (Millipore, Massachusetts, United States of America). Slides were imaged using an Evos FL Auto microscope (Life Technologies, California, United States of America). Brightness and contrast were adjusted uniformly across genotypes.

2.2.2.3.3 3,3'-diaminobenzidine immunohistochemistry of paraffin-embedded slices

Slides mounted with paraffin-embedded tissue were heated to 55˚C to melt paraffin, and then rehydrated through sequential placement in xylenes, Histo-Clear (National Diagnostics, Georgia, United States of America), 100% ethanol, 95% ethanol, 70% ethanol and water. Slides were then immersed in 10% H_2O_2 for 30 minutes to quench endogenous peroxidases, and then rinsed in Milli-Q® water. In order to retrieve antigens masked during PFA fixation, slides were placed in citric acid buffer (Abcam, Cambridgeshire, United Kingdom) and microwaved for 10 minutes in total. Slides were washed 3 times with TBS and 0.05% TWEEN® 20, and then incubated with a blocking solution consisting of 10% goat serum in TBST for 1 hour. Slides were then incubated with a primary antibody (Table 2.3) in the blocking solution overnight. Slides were next washed 3 times with TBS and 0.05% TWEEN® 20, and then incubated for 1 hour with a species-appropriate biotin-conjugated secondary antibody (all manufactured by Vector Laboratories, Peterborough, United Kingdom) diluted 1:200 in the blocking solution. Slides were then washed 3 times with TBS and 0.05% TWEEN® 20. Subsequently, slides were incubated in an ABC solution (Vectastain® Elite® ABC Kit, manufactured by Vector Laboratories, Peterborough, United Kingdom) for 1 hour. Sections were then washed 3 times in TBS. Finally, sections were exposed to a solution consisting of 3,3'-diaminobenzidine (DAB) and urea hydrogen peroxide (SIGMAFAST™ kit, prepared as per the manufacturer's instructions). Following DAB exposure, slides were again washed 3 times in TBS and 0.05% TWEEN® 20. Slides were then counterstained with haematoxylin (Gill's formula, Vector Laboratories, Peterborough, United Kingdom), then rinsed in Milli-Q® water, and dehydrated with sequential submersion in 70% ethanol, 95% ethanol, 100% ethanol and 100% xylenes. Coverslips were mounted on slides using DPX mounting medium and imaged using an Evos FL Auto microscope (Life Technologies, California,

United States of America). Brightness and contrast were adjusted uniformly across genotypes.

Table 2.3. Primary antibodies for immunohistochemistry

Antigen	Host species	Type	Product number	Company	Concentration
α-synuclein (all species)	Mouse	Monoclonal	610787	BD Biosciences	1:500
α-synuclein (human)	Mouse	Monoclonal	Ab80627 (syn211)	Abcam	1:500
DAT	Rat	Monoclonal	MAB369	Millipore	1:500
IBA1	Rabbit	Polyclonal	019-19741	Wako	1:500
P62	Rabbit	Monoclonal	EPR4844	Abcam	1:500
TH	Rabbit	Polyclonal	AB152	Millipore	
Ubiquitin	Rabbit	Polyclonal	Z0458	DAKO	1:250

DAT, dopamine transporter; IBA1, ionized calcium-binding adapter molecule 1; TH, tyrosine hydroxylase.

2.2.3 Stereology

Stereology was performed on 50 μm thick free-floating coronal sections of the whole brain, and stained as described in 1.2.2.2 with an antibody against TH. Every 3rd section through the SNc was stained and mounted on slides, for a total of eight sections per mouse. In each age group, mice of each genotype were processed together to prevent technical differences impacting neuron counts. TH positive neurons in the SNc and VTA were counted using an unbiased, online-counting optical fractionator method using Stereo Investigator software (MBF Bioscience, Vermont, United States of America) and a Zeiss Imager M2 microscope. The SNc and VTA were outlined using a 2x objective according the mouse brain atlas provided by Paxinos and Watson (2008). Neurons were subsequently counted at 100x. Pilot experiments with a 6 month-old control mouse were used to generate sampling parameters providing a Gundersen coefficient of error of less than 0.1. The parameters used were a sampling grid of 120 μm by 120 μm squares with a randomly placed counting frame of 60 μm by 60 μm, and an optical dissector height of 10 μm with a 2 μm guard distance.

2.2.4 Sodium dodecyl sulfate polyacrylamide gel electrophoresis and immunoblotting

2.2.4.1 Tissue preparation for protein electrophoresis

For sodium dodecyl sulfate polyacrylamide gel electrophoresis (SDS-PAGE), mice were subjected to cervical dislocation, the brain removed and the following brain regions dissected: hindbrain, midbrain, hippocampus, cortex and striatum. Samples were then immediately frozen at -80˚C. Protein samples were immersed in ice-cold radioimmunoprecipitation assay (RIPA) buffer (20mM Tris, 150mM NaCl, 1% NP-40, 1% sodium deoxycholate, 0.1% SDS, 1 "complete mini protease inhibitor cocktail tablet," deionised water) and then subjected to mechanical disruption by a rotor-type tissue homogeniser (Tissue-Tearor, Biospec Products, United States of America) for ten seconds. Samples were centrifuged for 2 minutes at 15000 *g*, to leave only soluble protein. Protein quantification was performed using a bicinchoninic acid assay (Smith *et al.* 1985). Protein samples were then diluted to a concentration of 0.5 μg per mL with RIPA lysis buffer, and 4x sample buffer was added in a ratio of 1:3 (final concentration of sample buffer components, 200 mM Tris HCl pH 6.8, 400 mM DTT, 8% SDS, 0.4% bromphenol blue, 50% glycerol by volume). Samples were denatured at 95˚C for 10 minutes, and then loaded into a polyacrylamide gel. A current was applied across the gel at 100 volts for approximately 2 hours at room temperature. Protein was transferred from the gel to a polyvinylidene fluoride membrane using the Bio-Rad Trans-Blot Turbo apparatus. The membrane was then placed in blocking solution (5% skim milk by weight in TBS with 0.1% TWEEN® 20) for 1 hour. Following blocking, the membrane was incubated in primary antibody against human α-synuclein (Ab80627 (syn211), mouse monoclonal, Abcam, Cambridgeshire, United Kingdom) in blocking solution overnight at 4˚C. The membrane was washed and probed with an HRP-conjugated secondary antibody (Bio-Rad,

California, United States of America) for 1 hour in blocking solution. Finally, the membrane was washed 3 times with TBS with 0.1% TWEEN® 20 and then developed using ECL+ chemiluminescent substrate (GE Healthcare, Illinois, United States of America) and imaged with a Chemidoc Touch (Bio-Rad, California, United States of America).

2.2.5 Fast-scan cyclic voltammetry

2.2.5.1 Preparation of recording electrodes for fast-scan cyclic voltammetry

For FCV, carbon-fibre microelectrodes (CFM) were prepared by hand, as performed previously (Threlfell *et al.* 2012; Janezic *et al.* 2013). A carbon fibre of 7 to 8 μm diameter (Goodfellow, Cambridgeshire, United Kingdom) was threaded into a 2 mm borosilicate capillary tube (Harvard Apparatus, Kent, United Kingdom) in a test-tube containing acetone. Once threaded, the capillary was drained of acetone and placed in a vertical electrode puller (Narishige, Tokyo, Japan). The capillary was pulled with heat under gravity to make a seal around the carbon fibre that was visible at 100x magnification. The carbon fibre was then trimmed to a length of between 50 and 100 μm under a 100x objective using a scalpel blade. An electrical connection to the carbon fibre was made via an insulated copper wire dipped in silver epoxy glue and inserted into the capillary. Finally, the wire was held in place by cyanoacrylate glue.

2.2.5.2 Preparation of acute striatal slices for fast-scan cyclic voltammetry

For FCV experiments, mice were transferred to a holding area for a minimum of 24 hours prior to experiments. Experiments were performed in age- and sex-matched pairs of mice, which had the following genotypes:

- *DAT*-IRES-cre control and *ATG7*cKO$^{DAT\text{-IRES-cre}}$
- hSNCA and hSNCA:*ATG7*cKO$^{DAT\text{-IRES-cre}}$
- *TH*-IRES-cre control and *ATG7*cKO$^{TH\text{-IRES-cre}}$

In this thesis, data from the first two pairs are plotted and analysed together for ease of comparison. FCV was performed as described previously (Threlfell *et al.* 2012; Janezic *et al.* 2013). Mice were killed by cervical dislocation and the brain removed into ice-cold artificial cerebrospinal fluid (aCSF) buffered by 4-(2-hydroxyethyl)-1-piperazineethanesulfonic (HEPES) acid and saturated with 95% O_2 and 5% CO_2. The composition of HEPES-buffered aCSF was 120 mM NaCl, 5 mM KCl, 20 mM $NaHCO_3$, 6.7 mM HEPES acid, 3.3 mM HEPES salt, 2 mM $CaCl_2$, 2 mM $MgSO_4$, 1.2 mM KH_2PO_4 and 10 mM glucose. Coronal slices (300 μm thick) containing the striatum were prepared using a VT 1200S vibratome (Leica Microsystems, Wetzlar, Germany) in HEPES-buffered aCSF. The order of mice for slice preparation in each pair was random. Slices were then maintained in HEPES-buffered aCSF at room temperature with a constant O_2 supply for 1 hour prior to experimentation. The genotype of mice for slice preparation in each pair was random.

2.2.5.3 Dopamine recordings with fast-scan cyclic voltammetry

For DA recordings, striatal slices were placed into a chamber where a constant flow of aCSF was maintained at approximately 1.5 mL per minute at a temperature of 31 to 32˚C.

The composition of aCSF used for recording was 124 mM NaCl, 3.8 mM KCl, 26 mM $NaHCO_3$, 2.4 mM $CaCl_2$, 1.3 mM $MgSO_4$, 1.2 mM KH_2PO_4 and 10 mM glucose, saturated with 95% O_2 and 5% CO_2. Prior to the start of recordings, slices were secured using silver pins and left to recover for a minimum of 20 minutes to allow both the brain slices to equilibrate at the recording bath temperature and the CFM to charge. A platinum/iridium concentric bipolar stimulating electrode of 25 μm diameter (FHC, Maine, USA) was placed at the surface of the striatal slice. A CFM was placed in the striatal slice at a depth of approximately 100 μm, approximately 150 μm away from the stimulating electrode.

The CFM was connected to a Millar voltammeter (Julian Millar, Barts and the London School of Medicine and Dentistry, London, United Kingdom), and the voltammeter to an oscilloscope (Tektronix, Berkshire, United Kingdom). A scanning waveform was swept across the CFM by the voltammeter, and the resulting voltammogram was recorded on a computer connected to the oscilloscope, using either Strathclyde Whole Cell Program (University of Strathclyde, Glasgow, Scotland) or AxoScope 10.5 (Molecular Devices, California, United States of America). The scanning waveform passing across the CFM swept from -0.7 V to 1.3 V and to -0.7 V at a rate of 800 V/s, i.e. each scan took 5 milliseconds. Voltammograms were recorded at a frequency of 8 Hz, and the CFM was switched out of circuit between scans. Electrical stimulation was delivered by the stimulating electrode for a duration of 200 μs at an amplitude of 600 μA. Electrical stimuli were delivered when the CFM was taken out of circuit, which precluded electrical stimuli from happening during a voltage sweep. Electrical stimuli were separated by 2.5 minutes to allow complete recovery of DA release. Following each experiment, electrodes were calibrated using 2 μM DA in aCSF. For the purposes of calibration a stock solution of 2.5

mM DA was kept at 4˚C and diluted to 2 μM in oxygenated-aCSF immediately prior to calibration.

2.2.5.4 Dopamine recording sites

In the studies described in this thesis, six recording sites were used to examine DA neurotransmission (Figure 2.1). four sites were used in the caudate-putamen, and two sites in the nucleus accumbens. As done in previous studies, data from the two nucleus accumbens sites were pooled, as were data from the four caudate-putamen sites, to provide accurate information regarding DA neurotransmission on average in each of these regions. In order to maximise the data obtained from each pair of mice, recordings were taken from two striatal slices per mouse per day at approximately ~ 1.5 to 0.5 mm from Bregma in the anteroposterior plane.

2.2.5.5 Analysis of cyclic voltammograms

Cyclic voltammograms generated during calibration were used to determine the location of the DA oxidation potential and to determine the sensitivity of the recording electrode. Calibration values were used with data acquired from acute striatal slices to determine changes in [DA]o over time. These data were applied to cyclic voltammograms generated from acute striatal slices to determine changes in $[DA]_o$ over time. Data from cyclic voltammograms was exported to Microsoft Excel and processed using custom macros (S. Cragg, unpublished). For experiments examining paired pulse depression (PPD) the size of the second peak in $[DA]_o$ (p2) is expressed as a proportion of the initial peak (p1) – this is denoted as p2/p1.

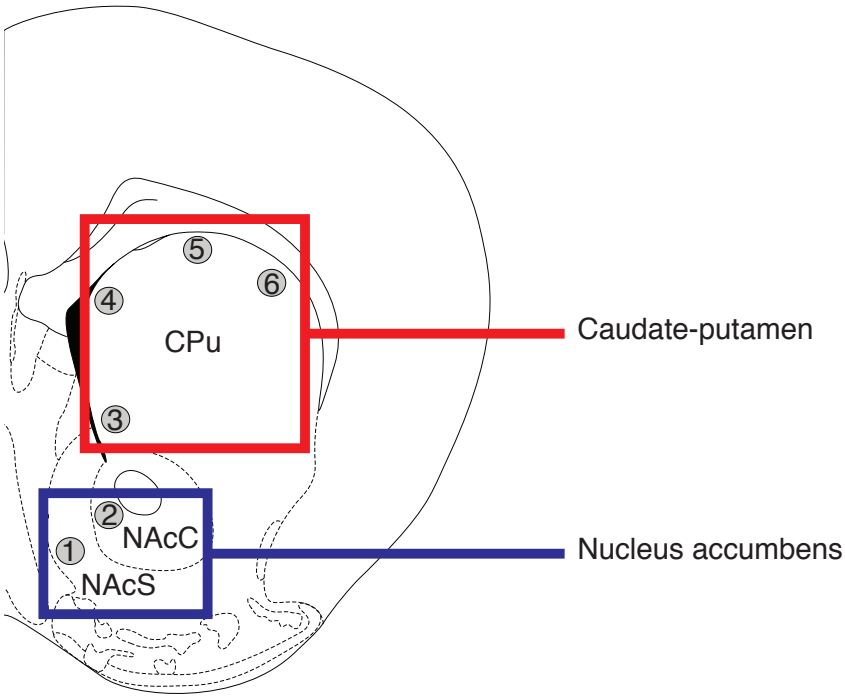


Figure 2.1. Sampling sites used for fast-scan cyclic voltammetry in Chapters 5 and 6. Electrodes were placed in (1) the shell of the nucleus accumbens (NAcS), (2) the core of the nucleus accumbens (NAcC), (3) the ventromedial caudate-putamen (CPu), (4) the dorsomedial CPu, (5) the dorsal CPu and (6) the dorsolateral CPu. Data from sites 1 and 2 were pooled together to provide information on dopamine neurotransmission in the nucleus accumbens, and sites 3 to 6 were pooled together to provide information on dopamine neurotransmission in the caudate-putamen.

2.2.6 High-performance liquid chromatography with electrochemical detection

2.2.6.1 Preparation of samples for high-performance liquid chromatography

Samples for high-performance liquid chromatograph (HPLC) with electrochemical detection were taken from the same striatal slices used for FCV experiments, immediately following the conclusion of FCV experiments, as performed previously (Janezic *et al.* 2013; Taylor *et al.* 2014; Sloan *et al.* 2016). From each striatal slice, two circular punches were taken from the caudate-putamen (diameter 2 mm, one from each hemisphere), and two circular punches were taken from the nucleus accumbens (diameter 1.2 mm, one from each hemisphere). Punches from the same slice and same region were stored together in 200 μL of 0.1M $HClO_4$ at -80˚C until an entire experimental set was complete and ready for analysis. Samples were then thawed at the same time for analysis and homogenised in $HClO_4$ through sonication. Samples were then centrifuged at 15000 *g* for 15 minutes at 4˚C to remove remnants of the cell membrane from the supernatant. The supernatant of caudate-putamen samples was diluted in 0.1M $HClO_4$ at a ratio of 1:10 or 1:15 to ensure that all neurotransmitters were within the range of detection of the HPLC electrode.

2.2.6.2 Electrochemical detection and measurement during high-performance liquid chromatography

To optimise detection of neurotransmitters, HPLC mobile phase was used that contained 13% methanol, 0.8 mM ethylenediaminetetraacetic acid (EDTA), 0.5 mM octanesulfonic acid and 0.12 M NaH_2PO_4. This solution was made to a pH of approximately 4.6, and passed through a 22 μM filter.

In order to determine that neurotransmitters could be detected and distinguished from each other, calibration standards of DA, 3,4-dihydroxyphenylacetic acid (DOPAC), noradrenaline (NA), homovanillic acid (HVA) and 5-hydroxyindoleacetic acid (5-HIAA) were prepared. 5 pmol (50 μL of 10^{-7} M) samples were injected into a C18 HPLC column (S150 x 4.6 mm; Agilent, California, USA) under high-pressure using an autosampler (AS-2057 PLUS, Jasco), at a flow rate of 1 mL per minute, over 15-20 minutes (adjusted to ensure overlap between different neurotransmitter peaks did not occur). Detection of neurotransmitters after they exited the column was performed by a Decade II SDS electrochemical detector (Antec, Zoeterwoude, the Netherlands) using a glassy carbon detecting electrode. Following clear identification of each standard individually, and in a mix of all standards, samples obtained from mouse striatal slices were run. Mixed standards were placed in the beginning, middle and end of each group of experimental samples. Peaks for each neurotransmitter were assigned from the mixed standard and applied to the experimental samples. In the data described in Chapter 3, the striatal punches from the three different age groups (1 month, 6 month, and 20 to 24 month), were run on different dates. In order to aid comparison of these different age groups, experimental data

were normalised to the values gained for control genotypes of the same age, as performed previously (Anwar *et al.* 2011).

2.3 Behavioural testing

All behavioural testing was performed in a blinded fashion. All tests were conducted in the light phase of the light-dark cycle. Behavioural testing groups contained mice of both sexes with no difference in sex ratio between transgenic mouse lines. Two groups of mice were used: one cohort with a mean age of 3 months (range 2.5 to 3.5 months), and one cohort with a mean age of 21 months (range 19 to 23 months).

2.3.1 Locomotor activity

Spontaneous locomotor activity was assessed by placing each mouse in a transparent plastic cage, and assessing locomotion by means of infra-red beam breaks over a 4-hour period in 30 minute intervals (apparatus manufactured by San Diego Instruments, California, United States of America). The floors of the cages were covered by a thin layer of saw dust, to a total volume of approximately 250 mL. Experiments were started between 0800 and 0900 hours.

2.3.2 Digital gait analysis

Mice were subjected to gait assessment using the CatWalk automated gait analysis system (Noldus Information Technology, Wageningen, the Netherlands). Mice were placed on a transparent glass platform that was cross-illuminated by a green light emitting diode. An orange contrasting light was placed over the mouse. Video recordings of 20 cm runs across

the platform were made, and were accepted for analysis if they were between 0.5 and 5 seconds in duration and there was less than 35% variation in speed. The first 5 compliant runs were analysed, or in the event of the mouse making 100 runs without reaching this target, all of the compliant runs within the first 100 were analysed. Runs were analysed using Catwalk software, and the average data for each mouse exported for analysis.

2.3.3 Rotarod

Mice were placed on a rotarod apparatus (Med Associates, Vermont, United States of America) facing away from the experimenter. Mice were trained for 4 days on a rotating rod apparatus that accelerated from 4 to 40 rpm over 5 minutes. The latency to fall was recorded. If a mouse turned to face the experimenter or fell within the first 10 seconds of a trial then the trial was stopped, the mouse returned to the rod and the trial restarted from the beginning.

2.3.4 Inverted screen

Mice were subjected to Kondziela's inverted screen test, performed as described by Deacon (2013a). Mice were placed on a 43 cm^2 wire mesh attached to a 4cm deep wooden frame, which was gently inverted. The latency to fall was recorded. The test was stopped at 60 seconds if the test subject had not fallen prior to this.

2.3.5 Stool collection

Mice were placed in a transparent plexiglass cage between the hours of 1600 and 1700, and the stool they expelled during this period collected, as previously described (Janezic *et al.* 2013). Stool pellets contaminated with urine were patted dry with paper towel. The number of pellets and the gross wet weight was recorded, before the samples were dried overnight at 60˚C and the dry weight obtained. Stool water was determined as the wet weight minus the dry weight (Kuo *et al.* 2010).

2.3.6 Spontaneous alternation in a T-maze

Spontaneous T-maze alternation was performed as described by Deacon and Rawlins (2006). A black-floored T-maze produced by the Department of Experimental Psychology at the University of Oxford was used. The T-maze consisted of three arms of length 30 cm, with walls of 20 cm in height, a central partition that extended 9 cm into the start arm, and guillotine doors that could be closed behind the mice as they entered each goal arm. Mice were placed in the start-arm of the T-maze, and allowed to explore the goal arms. Once the subject mouse had four feet and its tail tip inside one goal arm, it was considered to have entered that goal arm, and the guillotine door for that arm was shut. The mouse was then allowed to explore its surroundings for a further 30 seconds. Mice were then returned the start arm and the trial repeated. Alternation occurred if mice chose the previously unexplored goal arm on their second trial. Mice were tested twice daily on 5 consecutive days in a predetermined random order. The task was unrewarded.

2.3.7 Spatial novelty preference in a Y-maze

Spatial novelty preference in a Y-maze was assessed according to a modified version of the protocol described by Wolf *et al.* (2016). A plexiglass Y-maze produced by the Department of Experimental Psychology at the University of Oxford was used. The Y-maze consisted of three arms (width 8cm, height 20 cm, length 30cm), at 120˚ to each other: a start arm and two goal arms. Each of the goal arms could be blocked off by a guillotine door. A mixture of dirty and clean sawdust (3:1) was used in the maze to promote exploration. Before the start of each trial, one of the guillotine doors was shut, so that one of the goal arms was inaccessible (counterbalanced for genotype). The mouse was then allowed to explore the start arm and the open goal arm freely for 5 minutes. Subsequently the mouse was removed from the maze for 1 minute and the guillotine door opened so that all arms were accessible. The mouse was then allowed to freely explore for 2 minutes, and the time spent in the novel arm measured, and expressed as a preference index, which was calculated as time spent in the novel arm divided by time spent in the familiar and novel goal arms combined. The location of the mouse was tracked using EthoVisionXT ((Noldus Information Technology, Wageningen, the Netherlands). The task was unrewarded.

2.3.8 Tail suspension

The tail suspension test was performed as previously described (Steru *et al.* 1985; Can *et al.* 2012). Mice were suspended by their tails using adhesive tape, with a guard placed around the tails. The time spent immobile during a 5 minute period was recorded.

2.3.9 Elevated plus-maze

Elevated plus-maze testing was performed according the protocol described by Schank and colleagues (Schank *et al.* 2008). The apparatus consisted of two open arms and two enclosed arms arranged at right angles to each other, with open and closed arms alternating. The maze was elevated 70 cm from the ground. The arms were 35 cm long and 6 cm wide, with a central 6 cm by 6 cm square. The enclosed arms had walls 20 cm in height. Mice were placed in the centre of a plus-maze with two closed arms, facing toward an open arm, and timed for 5 minutes. Open arm time and open and closed arm entries were recorded. An arm entry was defined as placing all four paws into an arm. Data were recorded manually for the 3 month cohort, and using EthoVisionXT ((Noldus Information Technology, Wageningen, the Netherlands) for the 21 month cohort.

2.3.10 Olfactory testing

Olfaction was tested using a modified version of a habituation/dishabituation protocol described by Fleming *et al.* (2008). two glass vials were fixed to the floor of a cage containing bedding from the mouse's home cage. Initially, each glass vial held the same odour, and mice were habituated to this odour for three trials of 2 minutes duration (6 minutes total). At random, one of the glass vials was substituted with another vial containing a second odour, and a final trial of 2 minutes duration proceeded. The time spent exploring the novel odour, defined as presence of the nose of the mouse within 2 cm of the vial, was determined. Three pairs of odours were used, and whether odours were used as the habituation or novel odour was randomised. The odour pairs used were as follows: coconut/vanilla, orange/mango, and peppermint/jasmine. A novel odour

preference index was calculated as the time spent exploring the new odour, divided by the time spent investigating the original odour.

2.4 Statistical analysis

Experimenters were blinded to genotype in all experiments, and unblinded only at the time of analysis. Statistical analysis and presentation was performed using GraphPad Prism 6 for Macintosh (GraphPad Software, United States of America) and SPSS 24 (IBM, United States of America), according to standard texts by Keppel and Wickens (2004), Kirk (2013), and McDonald (2009). For FCV experiments, observations made in distinct anatomical locations in each animal were treated and analysed as biologically distinct, as performed previously by the Cragg group and other investigators (Rice and Cragg 2004; Chen *et al.* 2006; Senior *et al.* 2008; Li *et al.* 2010; Anwar *et al.* 2011; Patel *et al.* 2012; Janezic *et al.* 2013). In general, for experiments described in Chapters 3, 4, and 5, 3-way analysis of variance (ANOVA) was used for the following variables:

- Age (3 levels in Chapters 3 and 5; two levels in Chapter 4)
- h*SNCA* genotype (present or absent)
- *ATG7*cKO$^{DAT\text{-IRES-cre}}$ genotype (present or absent)

Where different statistical tests were performed, these are described in the text. The assumption of normality was tested using Q-Q plots, histograms and a Shapiro-Wilk test for data sets of less than 50, or a Kolgomorov-Smirnov test with Lilliefors correction test for data sets of greater than 50 (Shapiro and Wilk 1965; Kéry and Hatfield 2003; Ellison *et al.* 2009; Davis 2013). If data did not meet the assumption of normality, then it was transformed, and this is denoted in the figure legend. Logarithmic transformations were performed in base 10. Graphs display untransformed data for the ease of the reader. In

general, there was no difference between the results of analyses of transformed and untransformed data, and none of the major conclusions of this thesis were altered based on data transformation. In the event data could not be transformed to a more normal distribution this is noted in the figure, and a threeway ANOVA was performed, as there is no commonly used threeway non-parametric test and ANOVA is relatively robust to violations of the normality assumption, especially at larger values of *n* (Pearson 1931; Feir-Walsh and Toothaker 2016). If interactions were present between a genotype variable and age, these were investigated at each level of age. Pairwise comparisons were performed at each level of age if this was indicated, and a Bonferroni correction applied. In Chapter 6, all experiments were conducted in pairs of age- and sex-matched mice on the same day, with the only variable being the presence or absence of the *ATG7*cKO$^{TH\text{-IRES-cre}}$ genotype. Therefore, in Chapter 6, 2-tailed paired Student's *t* tests were performed. Tests for normality of pair differences were made (McDonald 2009). If transformation did not produce normality of pair differences, then a Wilcoxon signed-rank test was used. In all cases, p-values below 0.05 after multiple testing correction were considered significant.

Chapter 3: Generation and histological characterisation of a mouse model to examine the interaction between human alpha-synuclein and impaired macroautophagy in dopamine neurons

3 Generation and histological characterisation of a mouse model to examine the interaction between human alpha-synuclein and impaired macroautophagy in dopamine neurons

3.1 Overview

Macroautophagy is a major cellular process by which deleterious contents are degraded. Dysfunction of macroautophagy is implicated in both sporadic and genetic PD, and macroautophagy inducers are currently in PD clinical trials (e.g. nilotinib - see Pagan *et al.* 2016). However, little is known about the interaction between α-synuclein and macroautophagy *in vivo*. Similarly, the behavioural consequences of macroautophagic failure in DA neurons in the ageing mammalian brain are not well resolved. Hernandez and colleagues (2012) published data demonstrating that impaired macroautophagy boosts DA neurotransmission in young animals (the opposite of PD, where DA neurotransmission is reduced). However, other authors have demonstrated that impaired DA neuron macroautophagy produces a neuropathological phenotype that holds some similarities to PD (Ahmed *et al.* 2012; Friedman *et al.* 2012). In order to help resolve these open questions and contradictory findings, we generated a novel transgenic mouse that featured impaired macroautophagy in DA neurons, and expressed a full-length human *SNCA* BAC construct in all cells, as well as appropriate transgenic mouse control lines. This chapter describes the generation of mouse cohorts for longitudinal analysis, and the histological examination of these mice.

3.2 Aims of Chapter 3

1. To demonstrate the generation of transgenic mouse cohorts featuring:
    a. Overexpression of a human α-synuclein transgene from the complete human wild-type *SNCA* genomic locus (h*SNCA*);
    b. Impairment of macroautophagy in DA neurons (*ATG7*cKO$^{DAT\text{-IRES-cre}}$);
    c. Both impairment of macroautophagy in DA neurons and overexpression of a BAC human α-synuclein transgene from the complete human wild-type *SNCA* genomic locus (h*SNCA*:*ATG7*cKO$^{DAT\text{-IRES-cre}}$); or
    d. Neither genetic lesion (control).
2. To examine for evidence of progressive degeneration of the nigrostriatal system in transgenic mice.
3. To examine the brains of transgenic mice for evidence of pathology similar to that seen in PD.

3.3 Introduction

3.3.1 Choice of model species

When modeling human disease in other species, a balance must be met between species similarity to humans, the availability of investigative tools to examine biological questions, and practical matters such as cost and the time taken to reach old-age. These factors are particularly salient when modeling a disease associated with ageing, such as PD. Non-human primates feature the closest similarities to humans in terms of genetics, phenotypes and life-span, but the time taken to reach old-age, the reduced availability of genetic modifications to assist investigations and the ethical concerns precludes their widespread

use. On the opposite end of the spectrum, non-mammalian species such as *Drosophila* and *Caenorhabditis* are freely available and have a wide-range of genetic tools to assist investigators in asking biological questions, however their short life-span, and difficulties in determining parkinsonian phenotypes mean that they are of limited utility in modeling PD, and determining age-related phenotypes. Rodents such as rats and mice represent an effective middle-ground, as they have moderate life-spans, a large number of genetic tools are available to examine scientific questions, and their dopaminergic systems are reasonable analogues of the human system. Mice were used in the experiments described in this thesis, as the genetic tools used for conditional manipulation of macroautophagy are not available in rats. Likewise, both cDNA and BAC models of synucleinopathy are more commonly available in mice. In this experiment, we utilised an α-synuclein BAC transgene that the Wade-Martins laboratory had previously developed in mice (Janezic *et al.* 2013).

3.3.2 Methods of impairing macroautophagy *in vivo*

Macroautophagy can be impaired via genetic or chemical means. Absence of autophagy-essential genes in the whole organism is lethal in the embryonic or neonatal stages of life, preventing ageing and longitudinal analysis (Yue *et al.* 2003; Kuma *et al.* 2004; Komatsu *et al.* 2005). Likewise, systemic administration of macroautophagy inhibitors, such as bafilomycin, is toxic and not specific to a cell type. Therefore, in order to examine the consequences of impaired DA neuron macroautophagy, it was necessary to use conditional genetic means. In the present experiment, we utilised conditional deletion of *ATG7*, a gene essential for autophagy, in DA neurons. This breeding strategy took advantage of the cre-loxP system, in which the gene of interest, in this case *ATG7*, is flanked by two loxP sequences ("floxed"). These sequences are recognised by the cre recombinase, which

excises the target gene. Specificity of knockout can be achieved by driving the expression of the cre recombinase with a cell type-specific promoter. There are two conditional cre systems that are used to target DA neurons in which cre is knocked in to either the *DAT* locus or the *TH* locus. The *TH*-cre system has a number of limitations, including that *TH* is expressed in all catecholamine producing cells, including those of the adrenal gland and the locus coeruleus, and disruption of these structures may confound any behavioural findings (Lindeberg *et al.* 2004). Additionally, cre expression from *TH*-cre lines does not correlate well with *TH* expression assessed by conventional means (Lammel *et al.* 2015). Due to the limitations of *TH*-cre driver lines, *DAT* was used as the driver for cre recombinase for the majority of experiments in this thesis. In principle, cre recombinase can either be expressed from near the start codon of a gene, thus disrupting the transcription of one copy of the gene, or from an IRES at the end of the gene, thus conserving active expression. The two available *DAT* cre driver lines were developed by Zhuang *et al*. (2005), and Bäckman and colleagues (2006). The Zhuang mouse features a cre sequence immediately after the *DAT* promoter, and therefore has only one functional copy of *DAT*. In contrast, the Bäckman mouse expresses cre recombinase from an IRES in the 3' untranslated region (UTR), and thus preserves expression of *DAT*, at least partially. Mice that are heterozygotes for the Bäckman *DAT*-IRES-cre construct express 83% of the DAT seen in wildtype mice. The Bäckman *DAT*-IRES-cre line was used in this chapter, and the subsequent two chapters. The initial breeding of the *ATG7*cKO$^{DAT\text{-IRES-cre}}$ mouse in the Wade-Martins laboratory was performed by Dr. Javier Alegre-Abarretegui and Milena Cioroch. Subsequently, in-situ hybridisation (ISH) was performed by Prof. Peter Oliver (University of Oxford) to demonstrate the successful deletion of *ATG7* in *DAT* positive neurons (Figure 3.1).

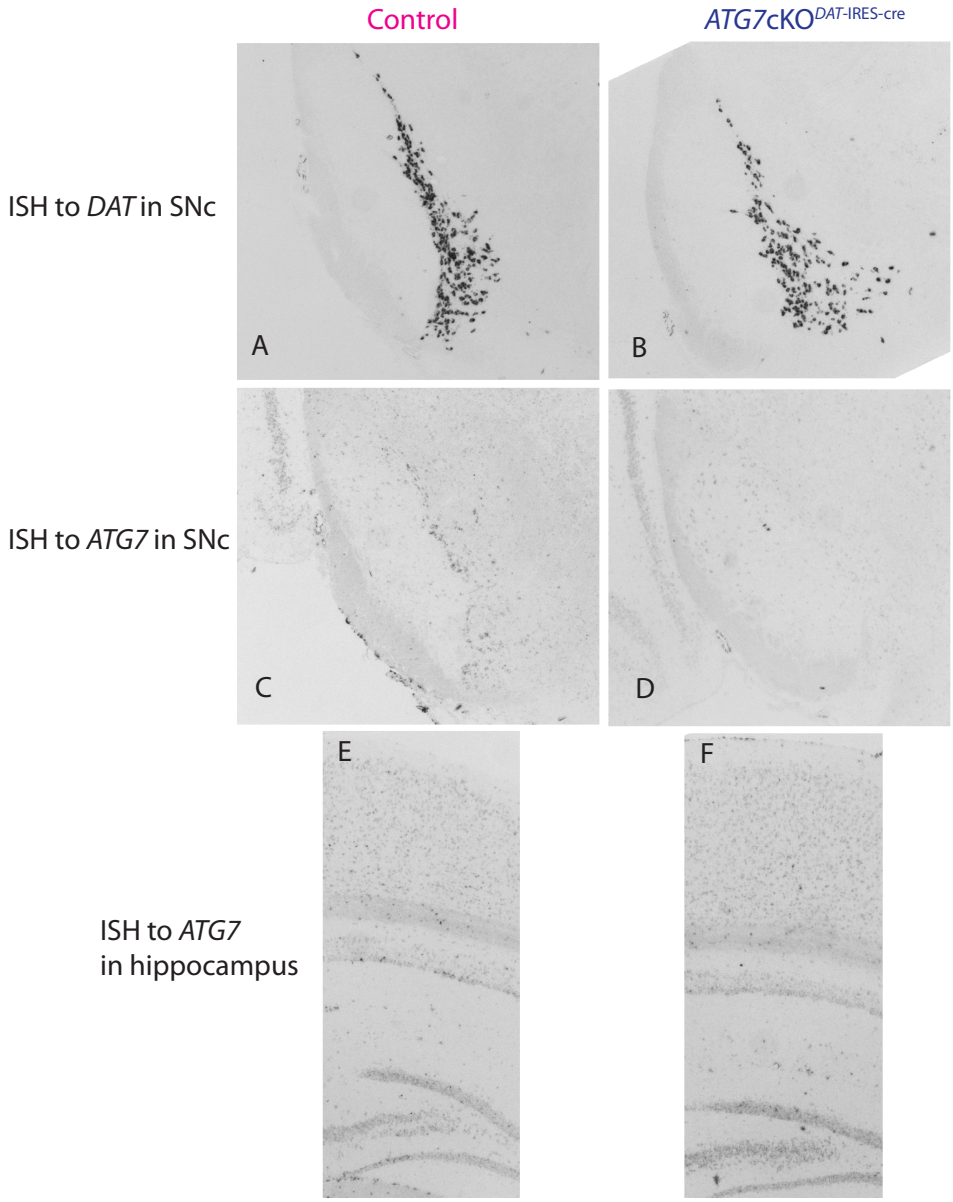


Figure 3.1. In-situ hybridisation studies in experimental mice demonstrate reduced *ATG7* expression in the midbrain of *ATG7*cKO$^{DAT\text{-IRES-cre}}$ mice.
In-situ hybridisation (ISH) was performed on adjacent 15 µM sections of the substantia nigra (SNc), using probes to *DAT* (A, B) and *ATG7* (C, D), demonstrating reduced *ATG7* expression in *ATG7*cKO$^{DAT\text{-IRES-cre}}$ mice. ISH using probes to *ATG7* was performed in the hippocampi and cortex of experimental mice (E, F) to demonstrate preservation of normal *ATG7* expression in areas where *DAT* is not expressed. All experiments performed by Prof. Peter Oliver.

3.3.3 Method of expressing human α-synuclein

There are two major methods of expressing human α-synuclein in transgenic mice: cDNA-based constructs and BAC constructs. BAC constructs have the advantage of retaining the regular promoter elements of the *SNCA* gene, thus helping to preserve normal spatiotemporal expression patterns. Previously, the Wade-Martins laboratory has developed the *SNCA*-OVX mouse, an α-synuclein BAC transgenic mouse that expresses α-synuclein at approximately twice the level of endogenous mouse α-synuclein (Janezic *et al.* 2013). This mouse had several key attributes associated with PD, including SNc neuron loss, reduced DA release, and behavioural attributes associated with PD such as reduced stride length. The *SNCA*-OVX BAC construct was therefore used in this experiment. The original *SNCA*-OVX mouse was developed on a mouse α-synuclein knockout background, in order to study the effects of human α-synuclein in isolation. However, the use of a mouse *SNCA* (m*SNCA*) knockout was precluded in this experiment as the floxed *ATG7* allele is located in close proximity to m*SNCA* on chromosome 6, and therefore breeding a mouse with both floxed *ATG7* allele and m*SNCA* knocked out would rely on rare homolgous recombination events. For this reason, the BAC h*SNCA* transgene was bred onto a regular C57/BL6 background, which was used for these experiments (work done by Milena Cioroch in the Wade-Martins laboratory).

3.4 Results

3.4.1 Generation of transgenic mouse lines

Mice were bred according to the breeding scheme described in Figure 3.2. A single copy of the *ATG7* allele allows relatively preserved macroautophagic function (Kuma *et al.* 2004; Komatsu *et al.* 2005), and thus mice with a single floxed copy of *ATG7* and one wild-type allele were used as controls, and compared with mice homozygous for the floxed *ATG7* allele, which had impaired macroautophagy. The h*SNCA* transgene was introduced into this breeding scheme, such that half of the mice in each group over-expressed human α-synuclein. All mice were heterozygous for wild-type *DAT* and *DAT* driving the cre recombinase from an IRES site, and homozygotes for m*SNCA*.

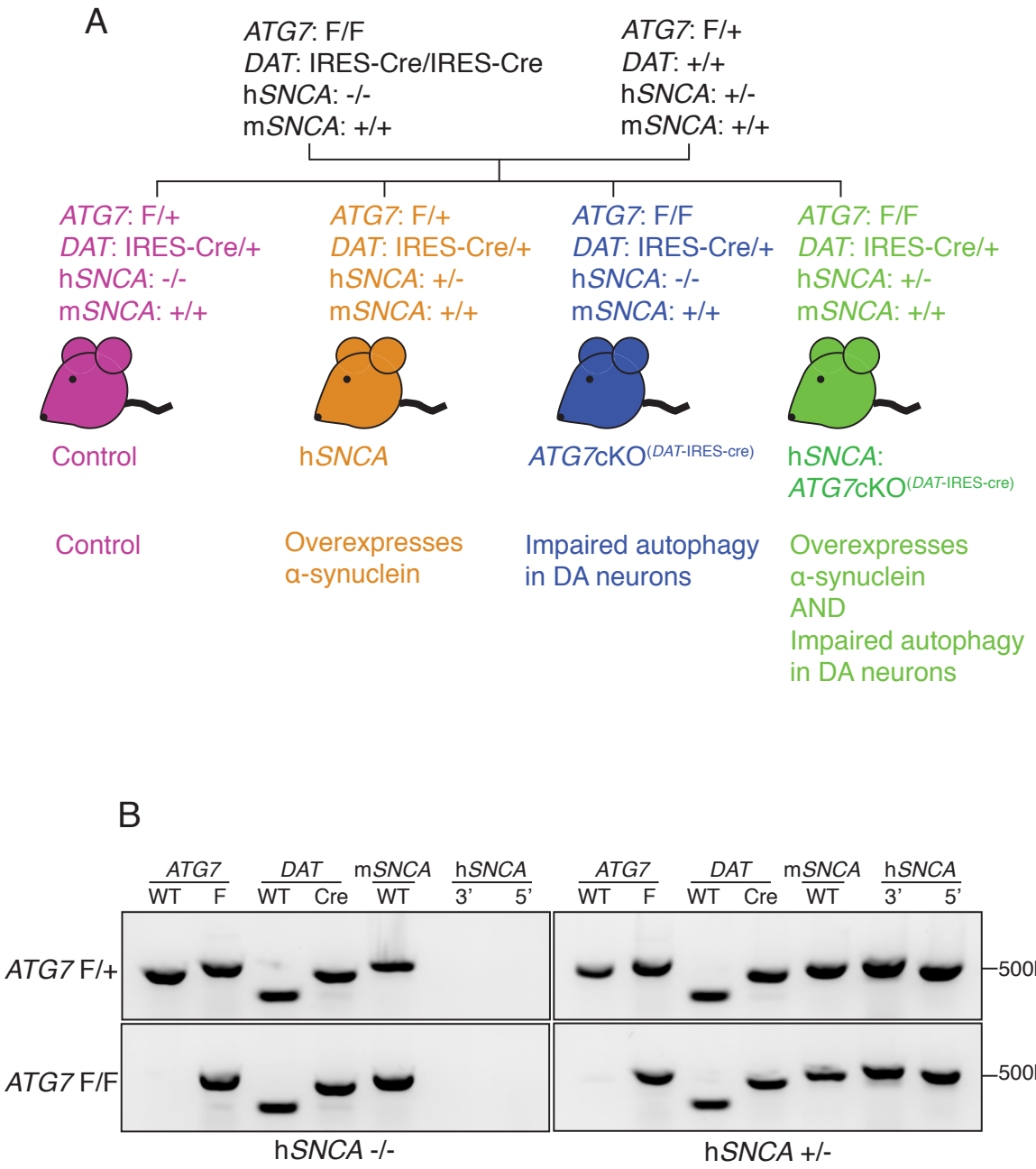
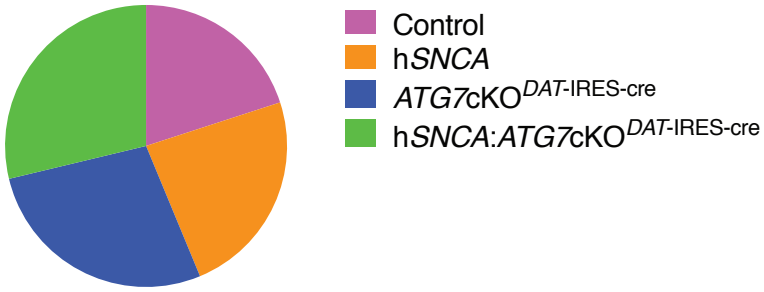


Figure 3.2. Generation of experimental genotypes.
(A) Example breeding strategy used to generate experimental animals. The experimental cross produced four genotypes. All mice were heterozygous for *DAT*-IRES-cre, and all were homozygous for wild-type mouse *SNCA* (m*SNCA*). These mice had either normal (ATG7 F/+) or impaired (ATG7 F/F) macroautophagic function in dopamine neurons, and expressed either no human *SNCA* (h*SNCA* -/-) or moderately overexpressed h*SNCA* (+/-). **(B) Experimental genotypes.** Three different genes, *ATG7*, *DAT*, and h*SNCA* were manipulated in this cross, with each gene determined using two different primer sets. An additional gene, mouse *SNCA* (m*SNCA*) is shown here to demonstrate its presence. *ATG7* was present as both wild-type (WT) and flanked by loxP sites ("floxed") (F). The *DAT* gene was present as wild-type (WT), or driving the expression of the cre-recombinase (Cre). The presence or absence of the h*SNCA* gene was confirmed by amplification of the 3' and 5' ends of the h*SNCA* BAC.

3.4.2 Confirmation of Mendelian inheritance of genetic modifications in experimental mouse cohorts

Following the generation of transgenic mice, it was necessary to confirm that mice were born in Mendelian ratios in order to exclude embryonic lethality as a consequence of genetic modification. It was expected that the four different genotypes in the experiment would be born in a 1:1:1:1 ratio, and the results of genotyping did not differ from this ratio (Figure 3.3).



Genotype	Expected ratio	Expected no.	Observed no.	Observed ratio
Control	1	20	16	0.80
h*SNCA*	1	20	19	0.95
*ATG7*cKO$^{DAT\text{-IRES-cre}}$	1	20	22	1.10
h*SNCA*:*ATG7*cKO$^{DAT\text{-IRES-cre}}$	1	20	23	1.15
Total	4	80	80	4

Figure 3.3. Experimental genotypes are inherited in Mendelian ratios.
All litters from three experimental breeding pairs were genotyped and enumerated. There was no statistically significant difference between expected and observed inheritance ratios (chi-square test, $\chi^2(2)=1.50$, $p=0.68$).

3.4.3 Confirmation of functionally impaired macroautophagy as a result of *ATG7* knockout in dopamine neurons

In order to provide evidence of conditional impairment of macroautophagy in *DAT*-positive neurons, fluorescent immunohistochemistry on midbrains from 6 month-old mice was performed for a recognized surrogate marker of macroautophagy impairment, P62 (Figure 3.4) (Friedman *et al.* 2012; Tang *et al.*). P62 accumulates in situations where macroautophagy is impaired. P62 puncta were present in the vast majority of DAT-positive neurons in midbrain sections from *ATG7*cKO$^{DAT\text{-IRES-cre}}$ and hSNCA:*ATG7*cKO$^{DAT\text{-IRES-cre}}$ mice, but were not present in control and h*SNCA* midbrains. These data were further confirmed by examination of the SNc and VTA in 20 to 24 month-old mice (Figures 3.13 and 3.14).

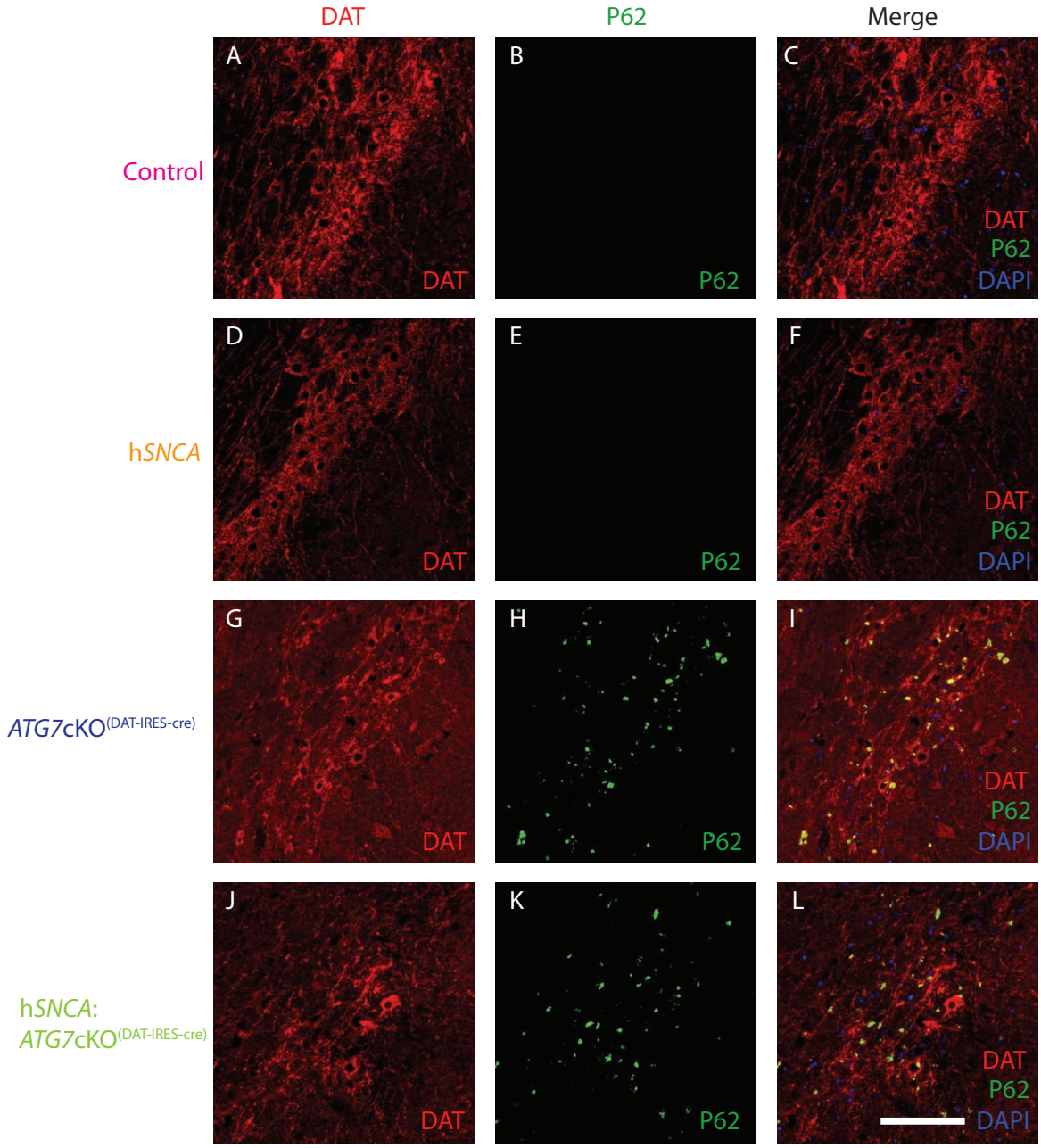


Figure 3.4. Increased P62 in the midbrain of 6 month-old *ATG7*cKO$^{DAT\text{-IRES-cre}}$ mice. Midbrain sections from experimental mice were probed with antibodies against DAT (red) and P62 (green). DAPI is blue. P62 accumulation was observed in DAT-positive neurons in *ATG7*cKO$^{DAT\text{-IRES-cre}}$ mice, consistent with impairment of macroautophagy in these neurons. Scale bar is 100 μM.

3.4.4 Confirmation of human α-synuclein expression in mice carrying the h*SNCA* transgene

In order to verify that human α-synuclein was expressed in mice that were positive for the h*SNCA* transgene, immunoblotting was performed on midbrain lysates from 6 month-old experimental mice (Figure 3.5). Further quantitative immunoblotting for α-synuclein has been carried out by other members of the Wade-Martins laboratory, and this is considered in the discussion section of this chapter.

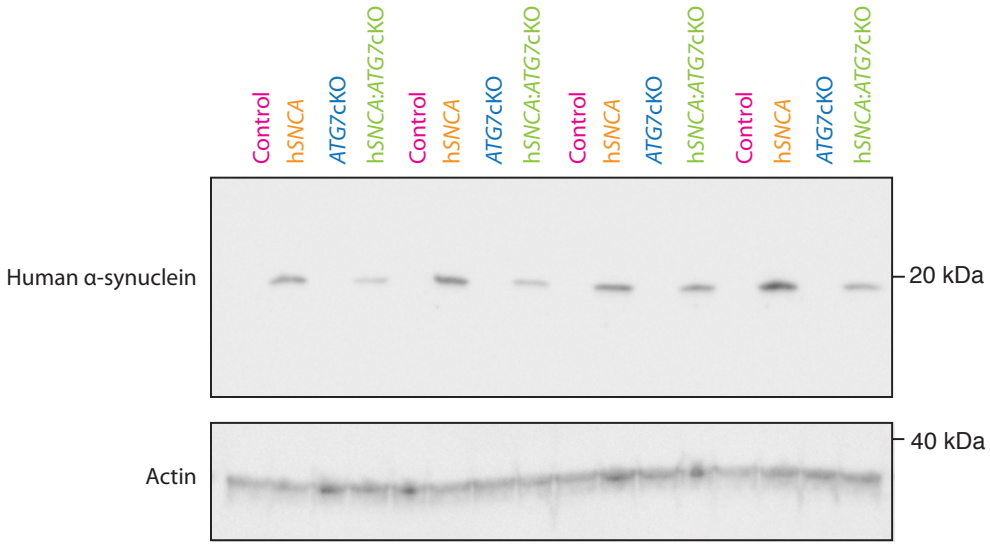


Figure 3.5 Expression of human α-synuclein in 6 month-old transgenic mice.
Midbrain lysates from experimental mice were subjected to immunoblotting and probed with an antibody specific to human α-synuclein (syn211, Abcam). Presence of human α-synuclein was confirmed in mice positive for the h*SNCA* transgene. n=4 mice per transgenic mouse line.

3.4.5 The *ATG7*cKO$^{DAT\text{-IRES-cre}}$ genotype is associated with selective loss of substantia nigra dopamine neurons

Loss of TH-positive DA neurons in the SNc is a cardinal feature of PD (Rudow *et al.* 2008). In order to assess for the effects of impaired macroautophagy and human α-synuclein expression on DA neuron number, unbiased stereological cell-counting of TH-positive neurons was performed on midbrain sections from all experimental genotypes at three different ages: 1 month, 6 months, and 20 to 24 months (Figure 3.6). TH-positive neurons from one hemisphere were counted. A three-way ANOVA demonstrated a reduction in SNc neurons associated with age, and in mice with the *ATG7*cKO$^{DAT\text{-IRES-cre}}$ genotype. Visual inspection of the data suggested that the association between the *ATG7*cKO$^{DAT\text{-IRES-cre}}$ genotype and SNc neuron loss was driven by reduced DA content in the 6 month and 20 to 24 month-old mouse cohorts. There was no association between h*SNCA* overexpression and SNc neuron number. In PD, the DA neurons of the SNc are preferentially lost, whereas the VTA is less affected (Hirsch *et al.* 1988). To further investigate DA neuron loss in the experimental mouse cohorts, stereological analysis was performed in the VTA. In the VTA there was evidence of neuron loss associated with age, but neither *ATG7* deletion, nor h*SNCA* was associated with neuron loss. Loss of DA neurons could also be observed qualitatively in the SNc of experimental mice at 6 and 24 months of age, while the VTA was relatively preserved. Neuron counts were similar to those previously reported by other investigators (Pascual *et al.* 2008; Garcia-Reitböck *et al.* 2010; Hauser *et al.* 2015; Verwey *et al.* 2016). An Appendix is attached at the conclusion of this thesis that gives mean neuron numbers in each genotype in each age group, and also analyses gene effects at each time point using separate two-way ANOVAs.

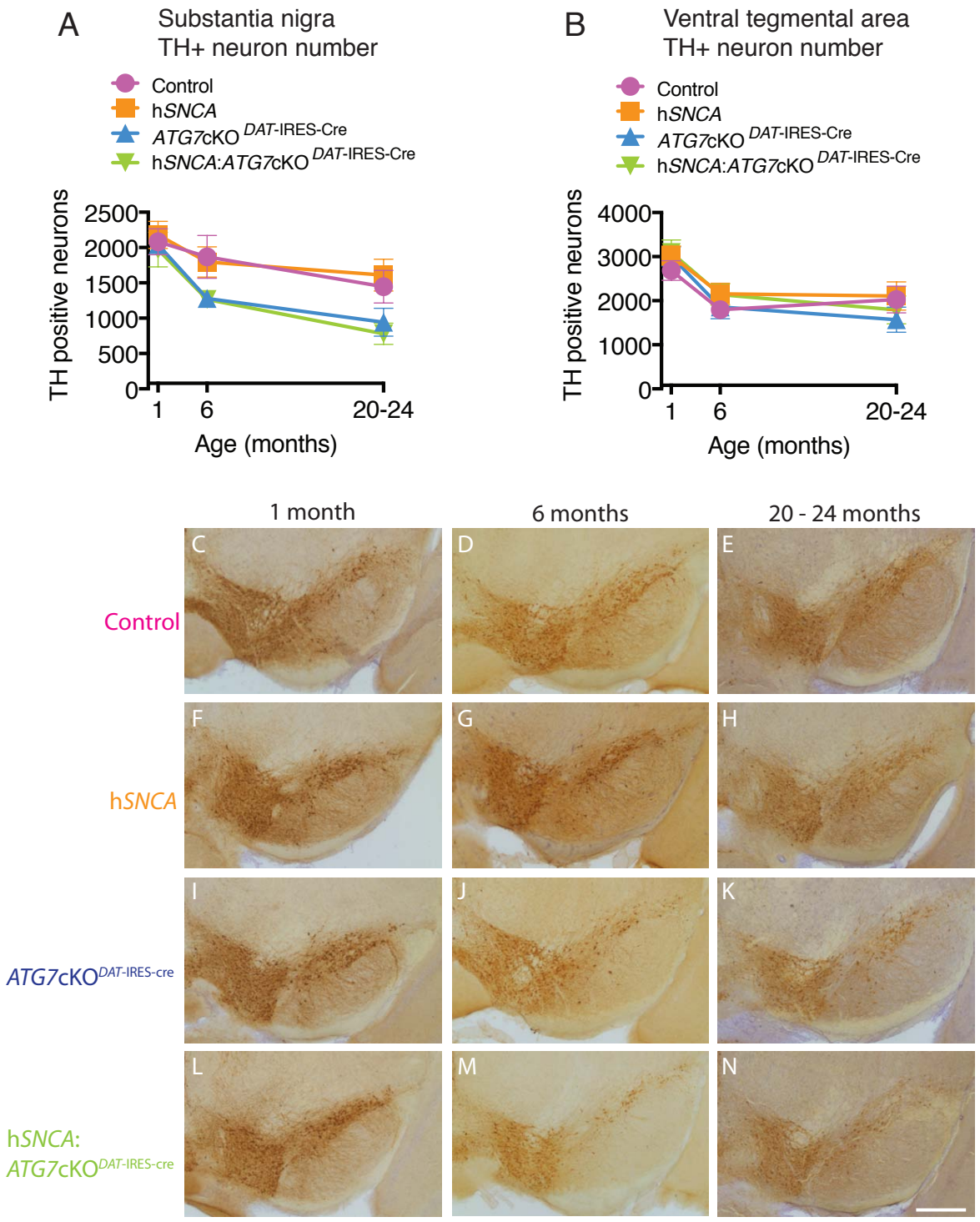


Figure 3.6. The *ATG7*cKO$^{DAT\text{-IRES-cre}}$ genotype is associated with dopamine neuron loss in the substantia nigra pars compacta, but not the ventral tegmental area.
(A) Results of stereological analysis of TH-positive neuron number in the substantia nigra. Three-way ANOVA for age, *ATG7*cKO$^{DAT\text{-IRES-cre}}$, and h*SNCA*. Main effect of age, $F_{(2,44)}$=20.571, p<0.001. Main effect of *ATG7*cKO$^{DAT\text{-IRES-cre}}$, $F_{(1,44)}$=15.133, p<0.001. No other effects or interactions. n=4-6 per transgenic mouse line per age group. **(B) Stereological analysis of TH-positive neuron number in the ventral tegmental area.** Three-way ANOVA for the effect of age, and *ATG7* and h*SNCA* genotypes**.** Main effect of age, $F_{(2,44)}$=19.174, p<0.001. n=4-6 per transgenic mouse line per age group. Data expressed as mean ± standard error of the mean (SEM). **(C-N) Representative midbrain sections of experimental genotypes stained for TH, genotypes and ages as labeled.** Scale bar is 500 μM.

3.4.6 Complex effects of h*SNCA* and *ATG7*cKO$^{DAT\text{-IRES-cre}}$ on caudate-putamen dopamine content

PD is characterised by reduced DA content in the caudate-putamen (Ehringer and Hornykiewicz 1960; Bernheimer *et al.* 1973). SNc neurons project to the caudate-putamen, whereas VTA neurons project primarily to the nucleus accumbens. Loss of SNc neurons, and their projections to the caudate-putamen, is thought to underlie reductions in caudate-putamen DA content in PD. In order to determine DA levels in the caudate-putamen and the nucleus accumbens, HPLC was performed on striatal tissue from mice at 1, 6 and 20 to 24 months of age. Three-way ANOVA of caudate-putamen DA content demonstrated an interaction between age and the h*SNCA* genotype. Pairwise comparisons demonstrated increased caudate-putamen DA in 1 month-old mice carrying the h*SNCA* transgene, but there was no effect of h*SNCA* in later age groups. These data concord with studies in combinatorial knockout mice which have suggested that α-synuclein plays a role in stabilising DA stores (Connor-Robson *et al.* 2016). The *ATG7*cKO$^{DAT\text{-IRES-cre}}$ genotype reduced caudate-putamen DA, independent of age. Visual inspection of the data suggests that the effect of the *ATG7*cKO$^{DAT\text{-IRES-cre}}$ genotype is primarily mediated by reduced caudate-putamen DA content in the 6 and 20 to 24 month age groups. DA content in the nucleus accumbens was unchanged. These data are in keeping with the stereology data, which found reductions in SNc DA neurons associated with the *ATG7*cKO$^{DAT\text{-IRES-cre}}$ genotype, but no changes in VTA DA neuron number.

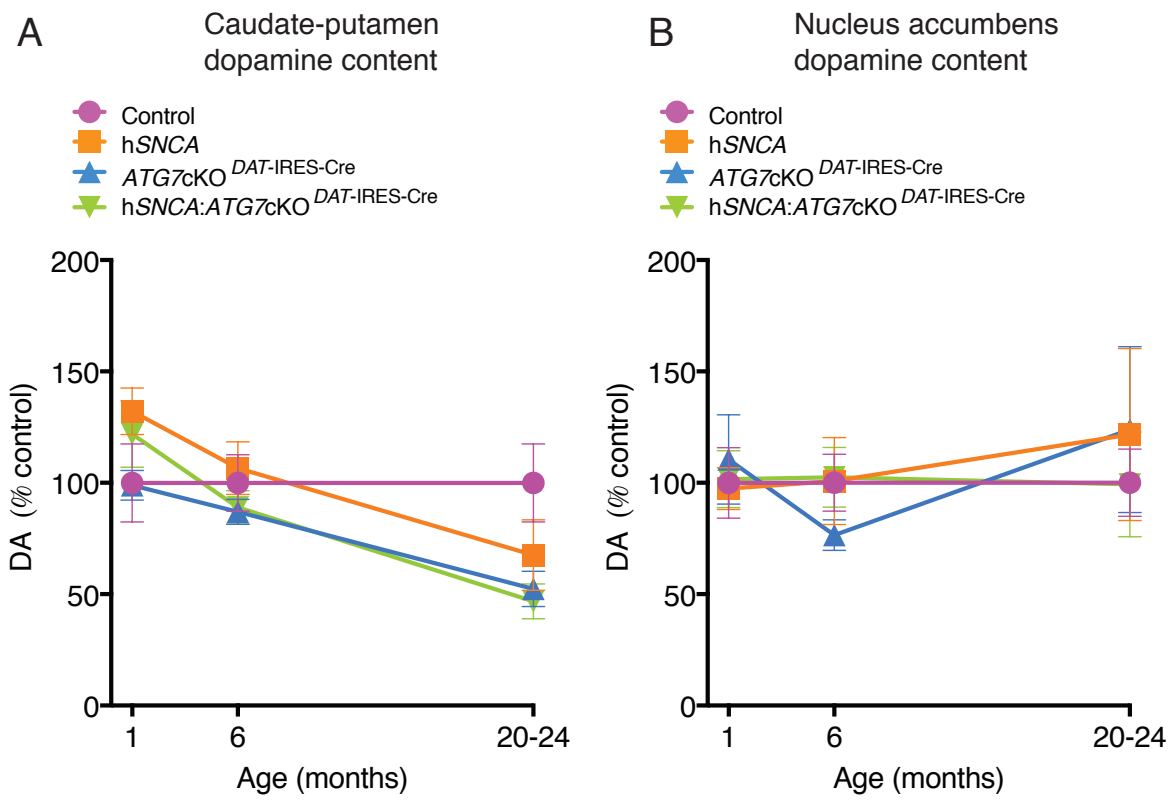


Figure 3.7. The *ATG7*cKO$^{DAT\text{-IRES-cre}}$ genotype is associated with reduced dopamine content in the caudate-putamen, and there are age-related changes in dopamine content associated with the h*SNCA* transgene.
(A) Analysis of dopamine content in the caudate-putamen. Three-way ANOVA for age, *ATG7*cKO$^{DAT\text{-IRES-cre}}$ and h*SNCA*. There was an interaction between age and h*SNCA* $F_{(2,42)}$=3.603, p=0.036. The effect of h*SNCA* was examined at each level of age, with a Bonferonni correction for multiple comparisons. In the 1 month age group, the h*SNCA* genotype was associated with increased dopamine content (126.97% of control ± 9.16% in the hSNCA group and 99.45% ± 9.16% in the group without h*SNCA*). In other age groups there was no significant effect of h*SNCA*. Main effect of age, $F_{(2,42)}$=14.94, p<0.001. Main effect of *ATG7*cKO$^{DAT\text{-IRES-cre}}$, $F_{(1,42)}$=6.73, p=0.013. No other effects or interactions. n=4-5 per transgenic mouse line per age group. **(B) Analysis of dopamine content in the nucleus accumbens.** Three-way ANOVA for the effect of age, and *ATG7*cKO$^{DAT\text{-IRES-cre}}$ and h*SNCA*. No effects or interactions. n=4-5 per transgenic mouse line per age group. Data expressed as mean ± SEM.

3.4.7 Absence of Lewy pathology in h*SNCA*:*ATG7*cKO$^{DAT\text{-IRES-cre}}$ mice aged 20 to 24 months

There are several key features of PD neuropathology. The most important are the loss of DA neurons, and the development of Lewy bodies and Lewy neurites. Evidence of loss of DA neurons was described in the previous section. In order to assess for the development of Lewy pathology, 50 μM thick brain sections from mice aged 20 to 24 months were probed using an antibody directed towards the N-terminus of α-synuclein that recognises both mouse and human α-synuclein. Increased α-synuclein immunoreactivity was observed in mice expressing the h*SNCA* transgene in the striatum, SNc, cortex and hippocampus, but no Lewy pathology was observed (Figures 3.8 and 3.9). In the SNc, cytoplasmic staining of neurons was observed in mice with the h*SNCA* transgene. In the cortex, expression of the h*SNCA* transgene was associated with cytoplasmic α-synuclein staining of cells in the external granule cell and external pyramidal cell layers (Figure 3.9). No major effect of conditional deletion of *ATG7* could be discerned. In order to compare results seen in experimental mice to those gained from standard analysis of human tissue, 4 μM thick paraffin-embedded sections were subjected to an antibody specific to the C-terminus of human of α-synuclein (Figures 3.10 and 3.11). α-Synuclein immunoreactivity was seen only in those mice expressing the h*SNCA* transgene, and, again, no evidence of Lewy pathology was seen. No interaction between *ATG7* deletion and the h*SNCA* transgene on neuropathology was observed.

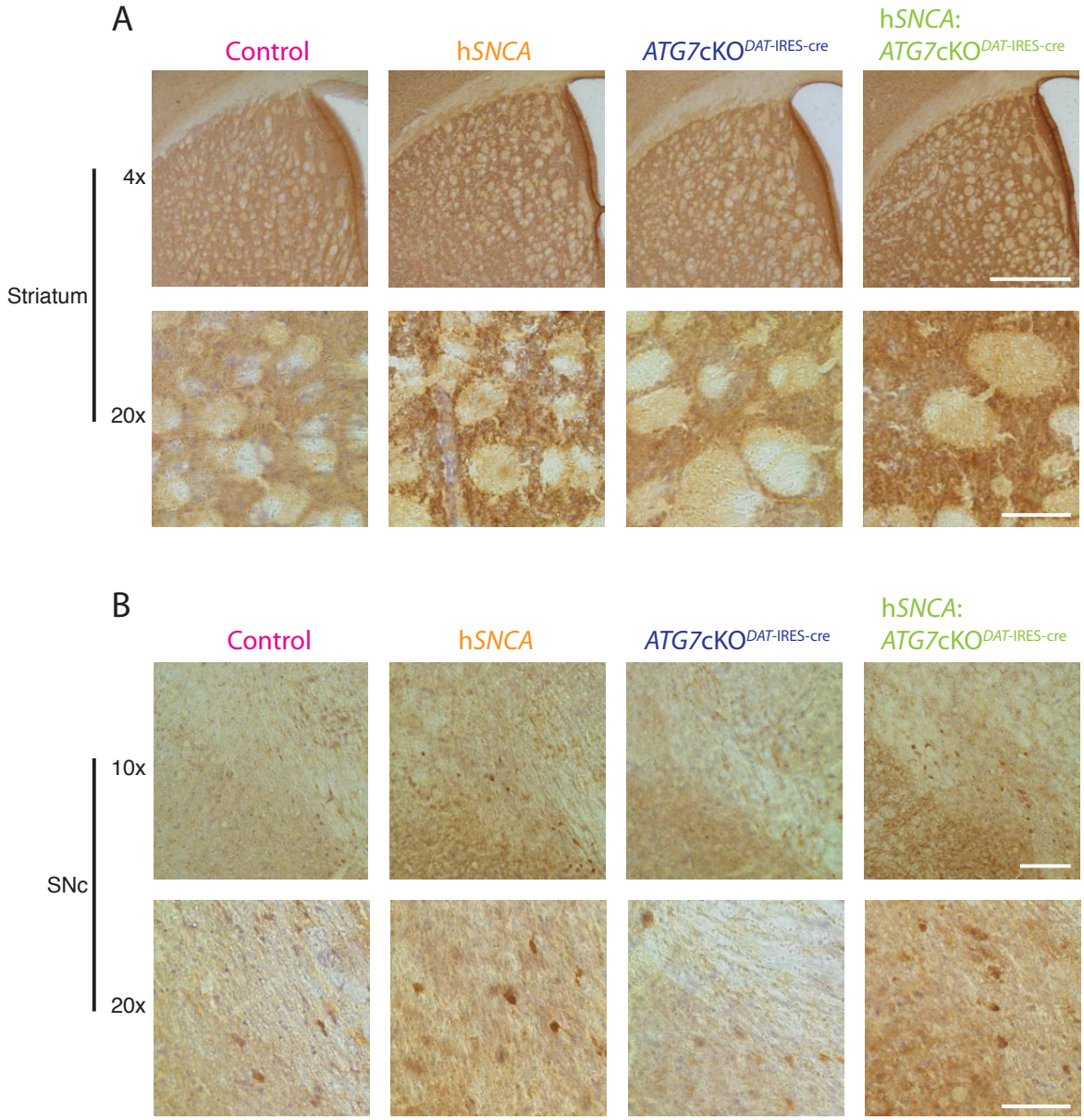


Figure 3.8. Immunohistochemical analysis of α-synuclein expression in the striatum and substantia nigra pars compacta of experimental mice aged 20 to 24 months.
(A) Striatum and (B) substantia nigra pars compacta. Immunohistochemical analyses using an antibody directed to an epitope at the N-terminus of α-synuclein, common to both human and mouse α-synuclein (antibody 610787, BD Biosciences). Note that increased α-synuclein immunoreactivity in the inferior-left quadrant of the 10x SNc images is in the substantia nigra pars reticulata. Representative images are shown of experiments including at least three mice per genotype. 4x scale bar is 500 μM, 10x scale bar is 200 μM, 20x scale bar is 100 μM.

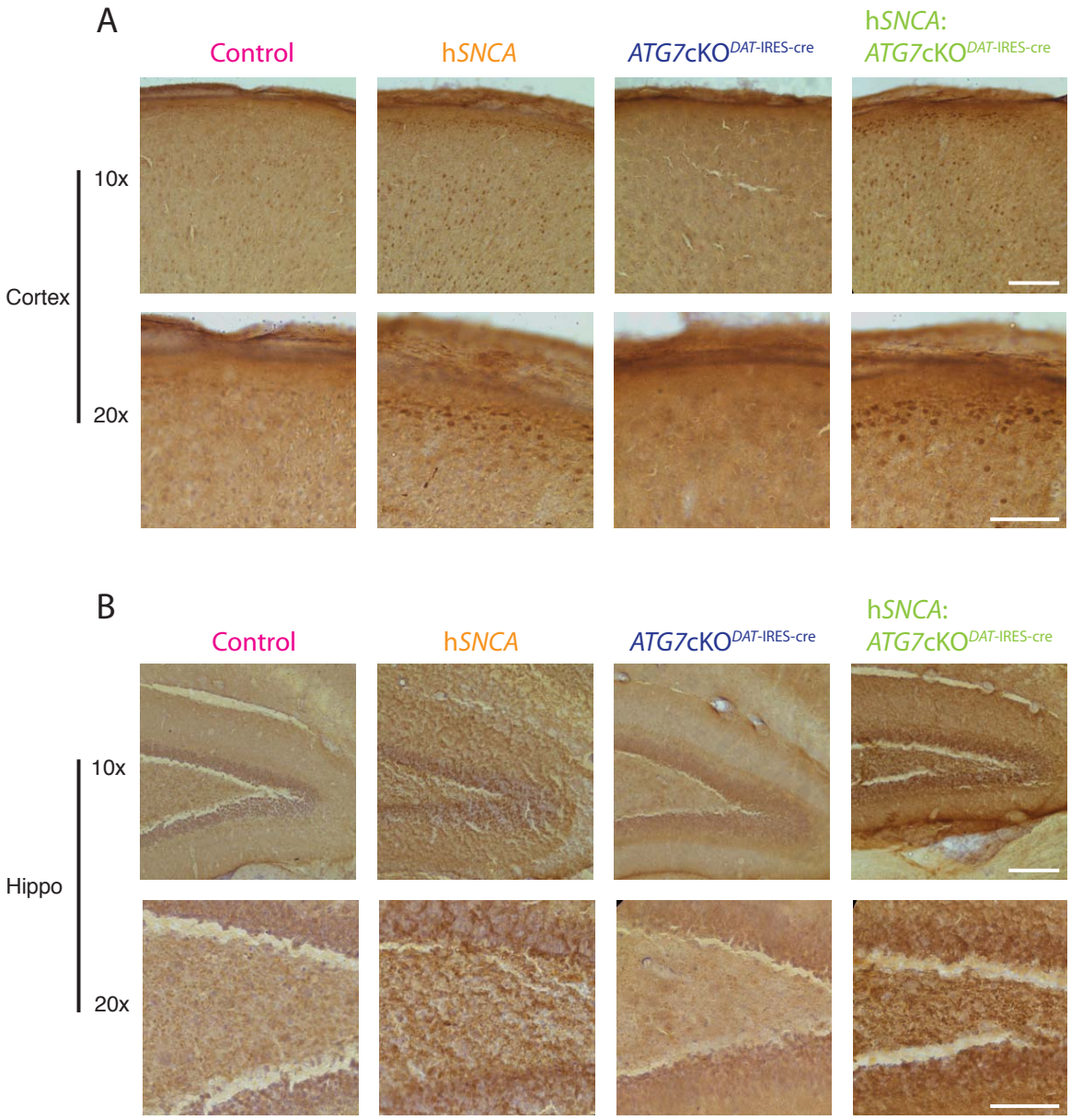


Figure 3.9. Immunohistochemical analysis of α-synuclein expression in the cortex and hippocampus of experimental mice aged 20 to 24 months.
(A) Cortex and (B) Hippocampus. Immunohistochemical analyses using an antibody directed to an epitope at the N-terminus of α-synuclein, common to both human and mouse α-synuclein (BD Biosciences, #610787). Representative images are shown of experiments including at least three mice per genotype. Hippo, hippocampus. 10x scale bar is 200 μM, 20x scale bar is 100 μM.

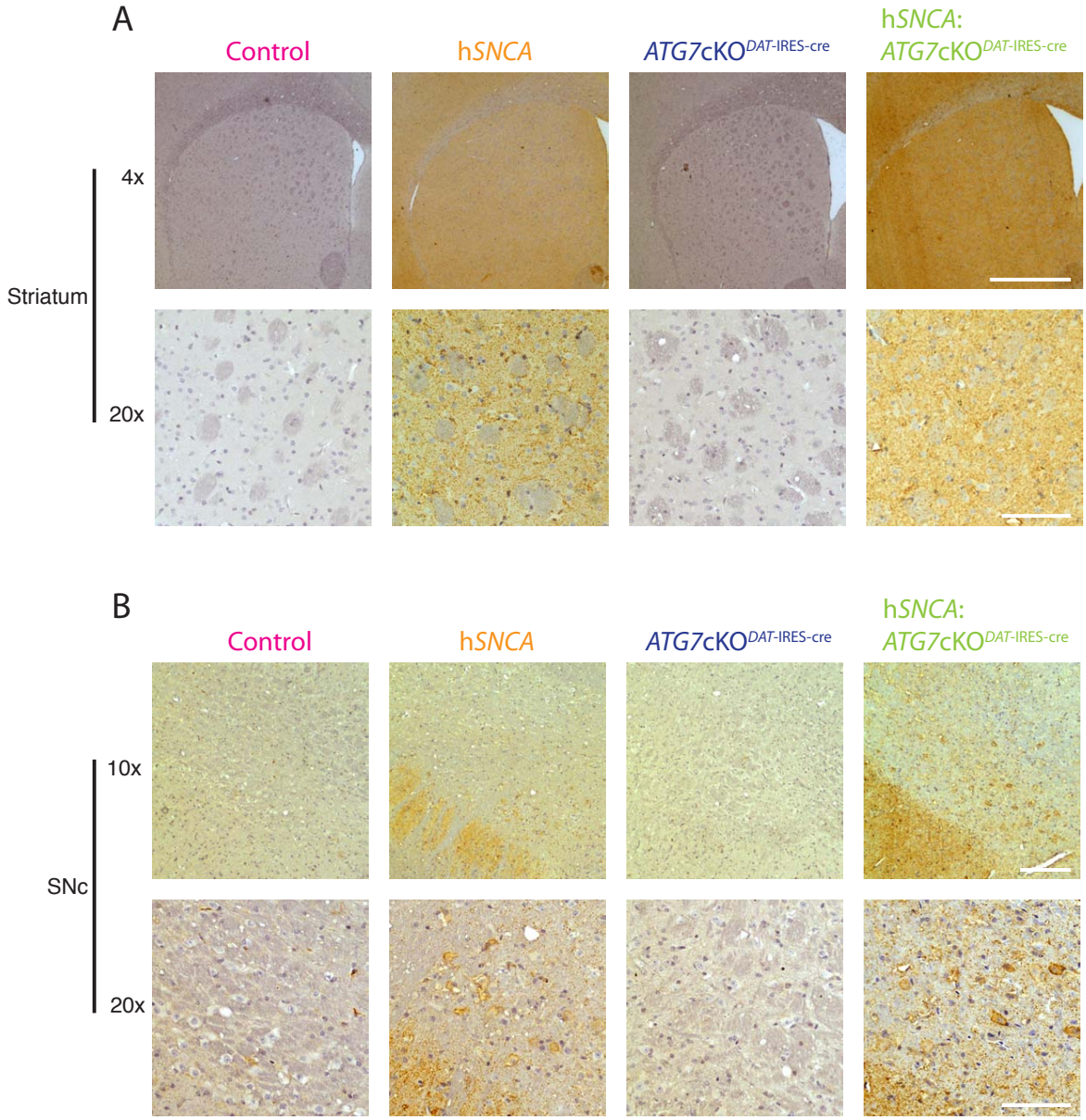


Figure 3.10. Immunohistochemical analysis of human α-synuclein expression in the striatum and substantia nigra pars compacta of experimental mice aged 20 to 24 months.

(A) Striatum and (B) Substantia nigra pars compacta. Immunohistochemical analyses using an antibody directed specfically to an epitope specific to the C-terminus of human α-synuclein (syn211, Abcam). Note that increased α-synuclein immunoreactivity in the inferior-left quadrant of the 10x SNc images is in the substantia nigra pars reticulata. Representative images are shown of experiments including at least three mice per genotype. 4x scale bar is 500 µM, 10x scale bar is 200 µM, 20x scale bar is 100 µM.

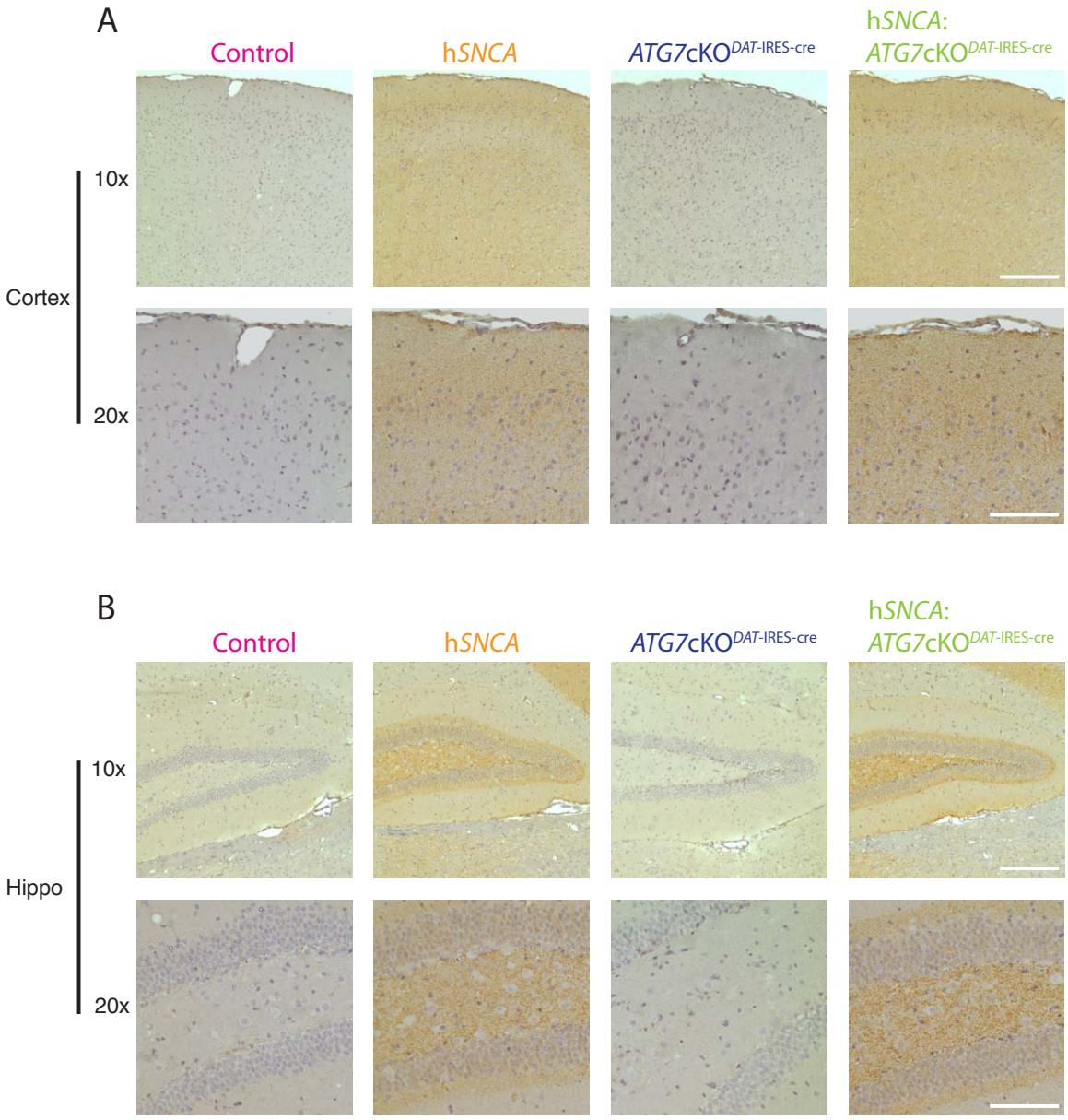


Figure 3.11. Immunohistochemical analysis of human α-synuclein expression in the cortex and hippocampus of experimental mice aged 20 to 24 months.
(A) Cortex and (B) Hippocampus. Immunohistochemical analyses using an antibody directed to an epitope at the C-terminus of α-synuclein, present in human but not mouse α-synuclein (syn211, Abcam). Representative images are shown of experiments including at least three mice per genotype. Hippo, hippocampus.10x scale bar is 200 μM, 20x scale bar is 100 μM.

3.4.8 The *ATG7*cKO$^{DAT\text{-IRES-cre}}$ genotype causes the accumulation of macroautophagic substrates in substantia nigra neurons, resembling some aspects of Parkinson's disease

In order to determine the extent to which impairment of macroautophagy in DA neurons causes a histological phenotype comparable to PD, a direct comparison was made between experimental mice and human PD neuropathology for three neuropathological markers of PD: α-synuclein, ubiquitin and P62 (Figure 3.17). Ubiquitin and P62 are both alternative markers of Lewy pathology, and also autophagic substrates, and the presence of these markers was assessed using DAB immunohistochemistry. In this comparison, it can be seen that α-synuclein immunoreactivity in experimental mice is punctate (Figure 3.12D and 3.12J) and there is no evidence of the Lewy-like aggregates seen in the PD brain (Figure 3.12M and 3.12P). Small ubiquitin-positive aggregates can be observed in mice with the *ATG7*cKO$^{DAT\text{-IRES-cre}}$ genotype (Figure 3.12H and 3.12K) that approach the size of intracellular ubiquitin aggregates seen in human PD, but do not reach the relative size or shape of a Lewy body. Donut-shaped P62 aggregates can be seen in *ATG7*cKO$^{DAT\text{-IRES-cre}}$ genotype (Figure 3.12I and 3.12L) that are similar to the intracellular Lewy bodies (relative to neuron size) seen in PD patients. No extracellular α-synuclein, ubiquitin or P62 aggregates were observed in these mice.

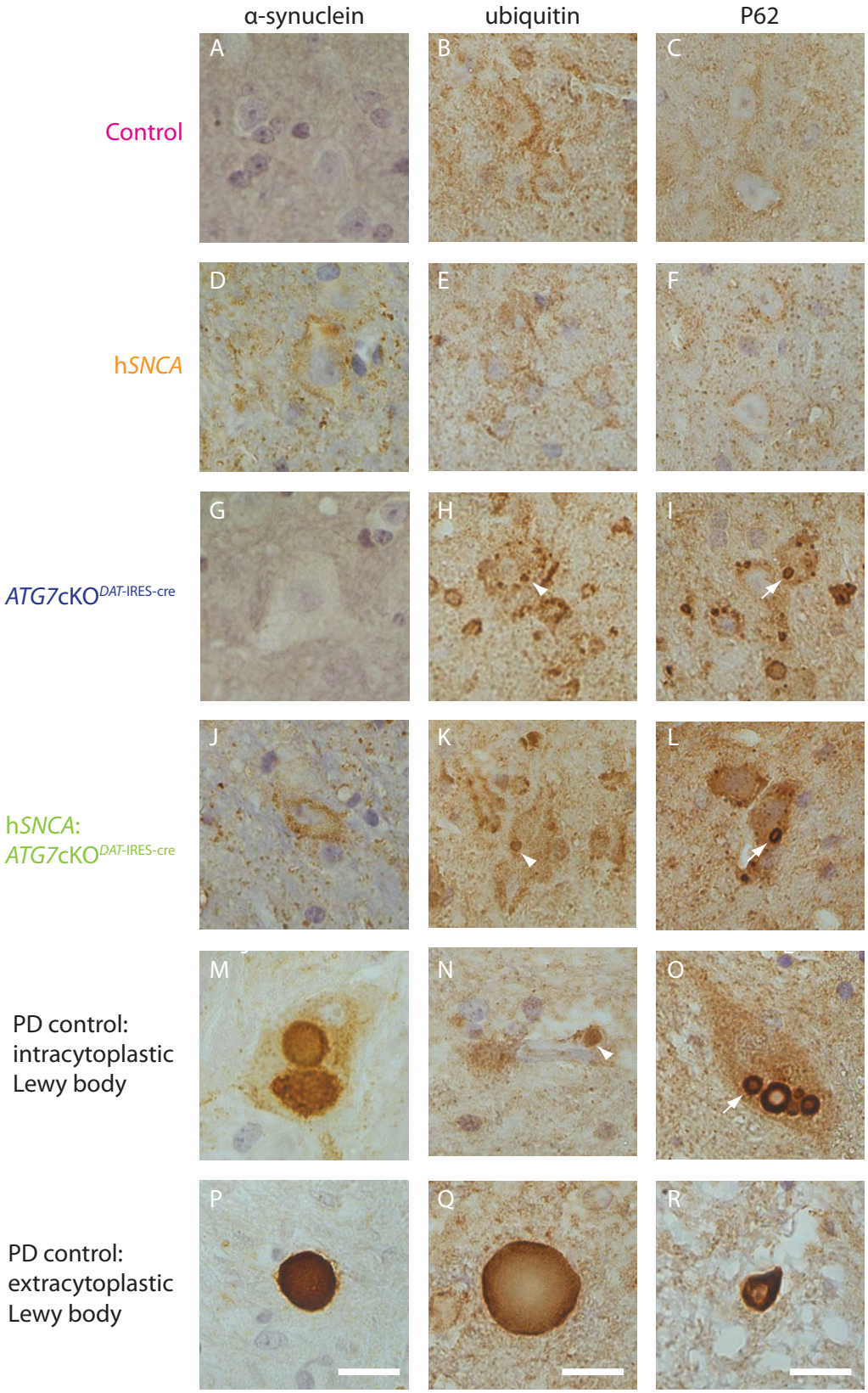


Figure 3.12. High-magnification comparison of human α-synuclein, ubiquitin and P62 staining in the substantia nigra of experimental mice and human Parkinson's disease controls.

(A-R) Sections from experimental mouse genotypes and human Parkinson's patients, as labeled. Representative images are shown of at least three mice per genotype. Scale bar is 20 μM. Ubiquitin inclusions are indicated with arrowheads, and P62 inclusions with arrows. α-Synuclein staining in panels M and P was performed by Dr. R. Roberts (Oxford) using the same techniques, as part of the routine characterisation of the patient cohort.

3.4.9 Characterisation of macroautophagic substrates in dopamine neurons neurons of mice aged 20 to 24 months using immunofluorescent immunohistochemistry

Further characterisation of P62 and ubiquitin inclusions was performed using immunofluorescent immunohistochemistry on brain slices from mice aged 20 to 24 months. Large P62 aggregates were visualised in DAT-positive neurons in the SNc, consistent with the findings previously described in 6 month-old mice (Figure 3.13). P62 was also examined in the VTA (Figure 3.14), in order to determine if there were any demonstrable differences between VTA and SNc neurons and their handling of autophagic cargo. If present, this might explain the relative preservation of VTA neurons when compared to SNc neurons, however no differences were found. There was a qualitative reduction in the number of SNc DAT-positive neurons, consistent with the stereological data discussed earlier. Compared to the P62 staining, smaller and less frequent ubiquitin aggregates were visualized in DAT-positive neurons (Figure 3.15).

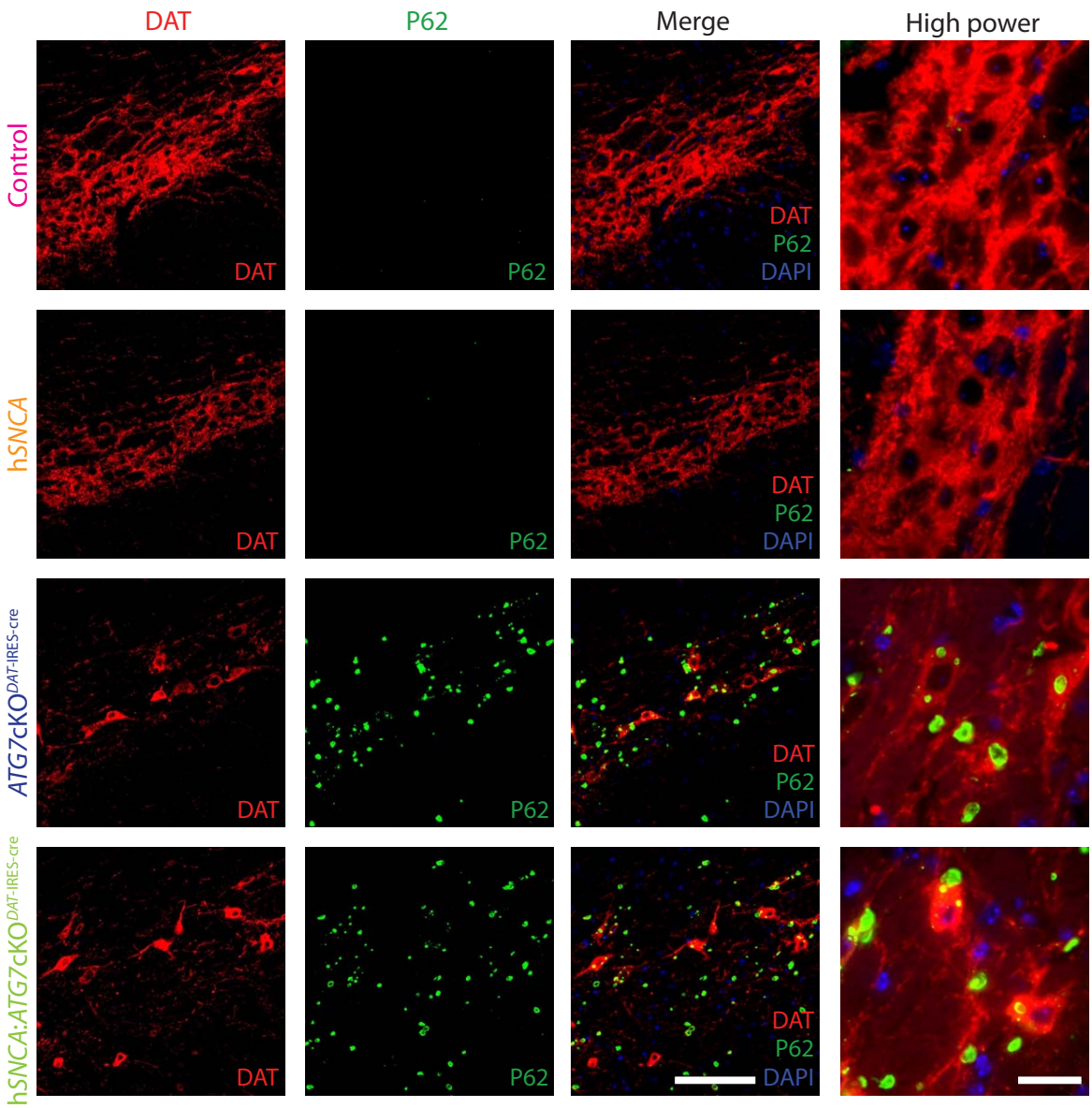


Figure 3.13. P62 aggregates develop in the substantia nigra pars compacta of 20 to 24 month-old mice when macroautophagy is impaired in DAT-positive neurons.
Midbrain sections from experimental mice were probed with antibodies against DAT (red) and P62 (green). DAPI is blue. Representative images are shown of experiments including at least three mice per genotype. A reduction in the number of DAT-positive neurons can also be observed, consistent with stereological data. Low magnification scale bar is 100 µM. High magnification scale bar is 25 µM.

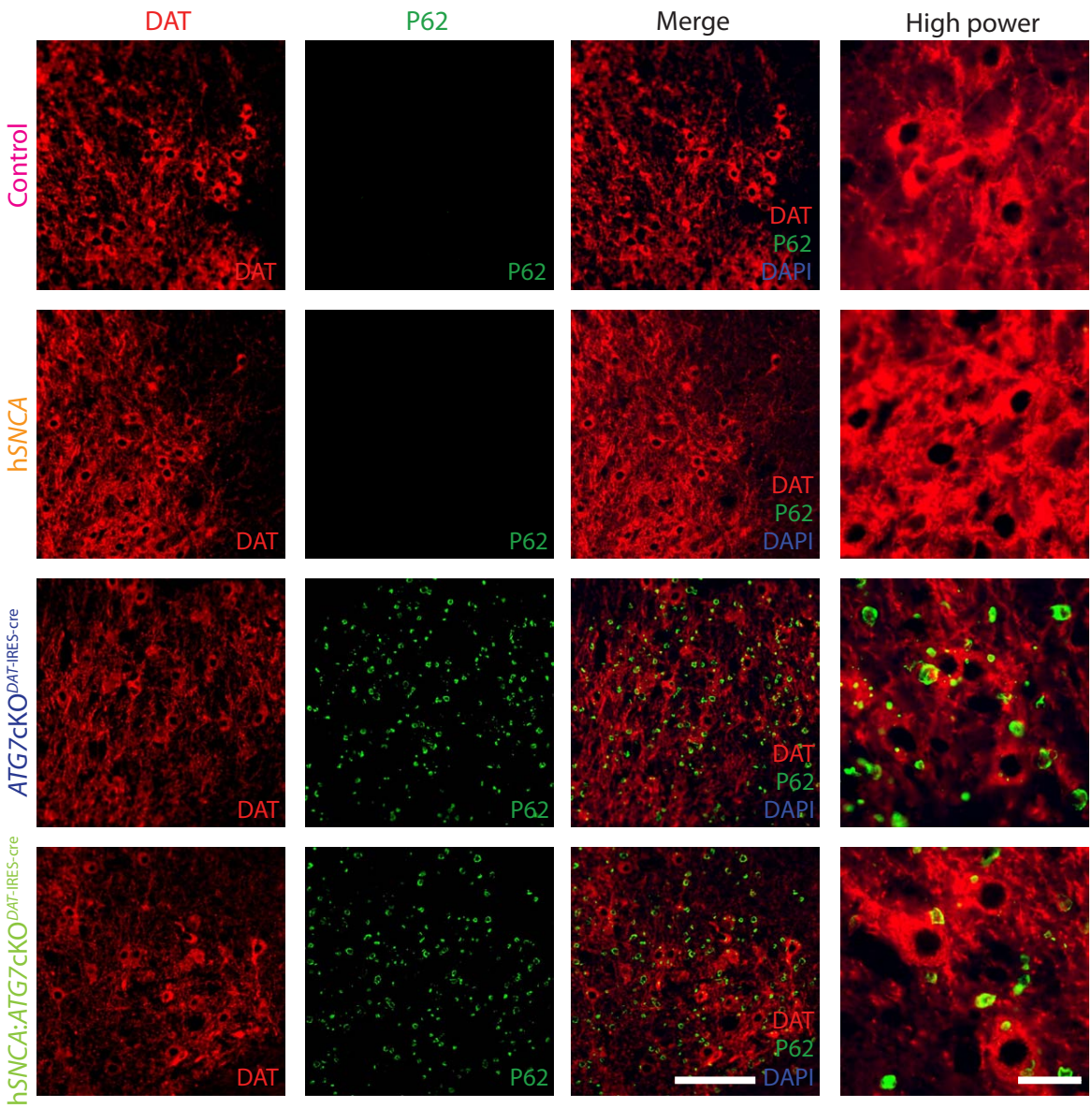


Figure 3.14. P62 aggregates in the ventral tegmental area of 20 to 24 month-old mice when macroautophagy is impaired in DAT-positive neurons.
Midbrain sections from experimental mice were probed with antibodies against DAT (red) and P62 (green). DAPI is blue. Representative images are shown of experiments including at least three mice per genotype. Low magnification scale bar is 100 μM. High magnification scale bar is 25 μM.

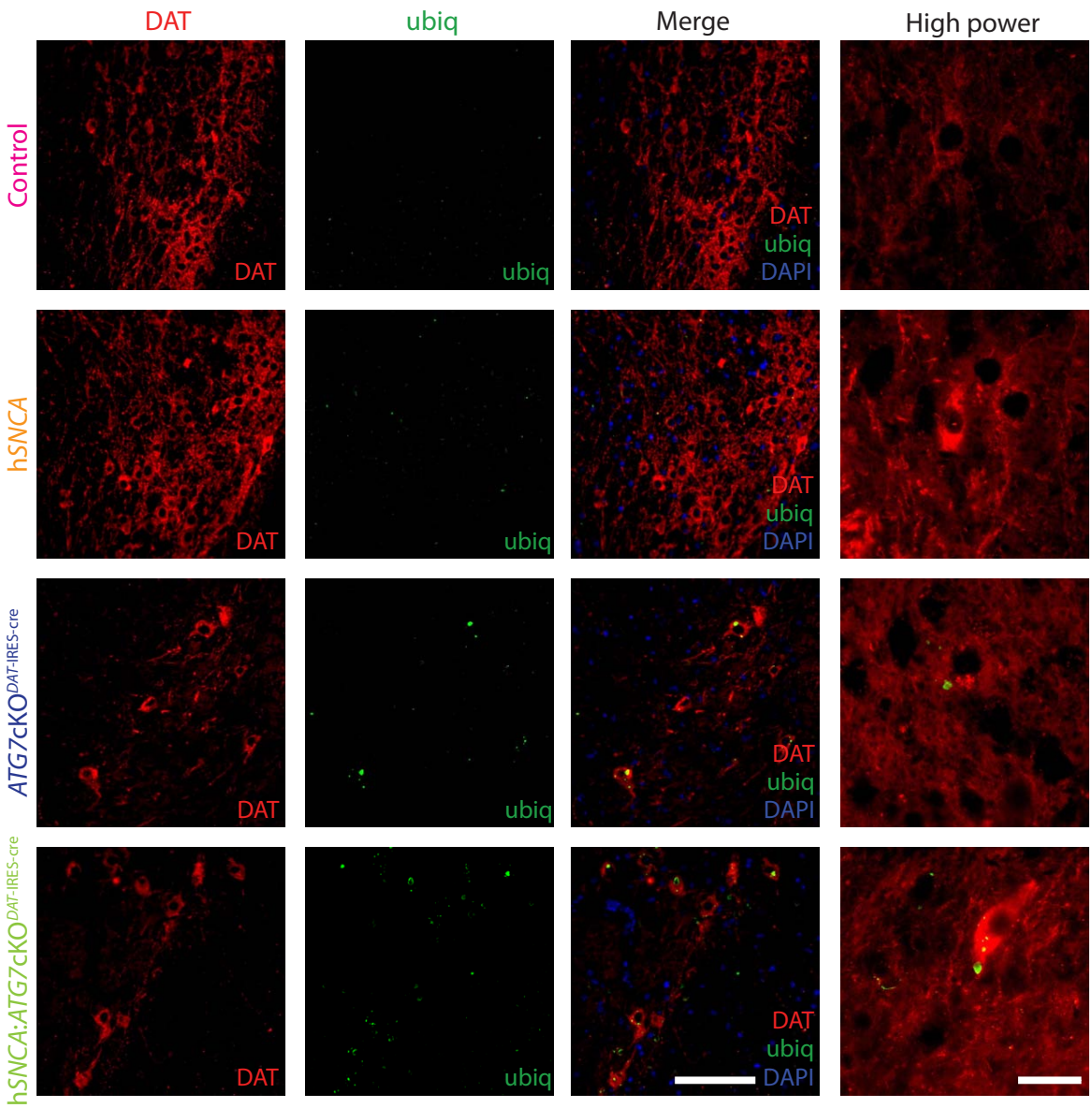


Figure 3.15. Occasional ubiquitin aggregates develop in substantia nigra dopamine neurons of 20 to 24 month-old mice when macroautophagy is impaired in DAT-positive neurons.
Midbrain sections from experimental mice were probed with antibodies against DAT (red) and ubiquitin (ubiq - green). DAPI is blue. Representative images are shown of at least three mice per genotype. A reduction in the number of DAT-positive neurons can also be observed, consistent with stereological data. Low magnification scale bar is 100 μM. High magnification scale bar is 25 μM.

3.5 Discussion

3.5.1 Data from collaborative experiments on hSNCA:*ATG7*cKO$^{DAT\text{-IRES-cre}}$ mice

Other researchers in the Wade-Martins laboratory have performed further experiments on the hSNCA:*ATG7*cKO$^{DAT\text{-IRES-cre}}$ mouse line that may prove informative for the interpretation of this thesis. Using sections from 20 to 24 month-old mice, an α-synuclein proximity ligation assay (PLA) was performed (N. Bengoa-Vergniory, in preparation). This assay detects oligomers of α-synuclein (Roberts *et al.* 2015). As expected, the h*SNCA* transgene increased the number of α-synuclein oligomers present in the midbrain and striatum, but there was no effect of the *ATG7*cKO$^{DAT\text{-IRES-cre}}$ genotype. This is consistent with the data presented in this chapter, which found that *ATG7*cKO$^{DAT\text{-IRES-cre}}$ did not have a modifying effect on α-synuclein histology in regards to increasing the observable amount of α-synuclein, or changing the way in which it was distributed. Quantitative western blotting has also been performed on 1 month-old mice, which found no differences in α-synuclein levels (S. Vingill, in preparation). However, striatal DAT levels were slightly reduced at 1-month, despite the absence of cell loss at this time point, suggesting an early pathological phenotype, or an effect of impaired macroautophagy on DAT expression. This reduction in DAT expression will become salient later in this thesis, when DA neurotransmission is considered.

3.5.2 Degeneration of the nigrostriatal system

Loss of SNc DA neurons is perhaps the single most important pathological feature of PD. In this study, deletion of *ATG7* in DA neurons was associated with loss of approximately

40% of SNc neurons, when compared with age-matched controls. This result is in line with previous studies (Friedman *et al.* 2012; Inoue *et al.* 2012; Ahmed *et al.* 2012; Niu *et al.* 2016), and is notable in that it probably represents the greatest loss of SNc DA neurons observed in a transgenic mouse model of PD. VTA DA neurons were not reduced in number in *ATG7*cKO$^{DAT\text{-IRES-cre}}$ mice, suggesting that ability to withstand impaired macroautophagy may be one of the features contributing to VTA neuron survival in PD. The extent of SNc DA neuron loss was very similar at 6 months and 20 to 24 months – approximately 40% of neurons were lost in both age groups. These raises the possibility that there may be a resistant population of DA neurons in the SNc that are not susceptible to macroautophagic impairment, and that are able to survive into old age. The relative preservation of VTA neurons mirrors the pattern seen in human disease (Hirsch *et al.* 1988). Some of the factors that have been put forward to account for the survival of VTA neurons in PD may be at play here. These include expression of calbindin and GIRK2. Calbindin is a calcium buffer that is enriched in VTA DA neurons when compared to SNc DA neurons, and is thought to protect against degeneration in PD (Yamada *et al.* 1990; Chung 2005). GIRK2 is a potassium channel that may mediate toxicity; its expression is higher in SNc neurons than VTA neurons (Chung 2005). Missense mutations in GIRK2 cause loss of SNc neurons in mice, with the VTA unaffected (Graybiel *et al.* 1990).

A limitation of the stereological study in this thesis is that a separate cell marker was not investigated. For example, some investigators use Nissl staining to demonstrate the total number of cells present in the SNc and VTA, and ensure that a reduction in TH-positive neurons is not due to down-regulation of TH. These experiments were not performed due to time limitations, and also because other researchers have already verified the finding of

reduced DA neurons in *ATG7*cKO$^{DAT\text{-IRES-cre}}$ mice using such techniques (Ahmed *et al.* 2012).

3.5.3 Histological features of Parkinson's disease neuropathology

The key histological features of PD neuropathology are Lewy bodies and Lewy neurites. Frank Lewy pathology did not develop in mice examined in this chapter. However, small P62-positive aggregates similar to intracytoplasmic Lewy bodies were observed, associated with macroautophagy impairment. This is consistent with P62 being much more specific for the macroautophagic pathway than, for example ubiquitin, which also has key roles in the UPS, and can be degraded by the UPS.

In the mice characterized in this chapter, the expression of the human α-synuclein transgene had no effect on neuron number or pathological features of PD, beyond increase α-synuclein immunoreactivity, which could be expected. This differs from the findings of our laboratory previously reported in Janezic *et al.* (2013). As discussed in a Section 3.5.5, this may be associated with the presence of endogenous mouse α-synuclein.

3.5.4 Absence of interaction between impaired macroautophagy and human α-synuclein

In the results presented in this chapter, there was little evidence of an interaction between macroautophagy impairment and human α-synuclein. This finding is pertinent to consideration of α-synuclein degradation pathways. For example, if macroautophagy was the only pathway by which α-synuclein was degraded, then DAT-positive neurons where

ATG7 was deleted should accumulate large amounts of α-synuclein with age – this was not the case. This suggests that, at least in this model, other pathways are sufficient to degrade excess α-synuclein. For example, the UPS or chaperone-mediated autophagy may have been able to eliminate excess α-synuclein from the cytoplasm, thus preventing the formation of aggregates.

3.5.5 Limitations of the model system

There are broad limitations to the mouse model system used in this thesis. The development of endogenous Lewy bodies has never been demonstrated in any mouse model of PD, and it may be that there are proteins or other molecules that prevent Lewy pathology from forming in mice. It may be necessary to use higher-order mammals, such as non-human primates, to accurately model Lewy body disease.

A factor that may have prevented the toxicity and aggregations of human α-synuclein used in this experiment is the presence of endogenous mouse α-synuclein. The mice described in this thesis are bred on a wild-type mouse α-synuclein background, as mouse *SNCA* and *ATG7* are in close proximity on chromosome 6 of the mouse genome, precluding breeding of a mouse featuring both knockout of mouse *SNCA* and a floxed *ATG7* allele in the absence of rare homologous recombination events. Cabin and colleagues (2005) have previously demonstrated that the presence of endogenous mouse α-synuclein mitigates toxicity of human A53T α-synuclein overexpression in a mouse model. Similarly, Fares *et al.* (2016) have shown that the presence of mouse α-synuclein prevents the fibrillisation and toxicity of human α-synuclein. However, the use of α-synuclein knockout mice is not

without problems; mice that lack α-synuclein have fewer DA neurons, in addition to DA release phenotypes which may confound any results associated with other genetic manipulations (Robertson *et al.* 2004).

In this thesis conditional deletion of *ATG7* has been used as a tool to impair macroautophagy. Accordingly, absence of *ATG7* is taken to be synonymous with impairment of macroautophagy. While deletion of *ATG7* is a common tool to cause macroautophagy impairment (Komatsu *et al.* 2006; Hernandez *et al.* 2012), it must be recognised that *ATG7* may have other, as yet unknown, functions outside the autophagic pathway. Therefore it may be more accurate to attribute the results presented in this thesis to be those of *ATG7* knockout, rather than impaired macroautophagy specifically.

As discussed in the introduction to this chapter, the options for studying the impairment of macroautophagy in DA neurons are limited. More general impairment of macroautophagy via genetic or chemical means is associated with reduced survival, precluding aging experiments. An alternative to the methods used here would be to inject a viral construct that impairs macroautophagy into the SNc or CPu, however this would have effects on both neurons and glia. A possible alternative to the use of conditional deletion of *ATG7* in DA neurons would be to use a similar breeding scheme, but to utilise deletion of *ATG5* instead. *ATG5* is on chromosome 10 in mice, and therefore mice with floxed *ATG5* on an *SNCA* knockout background could be generated.

3.5.6 Summary of findings from this chapter

In this chapter, the generation and validation of a novel transgenic mouse to model aspects of PD, and appropriate controls, was described. In addition, the histological characterisation of this model was performed. The model consisted of overexpression of the human α-synuclein gene and impairment of macroautophagy in DA neurons. The observations associated with this model are summarised in Table 3.1. Impairment of macroautophagy in DA neurons was associated with a 40% loss of DA neurons, the development of multiple P62-positive aggregates and smaller, more occasional, ubiquitin aggregates. No Lewy pathology was observed. h*SNCA* was associated with increased caudate-putamen DA content in young mice, and the *ATG7*cKO$^{DAT\text{-IRES-cre}}$ genotype was associated with reduced caudate-putamen DA, independent of age.

Table 3.1. Summary of neuropathological effects of *ATG7*cKO$^{DAT\text{-IRES-cre}}$ and h*SNCA* genotypes in experimental mice

Effect of gene on features of Parkinson's disease:	***ATG7*cKO$^{DAT\text{-IRES-cre}}$**	**h*SNCA***
SNc DA neuron number	Reduced	No effect
VTA DA neuron number	No effect	No effect
Caudate-putamen DA content	Reduced	Increased at 1 month
Nucleus accumbens DA content	No effect	No effect
Lewy bodies	None	None
Lewy neurites	None	None
P62 inclusions	Present	No effect
Ubiquitin inclusions	Present	No effect

DA, dopamine; DAT, dopamine transporter; SNc, substantia nigra pars compacta; VTA, ventral tegmental area.

Chapter 4: Behavioural characterisation of a mouse model to examine the interaction between human alpha-synuclein and impaired macroautophagy in dopamine neurons

4 Behavioural characterisation of a mouse model to examine the interaction between human alpha-synuclein and impaired macroautophagy in dopamine neurons

4.1 Overview

PD is characterised by the motor symptoms of bradykinesia, tremor, rigidity and postural instability. In addition, a number of non-motor symptoms contribute significantly to the burden of PD. Non-motor symptoms include olfactory dysfunction, constipation, cognitive deficits, anxiety and depression. Various tests have been proposed and utilised to examine transgenic rodents for the presence of symptoms analogous to those seen in PD. Commonly used tests of rodent motor function include latency to fall from an accelerating rotating rod ("rotarod"), gait analysis, and measurement of activity in an open field. Importantly, some of these motor tests have been validated using models that are known to have degeneration of the nigrostriatal system, such as mice intoxicated with MPTP (Colotla *et al.* 1990). A number of tests have been used to examine non-motor phenotypes, such as stool collection as an assessment of gastrointestinal function, olfactory discrimination tests to examine for hyposmia, and use of simple mazes to determine cognitive phenotypes. In this chapter, such tests have been utilised to examine for parkinsonian phenotypes in the experimental mice generated in Chapter 3. The behavioural tests used in this chapter are summarised in Table 4.1.

Table 4.1. Summary of behavioural assays used to phenotype experimental mice

Disease aspect	Behavioural assays
Motor function	Inverted screen, spontaneous locomotor activity, rotarod, digital gait analysis
Gastrointestinal function	Stool collection
Cognitive function	Spontaneous alternation in a T-maze, forced alternation in a Y-maze
Olfactory function	Paired odour discrimination
Depression	Tail suspension
Anxiety	Elevated-plus maze

4.2 Aims of Chapter 4

1. To examine experimental mice for the presence of motor phenotypes consistent with PD, including impairment of locomotor activity, motor coordination, and gait.
2. To examine experimental mice for the presence of non-motor phenotypes consistent with PD, including changes in gastrointestinal function, olfaction, cognitive deficits, and anxiety and depression-like symptoms.

4.3 Results

4.3.1 General health and characteristics of experimental mice

Mice were aged to either 3 or 21 months and subjected to a battery of tests to discern phenotypes relevant to PD. During the ageing process, mice were routinely monitored for the development of health defects or behavioural abnormalities. Some mice in the cohort aged to 21 months developed ulcerative dermatitis, although this did not differ between genotypes and was similar to that routinely found in the C57BL/6 strain (Kastenmayer *et al.* 2006). Mice carrying transgenes (either h*SNCA*, *ATG7*cKO$^{DAT\text{-IRES-cre}}$ or both) appeared identical to control mice. Weights of mice did not differ by genotype, although did increase with age (Figure 4.1).

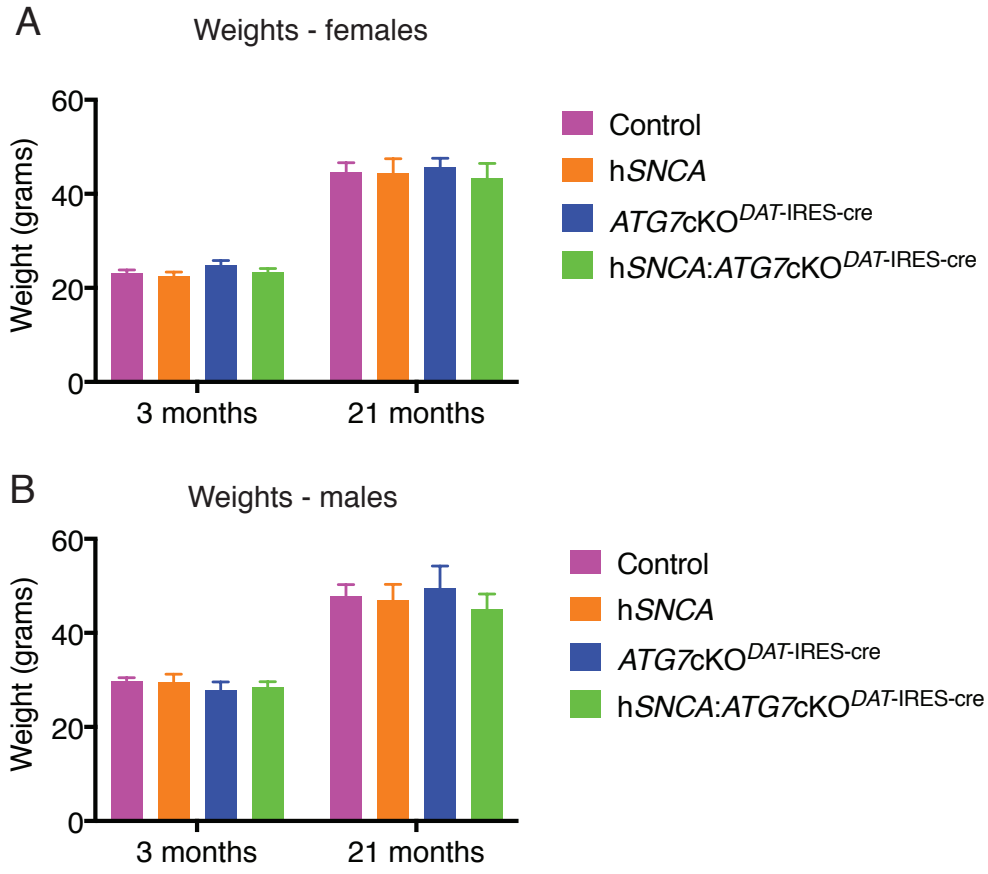


Figure 4.1. Weight does not differ between experimental genotypes.
Data separated by sex is shown for clarity. Three-way ANOVA for age, *ATG7*cKO$^{DAT\text{-IRES-cre}}$ and h*SNCA* genotypes. Main effect of age: $F_{(1,110)}$=278.784, p<0.001. No other effects or interactions. Data are expressed as mean ± SEM.

4.3.2 Assessment of the effects of impaired macroautophagy in dopamine neurons and human α-synuclein expression on motor function in transgenic mice

4.3.2.1 Older mice have reduced muscle strength

A number of tests were performed to assess motor function in the transgenic mouse cohorts that were established in Chapter 3. To begin with, muscle strength was assessed using Kondziela's inverted screen test, in which mice are placed on a wire grid, which is then inverted, and the fall latency of mice is measured (Figure 4.2). This is a screening test to establish if any deficits associated with impaired muscle strength are present between genotypes that may impact on tests of motor function. The maximum score is 60 seconds, after which time mice are removed from the grid. There was a reduction in performance on this test associated with age, but no differences were found associated with experimental genotypes.

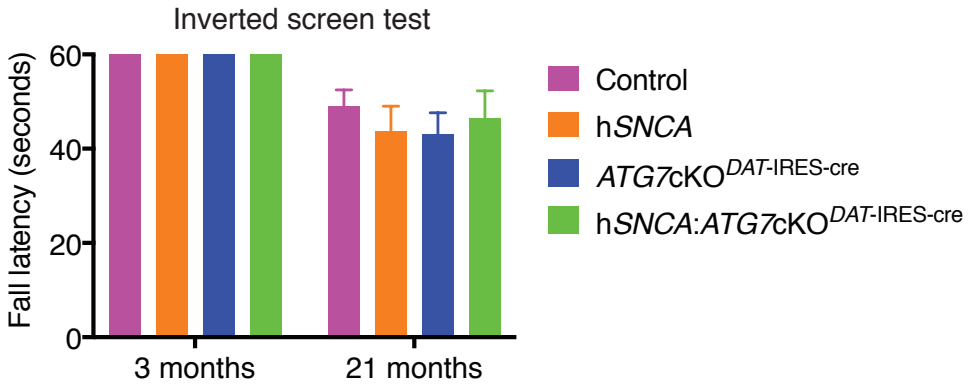


Figure 4.2. Muscle strength does not differ between experimental genotypes.
Data were not normally distributed. Three-way ANOVA for age, *ATG7*cKO$^{DAT\text{-IRES-cre}}$ and h*SNCA* genotypes. Main effect of age: $F_{(1,106)}$=47.776, p<0.001. No other effects or interactions. n=9-19 per transgenic mouse line per age group. Data are expressed as mean ± SEM.

4.3.2.2 The *ATG7*cKO$^{DAT\text{-IRES-cre}}$ genotype is associated with hyperlocomotion

Locomotor activity of mice was measured as an initial examination of motor function. Reductions in locomotor activity have been observed in toxin and genetic models of PD, however there is no demonstrable human corollary (Colotla *et al.* 1990; Baiguera *et al.* 2012). Mice were placed in the non-anxiogenic open field for 4 hours and total activity assessed by means of photobeam breaks. The *ATG7*cKO$^{DAT\text{-IRES-cre}}$ genotype was associated with increased locomotor activity, independent of age (Figure 4.3). This finding is consistent with previous reports in the literature (Ahmed *et al.* 2012).

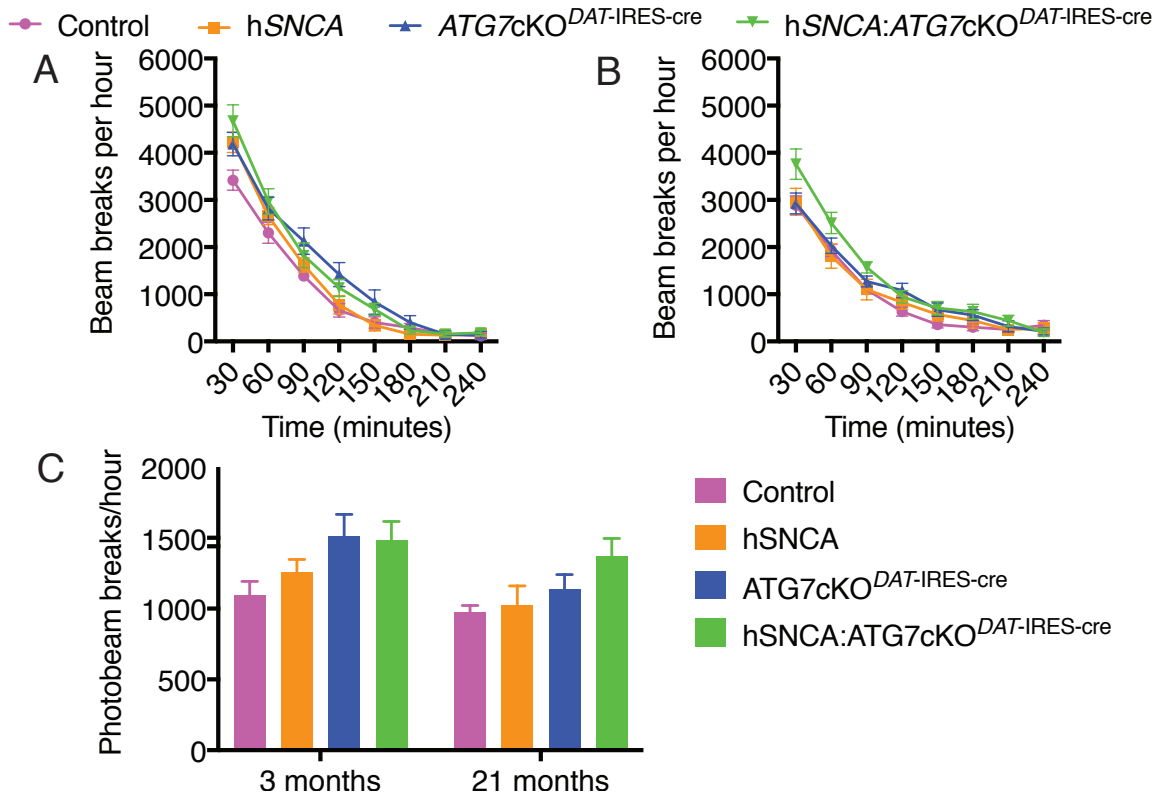


Figure 4.3. Impaired macroautophagy in dopamine neurons is associated with increased locomotor activity in the open-field.
(A) Locomotor activity of three month-old mice over four hours. Data are separated into 30 minute bins. **(B) Locomotor activity of 20 to 24 month-old mice over four hours**. Data are separated into 30 minute bins. **(C) Total locomotor activity over four hours.** Three-way ANOVA for age, *ATG7*cKO$^{DAT\text{-IRES-cre}}$ and h*SNCA*. Main effect of age: $F_{(1,113)}$=6.29, p=0.014. Main effect of *ATG7*cKO$^{DAT\text{-IRES-cre}}$: $F_{(1,113)}$=11.82, p=0.001. No other effects or interactions. n=11-20 per transgenic mouse line per age group. Data are expressed as mean ± SEM.

4.3.2.3 Improved rotarod performance in aged mice with the *ATG7*cKO$^{DAT\text{-IRES-cre}}$ genotype

In order to examine motor coordination, mice were tested on the accelerating rotarod (Jones and Roberts 1968; Deacon 2013b). Mice were trained on the rotarod for three trials per day (the performance on each day was averaged), for three consecutive days. The rotarod accelerated from four to forty revolutions per minute. On the fourth day mice were tested at the same speed, and again the average of three trials was taken (Figure 4.4). There was an age-dependent increase in rotarod performance associated with *ATG7*cKO$^{DAT\text{-IRES-cre}}$ genotype, such that performance was increased in 21 month-old animals with this genotype, but there was no difference in performance at 3 months. In order to verify the association of the *ATG7*cKO$^{DAT\text{-IRES-cre}}$ genotype with improved rotarod performance, training data from both cohorts was examined. Data from the training period of the 21 month-old cohort demonstrated improved performance of mice with the *ATG7*cKO$^{DAT\text{-IRES-cre}}$ genotype (Figure 4.5); there was no difference in the 3 month-old group (Figure 4.6).

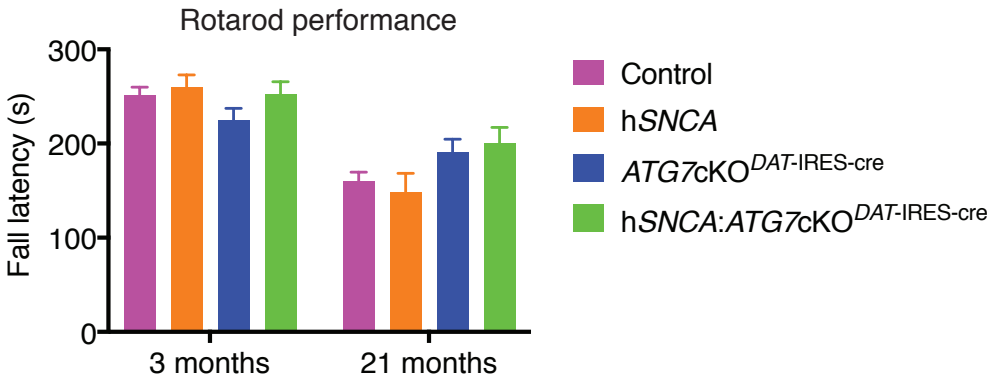


Figure 4.4. Impaired macroautophagy in dopamine neurons is associated with improved rotarod performance in old but not young mice.
Performance on a rotarod accelerating from four to forty revolutions per minute over 300 seconds was assessed following three days of training. Average of three trials is shown. Data was reflected and square-root transformed for analysis, but presented as raw data for ease of comparison. A Three-way ANOVA was performed for age, *ATG7*cKO$^{DAT\text{-IRES-cre}}$ and hSNCA. There was a significant 2-way interaction between *ATG7*cKO$^{DAT\text{-IRES-cre}}$ and age $F_{(1,107)}$=7.30, p=0.022. The effect of *ATG7*cKO$^{DAT\text{-IRES-cre}}$ at 3 and 21 months was then analysed. There was no effect of *ATG7*cKO$^{DAT\text{-IRES-cre}}$ at 3 months. In the 21 month group there was a significant effect of *ATG7*cKO$^{DAT\text{-IRES-cre}}$ improving rotarod performance (p=0.039). Mice carrying the *ATG7*cKO$^{DAT\text{-IRES-cre}}$ genotype had mean raw fall latency of 195.62 (95% CI 175.57 to 215.68) whereas mice without the *ATG7*cKO$^{DAT\text{-IRES-cre}}$ genotype had a mean raw fall latency of 154.09 (95% CI 133.58 to 174.61). Main effect of age: $F_{(1,107)}$=52.09, p<0.001. No other effects or interactions. n=9-19 per genotype per age group. Data are expressed as mean ± SEM.

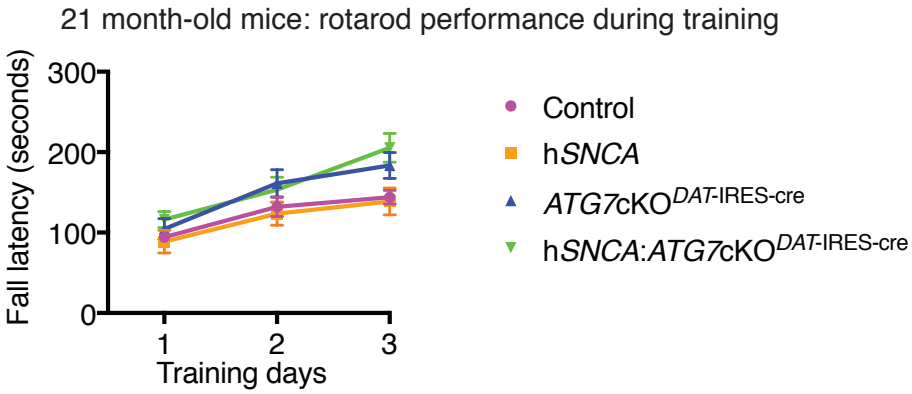


Figure 4.5. Impaired macroautophagy in dopamine neurons is associated with improved performance during rotarod training in 21 month-old mice.
Three-way mixed ANOVA for hSNCA, *ATG7*cKO$^{DAT\text{-IRES-cre}}$ and rotarod training day (as a within-subjects factor). Mauchly's test indicated that the assumption of sphericity had not been violated, $\chi^2(2) = 3.89$, p=0.143. There was a statistically significant interaction between training day and *ATG7*cKO$^{DAT\text{-IRES-cre}}$, $F_{(2,47)}=4.80$, p=0.010, such that mice with the *ATG7*cKO$^{DAT\text{-IRES-cre}}$ genotype performed significantly better on training day 3, but not on the other days (mean difference 53.04 seconds, 95% confidence intervals 23.51 seconds to 82.57 seconds, p=0.001, Bonferroni-adjusted). There was a significant within-subjects effect of training day ($F_{(2,94)}=71.43$, p<0.001). There was a significant between-subjects effect of *ATG7*cKO$^{DAT\text{-IRES-cre}}$ improving rotarod performance when the average of all training days was considered ($F_{(1,47)}=7.63$, p=0.008). No other effects or interactions. n=9-17 per genotype. Data are expressed as mean ± SEM.

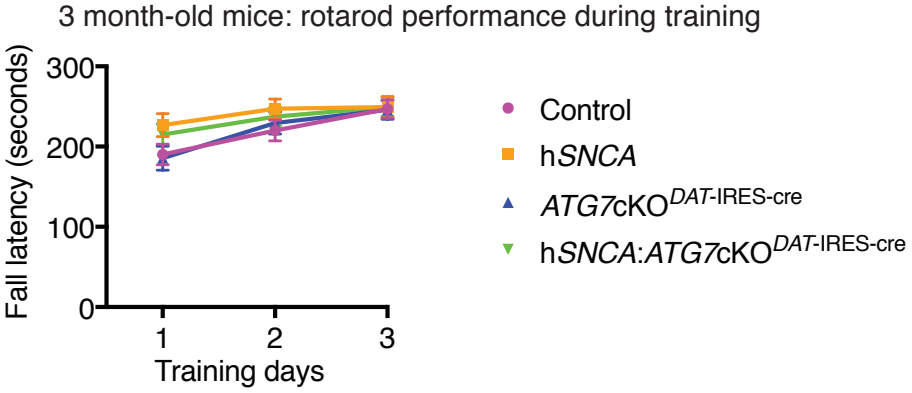


Figure 4.6. No effect of genotype on performance during rotarod training in 3 month-old mice.
Three-way mixed ANOVA for hSNCA, *ATG7*cKO$^{DAT\text{-IRES-cre}}$ and rotarod training day (as a within-subjects factor). Mauchly's test indicated that the assumption of sphericity had not been violated, $\chi^2(2) = 5.83$, p=0.054. There were no statistically significant genotype effects. There was a significant within-subjects effect of training day ($F_{(2,120)}=28.61$, p<0.001). No other effects or interactions. n=11-19 per genotype. Data are expressed as mean ± SEM.

4.3.2.4 The *ATG7*cKO$^{DAT\text{-IRES-cre}}$ genotype is associated with increases in forefoot swing speed and gait cadence

Impairment of gait is a cardinal feature of PD (Parkinson 1817; Jankovic 2008). Typically, PD patients develop a slowed, shuffling gait (Jankovic 2008). For this reason, gait was assessed in experimental mice by means of unforced locomotion across the Noldus Catwalk apparatus. This apparatus measures parameters of gait using video analysis of mice walking across a pressure-sensitive light-emitting walkway. No differences in stride length were observed between age groups or genotypes (Figure 4.7A). A small but statistically significant increase in forefoot swing speed was observed in mice with the *ATG7*cKO$^{DAT\text{-IRES-cre}}$ genotype (Figure 4.7B). Similarly, there was an increase in gait cadence (the number of steps taken per second) in mice with the *ATG7*cKO$^{DAT\text{-IRES-cre}}$ genotype (Figure 4.8A). There was an age-related reduction in gait velocity, but no effect of genotype (Figure 4.8B). Visual inspection of the data suggests that the effects observed in forefoot swing speed and gait cadence are driven primarily by differences associated with the *ATG7*cKO$^{DAT\text{-IRES-cre}}$ genotype in mice aged 21 months, consistent with the rotarod data described earlier.

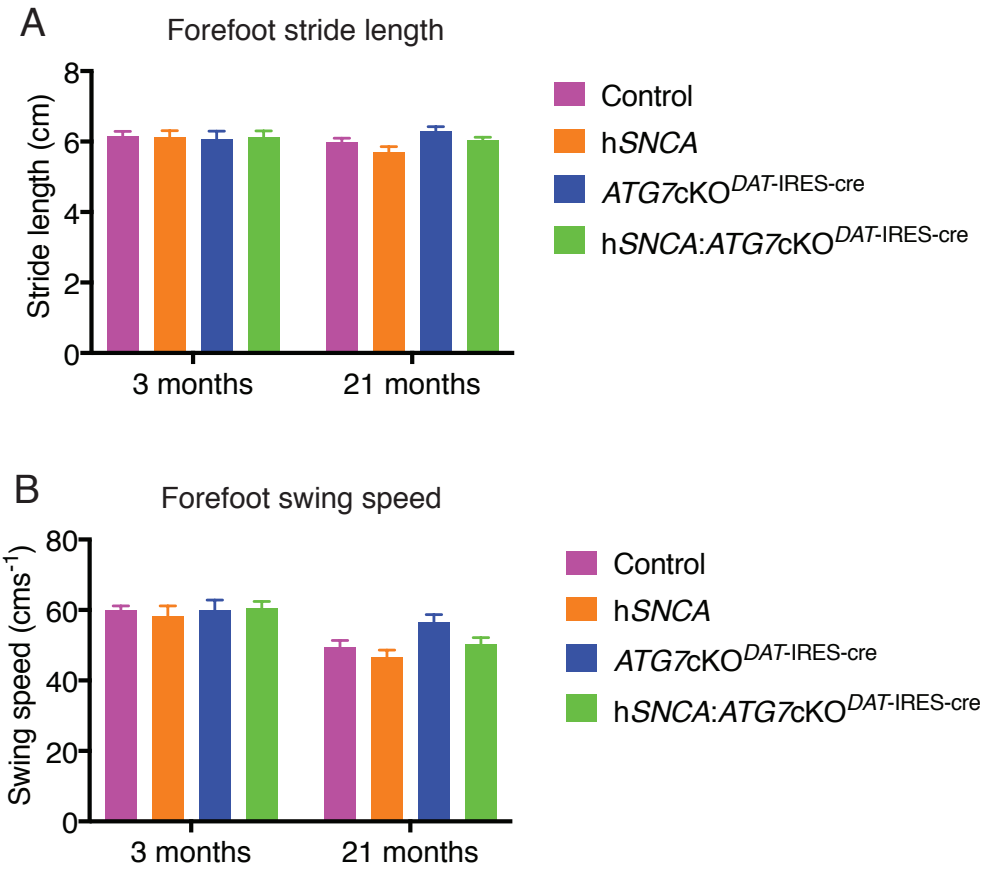


Figure 4.7. *ATG7*cKO$^{DAT\text{-IRES-cre}}$ mice have increased forefoot swing speed, but no changes in stride length.
(A) Forefoot stride length. No effects or interactions when assessed using a three-way ANOVA for age, *ATG7*cKO$^{DAT\text{-IRES-cre}}$ and h*SNCA*. n=11-20 per genotype per age group**.** **(B) Forefoot swing speed.** Three-way ANOVA for age, *ATG7*cKO$^{DAT\text{-IRES-cre}}$ and h*SNCA*. Main effect of age, $F_{(1,110)}= 34.34$, $p<0.001$. Main effect of *ATG7*cKO$^{DAT\text{-IRES-cre}}$, $F_{(1,110)}= 9.26$, $p<0.001$. No other effects or interactions. n=11-20 per genotype per age group. Data are expressed as mean ± SEM.

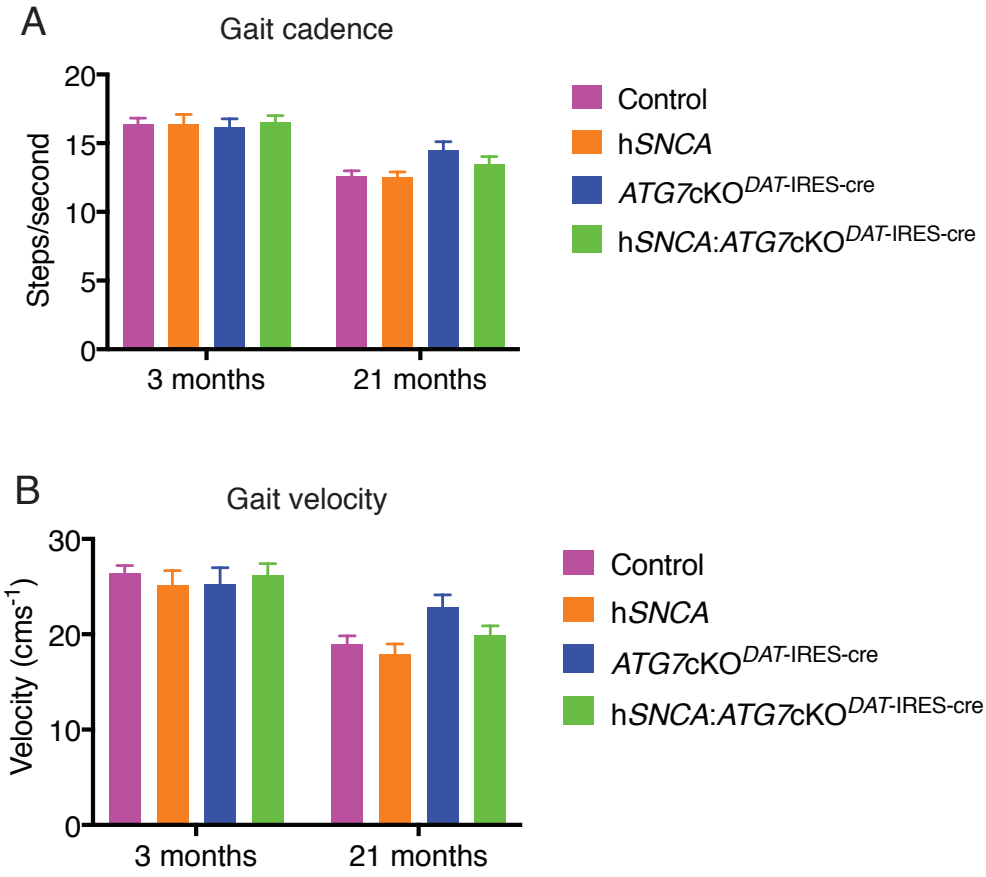


Figure 4.8. *ATG7*cKO$^{DAT\text{-IRES-cre}}$ mice have increased gait cadence, but no changes in gait velocity.
(A) Gait cadence. Data were log transformed for analysis, but presented as raw data for ease of comparison. Three-way ANOVA for age, *ATG7*cKO$^{DAT\text{-IRES-cre}}$ and h*SNCA*. Main effect of *ATG7*cKO$^{DAT\text{-IRES-cre}}$, $F_{(1,110)}= 4.10$, $p=0.045$. Main effect of age, $F_{(1,110)}= 12.07$, $p<0.001$. No other effects or interactions. n=11-20 per genotype per age group. **(B) Gait velocity.** Data were log transformed for analysis, but presented as raw data for ease of comparison. Three-way ANOVA for age, *ATG7*cKO$^{DAT\text{-IRES-cre}}$ and h*SNCA*. Main effect of age, $F_{(1,110)}= 50.49$, $p<0.001$. No other effects or interactions. n=11-20 per genotype per age group. Data are expressed as mean ± SEM.

4.3.3 The effects of impaired macroautophagy in dopamine neurons and human α-synuclein expression on parkinsonian non-motor phenotypes in transgenic mice

The non-motor symptoms of PD are some of the most troubling to patients, and are therefore important to examine in experimental animals (Alvarado-Bolanos *et al.* 2015). Common non-motor PD symptoms include cognitive dysfunction, constipation, depression, anxiety, and reduced olfaction (Hely *et al.* 2008; Chen *et al.* 2015).

4.3.3.1 The *ATG7*cKO$^{DAT\text{-IRES-cre}}$ genotype is associated with reduced successful spontaneous alternation in the T-maze, but no deficits were found in a Y-maze spatial novelty preference task

In order to examine for cognitive deficits in mice, an unrewarded T-maze spontaneous alternation task was used, according to the protocol described by Deacon and Rawlins (2006). The T-maze task relies on the motivation of animals to explore in order to find food, mates, safety and shelter. In this task, mice are placed in a start arm, and then allowed to freely explore. Once they enter a choice arm (either horizontal arm of the T), they are confined to this arm for 30 seconds. Subsequently, mice are returned to the start arm and allowed to explore freely. Most mice will choose the unexplored arm on the second trial, which requires hippocampus-dependent short-term memory (Deacon *et al.* 2002; Deacon and Rawlins 2006). Deficits in short-term memory may therefore result in a reduction in successful alternation. In the present study, the *ATG7*cKO$^{DAT\text{-IRES-cre}}$ genotype was associated with a reduction in successful alternation independent of age (Figure 4.9). In order to assess if this finding was associated with a more global cognitive deficit, or genotype-specific differences in habituation, the 21 month-old cohort of mice were

subjected to a spatial novelty preference task in a Y-maze. In the Y-maze task, mice are allowed to freely explore two arms of a three-arm Y-maze for 5 minutes. Mice were then removed from the Y-maze, and the third arm made accessible. The proportion of time that mice spent exploring the novel arm in a subsequent two minute trial was used to assess working memory. In this experiment, no differences between genotypes were observed (Figure 4.10). Possible reasons underlying the discrepancy between T-maze and Y-maze effects of the *ATG7*cKO$^{DAT\text{-IRES-cre}}$ genotype are considered in the discussion section of this chapter.

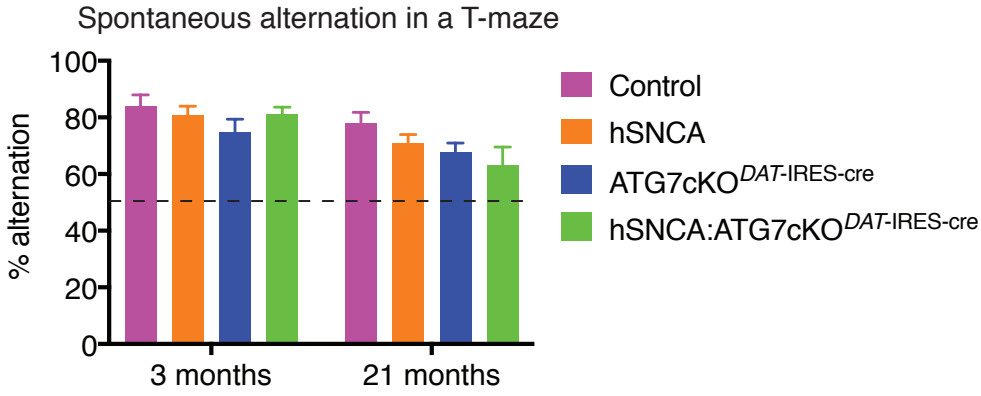


Figure 4.9. Impaired macroautophagy in dopamine neurons is associated with a reduced rate of spontaneous alternation in the T-maze.
Data were reflected and square root transformed for analysis, but presented here as raw data for ease of comparison. A three-way ANOVA was performed for age, *ATG7*cKO$^{DAT\text{-}IRES\text{-}cre}$ and h*SNCA*. There was a statistically significant decrease in successful alternation with age, $F_{(1,105)}$=12.69, p=0.001. There was a reduced rate of successful alternation associated with the *ATG7*cKO$^{DAT\text{-}IRES\text{-}cre}$ genotype, $F_{(1,105)}$= 5.93, p=0.028. There were no other effects or interactions. n=10-20 per genotype per age group. Dashed line represents chance. Data are expressed as mean ± SEM.

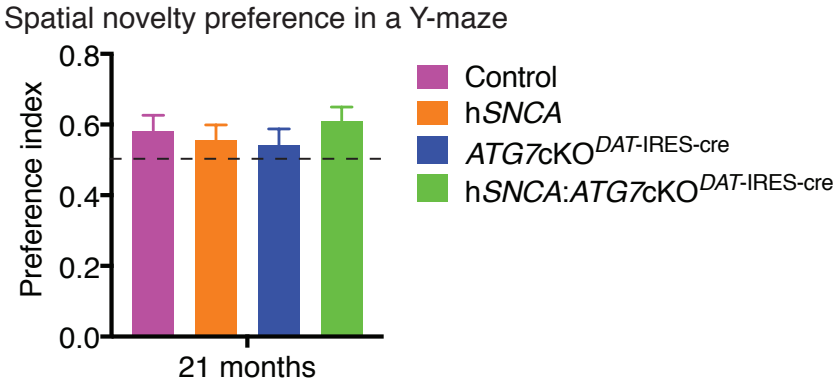


Figure 4.10. No deficit associated with experimental genotypes in 21 month-old mice tested using a spatial novelty preference test in a Y-maze.
A 2-way ANOVA was performed for the *ATG7*cKO$^{DAT\text{-}IRES\text{-}cre}$ and h*SNCA* genotypes. There were no effects or interactions. n=10-17 per genotype. Dashed line represents chance. Data are expressed as mean ± SEM.

4.3.3.2 No association between genotype and measures of gastrointestinal function

Constipation is a common premorbid symptom in PD, and contributes significantly to the burden of disease in some patients (Chen *et al.* 2015; Adams-Carr *et al.* 2016). In order to investigate for the presence of gastrointestinal dysfunction in the 3 and 21 month-old transgenic mouse cohorts, stool was collected over a 1-hour period, between 1600 and 1700 hours. The total number of pellets, dry weight of the stool and the proportion of water in stool was determined. There were no difference in any of these measures associated with the either the *ATG7*cKO$^{DAT\text{-IRES-cre}}$ genotype, or the h*SNCA* genotype (Figure 4.11). In a previous study of *SNCA*-OVX mice in the Wade-Martins laboratory (Janezic *et al.* 2013), male *SNCA*-OVX mice demonstrated an increase in dry stool mass, independent of age, however this could not be replicated in the current experiment, even when data from each sex was analysed separately, and when each age group was analysed separately or together. DAT-positive neurons can be occasionally found in the myenteric plexuses of the mouse gastrointestinal system, however it appears impairment of macroautophagy in these neurons is not sufficient to cause an overt gastrointestinal phenotype (Li *et al.* 2004).

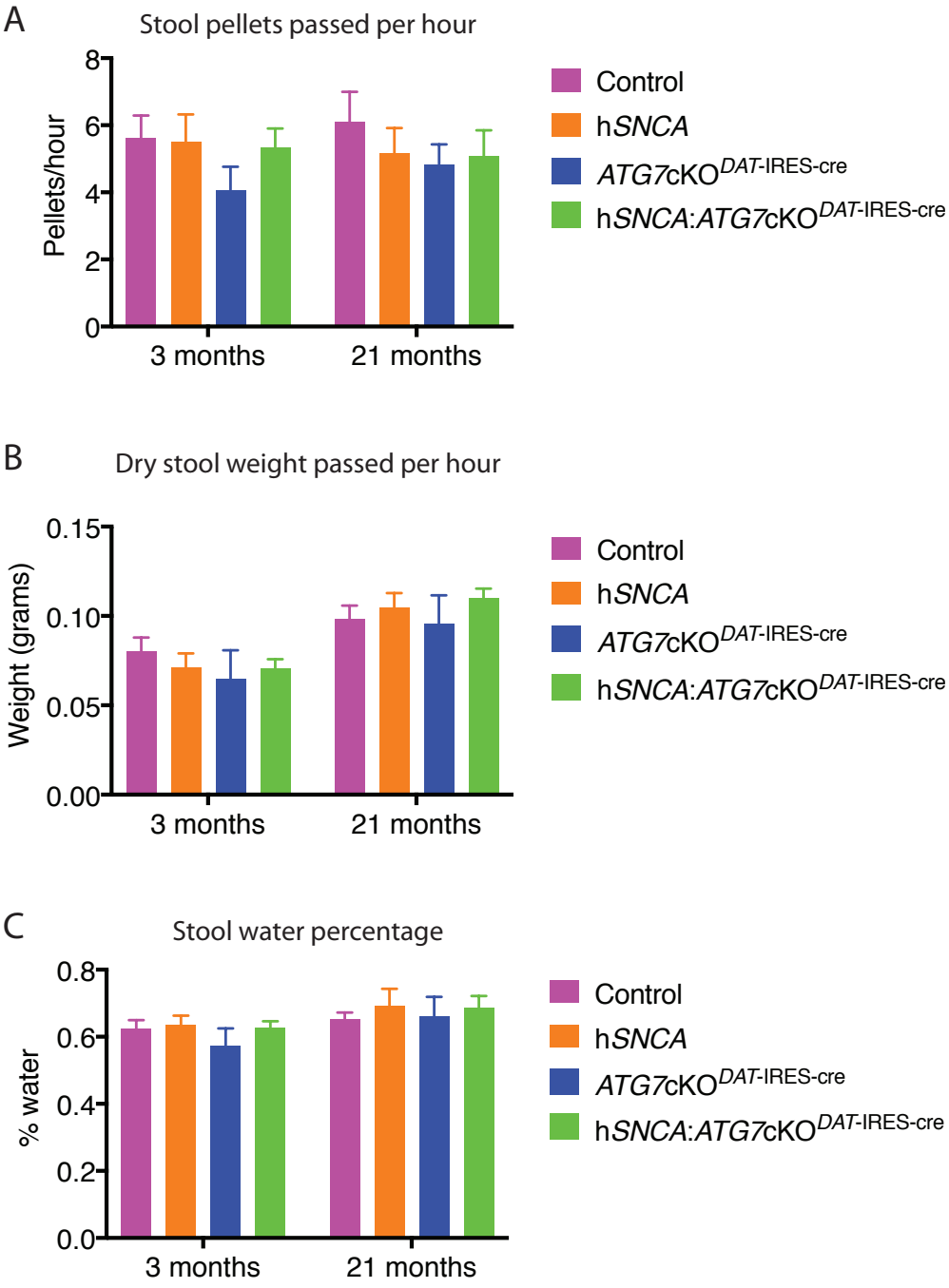


Figure 4.11. No effect of impaired dopamine neuron macroautophagy or human α-synuclein expression on gastrointestinal function.
(A) Stool pellets expelled per hour by experimental mice. Three-way ANOVA for age, hSNCA and *ATG7*cKO$^{DAT\text{-IRES-cre}}$. No effects or interactions. n=12-21 per genotype per group. **(B) Dry weight of stool expelled per hour.** Data were square root transformed for analysis, but presented as raw data for analysis. Three-way ANOVA for age, hSNCA and *ATG7*cKO$^{DAT\text{-IRES-cre}}$. Effect of age, $F_{(1,112)}$=5.69, p=0.019. No other effects or interactions. n=12-21 per genotype per group. **(C) Water percentage of stool.** Data were not normally distributed. Three-way ANOVA for age, hSNCA and *ATG7*cKO$^{DAT\text{-IRES-cre}}$. Effect of age, $F_{(1,112)}$= 5.451, p=0.021. No other effects or interactions. n=12-21 per genotype per group. Data are expressed as mean ± SEM.

4.3.3.3 No association between genotype and depression- or anxiety-like phenotypes

Depression is a frequent comorbidity in PD (Chen *et al.* 2015). A common laboratory test for depression-like phenotypes is the tail suspension test (Steru *et al.* 1985). In this test, a mouse is suspended by its tail and the time that it spends immobile, rather than attempting to escape from its predicament, is measured. The immobility time is thought to be a measure of 'behavioural helplessness' and is negatively correlated with administration of clinical antidepressant drugs (Steru *et al.* 1985; Ripoll *et al.* 2003; Cryan *et al.* 2005). There were no genotype-specific differences in immobility time in the tail suspension test in the transgenic mouse cohorts (Figure 4.12A).

A second common comorbid neuropsychiatric disorder in PD is anxiety (Chen *et al.* 2015). Anxiety-like phenotypes in mice can be determined using the elevated plus-maze. In this test, two arms of a plus-maze are open, and two are enclosed on either side. Mice tend to avoid the open arms of the maze, and it is thought that forays into these arms provokes anxiety (Lister 1987; Walf and Frye 2007). Mice administered anxiolytic drugs, such as benzodiazepines, spend more time in the open arms (Pellow and File 1986). Neither the h*SNCA* or *ATG7*cKO$^{DAT\text{-IRES-cre}}$ genotypes were associated with the number of open arm entries, or open arm time in this experiment (Figure 4.12B and C).

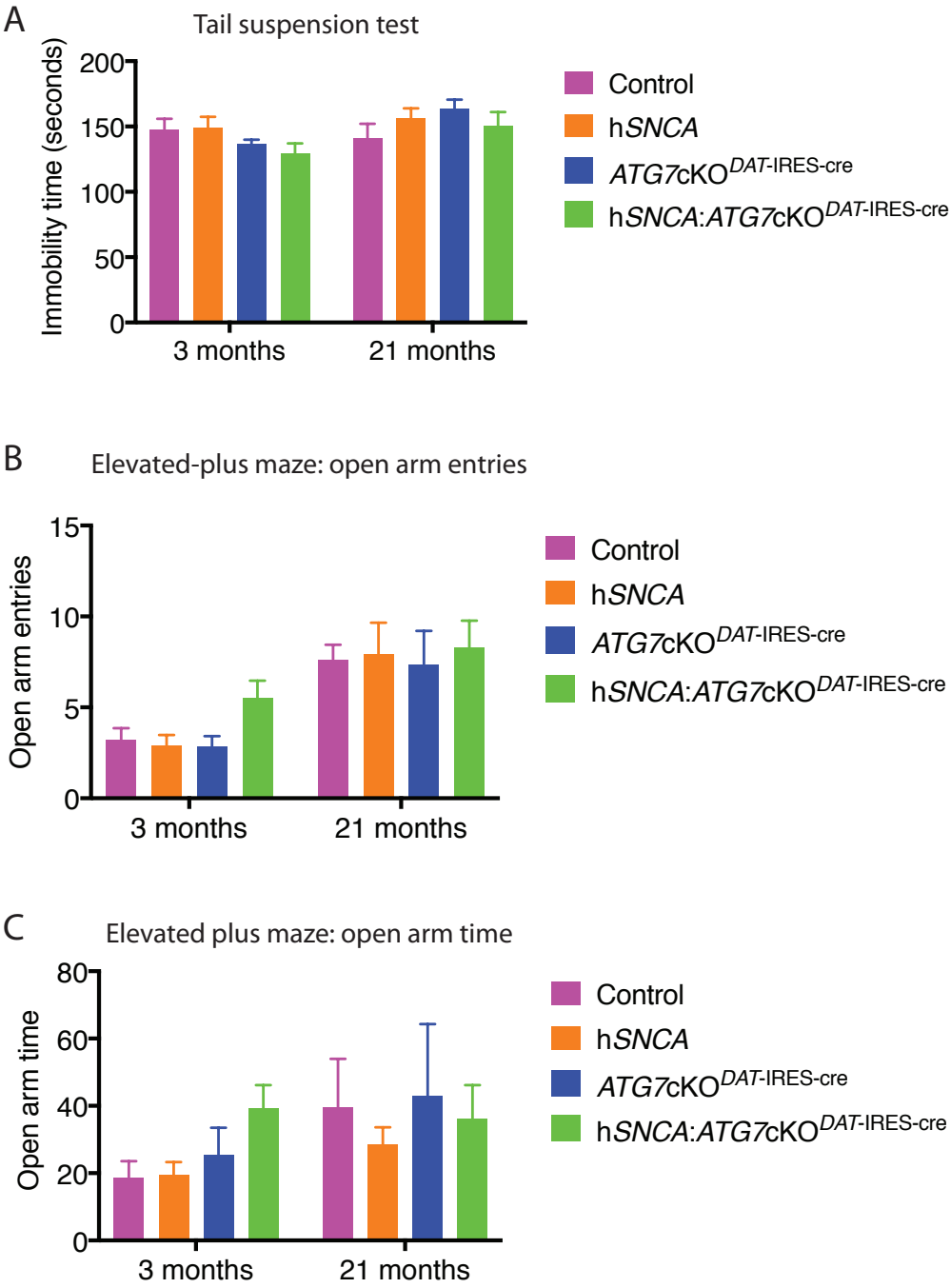


Figure 4.12. Absence of depression- or anxiety-like phenotypes associated with experimental genotypes.
(A) Immobility time in the tail suspension test. A three-way ANOVA was performed for age, *ATG7*cKO$^{DAT\text{-IRES-cre}}$and h*SNCA*. There were no significant effects or interactions. n=10-17 per genotype per group. **(B) Open arm time in the elevated-plus maze.** Data were square root transformed for analysis, but presented as raw data for ease of comparison. A three-way ANOVA was performed for age, *ATG7*cKO$^{DAT\text{-IRES-cre}}$ and h*SNCA*. No effects or interactions. n=10-20 per genotype per group. **(C) Open arm entries in the elevated-plus maze.** Data were square root transformed to a distribution that was assessed as normal by Q-Q plot and histogram, but did not pass the Kolmogorov-Smirnov test. Raw data are presented for ease of comparison. A three-way ANOVA was performed for age, *ATG7*cKO$^{DAT\text{-IRES-cre}}$ and h*SNCA*. Effect of age, $F_{(1,107)}=27.92$, $p<0.001$. There were no other significant effects or interactions. n=10-20 per genotype per group. Data are expressed as mean ± SEM.

4.3.3.4 No association between genotype and olfactory function in aged mice

Finally, olfaction was assessed in the 21 month-old transgenic mouse cohort. Olfactory deficits are a frequent accompaniment to PD, and may precede the development of PD by some decades. In order to assess for any olfactory problems, a modified version of a habituation/dishabituation protocol used by Fleming and colleagues (2008) was administered to transgenic mice. Mice were exposed to one odour, which was held in two glass vials at either end of a cage containing bedding from the mouse's home cage, for three trials of 2 minutes each. Subsequently, a second odour was placed in one of the glass vials for a final trial. The time spent exploring the new odour was determined, and divided by the time spent exploring the original odour to calculate a novel odour preference index. In general, this index was greater than 1, indicating a proclivity to investigate the novel odour, and this was confirmed statistically by comparing preference indices to chance. Three odour pairs were used: orange/mango, coconut/vanilla and peppermint/jasmine. However, no differences between experimental genotypes were found, and there was a wide degree of variation in the results obtained from this assay (Figure 4.13).

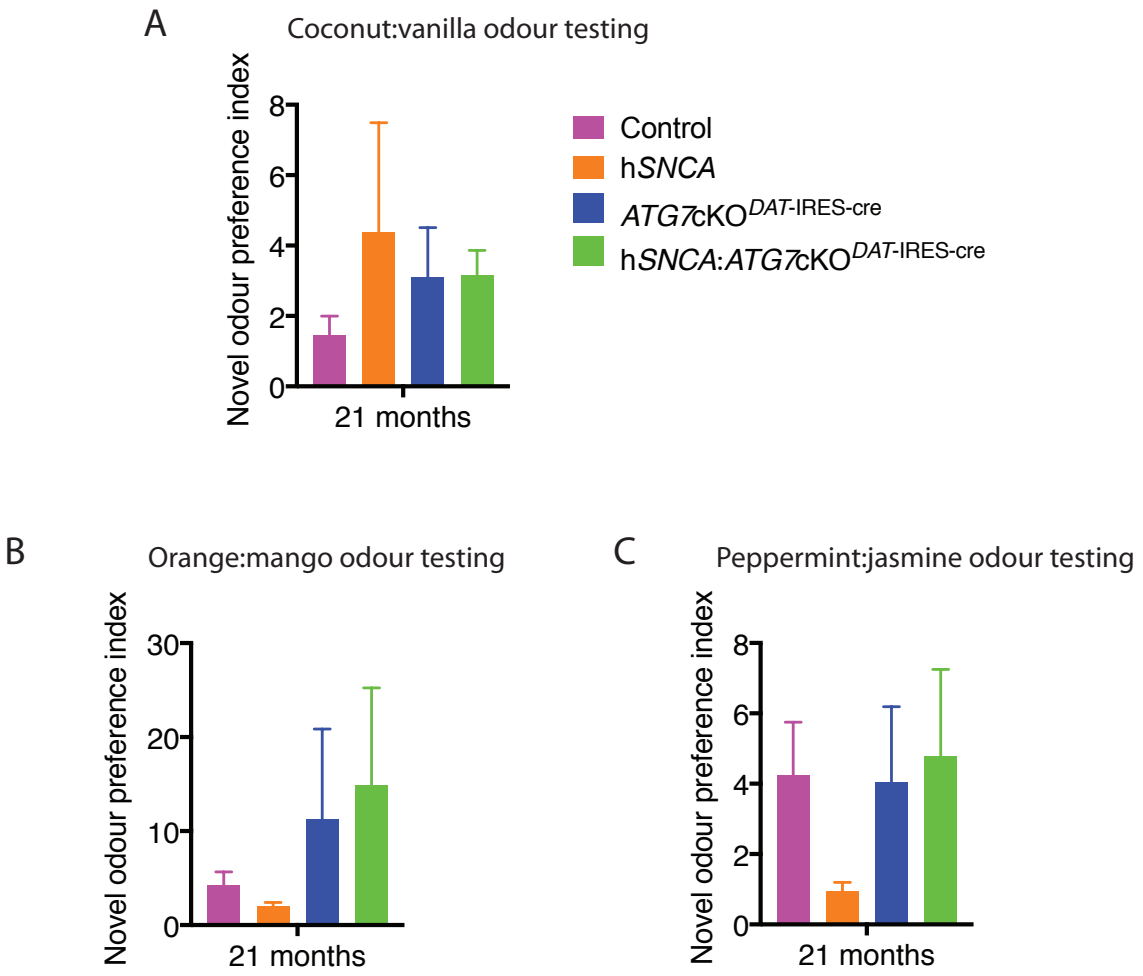


Figure 4.13. No evidence of olfactory deficit associated with experimental genotypes in 21 month-old mice.
(A) Coconut:vanilla odour pairing. (B) Orange:mango odour pairing. (C) Peppermint:jasmine odour pairing. Data from all genotypes was compared to chance for each odour pair using a unpaired Student's *t*-tests. In all odour pairs mice showed a statistically greater preference for the novel odour. For coconut:vanilla, unpaired two-tailed *t*-test, $t(101)=2.26$, $p=0.026$. For orange:mango, unpaired two-tailed *t*-test, $t(101)=2.06$, $p=0.042$. For peppermint:jasmine, unpaired two-tailed *t*-test, $t(100)=2.90$, $p=0.004$. Pairs were then analysed separately using a two-way ANOVA for *ATG7*cKO$^{DAT\text{-IRES-cre}}$ and h*SNCA*. Data were log transformed for analysis but presented as raw data for ease of comparison. There was no significant effects or interactions. n=12-20 per genotype per group. Data are expressed as mean ± SEM.

4.4 Discussion

4.4.1 Association of *ATG7*cKO$^{DAT\text{-IRES-cre}}$ genotype with improved motor function

In Chapter 3 of this thesis, loss of SNc neurons in mice carrying the *ATG7*cKO$^{DAT\text{-IRES-cre}}$ genotype was described, consistent with the findings of several other investigators. In parallel, striatal DA content was found to be reduced in mice with the *ATG7*cKO$^{DAT\text{-IRES-cre}}$ genotype. Based on what has been traditionally described in the literature, it would be expected that these mice would display parkinsonian behavioural phenotypes, such as reduced locomotor activity, bradykinesia, and reduced rotarod fall latency. Paradoxically, however, in the current chapter the opposite has been found; mice with the *ATG7*cKO$^{DAT\text{-IRES-cre}}$ genotype are hyperlocomotor, have quickened limb movements and gait cadence, and perform better on the rotarod. The extent of the heightened motor performance of *ATG7*cKO$^{DAT\text{-IRES-cre}}$ in the 21 month-old cohort of mice was in the region of 20% for both rotarod performance and locomotor activity, a sizeable increment that is comparable to the effect of dopamine agonist administration to MPTP-lesioned mice (Ayton *et al.* 2013).

There are some findings in the literature that are consistent with these results. Ahmed *et al.* (2012) reported that *ATG7*cKO$^{DAT\text{-cre}}$ mice are hyperlocomotor at 7 months of age, despite SNc neuron loss, and reduced striatal DA content. Ahmed and colleagues went on to demonstrate that the same phenotype was not present at 12 months of age, however the sample used was relatively small (four to six per genotype).

Many of the behavioural phenotypes found associated with the *ATG7*cKO$^{DAT\text{-IRES-cre}}$ genotype are consistent with hyperdopaminergia. *DAT* is the major determinant of synaptic dopamine. Mice lacking the *DAT* gene thus have greatly elevated levels of striatal dopamine, and are found to be hyperlocomotor (Giros *et al.* 1996). Similarly, administration of agents that increase the bioavailability of DA causes hyperlocomotion, and improves rotarod performance (Ayton *et al.* 2013; Sloan *et al.* 2016). Previously Hernandez *et al.* (2012) have demonstrated that DA neurotransmission is enhanced when macroautophagy is impaired, and this effect may underlie enhanced motor performance of mice carrying the *ATG7*cKO$^{DAT\text{-IRES-cre}}$ genotype.

4.4.2 *ATG7*cKO$^{DAT\text{-IRES-cre}}$ and measures of memory

In this chapter, mice with the *ATG7*cKO$^{DAT\text{-IRES-cre}}$ genotype were found to have a reduced rate of alternation in a T-maze task. This apparent short-term memory deficit was not found in a second task involving spatial novelty preference in a Y-maze. There may be several, possibly overlapping reasons underlying this discrepancy. The Y-maze task was only conducted on the 21 month-old cohort, and therefore sample size was reduced by approximately half, reducing the power of the study to detect any differences. Alternatively, it may be that the reduced rate of spontaneous alternation in the T-maze reflects a deficit in short-term working memory, whereas the Y-maze task relies on habituation, which is not impaired, or not impaired to the same extent (Sanderson and Bannerman 2012). It is possible, also, that the reduced rate of successful alternation in the T-maze task is indicative of a hyperdopaminergic state. Previous work in the Wade-Martins laboratory has demonstrated that mice that lack α- and γ-synuclein have increased DA release, are hyperlocomotor, and have a reduced rate of spontaneous alternation in the

T-maze (Senior *et al.* 2008). In any event, a possible anatomical substrate for any association between differences in spatial working memory and the *ATG7*cKO$^{DAT\text{-IRES-cre}}$ genotype exists, in the form of multiple DA inputs to the hippocampus from the SNc and nucleus accumbens (Carter and Fibiger 1977; Scatton *et al.* 1980). In the hippocampus, DA has been shown to play a role in long-term potentiation of synapses, a key process underlying memory formation, particularly in relation to spatial novelty (Frey *et al.* 1990; Li *et al.* 2003).

4.4.3 Absence of association between h*SNCA* and parkinsonian phenotypes

In concordance with the observations described in Chapter 3, there were no phenotypes associated with presence of the h*SNCA* transgene in the behavioural experiments described in this chapter. This may be expected, given the absence of an overt neuropathological phenotype. Again, the differences between the results of the Janezic study and the present study may be associated with the presence of endogenous mouse α-synuclein, interfering with the toxicity of human α-synuclein.

4.5 Chapter summary

This chapter has demonstrated that mice with deletion of *ATG7* in DA neurons perform better on measures of motor function, and are impaired in a T-maze alternation task, but not in a Y-maze forced alternation task. In the experiments described in this chapter, summarised in Table 4.2. (below), there was no behavioural effect of the h*SNCA* transgene. The reasons underlying the apparently contradictory effects of conditional *ATG7* knockout (fewer DA neurons but improved motor function) will be further explored in the following chapter, which examines DA neurotransmission.

Table 4.2. Summary of behavioural effects of *ATG7*cKO$^{DAT\text{-IRES-cre}}$ and h*SNCA* genotypes

Effect of gene on behavioural correlates of Parkinson's disease:	***ATG7*cKO$^{DAT\text{-IRES-cre}}$**	**h*SNCA***
Locomotor activity	Increased	No effect
Rotarod performance	Increased at 21 months	No effect
Stride length	No effect	No effect
Stride swing speed	Increased	No effect
Gait cadence	Increased	No effect
Gait velocity	No effect	No effect
Spontaneous alternation in a T-maze	Reduced	No effect
Forced alternation in a Y-maze	No effect	No effect
Constipation-like phenotype	No effect	No effect
Depression-like phenotype	No effect	No effect
Anxiety-like phenotype	No effect	No effect
Olfactory deficit	No effect	No effect

Chapter 5: Characterisation of dopamine neurotransmission in a mouse model examining the interaction between human alpha-synuclein and impaired macroautophagy in dopamine neurons

5 Characterisation of dopamine neurotransmission in a mouse model examining the interaction between human alpha-synuclein and impaired macroautophagy in dopamine neurons

5.1 Introduction

Impairment of DA neurotransmission is thought to be the key mechanism underlying the development of motor symptoms in PD. Loss of DA-producing neurons in the SNc is the key pathological feature of PD, and the major projection target of the SNc, the striatum, has reduced levels of DA in PD (Pakkenberg and Brody 1965; Rudow *et al.* 2008). The most commonly used therapies to treat PD (L-DOPA and DA agonists) supplement or mimic endogenous DA neurotransmission and are efficacious in treating the motor symptoms of PD (Connolly and Lang 2014).

In the data presented in Chapter 3, impairment of macroautophagy in DA neurons is associated with a loss of DA-producing cells in the SNc, but not the VTA. Reflecting this, DA content was reduced in the caudate-putamen but not the nucleus accumbens. All other factors being equal, loss of SNc neurons would be expected to cause a parkinsonian behavioural phenotype, comprising such features as reduced locomotion, bradykinesia, and impaired rotarod performance. However, the results of Chapter 4 demonstrate the opposite of this: mice with impaired macroautophagy in DA neurons are hyperlocomotor, hyperkinetic, and have improved rotarod performance in old age. One explanation of these two, apparently contradictory, findings could be that impairment of macroautophagy has a net positive effect on DA neurotransmission.

One study in the literature suggests that impaired macroautophagy may improve DA neurotransmission. Work by Hernandez *et al.*(2012) using a *ATG7*cKO$^{DAT\text{-cre}}$ model demonstrated that, in the caudate-putamen, impairment of autophagy in DA neurons causes increased evoked DA levels in mice aged 8 to 10 weeks. Additionally, Hernandez and colleagues found that paired-pulse depression (PPD) was reduced in *ATG7*cKO$^{DAT\text{-cre}}$ mice. Of importance for the results presented in this chapter, it was reported that DA reuptake was unaltered by impaired macroautophagy, because although there was a trend towards increased DA half-life in *ATG7*cKO$^{DAT\text{-cre}}$ mice, this increase was not statistically significant.

Previous work in the Cragg laboratory has used FCV to demonstrate that, in mice with a *SNCA* knockout background, overexpression of human α-synuclein reduced evoked $[DA]_o$ by 3 months of age (Janezic *et al.* 2013). To date, no studies have examined DA neurotransmission and its relationship to impaired macroautophagy in aged mice, whether effects are restricted to the caudate-putamen or also involve the nucleus accumbens, or the interaction between increased levels of α-synuclein and impaired macroautophagy. The present chapter will seek to address these areas, and test the hypothesis that impaired macroautophagy enhances DA neurotransmission.

5.2 Aims of Chapter 5:

To test whether the *ATG7*cKO$^{DAT\text{-IRES-cre}}$ and h*SNCA* genotypes modify DA neurotransmission in the caudate putamen and nucleus accumbens, across the lifespan of experimental mice, specifically determining:

1. Peak $[DA]_o$.
2. DA reuptake kinetics.
3. The ratio of $[DA]_o$ released in response to single and burst stimuli, as an indicator of DA release probability.
4. The frequency dependence of peak $[DA]_o$.
5. Paired-pulse depression.

5.3 The electrochemical basis of fast-scan cyclic voltammetry

Chapter 2 contains detailed experimental procedures for the FCV experiments described in this thesis. FCV utilises the electroactive properties of DA to facilitate its detection. In FCV, a potential difference is ramped across a carbon fibre microelectrode, at a rate of 800 volts per second. The potential difference changes from -0.7 volts to 1.3 volts and back to -0.7 volts, a process which takes five milliseconds. In the experiments described here, a five millisecond scan is performed eight times per second. When the electrode potential reaches approximately 600 millivolts, DA is oxidized to DA-o-quinone, and the liberated electrons are transferred to the recording carbon fibre microelectrode (CFM). When the potential drops to approximately -200 millivolts, DA-o-quinone is reduced, and electrons return from the recording electrode. This flow of electrons is measured as an electrical current,

and is directly proportional to the concentration of DA. Therefore, using FCV, the concentration of DA in the extracellular space ([DA]o) can be assessed in real-time at high temporal resolution. In the experiments described here, electrical stimuli are used to evoke DA release.

5.4 Results

5.4.1 The *ATG7*cKO$^{DAT\text{-IRES-cre}}$ genotype is associated with increased peak evoked $[DA]_o$ in the caudate-putamen at 1 month, but lower peak release at 6 and 20 to 24 months.

In order to determine the basic DA neurotransmission properties in the experimental mouse cohorts generated in Chapter 3, peak DA release in response to a single stimulation was measured in all experimental genotypes at 1, 6, and 20 to 24 months of age in the caudate-putamen (Figure 5.1) and nucleus accumbens (Figure 5.2). At 1 month, presence of the *ATG7*cKO$^{DAT\text{-IRES-cre}}$ genotype was associated with a small but statistically significant increase in peak evoked $[DA]_o$ in the caudate-putamen (Figure 5.1). In the 6 and 20 to 24 month-old age groups however, presence of *ATG7*cKO$^{DAT\text{-IRES-cre}}$ was associated with reduced peak DA release (Figure 5.1). In Chapter 3, there was a large reduction in SNc neurons in the 6 and 20 to 24 month age group (see Figure 3.6). As the SNc is the primary DA input to the caudate-putamen, the reduction in SNc neuron number associated with *ATG7*cKO$^{DAT\text{-IRES-cre}}$ is therefore likely to account for reduced peak caudate-putamen DA release in older age groups. In the nucleus accumbens, peak evoked $[DA]_o$ was increased in mice with the *ATG7*cKO$^{DAT\text{-IRES-cre}}$ genotype. There was no change in VTA neuron number by genotype, which provide the primary DA innervation of the nucleus accumbens. Taken together, these data support the notion that the *ATG7*cKO$^{DAT\text{-IRES-cre}}$ genotype may increase evoked $[DA]_o$ in the absence of neuron loss.

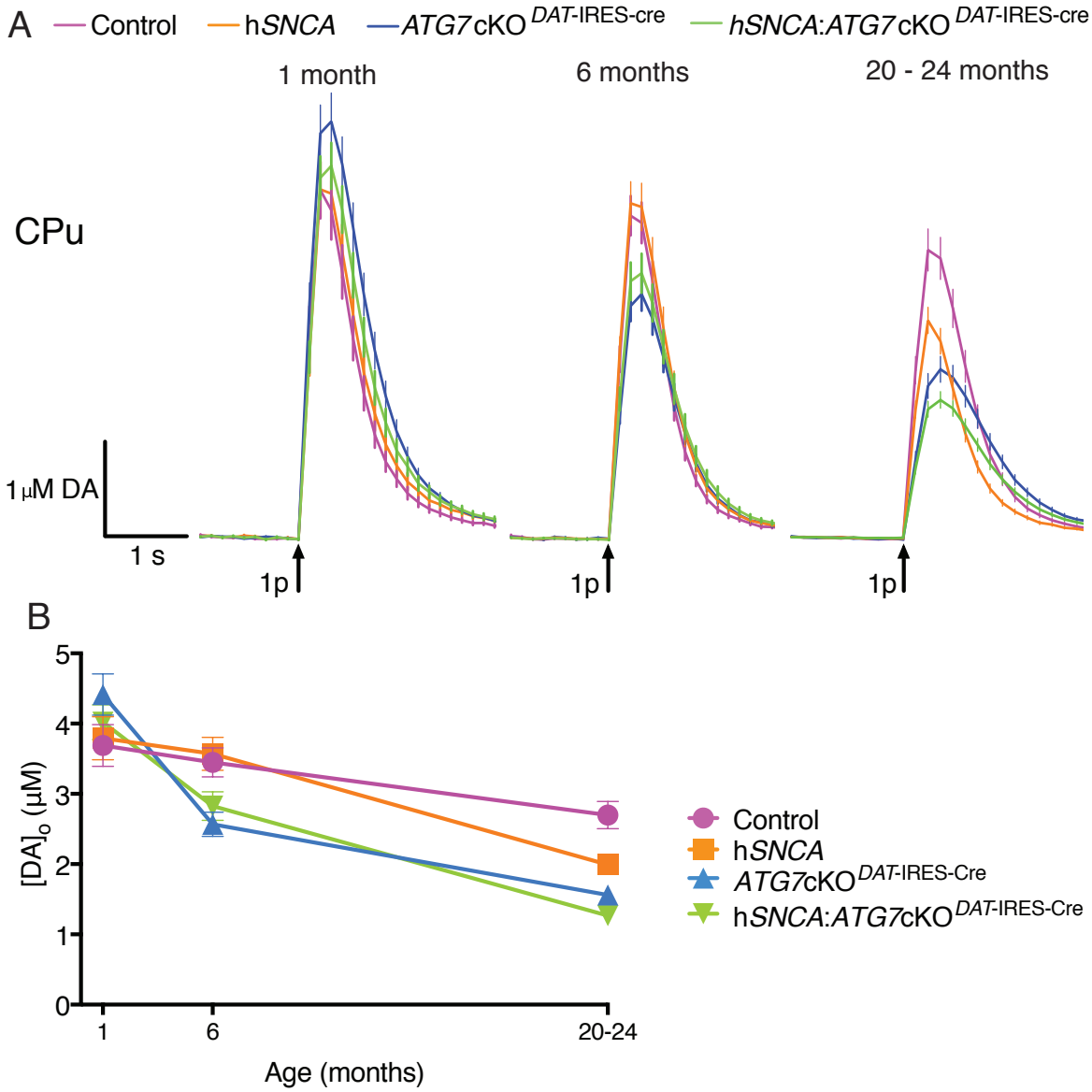


Figure 5.1. The *ATG7*cKO$^{DAT\text{-IRES-cre}}$ genotype is associated with increased peak evoked $[DA]_o$ in the caudate-putamen at 1 month, but lower peak release at 6 and 20 to 24 months. The h*SNCA* gene is associated with reduced evoked $[DA]_o$ at 20 to 24 months.

(A) Mean evoked $[DA]_o$ profiles over time following single pulse stimuli in the caudate-putamen, in three different age groups. Data from four sites in the caudate-putamen were pooled. **(B) Analysis of peak dopamine release in the caudate-putamen in three different age groups.** Data were log transformed for analysis, but presented here as raw data. Three-way ANOVA for age, *ATG7*cKO$^{DAT\text{-IRES-cre}}$ and h*SNCA*. There was a two-way interaction between *ATG7*cKO$^{DAT\text{-IRES-cre}}$ and age: $F_{(2,420)}$=13.34, p<0.001. Therefore, the effect of *ATG7*cKO$^{DAT\text{-IRES-cre}}$ was determined at each level of age, with a Bonferroni adjustment. At 1 month, raw peak $[DA]_o$ was 3.74 ± 0.16 µM in mice without *ATG7*cKO$^{DAT\text{-IRES-cre}}$ and 4.22 ± 0.16 µM in mice with *ATG7*cKO$^{DAT\text{-IRES-cre}}$, a difference of 0.48 (95% CI .044 to 0.91) µM, transformed p=0.049. At 6 and 20 to 24 months, *ATG7*cKO$^{DAT\text{-IRES-cre}}$ was associated with reduced raw peak $[DA]_o$ of 0.81 (95% CI 0.40 to 1.22) and 0.93 (95% CI 0.54 to 1.32) µM respectively, in both cases p<0.001. There was a two-way interaction between h*SNCA* and age: $F_{(2,420)}$=4.36, p=0.013. The effect of h*SNCA* was determined at each level of age with a Bonferonni correction. There was no effect of h*SNCA* at 1 or 6 months, but was significantly reduced at 20 to 24 months (p=0.002), with a raw difference of 0.50 µM (95% CI 0.11 to 0.89). n=32-40 from 4-5 mice in each transgenic mouse line. Data are shown as mean ± SEM.

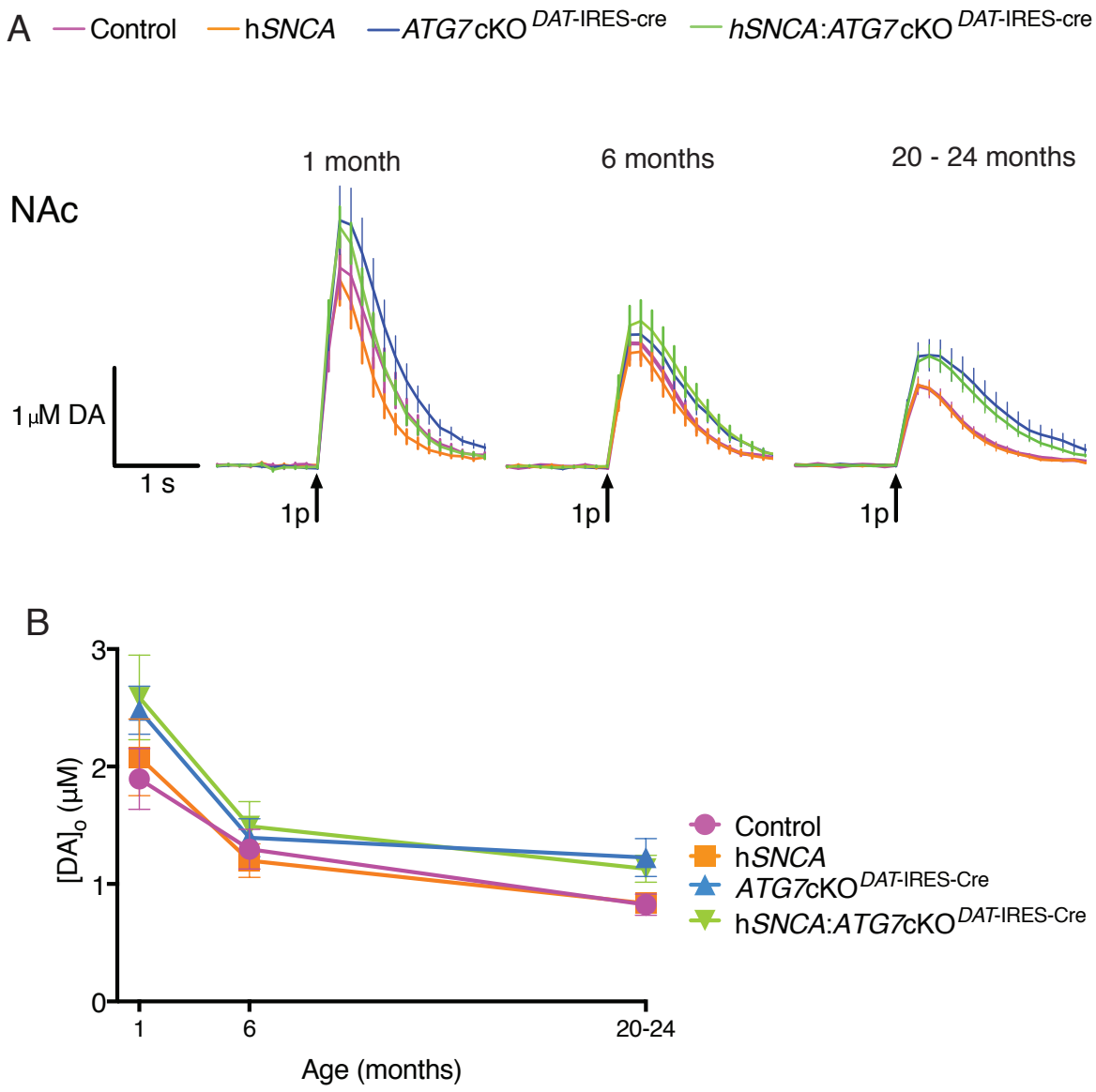


Figure 5.2. *ATG7*cKO$^{DAT\text{-IRES-cre}}$ is associated with increased peak evoked $[DA]_o$ in the nucleus accumbens, independent of age.
(A) Mean evoked $[DA]_o$ profiles over time following single pulse stimuli in the caudate-putamen, in three different age groups. Data from two sites in the nucleus accumbens were pooled. **(B) Analysis of peak dopamine release in nucleus accumbens in three different age groups.** Data are square-root transformed but shown here as raw data for ease of comparison. Three-way ANOVA for age, *ATG7*cKO$^{DAT\text{-IRES-cre}}$ and h*SNCA*. Main effect of *ATG7*cKO$^{DAT\text{-IRES-cre}}$: $F_{(1,204)}$=9.84, p=0.002. Main effect of age: $F_{(2,204)}$=42.46, p<0.001. No other effects or interactions. n=16-20 from 4-5 mice in each age group in each transgenic mouse line. Data are shown as mean ± SEM.

5.4.2 Impairment of macroautophagy in dopamine neurons is associated with reduced rates of dopamine reuptake independent of age, in both the caudate-putamen and nucleus accumbens

One of the key determinants of DA neurotransmission is the rate of DA decay following a release event. The rate of DA decay is determined largely by the reuptake of DA by DAT. In the absence of DAT, DA can leave the release site via simple diffusion, extracellular degradation or uptake by non-neuronal cells. However, in DAT knockout mice, $[DA]_o$ persists over 100 times longer than in mice homozygous for DAT, illustrating the overwhelming importance of DAT for clearance of DA from the release site (Giros *et al.* 1996). In order to determine the rate of DA reuptake in both the caudate-putamen and nucleus accumbens, the falling phases of DA transients were examined following single pulse stimulation. The falling phases were concentration-matched when $[DA]_o$ reached 2 μM ± 0.4 μM in the caudate-putamen and 1 μM ± 0.2 μM in the nucleus accumbens. Each curve that met these criteria was fitted with a one-phase exponential decay curve, to give a decay constant, *K*, with units of s^{-1}. Data from the caudate-putamen are displayed in Figure 5.3 and from the nucleus accumbens in Figure 5.4. A three-way ANOVA was performed on data from the caudate-putamen, and this demonstrated an interaction between age and *ATG7*cKO$^{DAT\text{-IRES-cre}}$, with K values being lower in association *ATG7*cKO$^{DAT\text{-IRES-cre}}$ at every level of age. There was no effect of h*SNCA*. The same analysis was applied to data from the nucleus accumbens, and this demonstrated reductions in *K* values associated with *ATG7*cKO$^{DAT\text{-IRES-cre}}$, h*SNCA*, and age. In summary, these data demonstrate a reduction in DA reuptake in association with the *ATG7*cKO$^{DAT\text{-IRES-cre}}$ genotype in both regions studied, independent of age. Differences in *K* observed between age groups resemble the pattern of DA neuron loss (see Figure 3.6), and this may underlie slowed reuptake, in particular in the caudate-putamen.

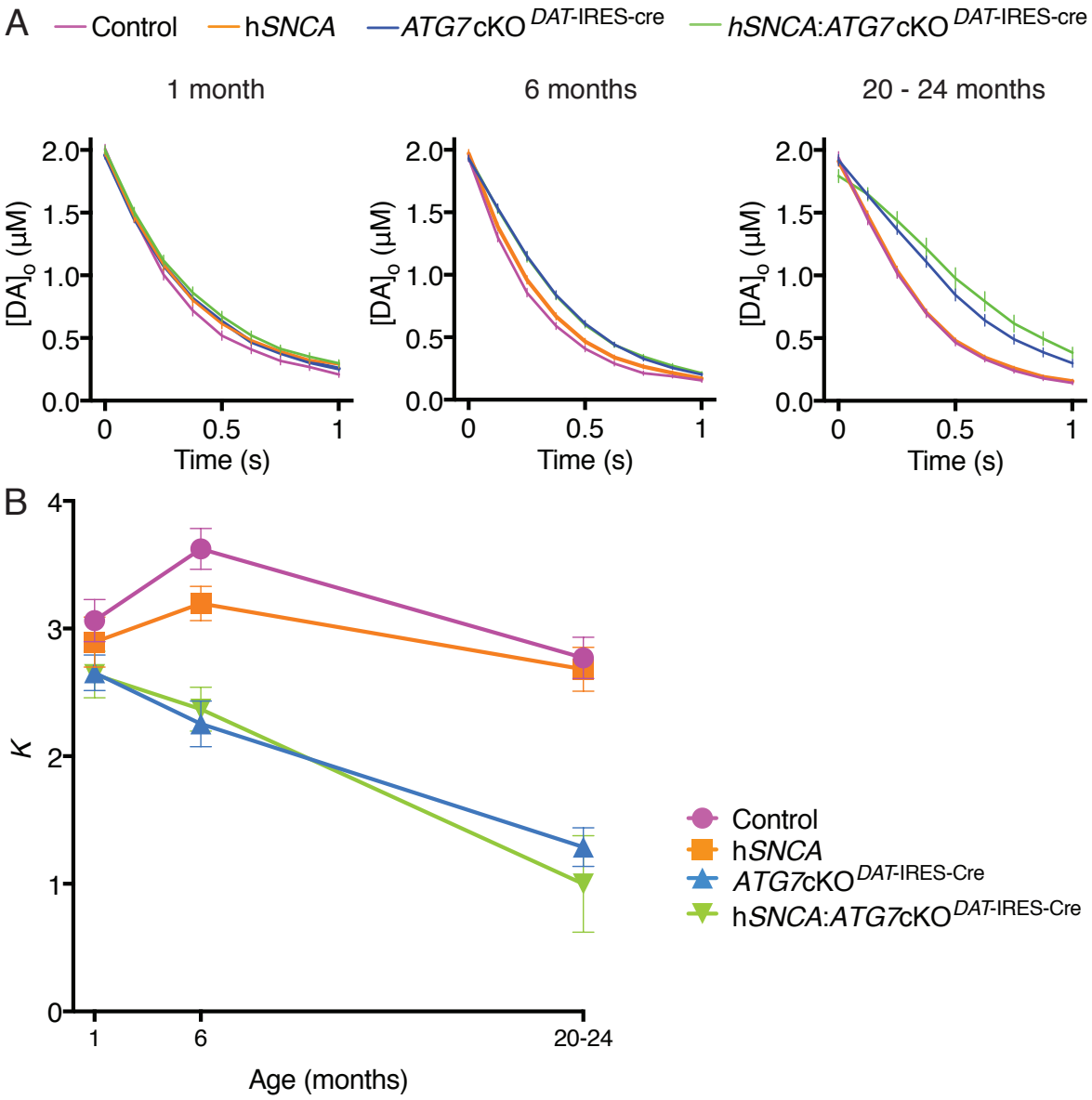


Figure 5.3. *ATG7*cKO$^{DAT\text{-IRES-cre}}$ is associated with a reduced rate of caudate-putamen dopamine reuptake, independent of age.

(A) Mean $[DA]_o$ reuptake profiles in the caudate-putamen in three different age groups, concentration matched at 2 µM [DA]. Data from four sites in the caudate-putamen were pooled. Time 0 is when the falling phase of the dopamine transient passed closest to 2 µM [DA]. **(B) Analysis of dopamine reuptake in the caudate-putamen in three different age groups.** Three-way ANOVA for age, *ATG7*cKO$^{DAT\text{-IRES-cre}}$ and h*SNCA*. There was a two-way interaction between *ATG7*cKO$^{DAT\text{-IRES-cre}}$ and age: $F_{(2,322)}$=9.74, p<0.001. Therefore, the effect of *ATG7*cKO$^{DAT\text{-IRES-cre}}$ was determined at each level of age, with a Bonferroni adjustment. The *ATG7*cKO$^{DAT\text{-IRES-cre}}$ was significantly associated with slower dopamine reuptake at every level of age. No other effects or interactions. n=6-20 from 4-5 mice in each age group in each transgenic mouse line. Data are shown as mean ± SEM.

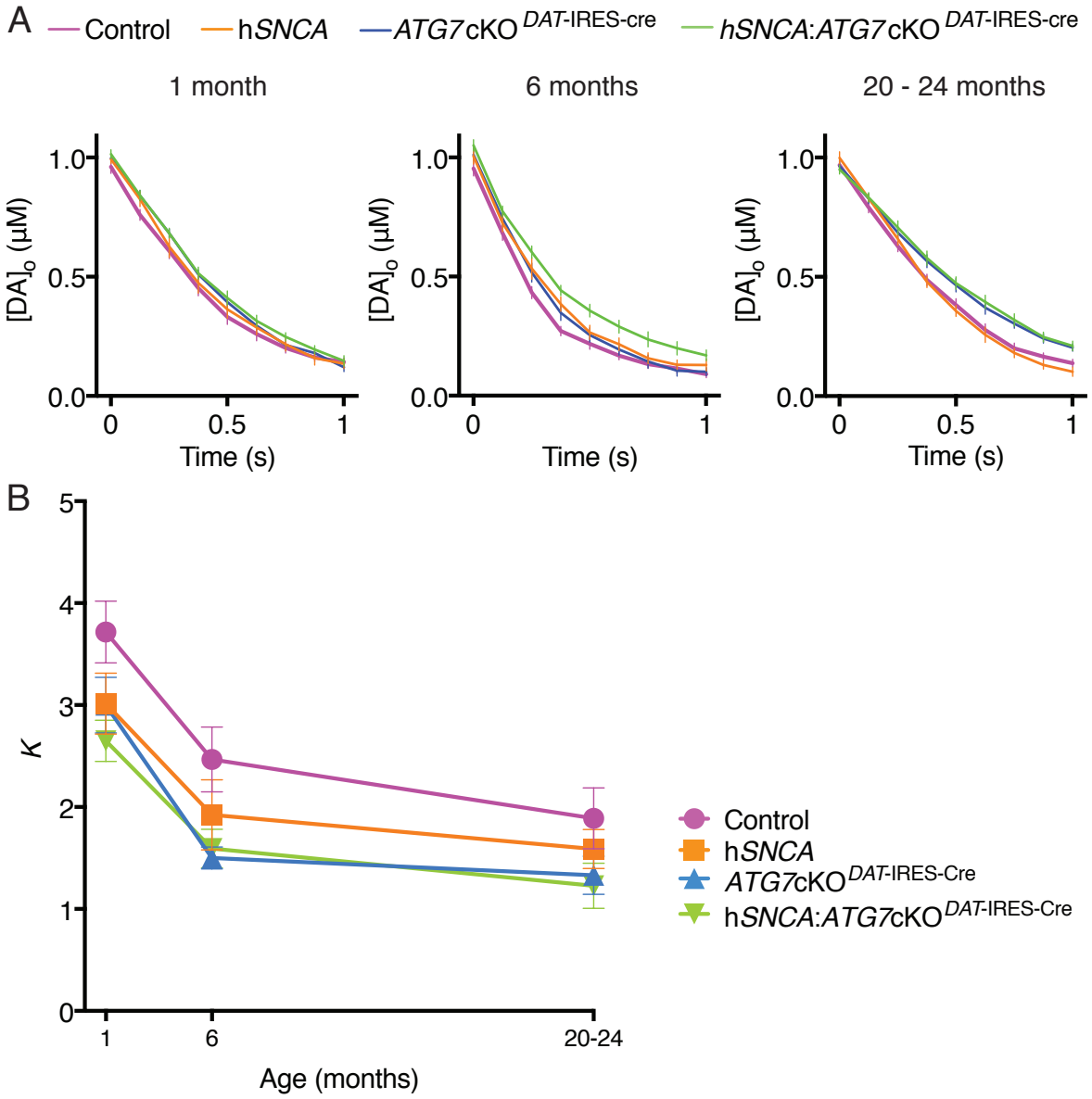


Figure 5.4. Both *ATG7*cKO$^{DAT\text{-IRES-cre}}$ and h*SNCA* reduce dopamine reuptake rate in the nucleus accumbens, independent of age.
(A) Mean $[DA]_o$ reuptake profiles in the nucleus accumbens in three different age groups, concentration matched at 1 µM [DA]. Data from two sites in the nucleus accumbens were pooled. Time 0 is when the falling phase of the dopamine transient passed closest to 1 µM [DA]. **(B) Analysis of dopamine reuptake in the nucleus accumbens in three different age groups.** Data were square root transformed for analysis, but presented here as raw data for ease of comparison. Three-way ANOVA for age, *ATG7*cKO$^{DAT\text{-IRES-cre}}$ and h*SNCA*. Main effect of age: $F_{(2,139)}$=43.10, p<0.001. Main effect of *ATG7*cKO$^{DAT\text{-IRES-cre}}$: $F_{(1,139)}$=13.06, p<0.001. Main effect of h*SNCA*: $F_{(1,139)}$=4.19, p=0.043 No other effects or interactions. n=9-12 from 4-5 mice in each age group in each transgenic mouse line. Data are shown as mean ± SEM.

5.4.3 Assessment of dopamine release probability

One factor that may account for the changes in evoked $[DA]_o$ in response to single electrical pulses is DA release probability. DA release probability can be defined as the likelihood that an action potential will cause release of neurotransmitter at a given synapse (Daniel *et al.* 2009).

A single electrical stimulus causes release of DA that is determined by the DA release probability. Multiple pulses will result in activation of almost all DA release sites, and this is thought to represent the maximum possible amount of DA that can be released. DA release probability can therefore be assessed by comparing the ratio of $[DA]_o$ following multiple pulses at high-frequency to $[DA]_o$ following a single pulse (Cragg 2003; Rice and Cragg 2004). Using this paradigm, the ratio of multiple pulse $[DA]_o$ to single pulse $[DA]_o$ is inversely proportional to DA release probability. Therefore, if any of the changes in DA release observed in the preceding experiments in this chapter were associated with differences in DA release probability, then differences in the ratio of a multiple pulse to single pulse ratio would be observed.

To determine DA release probability, $[DA]_o$ following four pulses at 100 Hz (4p) was normalised to $[DA]_o$ following a single pulse (Figure 5.5). There was an age-dependent change in the 4p:1p ratio in the caudate-putamen, such that the 4p:1p ratio was increased in association with the *ATG7*cKO$^{DAT\text{-IRES-cre}}$ in acute slices from mice at one month of age, but not in older age groups. There was no difference between genotypes at any age in the nucleus accumbens.

These data suggest that there is a reduction in caudate-putamen DA release probability at one month associated with the *ATG7*cKO$^{DAT\text{-IRES-cre}}$ genotype, which would have the effect of reducing peak evoked $[DA]_o$. Despite this, the *ATG7*cKO$^{DAT\text{-IRES-cre}}$ was associated with increased peak evoked $[DA]_o$ at 1-month, the opposite of what would be expected from a decrease in DA release probability. Therefore, this reduction in one month DA release probability may occur in order to counter the increased peak evoked $[DA]_o$ that occurs by another mechanism. Potential mechanisms mediating changes in DA release probability are considered in the discussion section of this chapter.

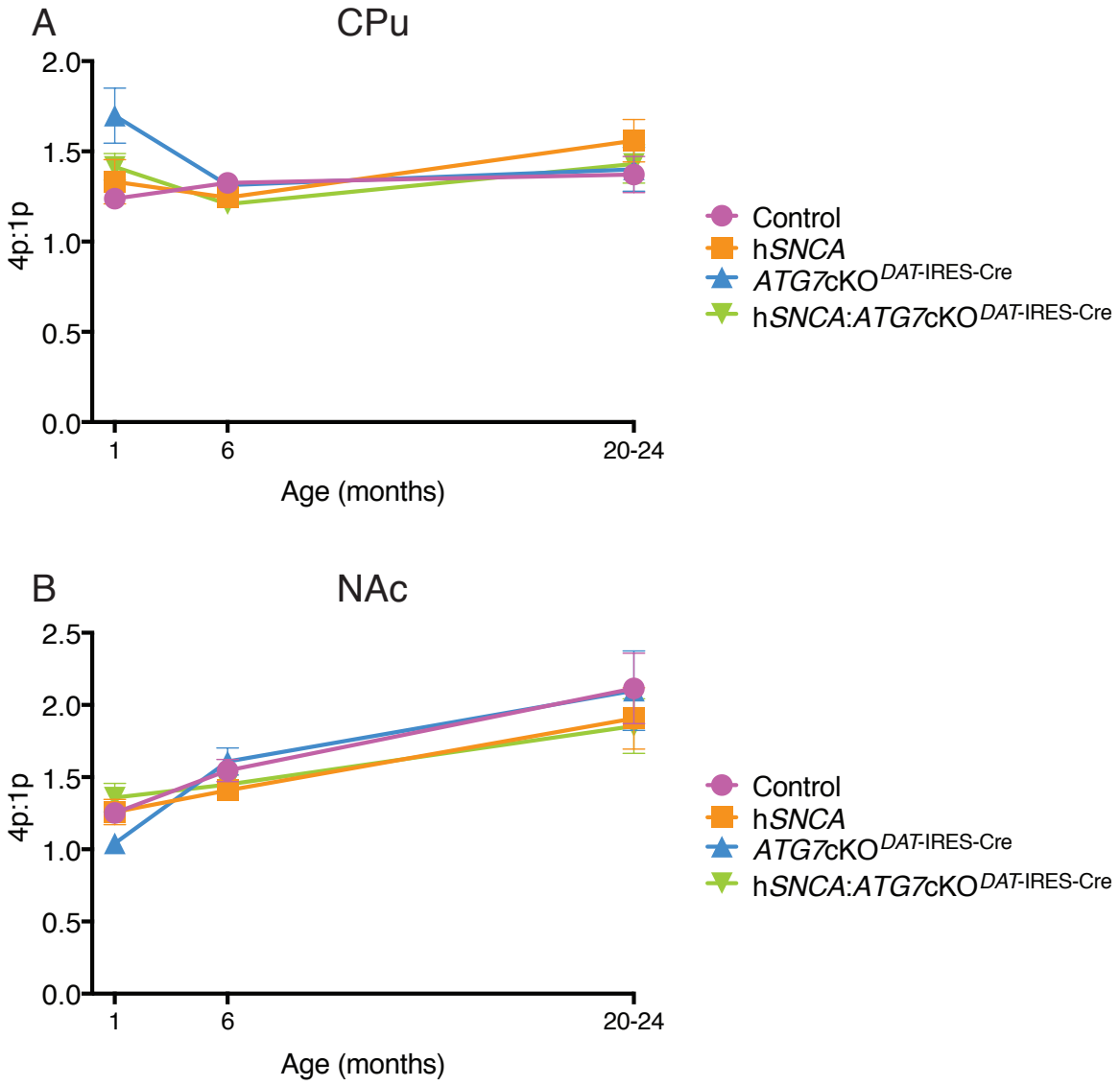


Figure 5.5. *ATG7*cKO$^{DAT\text{-IRES-cre}}$ is associated with increased quadruple pulse to single pulse ratio in the caudate-putamen in 1 month-old mice, but not in older mice, or in the nucleus accumbens.

(A) Analysis of quadruple pulse to single pulse ratio in the caudate-putamen in three different age groups. Three-way ANOVA for age, *ATG7*cKO$^{DAT\text{-IRES-cre}}$ and h*SNCA*. There was a two-way interaction between *ATG7*cKO$^{DAT\text{-IRES-cre}}$ and age: $F_{(2,420)}$=4.531, p=0.011. Therefore, the effect of *ATG7*cKO$^{DAT\text{-IRES-cre}}$ was determined at each level of age, with a Bonferroni adjustment. At 1 month, the 4p:1p ratio was 1.35 ± 0.06 in mice without *ATG7*cKO$^{DAT\text{-IRES-cre}}$ and 1.55 ± 0.06 in mice with *ATG7*cKO$^{DAT\text{-IRES-cre}}$, a statistically significant difference of 0.20 (95% CI 0.05 to 0.35), p=0.01. At 6 and 20 to 24 months, there was no association with the *ATG7*cKO$^{DAT\text{-IRES-cre}}$ and 4p:1p ratio. Main effect of age: $F_{(2,420)}$=6.04, p=0.003. n=32-40 from 4-5 mice in each transgenic mouse line in each age group. **(B) Analysis of quadruple pulse to single pulse ratio in the nucleus accumbens in three different age groups.** Data were log-transformed for analysis to a normal distribution as assessed by Q-Q plot and hustogram, although remained significantly different from a normal distribution using the Kolmogorov-Smirnov test with Lilliefors correction. Raw data are presented here. Three-way ANOVA for age, *ATG7*cKO$^{DAT\text{-IRES-cre}}$ and h*SNCA*. Main effect of age: $F_{(2,204)}$=17.19, p<0.001. No other effects or interactions. n=16-20 from 4-5 mice in each transgenic mouse line in each age group. Data are shown ± SEM

5.4.4 Evoked dopamine levels in response to stimuli of different frequencies

SNc and VTA DA neurons have both tonic and phasic firing patterns. Tonic firing of DA neurons is generally considered to occur at frequencies of less than 6 Hz, whereas phasic firing can occur at rates of up to 100 Hz (Grace and Bunney 1984; Hyland *et al.* 2002). The magnitude of DA release is dependent on the frequency of stimulation. In order to assess if the presence of the *ATG7*cKO$^{DAT\text{-IRES-cre}}$ or h*SNCA* genotypes had any effect on the response of DA release to stimulation frequency, striatal slices from 1 month-old mice were used, in order to eliminate any confounding effect that differences in DA neuron number and associated density of striatal innervation may have on frequency responsiveness.

Striatal slices were subjected to stimuli of different frequencies (5, 10, 25 and 100 Hz) in two sites: the dorsolateral caudate-putamen and the nucleus accumbens core. Data were normalised to one pulse release. In the caudate-putamen, there were no differences associated with the *ATG7*cKO$^{DAT\text{-IRES-cre}}$ or h*SNCA* genotypes or genotypes (Figure 5.6A). As expected, there was a strong association between stimulation frequency and magnitude of evoked $[DA]_o$. In the nucleus accumbens, presence of *ATG7*cKO$^{DAT\text{-IRES-cre}}$ was associated with increased DA release across at higher frequencies (Figure 5.6B). Again, there was a strong association between stimulation frequency and magnitude of evoked $[DA]_o$.

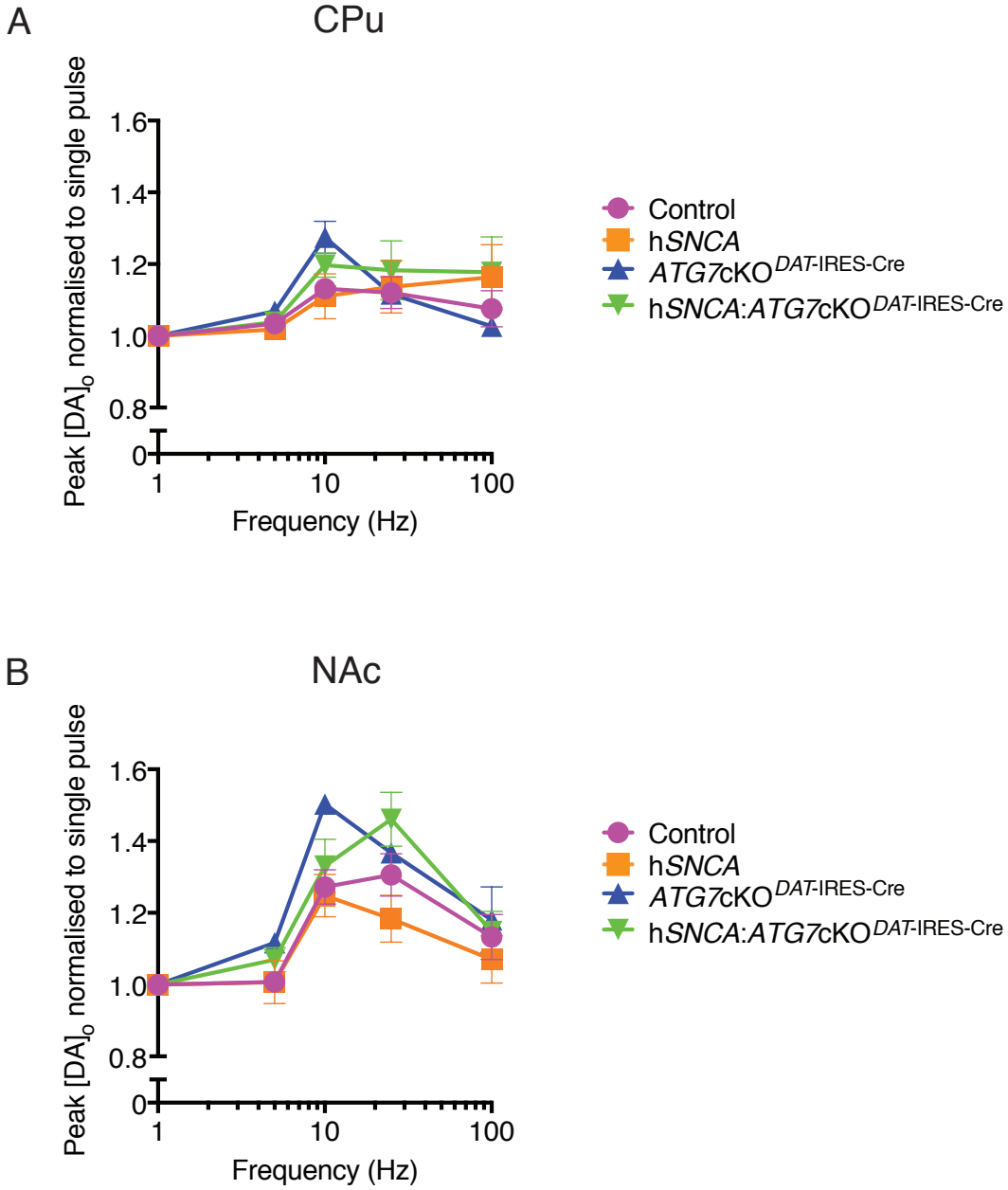


Figure 5.6. In striatal slices from 1 month-old mice, *ATG7*cKO$^{DAT\text{-IRES-cre}}$ is associated with increased dopamine release in the nucleus accumbens across all frequencies, but not in the caudate putamen.

(A) Analysis of dopamine release in the caudate-putamen in response to different physiologically relevant frequencies. Three-way ANOVA for frequency, *ATG7*cKO$^{DAT\text{-IRES-cre}}$ and h*SNCA*. Main effect of frequency: $F_{(4,135)}$=8.94, p<0.001. No other effects or interactions. n=7-8 from four mice in each transgenic mouse line. **(B) Analysis of dopamine release in the nucleus accumbens in response to different physiologically relevant frequencies.** Three-way ANOVA for frequency, *ATG7*cKO$^{DAT\text{-IRES-cre}}$ and h*SNCA*. Main effect of *ATG7*cKO$^{DAT\text{-IRES-cre}}$: $F_{(1,140)}$=17.29, p<0.001. Main effect of frequency: $F_{(4,135)}$=37.74, p<0.001. No other effects or interactions. n=8 from four mice in each transgenic mouse line. Data are shown ± SEM.

5.4.5 The ability to respond to repeated stimuli: paired-pulse depression

Neurons of the SNc and VTA facilitate movement by acting in a coordinated manner of repeated firing in both tonic and phasic fashions. For this reason, it is important to consider the magnitude of $[DA]_o$ in response to repeated stimuli. PPD is one metric that is commonly used to assess the ability of DA synapses to respond to a second stimulus, and is thought to reflect short-term, activity-dependent plasticity (Abeliovich *et al.* 2000; Cragg 2003; Hernandez *et al.* 2012). Previous work has shown a reduction in PPD in the caudate-putamen of *ATG7*cKO$^{DAT\text{-IRES-cre}}$ mice (Hernandez *et al.* 2012). α-Synuclein knockout mice show a similar reduction in PPD in response to single pulses (Abeliovich *et al.* 2000), although this finding is not consistent (S.J. Cragg, unpublished data). The behavioural corollaries of changes in PPD depression are not well resolved in the literature. However, it could be supposed that a reduction in PPD, for example, will result in increased evoked DA at a second stimulus, thereby increasing DA availability and facilitating movement.

In the set of experiments described in the following six figures, evoked $[DA]_o$ was assessed in the caudate-putamen and nucleus accumbens in response to two electrical stimuli, each 3 seconds apart. The stimuli used were either single pulses, or four pulses at a frequency of 100 Hz. The protocols used were as follows:

- 1 pulse – 3 seconds – 1 pulse (1p:1p. Shown in figures 5.7 and 5.10)
- 4 pulses – 3 seconds – 4 pulses (4p:4p. Shown in figures 5.8 and 5.11)
- 1 pulse – 3 seconds – 4 pulses (1p:4p. Shown in Figures 5.9 and 5.12)

In these experiments, the size of the second peak in $[DA]_o$ (p2) is expressed as a proportion of the initial peak (p1) – this is denoted as p2/p1. A higher p2/p1 indicates less PPD. A summary of the results is provided in the following table, for ease of comparison.

Table 5.1. Summary of effects of *ATG7*cKO$^{DAT\text{-IRES-cre}}$ and hSNCA on paired-pulse depression

Anatomical location:	**Protocol:**	***ATG7*cKO$^{DAT\text{-IRES-cre}}$**	**h*SNCA***	**Figure**
Caudate-putamen	1p:1p	Reduced	Increased	5.7
	4p:4p	Reduced	Increased	5.8
	1p:4p	Reduced	Increased at 20-24 months only	5.9
Nucleus accumbens	1p:1p	Reduced	No effect	5.10
	4p:4p	Reduced	No effect	5.11
	1p:4p	No effect	Increased at 20-24 months only	5.12

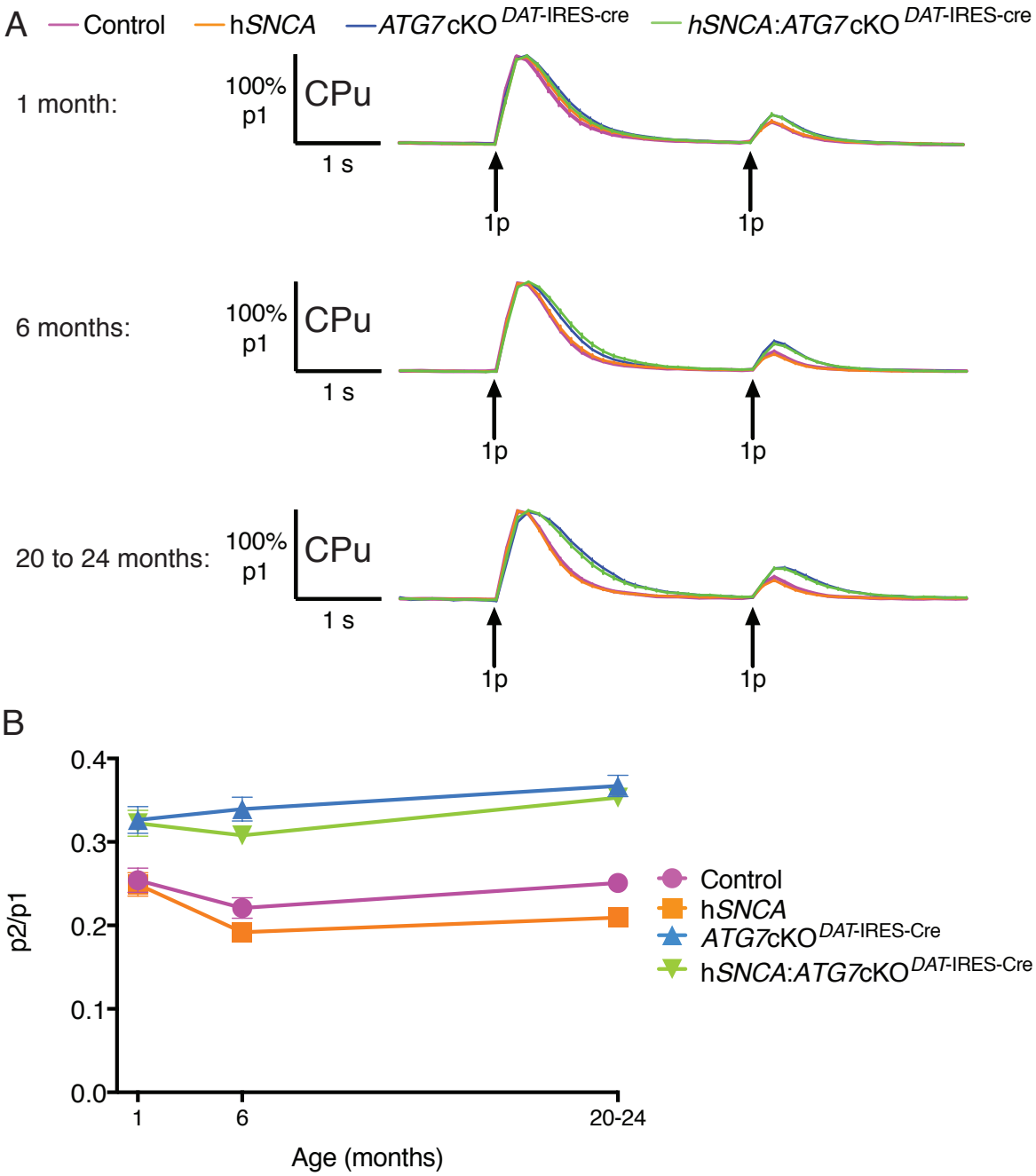


Figure 5.7. Paired-pulse depression in a paired single pulse protocol in the caudate-putamen is reduced by *ATG7*cKO$^{DAT\text{-IRES-cre}}$ and increased by h*SNCA*.
(A) Mean evoked $[DA]_o$ profiles over time following paired single pulse stimuli in the caudate-putamen, in three different age groups. Data from four sites in the caudate-putamen were pooled. **(B) Analysis of paired-pulse depression in three different age groups.** Data were normally distributed as assessed by Q-Q plot and histogram, but were significantly different from a normal distribution using a Kolmogorov-Smirnov test with Lilliefors correction. Three-way ANOVA for age, *ATG7*cKO$^{DAT\text{-IRES-cre}}$ and h*SNCA*. There was a two-way interaction between *ATG7*cKO$^{DAT\text{-IRES-cre}}$ and age: $F_{(2,420)}$=13.34, p<0.001. At every level of age, *ATG7*cKO$^{DAT\text{-IRES-cre}}$ was associated with reduced paired-pulse depression (p<0.001, Bonferroni corrected). Main effect of age: $F_{(2,419)}$=6.54, p=0.002. Main effect of *ATG7*cKO$^{DAT\text{-IRES-cre}}$: $F_{(1,419)}$=220.52, p<0.001. Main effect of h*SNCA*: $F_{(1,419)}$=7.88, p=0.005. No other effects or interactions. n=32-40 from 4-5 mice in each age group in each transgenic mouse line. Data are shown as mean ± SEM.

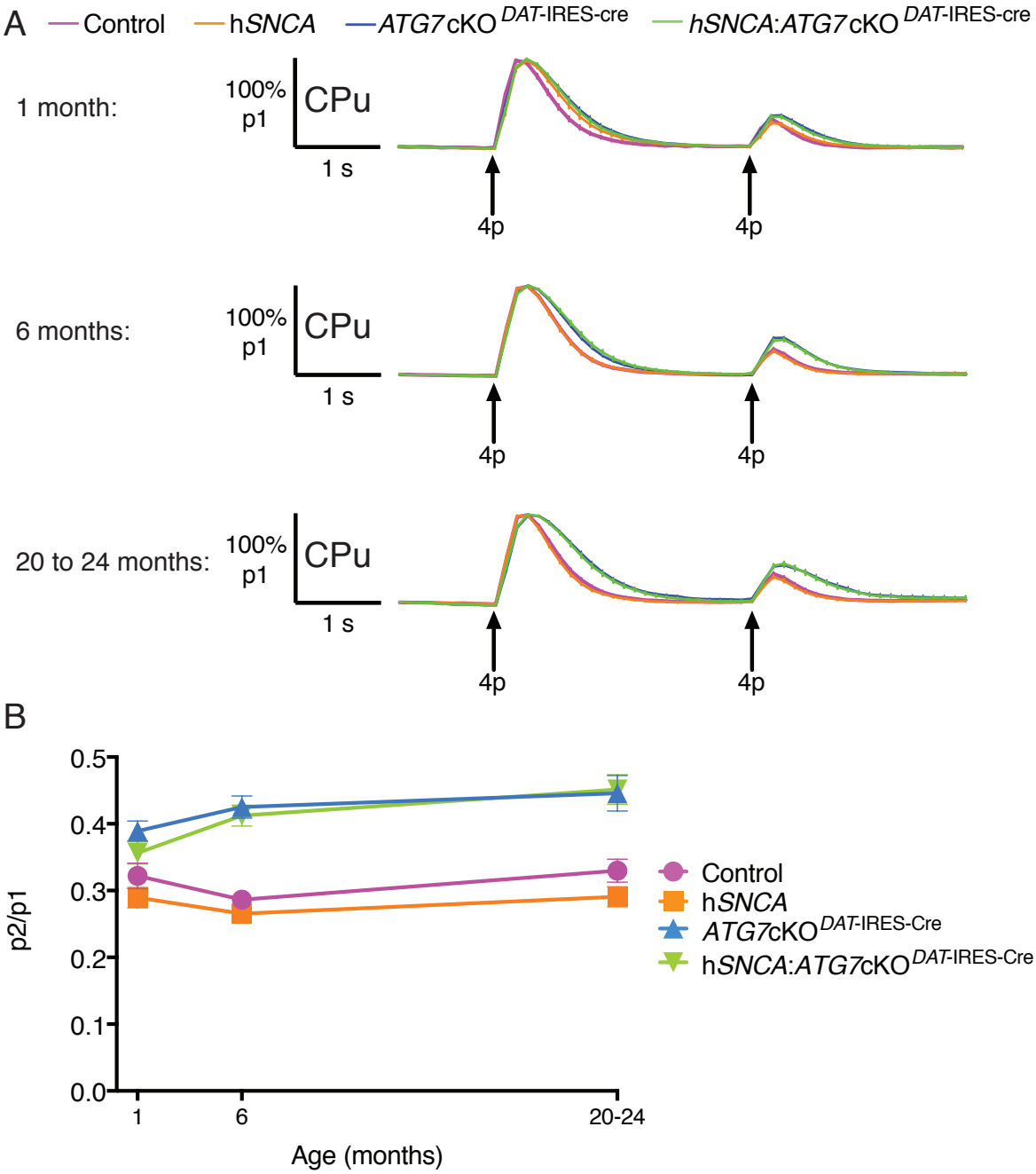


Figure 5.8. Paired-pulse depression in a paired quadruple pulse protocol in the caudate-putamen is reduced by *ATG7*cKO$^{DAT\text{-IRES-cre}}$ and increased by h*SNCA*.
(A) Mean evoked $[DA]_o$ profiles over time following paired quadruple pulse stimuli in the caudate-putamen, in three different age groups. Data from four sites in the caudate-putamen were pooled. **(B) Analysis of paired-pulse depression in three different age groups.** Three-way ANOVA for age, *ATG7*cKO$^{DAT\text{-IRES-cre}}$ and h*SNCA*. There was a two-way interaction between *ATG7*cKO$^{DAT\text{-IRES-cre}}$ and age: $F_{(2,418)}$=5.06, p=0.007. At every level of age, *ATG7*cKO$^{DAT\text{-IRES-cre}}$ was associated with reduced paired-pulse depression (p<0.001, Bonferroni corrected). Main effect of *ATG7*cKO$^{DAT\text{-IRES-cre}}$: $F_{(1,418)}$=119.93, p<0.001. Main effect of h*SNCA*: $F_{(1,418)}$=4.30, p=0.039. No other effects or interactions. n=32-40 from 4-5 mice in each age group in each transgenic mouse line. Data are shown as mean ± SEM.

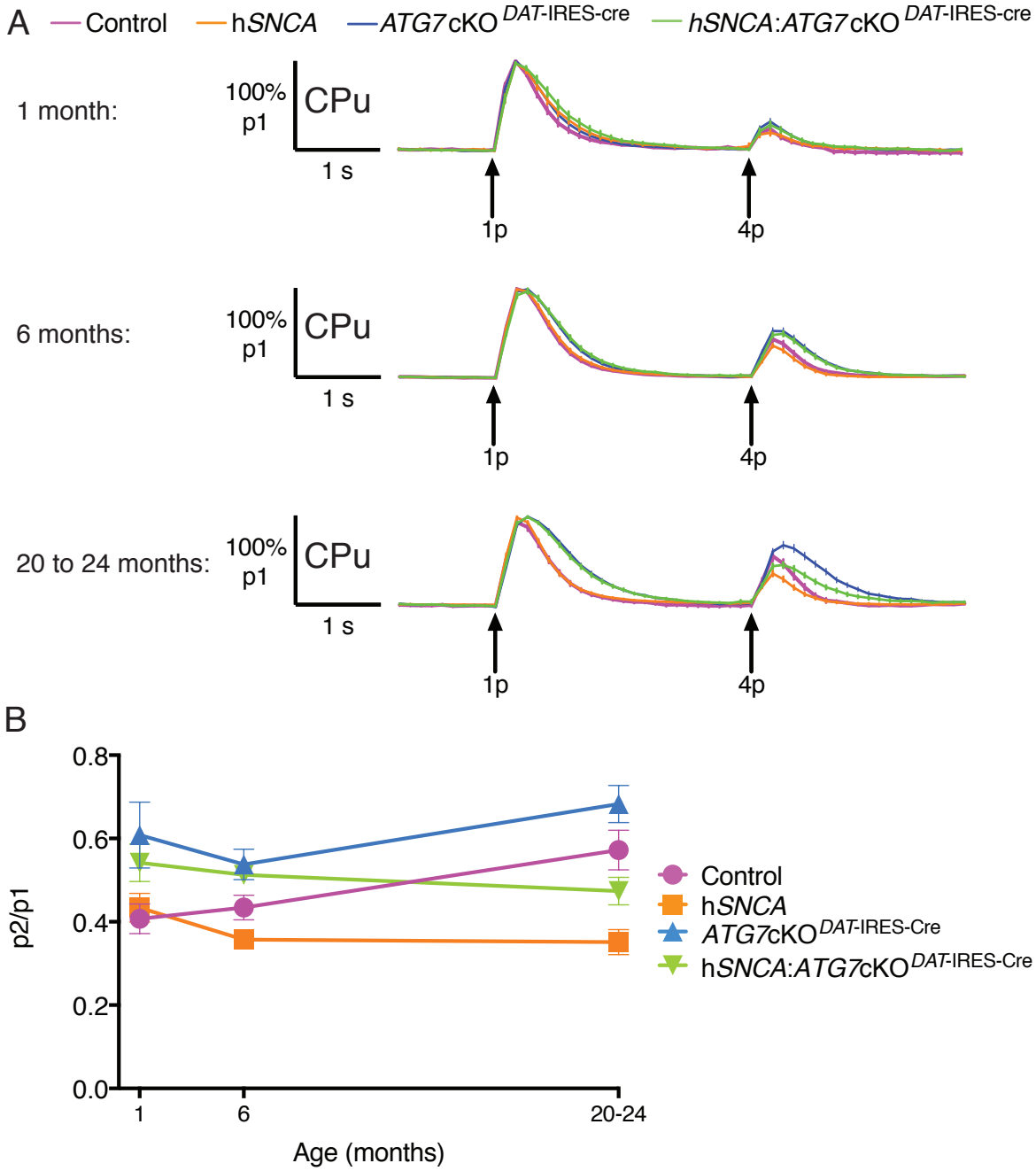


Figure 5.9. Paired-pulse depression in a single pulse-quadruple pulse protocol in the caudate-putamen is reduced by *ATG7*cKO$^{DAT\text{-IRES-cre}}$ independent of age and increased by h*SNCA* in 20 to 24 month-old mice.

(A) Mean evoked $[DA]_o$ profiles over time following single pulse-quadruple pulse stimuli in the caudate-putamen, in three different age groups. Data from four sites in the caudate-putamen were pooled. **(B) Analysis of paired-pulse depression in three different age groups.** Data were log transformed to a normal distribution as assessed by Q-Q plot and histogram, but were significantly different from a normal distribution using a Kolmogorov-Smirnov test with Lilliefors correction. Three-way ANOVA for age, *ATG7*cKO$^{DAT\text{-IRES-cre}}$ and h*SNCA*. There was a two-way interaction between h*SNCA* and age: $F_{(2,413)}$=12.95, p<0.001. Therefore, the effect of h*SNCA* was assessed at each level of age, with a Bonferroni adjustment. There was no effect of h*SNCA* in the 1 or 6 month-old groups, but a significant increase in paired-pulse depression was observed in the 20 to 24 month-old group (mean raw difference 0.22 ± 0.04, p<0.001). Main effect of *ATG7*cKO$^{DAT\text{-IRES-cre}}$: $F_{(1,413)}$=38.80, p<0.001. No other effects or interactions. n=32-40 from 4-5 mice in each age group in each transgenic mouse line. Data are shown as mean ± SEM.

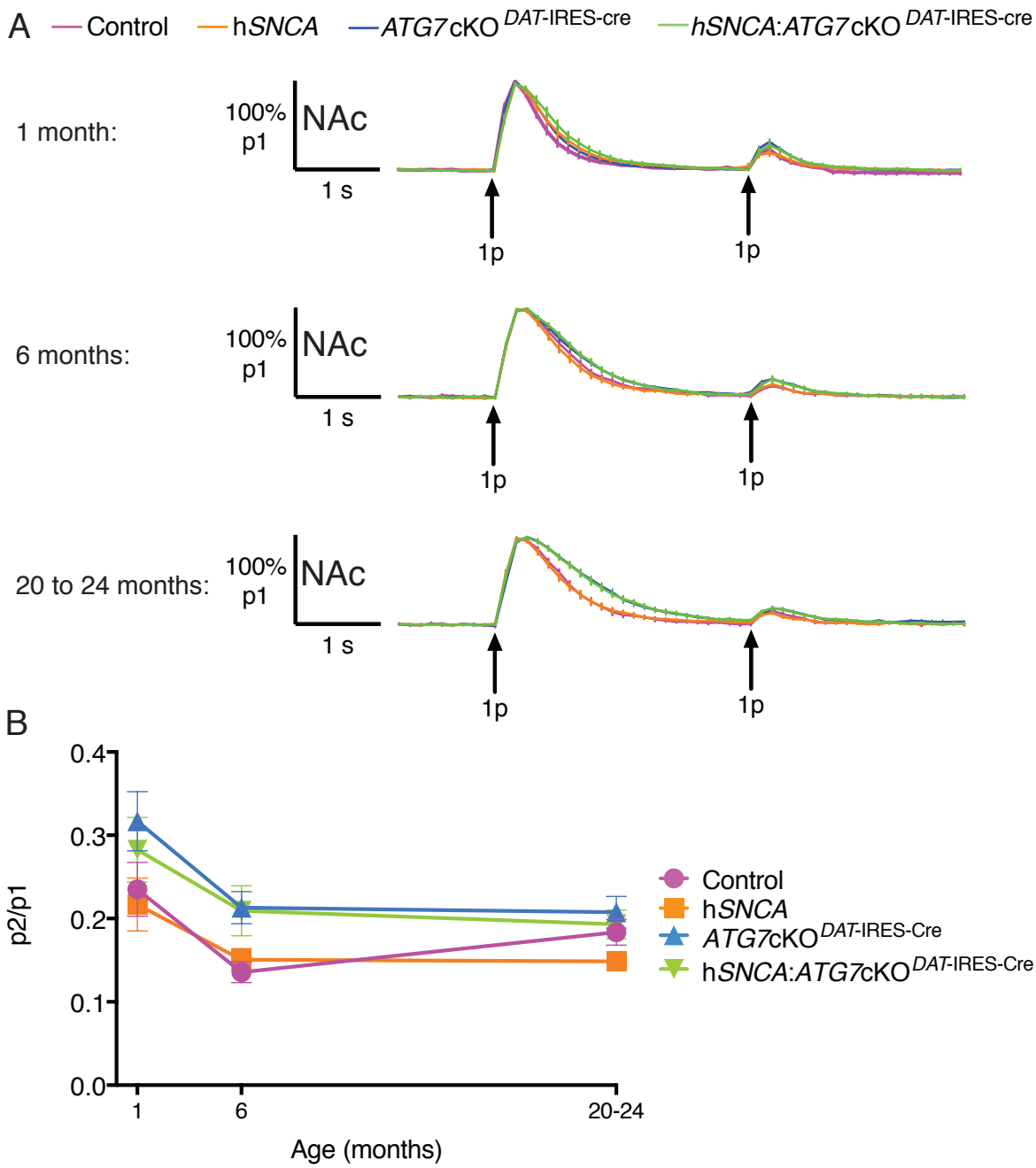


Figure 5.10. Paired-pulse depression in a paired single pulse protocol in the nucleus accumbens is reduced by *ATG7*cKO$^{DAT\text{-IRES-cre}}$.
(A) Mean evoked $[DA]_o$ profiles over time following paired single pulse stimuli in the nucleus accumbens, in three different age groups. Data from two sites in the nucleus accumbens were pooled. **(B) Analysis of paired-pulse depression in three different age groups.** Data were log-transformed for analysis, but presented here as raw data for ease of comparison. Three-way ANOVA for age, *ATG7*cKO$^{DAT\text{-IRES-cre}}$ and h*SNCA*. Main effect of age: $F_{(2,204)}$=9.00, p<0.001. Main effect of *ATG7*cKO$^{DAT\text{-IRES-cre}}$: $F_{(1,204)}$=17.38, p<0.001. No other effects or interactions. n=16-20 from 4-5 mice in each age group in each transgenic mouse line. Data are shown as mean ± SEM.

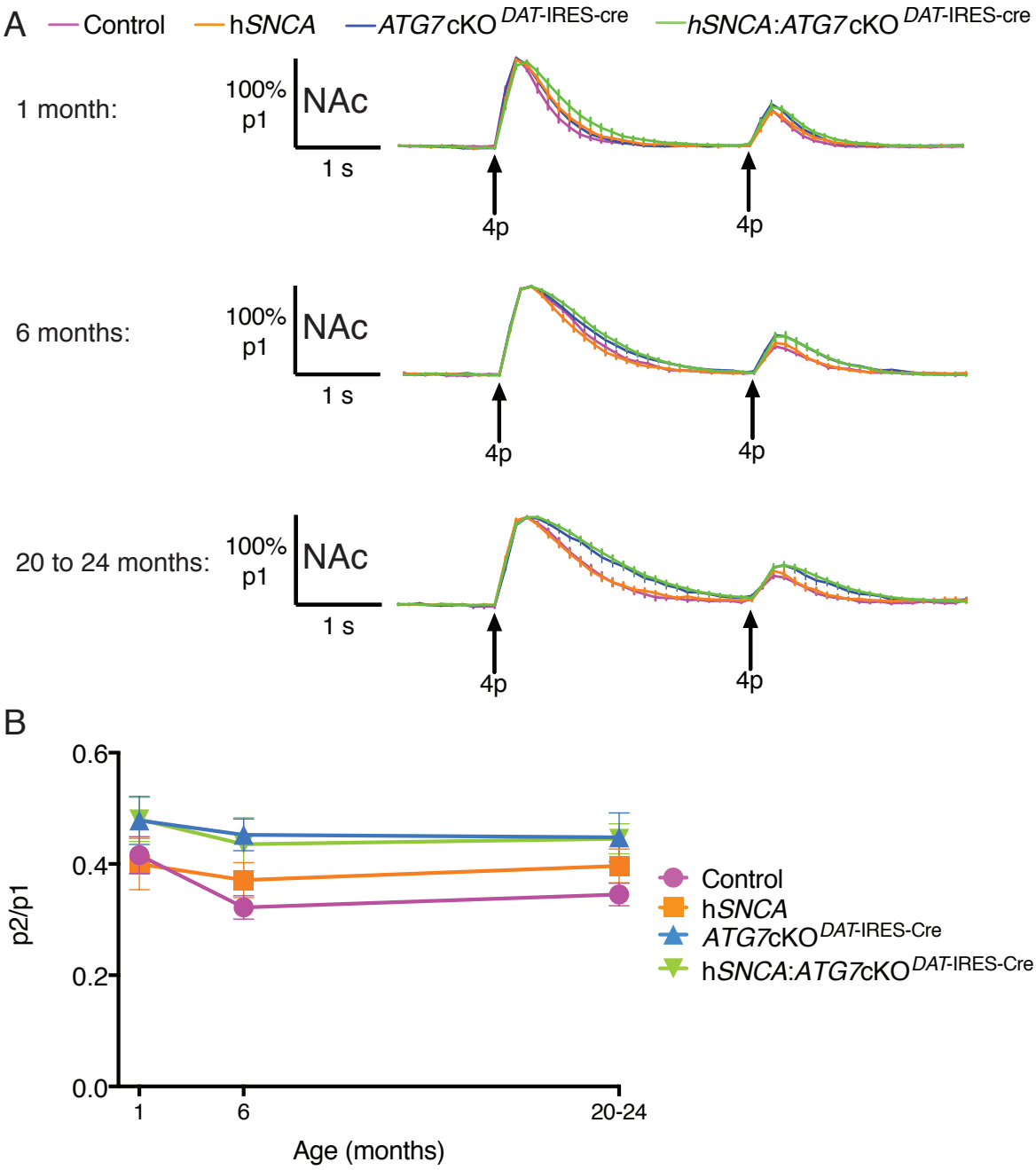


Figure 5.11. Paired-pulse depression in a paired quadruple pulse protocol in the nucleus accumbens is decreased by *ATG7*cKO$^{DAT\text{-IRES-cre}}$.
(A) Mean evoked $[DA]_o$ profiles over time following paired quadruple pulse stimuli in the nucleus accumbens, in three different age groups. Data from two sites in the nucleus accumbens were pooled. **(B) Analysis of paired-pulse depression in three different age groups.** Three-way ANOVA for age, *ATG7*cKO$^{DAT\text{-IRES-cre}}$ and h*SNCA*. Main effect of *ATG7*cKO$^{DAT\text{-IRES-cre}}$: $F_{(1,204)}=16.32$, $p<0.001$. No other effects or interactions. n=16-20 from 4-5 mice in each age group in each transgenic mouse line. Data are shown as mean ± SEM.

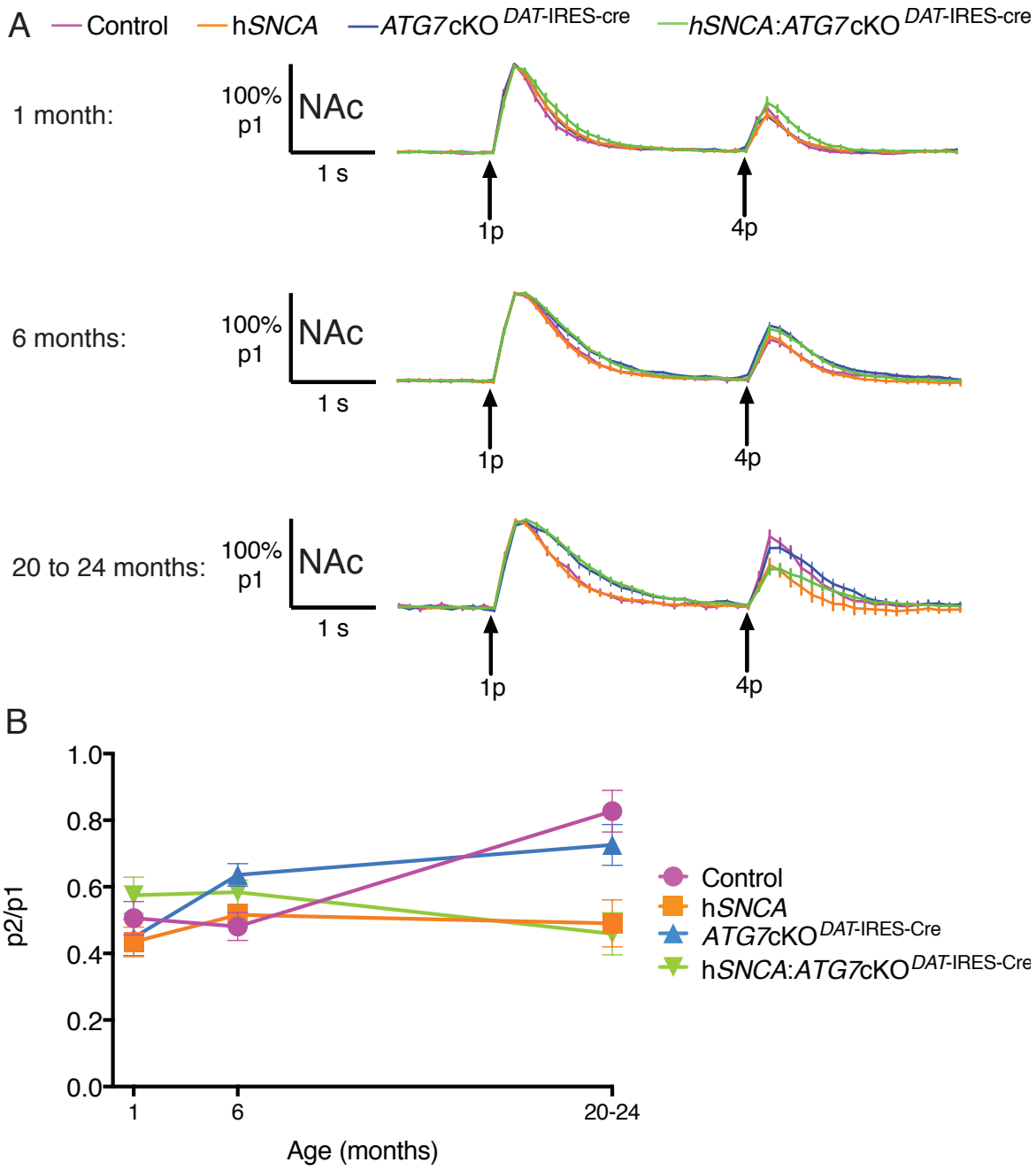


Figure 5.12. Age-dependent increase in paired-pulse depression of dopamine release associated with h*SNCA* in a single pulse-quadruple pulse protocol in the nucleus accumbens.

(A) Mean evoked $[DA]_o$ profiles over time following single pulse-quadruple pulse stimuli in the nucleus accumbens, in three different age groups. Data from two sites in the nucleus accumbens were pooled. **(B) Analysis of paired-pulse depression in three different age groups.** Three-way ANOVA for age, *ATG7*cKO$^{DAT\text{-IRES-cre}}$ and h*SNCA*. There was a two-way interaction between h*SNCA* and age: $F_{(2,204)}$=11.77, p<0.001. Therefore, the effect of h*SNCA* was assessed at each level of age, with a Bonferroni adjustment. There was no effect of h*SNCA* in the 1 or 6 month-old groups, but a significant increase in paired-pulse depression was observed in the 20 to 24 month-old group (mean difference 0.30 ± 0.05, p<0.001). Main effect of age: $F_{(1,204)}$=6.33, p=0.002. No other effects or interactions. n=16-20 from 4-5 mice in each age group in each transgenic mouse line. Data are shown as mean ± SEM.

5.5 Discussion

5.5.1 Impaired macroautophagy in dopamine neurons increases evoked dopamine concentrations

In the present study, evoked $[DA]_o$ was assessed following a single pulse electrical stimulation. The *ATG7*cKO$^{DAT\text{-IRES-cre}}$ genotype was associated with increased peak $[DA]_o$ in the caudate-putamen of 1 month-old mice; this same genotype was associated with reduced evoked $[DA]_o$ in mice aged 6 and 20 to 24 months.

It is important to note that at 6 and 20 to 24 months, mice with the *ATG7*cKO$^{DAT\text{-IRES-cre}}$ had large reductions the numbers of SNc neurons, the primary projection neurons to the caudate-putamen. Therefore, it would be expected that mice with the *ATG7*cKO$^{DAT\text{-IRES-cre}}$ genotype in these age groups would have fewer dopaminergic terminals in the caudate-putamen, and thus reduced peak evoked $[DA]_o$.

The primary DA projection neurons to the nucleus accumbens are located in the VTA, where there is no genotype-associated cell loss. In the nucleus accumbens, *ATG7*cKO$^{DAT\text{-IRES-cre}}$ was associated with increased peak evoked $[DA]_o$. Similarly, there is no loss of SNc DA neurons in 1 month-old mice, which project to the caudate-putamen, and here there is increased peak evoked $[DA]_o$ associated with the *ATG7*cKO$^{DAT\text{-IRES-cre}}$ genotype. These data suggest that in settings where there is no loss of DA projection neurons, the *ATG7*cKO$^{DAT\text{-IRES-cre}}$ genotype increases evoked $[DA]_o$. These findings are consistent with those described by Hernandez *et al.* (2012), the only previous group to have published data on the relationship between impaired macroautophagy and DA neurotransmission.

The potential mechanisms by which impaired macroautophagy increases peak $[DA]_o$ merit consideration. Peak $[DA]_o$ may be increased solely by a reduced rate of DA reuptake; a possibility that is discussed in section 1.5.2. Another potential explanation is that synaptic vesicles are degraded via macroautophagy (Hernandez *et al.* 2012). Therefore, when macroautophagy is impaired there are more synaptic vesicles to fuse with the presynaptic membrane and thus peak $[DA]_o$ is increased. This would tally with classical studies that demonstrate a role for lysosomal degradation in breakdown of synaptic vesicles (Holtzman *et al.* 1971). Macroautophagy has also been implicated in the degradation of synaptic receptors, and it is possible that impairment of macroautophagy perturbs degradation of presynaptic receptors such that peak $[DA]_o$ is increased (Rowland *et al.* 2006; Matsuda *et al.* 2008).

It is unlikely that the increased peak $[DA]_o$ observed in this chapter is a result of changes in DA release probability. DA release probability can be screened by examining the ratio of evoked $[DA]_o$ in response to multiple stimuli (e.g. four pulses) and comparing this to evoked $[DA]_o$ in response to a single pulse (Cragg 2003; Rice and Cragg 2004). This ratio is inversely proportional to DA release probability. In the caudate-putamen of 1 month-old *ATG7*cKO$^{DAT\text{-IRES-cre}}$ mice, the 4p:1p ratio was increased, suggesting that DA release probability was reduced in these mice, the opposite of the effect that would increase evoked $[DA]_o$. The DA release probability in these mice may be reduced in order to counter the observed increase in evoked $[DA]_o$. One of the most important factors determining DA release probability is the contribution of cholinergic interneuron innervation to DA neurons, which serves to reduce evoked $[DA]_o$ in response to a single

pulse, but enhances response to burst stimuli (Rice and Cragg 2004; Threlfell *et al.* 2012). Thus, increased cholinergic tone may be mediating this reduction in DA release probability in the caudate-putamen of 1 month-old *ATG7*cKO$^{DAT\text{-IRES-cre}}$ mice, but this hypothesis is not tested further here.

5.5.2 Dopamine reuptake is impaired when macroautophagy is impaired

In the present study, DA reuptake was reduced in all regions and age groups sampled. The major determinant of DA reuptake is the DA Transporter (DAT); when DAT is absent or saturated, DA can only leave the synapse via simple diffusion (Giros *et al.* 1996; Jones *et al.* 1998). Therefore, if DA release is unchanged, a reduction in DAT activity is associated with increased peak $[DA]_o$. This effect can be observed in striatal slices through acute application of DAT antagonists, such as cocaine and GBR-12909 (Cragg *et al.* 2000). A reduction in DAT activity may therefore explain the increased evoked $[DA]_o$ observed in experiments where there was no DA cell loss.

A reduction in DAT availability, independent of neuron number, is consistent with findings reported by Niu et al. (2016), who found that impaired autophagy in DA neurons, achieved using an *ATG7*cKO$^{TH\text{-cre}}$ model, was associated with reduced susceptibility to MPTP intoxication. The selectivity of MPTP for DA neurons is driven by its selective uptake by DAT (Javitch *et al.* 1985). Therefore, when less DAT is available, the uptake of MPTP would be reduced, and its toxicity abrogated.

DAT is rapidly trafficked to and from the synaptic membrane, providing dynamic spatiotemporal regulation of synaptic DA. For example, within thirty seconds of stimulation with amphetamine, membrane DAT levels increase by 60% (Johnson *et al.* 2005). Within the cell, DAT principally resides in endosomes, which can fuse with the plasma membrane, thereby inserting DAT (Melikian and Buckley 1999; Loder and Melikian 2003; Hong and Amara 2013). Impairment of macroautophagy, and the accumulation of autophagic vesicles that this entails, may impede the cycling of DAT to and from the plasma membrane, thus reducing the availability of DAT to return DA from the synapse. Alternatively, one of the mechanisms by which DAT is regulated is via ubiquitylation, where DAT is tagged with ubiquitin, prompting its internalisation and degradation (Miranda *et al.* 2007). In Chapter 3, ubiquitin aggregates were visualised in DA neurons when macroautophagy was impaired. It is possible that ubiquitylation mechanisms in DA neurons of *ATG7*cKO$^{DAT\text{-IRES-cre}}$ mice are disturbed, altering DAT ubiquitylation and therefore reducing the rate of DAT activity.

In order to overcome the problem of changes in DA neuron number confounding DA reuptake data, alternative approaches could be employed in future. For example, cell lines that express DAT could be subjected to chemical modifiers of autophagy, such as bafilomycin or rapamycin, and DA uptake measured. Alternatively, acute chemical or genetic (e.g. *ATG7* siRNA) modifiers of autophagy may be introduced into the midbrain of rodents, and FCV or other DA reuptake assays performed. The recent literature suggests that the latter approach may have effects on DAT function. Hung *et al.* (2014) infused *ATG7* siRNA into the substantia nigra of rats, and found that this reduced the toxicity of MPP+ administered 4 days later.

It is worthy of note that the *DAT*-IRES-cre system used so far in this thesis is based upon genetic editing of the *DAT* locus. Although every mouse used has the same *DAT* genotype, it is possible that the reuptake effects observed are an artifact of this expression system. In part to address these shortcomings, in Chapter 6 of this thesis, the effect of *ATG7*cKO on DA neurotransmission is examined using the *TH*-IRES-cre driver line.

5.5.3 In most contexts, impaired macroautophagy in dopamine neurons reduces paired-pulse depression, whereas human α-synuclein increases paired-pulse depression

In this chapter, the *ATG7*cKO$^{DAT\text{-IRES-cre}}$ genotype was associated with a reduction in PPD in all protocols used in the caudate-putamen, and in two of the three protocols used in the nucleus accumbens. A reduction in PPD increases DA availability after a second stimulus, providing a potential mechanism for increased locomotion in these mice. Synaptic depression may result from a reduction in the readily releasable pool of synaptic vesicles. If impaired macroautophagy brought about an increase in the readily releasable pool, this could account for reduced PPD. For example, macroautophagy may be responsible for degrading some synaptic vesicles; when macroautophagy is impaired (the *ATG7*cKO$^{DAT\text{-IRES-cre}}$ genotype), these vesicles remain, increasing the size of the readily releasable pool. Alternatively, changes in presynaptic receptor activation, such as the D_2 autoreceptor, may influence DA release at the second stimulus. However, D_2-related effects in the mouse striatum disappear after 600 milliseconds (Benoit-Marand *et al.* 2001), so they are unlikely to play a role in PPD differences in the PPD experiments described here, where the stimuli are separated by 3 seconds.

5.5.4 Dopamine neurotransmission and tests of motor function: correlation does not equal causation

In the set of experiments described in this chapter, a number of factors were identified that serve to enhance DA neurotransmission in *ATG7*cKO$^{DAT\text{-IRES-cre}}$ mice. These findings correlate with the improved motor function observed in mice with the *ATG7*cKO$^{DAT\text{-IRES-cre}}$ genotype. However, it has not been demonstrated that the improved motor performance was a direct consequence of the enhancement of DA neurotransmission, although it does remain a likely explanation.

In addition it is difficult to determine whether the effects observed in the caudate-putamen, or in the nucleus accumbens would be the primary drivers of improved motor performance. The caudate-putamen is primarily associated with motor phenotypes, derived in part from its degeneration in association with PD. However, increased DA in the nucleus accumbens is reliably associated with increased locomotion (Pijnenburg and van Rossum 1973; Kelly *et al.* 1975; Delfs *et al.* 1990), and it is in the nucleus accumbens that evoked $[DA]_o$ is unaffected by cell loss, and where evoked $[DA]_o$ is particularly increased at physiological firing frequencies associated with motor function.

5.5.5 Strengths and limitations of examining dopamine neurotransmission using fast-scan cyclic voltammetry

Multiple techniques can be utilised to examine DA neurotransmission. Each of these has advantages, drawbacks and limitations. In this chapter, *ex vivo* FCV was used. *Ex vivo*

FCV has advantages over *in vivo* FCV, as the synapses have been separated from neuronal cell bodies, which allows for precise manipulation of firing frequencies, and assessment of synaptic function without the confounding effects of cellular pathology. Additionally, use of *ex vivo* striatal slices has practical advantages, allowing specific brain regions to be easily accessible. The major advantage of *in vivo* FCV is the ability to correlate DA recordings with behavioural tasks directly. For example, if *in vivo* FCV had been used in the mouse lines described in this thesis, the $[DA]_o$ could be correlated with a rotarod task. Microdialysis is another commonly used technique to examine DA neurotransmission that involves periodic sampling of extracellular DA using a striatal catheter that is perfused with aCSF. This technique lacks temporal resolution, precluding accurate measures of parameters such as reuptake, frequency responsiveness and PPD.

5.5.6 Chapter summary

The data collected in this chapter are summarised in Table 5.2. In general, factors associated with increased DA availability, such as higher evoked $[DA]_o$, slower DA reuptake, and reduced PPD were found in acute striatal slices from *ATG7*cKO$^{DAT\text{-IRES-cre}}$ mice. These data provide a physiological basis for enhanced motor performance observed in these mice. It should be noted, however, that these findings are in a mouse model, and one that is based upon genetic alteration of DAT, a major determinant of DA neurotransmission. Chapter 6 uses *ATG7*cKO$^{TH\text{-IRES-cre}}$ mice to confirm the effects of macroautophagy impairment on DA neurotransmission, independent of cre driver line.

Table 5.2. Dopamine neurotransmission phenotypes associated with *ATG7*cKO$^{DAT\text{-IRES-cre}}$ and h*SNCA* genotypes in experimental mice

Anatomical region	Parameter	*ATG7*cKO$^{DAT\text{-IRES-cre}}$	h*SNCA*
Caudate-putamen	1p release	Increased at 1 month, decreased at 6 and 20 to 24 months	No effect
	DA reuptake	Reduced	No effect
	Release probability	Reduced at 1 month	No effect
	Frequency-response	No effect	No effect
	1p:1p PPD	Reduced	Increased
	4p:4p PPD	Reduced	Increased
	1p:4p PPD	Reduced	Increased at 20 to 24 months
Nucleus accumbens	1p release	Increased	No effect
	DA reuptake	Reduced	Reduced
	Release probability	No effect	No effect
	Frequency-response	Increased	No effect
	1p:1p PPD	Reduced	No effect
	4p:4p PPD	Reduced	No effect
	1p:4p PPD	No effect	Increased at 20 to 24 months

1p, 1 pulse. 4p, 4 pulse. DA, dopamine. PPD, paired-pulse depression.

Chapter 6: Examination of dopamine neurotransmission when macroautophagy is impaired in dopamine neurons, using a *TH*-IRES-cre driver line

6 Examination of dopamine neurotransmission when macroautophagy is impaired in dopamine neurons, using a *TH*-IRES-cre driver line

6.1 Introduction

In Chapter 5, a number of changes in DA neurotransmission were shown to occur when macroautophagy was impaired by means of conditional deletion of *ATG7* in *DAT*-expressing neurons. Such changes included enhanced evoked $[DA]_o$ in the caudate-putamen and nucleus accumbens at a young age, reduced PPD, and a reduced rate of $[DA]_o$ reuptake. Similar findings, save for the difference in DA reuptake, were reported by Hernandez and colleagues (2012) in 8 to 10 week-old *ATG7*cKO$^{DAT\text{-IRES-cre}}$ mice. These changes in $[DA]_o$ dynamics correlate with an improvement in motor performance of *ATG7*cKO$^{DAT\text{-IRES-cre}}$ mice, as discussed in Chapter 4. However, these results may be confounded by, or specific to, the *DAT*-IRES-cre expression system used, which by its nature requires the manipulation of DAT. DAT is the major determinant of dopaminergic neurotransmission, and thus even small differences in trafficking, conformation or orientation can have major effects on neurotransmission (Giros *et al.* 1996; Jones *et al.* 1998). Therefore, in this chapter, conditional deletion of *ATG7* in DA neurons was achieved using a *TH*-IRES-cre system. *ATG7*cKO$^{TH\text{-IRES-cre}}$ mice have both wild-type DAT alleles, removing artificial changes in DAT as a potential cause of any DA neurotransmission differences observed.

Two previous studies of *ATG7* deletion in DA neurons utilising the *TH* promoter to drive cre expression have been conducted. The first, by Friedman and colleagues (2012), used

the same *TH*-IRES-cre system used in this chapter. In the *ATG7*cKO$^{\text{TH-IRES-cre}}$ mouse, Friedman *et al.* found that there was a normal complement of SNc DA neurons at 4 months, but a 40% reduction at 9 months. There was no change in striatal DA levels, assessed using HPLC, at 1 month, but a 50% reduction at 4 months. Behavioural tests demonstrated reduced locomotor activity at 9 months compared with controls, a phenotype that was absent at 4 months. Later studies were conducted by Niu et al. (2016) using the *TH*-cre driver line developed by Gelman and colleagues (2003). In *ATG7*cKO$^{\textit{TH}\text{-cre}}$ mice a reduction in DA neuron number was found at 5 months, with no earlier timepoints examined. Niu and colleagues found that the remaining SNc neurons were resistant to MPTP toxicity, a phenotype that persisted at 12 months. A reduction in MPTP toxicity could be explained by reduced DAT availability, as DAT is the entry point for MPTP into the DA neuron (Javitch *et al.* 1985).

DA neurotransmission has not been previously examined in the *ATG7*cKO$^{\textit{TH}\text{-IRES-cre}}$ mouse model and therefore a thorough characterisation will serve as a platform for further studies by other members of the Wade-Martins group. The h*SNCA* transgene was not used in these experiments, as the major effects observed in Chapters 3, 4, and 5 were attributable only to impaired macroautophagy in DA neurons. Enhanced DA neurotransmission was observed in *ATG7*cKO$^{\textit{DAT}\text{-IRES-cre}}$ mice, including increased evoked $[DA]_o$, reduced rates of DA reuptake, and reduced PPD. Therefore, in this chapter, the hypothesis that *ATG7*cKO$^{\textit{TH}\text{-IRES-cre}}$ mice have enhanced DA neurotransmission characteristics is tested.

6.2 Chapter aims

1. To describe the generation of a mouse line featuring macroautophagy impairment in DA neurons, utilising conditional deletion of *ATG7* in a *TH*-IRES-cre driver line (a *ATG7*cKO$^{TH\text{-IRES-cre}}$ mouse).
2. To test whether macroautophagy impairment in DA neurons, using an *ATG7*cKO$^{TH\text{-IRES-cre}}$ model, enhances DA neurotransmission. This aim will be tested by examining the following measurements in the caudate-putamen and nucleus accumbens:
    a. Peak evoked extracellular DA concentrations in response to single pulse electrical stimulation.
    b. DA reuptake kinetics.
    c. DA release probability.
    d. Evoked DA release in response to trains of electrical stimuli at physiologically-relevant frequencies.
    e. Paired-pulse depression of DA release.
3. To determine the effect of macroautophagy impairment in DA neurons, using an *ATG7*cKO$^{TH\text{-IRES-cre}}$ model, on DA content in the caudate-putamen and nucleus accumbens.

6.3 Results

6.3.1 Generation of *ATG7*cKO$^{TH\text{-IRES-cre}}$ mice

In order to generate *ATG7*cKO$^{TH\text{-IRES-cre}}$ mice and appropriate control mice (Figure 6.1), a mouse heterozygous for wild-type *TH* and *TH*-IRES-cre was obtained from Prof. Keith Channon (University of Oxford), and crossbred with mice featuring floxed *ATG7* alleles. The *TH*-IRES-cre line was originally generated and characterised by Lindeberg and colleagues (2004). Following several crosses, mice homozygous for *TH*-IRES-cre and homozygous for the floxed *ATG7* allele were generated, and crossed with a mouse homozygous for wild-type *TH* and heterozygous for the floxed *ATG7* allele (Figure 6.1). For the FCV and HPLC experiments described in this chapter, 1 month-old mice were used. This age group was chosen to match the youngest age group used in Chapters 3 and 5, and in consideration of evidence from a previous study by Friedmann *et al.* (2012) which demonstrated that there was no loss of SNc DA neurons at 4 months of age in *ATG7*cKO$^{TH\text{-IRES-cre}}$ mice, indicating that it was very unlikely that SNc neuron number would be reduced at 1 month of age.

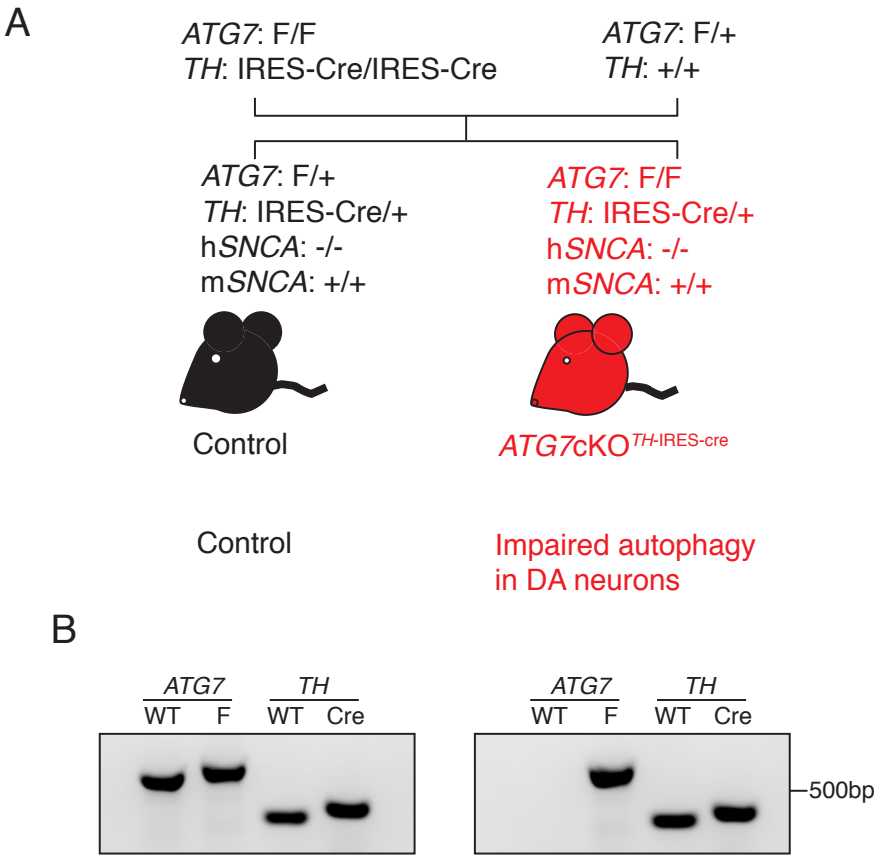


Figure 6.1. Generation of experimental genotypes.
(A) Example breeding strategy used to generate experimental animals. The experimental cross produced two genotypes. All mice were heterozygous for *TH*-IRES-cre, and all were homozygous for wild-type mouse *SNCA* (m*SNCA*). These mice had either normal (*ATG7* F/+) or impaired (F/F) macroautophagic function in dopamine neurons, and none expressed human *SNCA* (h*SNCA* -/-). **(B) Experimental genotypes.** *ATG7* and *TH* were manipulated in this cross, with each gene determined using two different primer sets. *ATG7* was present as both wild-type (WT) and flanked by loxP sites ("floxed") (F). The *TH* gene was present as wild-type (WT), or driving the expression of the cre-recombinase (Cre).

6.3.2 Peak dopamine release is increased in mice with impaired macroautophagy in dopamine neurons using an *ATG7*cKO$^{TH\text{-IRES-cre}}$ model

In order to assess the effect of impaired macroautophagy on peak evoked $[DA]_o$, acute striatal slices from 1 month-old control and *ATG7*cKO$^{TH\text{-IRES-cre}}$ mice were subjected to multi-site FCV recordings in the caudate-putamen and nucleus accumbens (Figure 6.2).

Peak evoked $[DA]_o$ in response to a single electrical stimulus in the caudate-putamen was higher in *ATG7*cKO$^{TH\text{-IRES-cre}}$ mice (Figure 6.2A). These data were consistent with the findings in Chapter 5 in 1 month-old mice featuring the *ATG7*cKO$^{DAT\text{-IRES-cre}}$ genotype.

Similarly, peak evoked $[DA]_o$ in the nucleus accumbens was increased in acute striatal slices from *ATG7*cKO$^{TH\text{-IRES-cre}}$ mice, when compared with data from control mice (6.2B). These observations are relatively consistent with findings in Chapter 5 investigating *ATG7*cKO$^{DAT\text{-IRES-cre}}$ mice.

Taken together, these data corroborate the evidence supplied in Chapter 5 indicating that impaired macroautophagy increases peak evoked $[DA]_o$ neurotransmission, thus providing a neurochemical basis for the improved motor performance observed in *ATG7*cKO$^{DAT\text{-IRES-cre}}$ mice in Chapter 4.

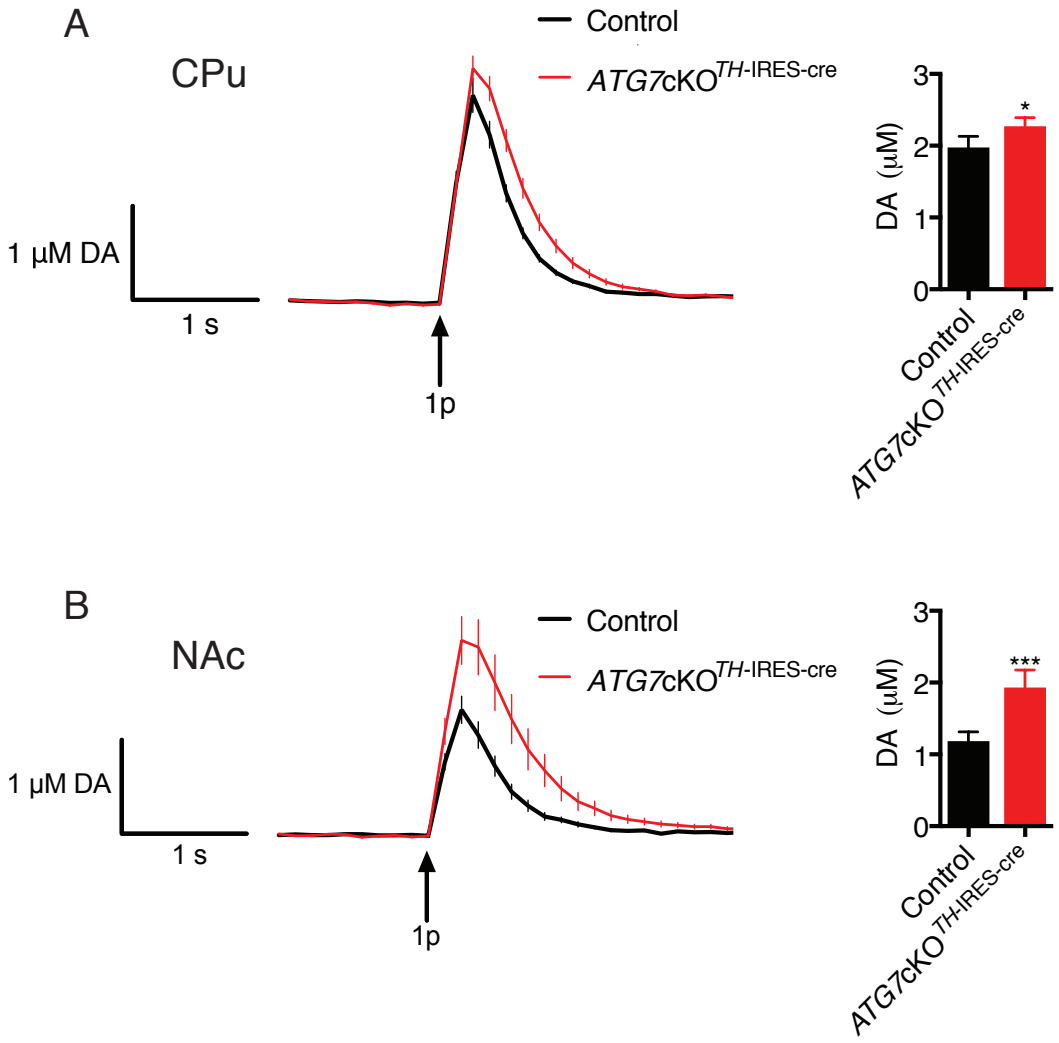


Figure 6.2. Increased evoked $[DA]_o$ release in response to a single stimulus in the caudate-putamen and nucleus accumbens in striatal slices from 1 month-old *ATG7*cKO$^{TH\text{-IRES-cre}}$ mice.

(A) $[DA]_o$ in the caudate-putamen following a single stimulation. n=60 from 5 mice in each genotype. Paired t-test, $t(39)=2.16$ * p=0.037. CPu, caudate-putamen. **(B) $[DA]_o$ in the nucleus accumbens following a single stimulation.** Data were log transformed for analysis, but presented as raw data for ease of comparison. Paired t-test, $t(19)=4.62$, *** $p<0.001$. n=20 from 5 mice in each genotype. NAc, nucleus accumbens. Data are shown ± SEM.

6.3.3 The rate of dopamine reuptake is reduced in the caudate-putamen, but not the nucleus accumbens, in mice with impaired macroautophagy in dopamine neurons, using an *ATG7*cKO$^{TH\text{-IRES-cre}}$ model

In Chapter 5, a reduction in the rate of DA reuptake was observed in the caudate-putamen and nucleus accumbens in association with the *ATG7*cKO$^{DAT\text{-IRES-cre}}$ genotype. In similar experiments, DA transients from control and *ATG7*cKO$^{TH\text{-IRES-cre}}$ were concentration matched at 2 μM $[DA]_o$ ± 0.4. In the caudate-putamen, $[DA]_o$ was high enough that this analysis could be performed on transients following a single pulse. In the nucleus accumbens, it was necessary to administer a train of 20 stimuli at 50 Hz in order to raise $[DA]_o$ sufficiently, especially in the control genotype. Reuptake constants *(K)* were calculated for the mean curves in each genotype, as performed previously (Anwar *et al.* 2011; Brimblecombe and Cragg 2014). The speed of DA reuptake was reduced in the caudate-putamen, and there was a trend towards reduction in the reuptake rate in the nucleus accumbens.

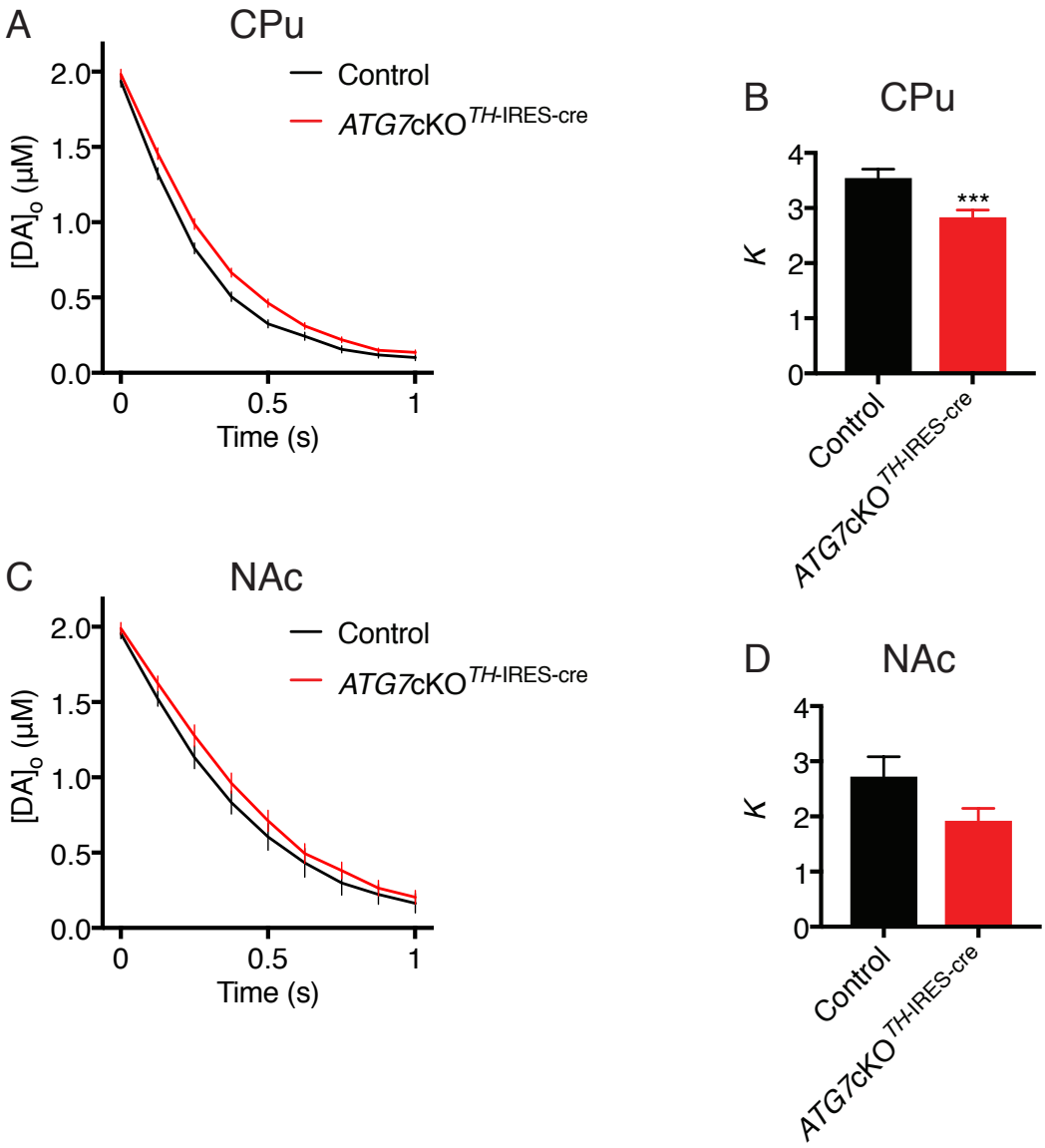


Figure 6.3. The *ATG7*cKO$^{TH\text{-IRES-cre}}$ genotype is associated with a reduced rate of dopamine reuptake in the caudate-putamen, but not the nucleus accumbens.
(A) Concentration-matched dopamine transients in the caudate-putamen. Dopamine transients were cropped at the point where they passed closes to 2 µM $[DA]_o$, and this point was taken as time=0. **(B) Analysis of reuptake coefficients in the caudate-putamen.** Significant effect of genotype, *** $p < 0.001$. n=20-30 from 5 mice per genotype. CPu, caudate-putamen. **(C) Concentration-matched dopamine transients in the nucleus accumbens.** Dopamine transients were cropped at the point where they passed closes to 2 µM $[DA]_o$, and this point was taken as time=0. **(D) Analysis of reuptake coefficients in the nucleus accumbens.** Significant effect of genotype, *** $p < 0.001$. n=20-30 from 5 mice per genotype. NAc, nucleus accumbens. Data are shown ± SEM.

6.3.4 Dopamine release probability is unchanged in mice with impaired macroautophagy in dopamine neurons using an *ATG7*cKO$^{TH\text{-IRES-cre}}$ model

DA release probability is defined as the likelihood that a single action potential will evoke a release event (Daniel *et al.* 2009). An experimental corollary is that if release probability is reduced, a single electrical stimulation during FCV will produce fewer release events than a burst stimulus, and this will be reflected by changes in evoked $[DA]_o$. In this thesis, DA release probability has been determined by examining the ratio of evoked $[DA]_o$ detected following four pulses at 100 Hz frequency, and dividing this figure by the $[DA]_o$ following a single pulse. In Chapter 5, it was demonstrated that there was an increase in DA release probability assessed by this method in the caudate-putamen of acute striatal slices from 1 month-old mice carrying the *ATG7*cKO$^{DAT\text{-IRES-cre}}$ genotype. In *ATG7*cKO$^{TH\text{-IRES-cre}}$, there was no difference in DA release probability assessed via this method. Possible reasons for this discrepancy are advanced in the discussion section of this chapter.

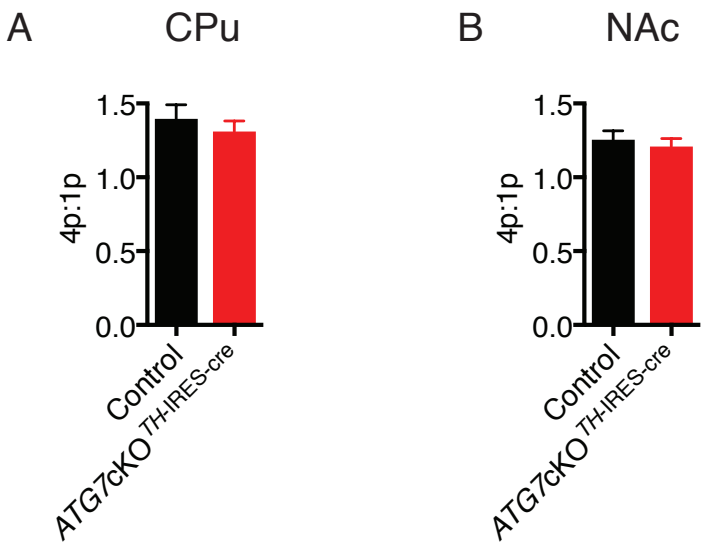


Figure 6.4. Dopamine release probability is unchanged by impaired macroautophagy in dopamine neurons in an *ATG7*cKO$^{TH\text{-IRES-cre}}$ model.
(A) Ratio of evoked $[DA]_o$ following four pulses at 100 Hz compared to single pulse in the caudate-putamen. Data were log transformed for analysis, but presented here as raw data for ease of comparison. No difference between genotypes, Wilcoxon signed-rank test. n=40 from 5 mice per genotype. CPu, caudate-putamen. **(B) Ratio of evoked $[DA]_o$ following four pulses at 100 Hz compared to single pulse in the caudate-putamen.** No difference between genotypes, paired t-test. n=20 from 5 mice per genotype. NAc, nucleus accumbens. Data are shown ± SEM.

6.3.5 Impairment of macroautophagy in dopamine neurons does not change frequency responsiveness of evoked $[DA]_o$ in an *ATG7*cKO$^{TH\text{-IRES-cre}}$ model

DA neurons of the SNc and VTA are tonically active and can fire in bursts of higher frequency in response to a multitude of stimuli. Therefore, it is important to consider the amplitude of evoked $[DA]_o$ in response to different firing frequencies. In this thesis frequency-responsiveness of evoked $[DA]_o$ has been examined by administering burst stimuli of four pulses at frequencies of 5, 10, 25 and 100 Hz. These data have been normalised to the evoked $[DA]_o$ following a single pulse. Two representative sites were interrogated in this manner: the dorsolateral caudate-putamen and the nucleus accumbens core.

In Chapter 5, analysis of evoked $[DA]_o$ in acute striatal slices from 1 month-old mice demonstrated that the *ATG7*cKO$^{DAT\text{-IRES-cre}}$ genotype was associated with increased evoked $[DA]_o$ at higher frequencies when compared to mice without *ATG7*cKO$^{DAT\text{-IRES-cre}}$. In the *ATG7*cKO$^{TH\text{-IRES-cre}}$ mice (Figure 6.5), there was no difference between genotypes in either the caudate-putamen or nucleus accumbens. It should be noted that because these data are normalised to single pulse evoked $[DA]_o$ – which is higher in *ATG7*cKO$^{TH\text{-IRES-cre}}$ mice in both regions – the absolute value of $[DA]_o$ remains higher in *ATG7*cKO$^{TH\text{-IRES-cre}}$ mice at all frequencies examined.

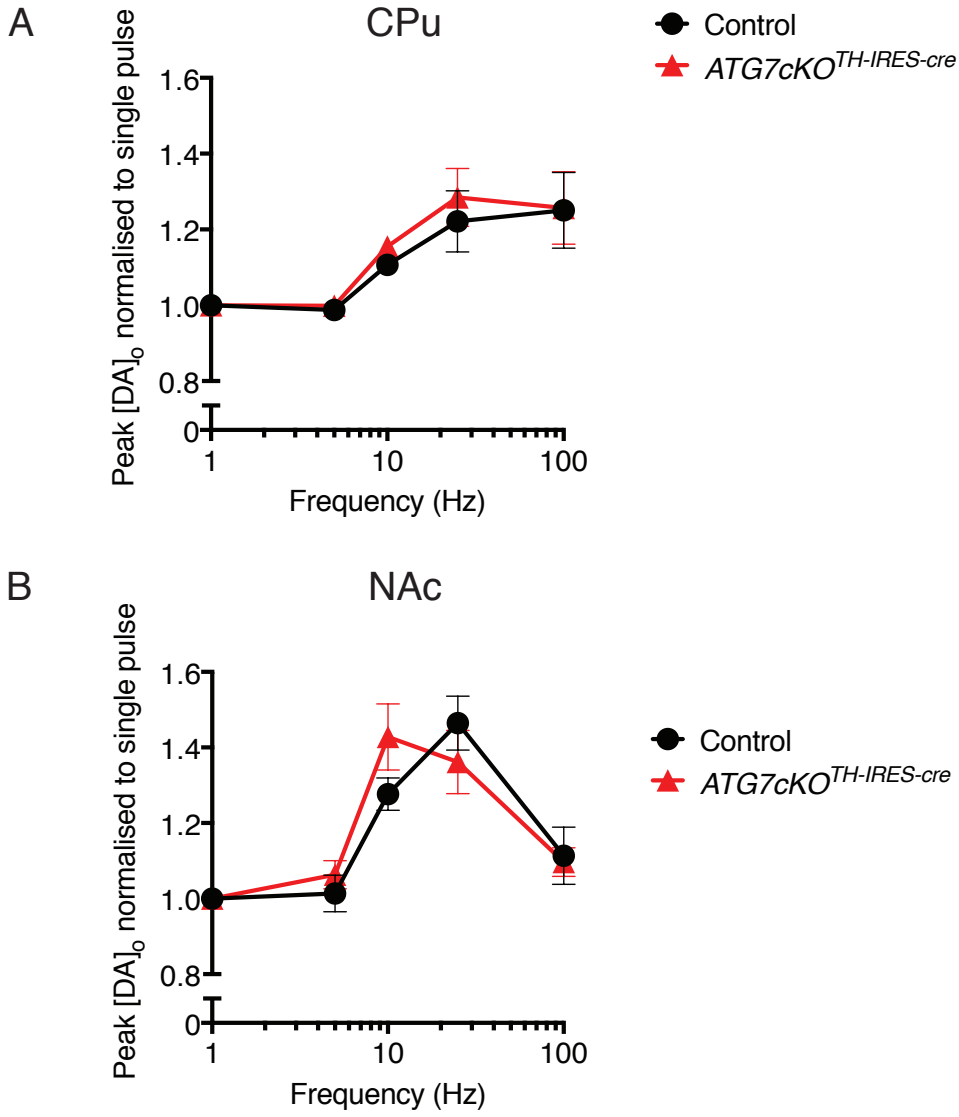


Figure 6.5. Magnitude of evoked $[DA]_o$ in response to physiologically-relevant stimulation frequencies is unchanged by the *ATG7*cKO$^{TH\text{-IRES-cre}}$ genotype in the caudate-putamen and nucleus accumbens.
(A) Evoked $[DA]_o$ in the dorsolateral caudate-putamen in response to four pulse stimuli of 5, 10, 25 and 100 Hz, normalised to single pulse release. Two-way ANOVA for genotype and frequency, no effect of genotype and no interaction. n=10 from 5 mice. CPu, caudate-putamen. **(B) Evoked $[DA]_o$ in the nucleus accumbens core in response to four pulse stimuli of 5, 10, 25 and 100 Hz, normalised to single pulse release.** Two-way ANOVA for genotype and frequency, no effect of genotype and no interaction. n=10 from 5 mice. NAc, nucleus accumbens. Data are shown ± SEM.

6.3.6 Impairment of macroautophagy in dopamine neurons is associated with reduced paired-pulse depression in an *ATG7*cKO$^{TH\text{-IRES-cre}}$ model

PPD describes an effect where, when two electrical stimuli are given in close temporal and spatial proximity, peak evoked $[DA]_o$ is reduced in response to the second stimulus. PPD is thought to reflect short-term synaptic plasticity (Abeliovich *et al.* 2000; Cragg 2003; Hernandez *et al.* 2012). The behavioural corollaries of changes in PPD are unclear, however reductions in PPD may facilitate improved motor function by increasing DA availability during prolonged periods of movement. In Chapter 5 of this thesis, a reduction in PPD was observed in association with the *ATG7*cKO$^{DAT\text{-IRES-cre}}$ genotype in almost all contexts tested. Therefore, in this chapter, PPD was examined in *ATG7*cKO$^{TH\text{-IRES-cre}}$ mice in order to determine if this phenotype persisted. As for Chapter 5, the protocols used were as follows:

- 1 pulse – 3 seconds – 1 pulse (1p:1p. Shown in figures 6.6A and 6.7A)
- 4 pulses – 3 seconds – 4 pulses (4p:4p. Shown in figures 6.6B and 6.7B)
- 1 pulse – 3 seconds – 4 pulses (1p:4p. Shown in Figures 6.6C and 6.7C)

A summary of results is provided in Table 6.1 (below), for ease of comparison.

Table 6.1. Summary of effects of *ATG7*cKO$^{TH\text{-IRES-cre}}$ on paired-pulse depression

Anatomical location:	Protocol:	*ATG7*cKO$^{TH\text{-IRES-cre}}$	Figure
Caudate-putamen	1p:1p	Reduced	6.6A
	4p:4p	Reduced	6.6B
	1p:4p	Reduced	6.6C
Nucleus accumbens	1p:1p	Reduced	6.7A
	4p:4p	No effect	6.7B
	1p:4p	Reduced	6.7C

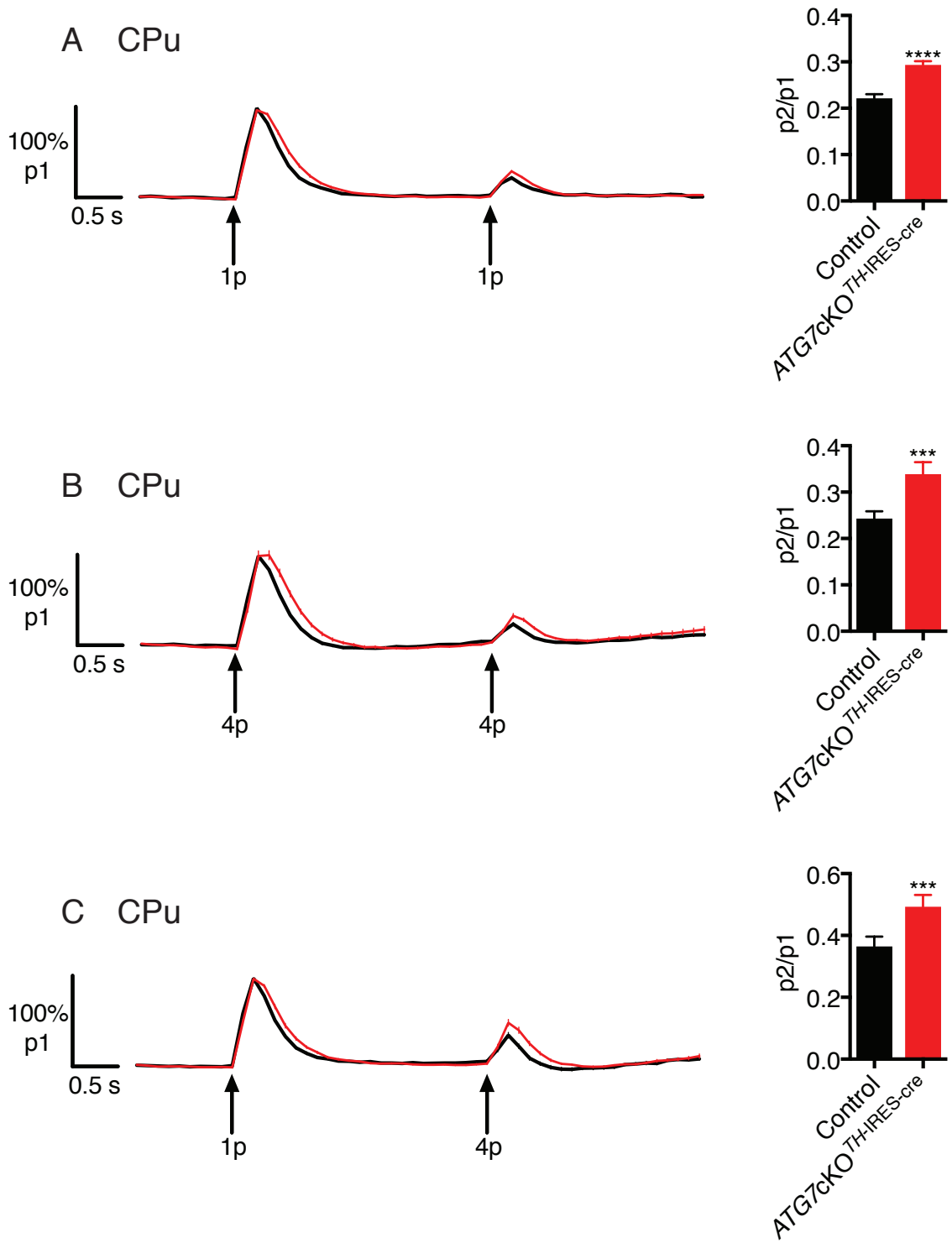


Figure 6.6. Macroautophagy impairment in dopamine neurons reduces paired-pulse depression of evoked $[DA]_o$ in the caudate-putamen in a *ATG7*cKO$^{TH\text{-IRES-cre}}$ model. **(A) Paired-pulse depression of evoked $[DA]_o$ in a paired single pulse protocol.** Paired t-test, $t(39)=5.92$ **** $p<0.0001$. **(B) Paired-pulse depression of evoked $[DA]_o$ in a paired quadruple pulse protocol.** Data are log transformed for analysis, but presented as raw data for ease of comparison. Paired t-test, $t(39)=3.82$ *** $p< 0.001$. **(C) Paired-pulse depression of evoked $[DA]_o$ in a single pulse – quadruple pulse protocol.** Data are square root transformed for analysis, but presented as raw data for ease of comparison. Paired t-test, $t(39)=3.88$ *** $p< 0.001$. n=60 from 5 mice per genotype. CPu, caudate-putamen. Data are shown ± SEM.

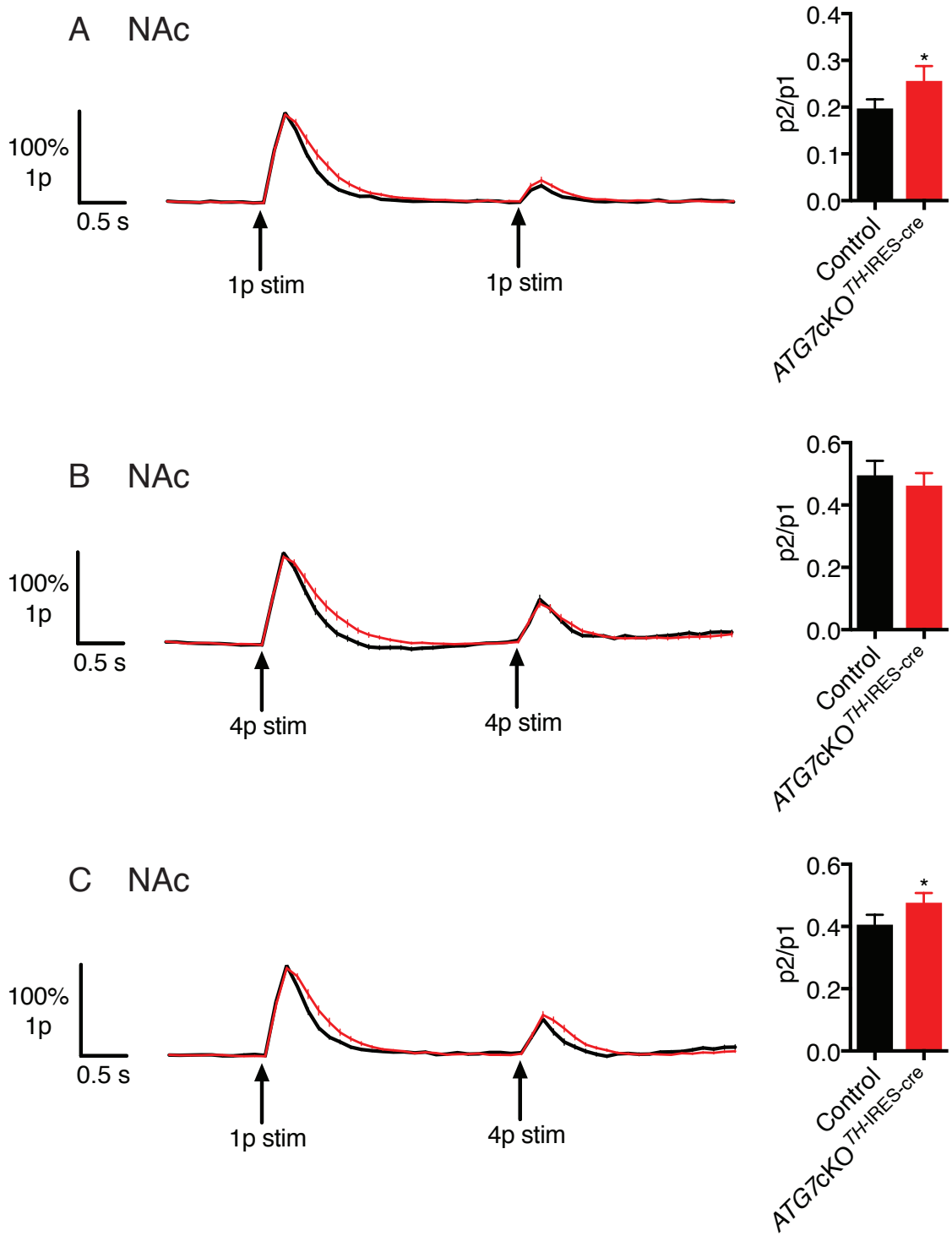


Figure 6.7. Macroautophagy impairment in dopamine neurons reduces paired-pulse depression of evoked $[DA]_o$ in the nucleus accumbens in some contexts in a *ATG7*cKO$^{TH\text{-IRES-cre}}$ model.

(A) Paired-pulse depression of evoked $[DA]_o$ in a paired single pulse protocol. Data were log-transformed for analysis, but presented as raw data for ease of comparison. Paired t-test, $t(19)=2.46$ * $p = 0.024$. **(B) Paired-pulse depression of evoked $[DA]_o$ in a paired quadruple protocol.** Data were log-transformed for analysis, but presented as raw data for ease of comparison. No significant difference, paired t-test. **(C) Paired-pulse depression of evoked $[DA]_o$ in a single pulse – quadruple pulse protocol.** Paired t-test, $t(19)=2.17$ * $p = 0.043$. n=20 from 5 mice in each genotype. NAc, nucleus accumbens. Data are shown ± SEM.

6.3.7 No effect of macroautophagy impairment on dopamine content in the caudate-putamen or nucleus accumbens in an *ATG7*cKO$^{TH\text{-IRES-cre}}$ model

In PD, there is a reduction in striatal DA content (Ehringer and Hornykiewicz 1960). In Chapter 3, reductions in DA were observed in the caudate-putamen in mice carrying the *ATG7*cKO$^{DAT\text{-IRES-cre}}$ genotype at older ages. Changes in DA content may impact on evoked $[DA]_o$ and PPD. For these reasons, DA content was analysed in the caudate-putamen and nucleus accumbens of *ATG7*cKO$^{TH\text{-IRES-cre}}$ and compared to control mice, with no differences being found.

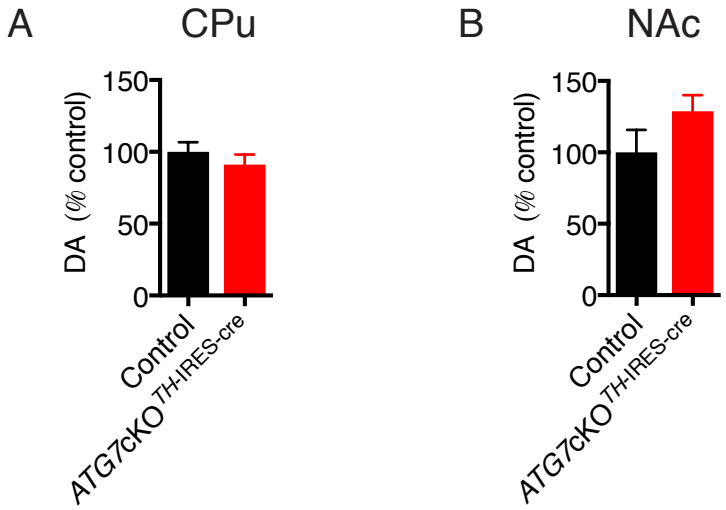


Figure 6.8. No effect of macroautophagy impairment on dopamine content in the caudate-putamen or nucleus accumbens.
(A) Dopamine content in the caudate-putamen. No effect of genotype, paired t-test. CPu, caudate-putamen. n=5 per genotype. **(B) Dopamine content in the nucleus accumbens.** No effect of genotype, paired t-test. n=5 per genotype. Data are shown ± SEM. NAc, nucleus accumbens.

6.4 Discussion

6.4.1 The effect of macroautophagy impairment in dopamine neurons on neurotransmission is similar between *ATG7*cKO$^{TH\text{-IRES-cre}}$ and *ATG7*cKO$^{DAT\text{-IRES-cre}}$ mice

One of the major aims of this chapter was to determine of *ATG7*cKO$^{TH\text{-IRES-cre}}$ mice had similar changes in DA neurotransmission to those observed in *ATG7*cKO$^{DAT\text{-IRES-cre}}$ mice in Chapter 5. The results of this chapter, and a comparison to the data generated in Chapter 5 are provided in Table 6.2 (overleaf). Such a comparison has not been performed previously, and there are no data in the literature regarding DA neurotransmission in *ATG7*cKO$^{TH\text{-IRES-cre}}$ mice. It can be seen from Table 6.2 that DA neurotransmission characteristics in acute striatal slices from 1 month-old *ATG7*cKO$^{TH\text{-IRES-cre}}$ and *ATG7*cKO$^{DAT\text{-IRES-cre}}$ mice are similar, particularly in the caudate-putamen. In particular, the core observations observed in Chapter 5 are the same: that impaired macroautophagy in DA neurons increases evoked $[DA]_o$ in the caudate-putamen and nucleus accumbens, and this is associated with reduced rates of DA reuptake, and reduced PPD. The four parameters in which the data from Chapter 5 and 6 differ are: (1) DA release probability in the caudate-putamen, (2) DA reuptake kinetics in the nucleus accumbens, (3) the magnitude of evoked $[DA]_o$ in response to increasing stimulation frequency in the nucleus accumbens, and (4) small differences in PPD in the nucleus accumbens. Possible explanations for these differences are considered in the following section. There are inherent general limitations to the *TH*-IRES-cre driver line used in this chapter, and these may account for some of the differences observed between *ATG7*cKO$^{TH\text{-IRES-cre}}$ and *ATG7*cKO$^{DAT\text{-IRES-cre}}$ mice; these limitations are discussed in Section 6.4.3.

Table 6.2. Comparison of the effects of the *ATG7*cKO$^{TH\text{-IRES-cre}}$ and *ATG7*cKO$^{DAT\text{-IRES-cre}}$ genotypes on dopamine neurotransmission in acute striatal slices from 1 month-old mice				
Anatomical region	**Parameter**	***ATG7*cKO$^{TH\text{-IRES-cre}}$**	***ATG7*cKO$^{DAT\text{-IRES-cre}}$**	**Concordant?**
Caudate-putamen	1p release	Increased	Increased	✓
	DA reuptake	Reduced	Reduced	✓
	Release probability	No effect	Reduced	×
	Frequency	No effect	No effect	✓
	1p:1p PPD	Reduced	Reduced	✓
	4p:4p PPD	Reduced	Reduced	✓
	1p:4p PPD	Reduced	Reduced	✓
Nucleus accumbens	1p release	Increased	Increased	✓
	DA reuptake	No effect	Reduced	×
	Release probability	No effect	No effect	✓
	Frequency	No effect	Increased	×
	1p:1p PPD	Reduced	Reduced	✓
	4p:4p PPD	No effect	Reduced	×
	1p:4p PPD	Reduced	No effect	×

6.4.2 Differences in dopamine neurotransmission between *ATG7*cKO$^{DAT\text{-IRES-cre}}$ and *ATG7*cKO$^{TH\text{-IRES-cre}}$ mice

The majority of the differences observed between *ATG7*cKO in the *DAT*-IRES-cre line and *ATG7*cKO the *TH*-IRES-cre line are found in the nucleus accumbens. Importantly, one of the major criticisms of the *TH*-IRES-cre line has been poor expression of the cre recombinase in the VTA, which projects to the nucleus accumbens (Lammel *et al.* 2015). The suboptimal performance of the *TH*-IRES-cre line in this regard may account for some of the discrepancies between *ATG7*cKO$^{DAT\text{-IRES-cre}}$ and *ATG7*cKO$^{TH\text{-IRES-cre}}$ mice. However, it is noteworthy that in all cases there where there was a discrepancy of *ATG7*cKO between the *DAT*-IRES-cre and *TH*-IRES-cre driver lines, in general, the direction of the effect remained towards increased DA availability in the nucleus accumbens.

For example, ATG7cKO in the DAT-IRES-cre line slowed DA reuptake in the nucleus accumbens, and the same direction of effect was apparent using the TH-IRES-cre driver

line, although it was not statistically significant. Likewise, ATG7cKO reduced PPD in the nucleus accumbens in two out of three protocols in both the DAT-IRES-cre and TH-IRES-cre driver lines, but the two protocols were not the same for both lines.

Some of the observed differences may be due to reduced statistical power in the *TH*-IRES-cre dataset. For example, in 1 month-old mice alone there were 32 observations of the effect of *ATG7*cKO in the nucleus accumbens of *DAT*-IRES-cre mice, whereas there were only 20 in the *TH*-IRES-cre line. Alternatively, some of the changes in DA neurotransmission observed in the nucleus accumbens of *ATG7*cKO$^{DAT\text{-IRES-cre}}$ mice may be an artifact of the manipulation of DAT. As mentioned in the previous chapter, experiments conducted using alternative tools such as cell lines and acute injection models may serve to better delineate changes in DA reuptake as a direct consequence of impaired macroautophagy.

In the caudate-putamen, there was only one discrepant effect of *ATG7*cKO between the *TH*-IRES-cre and *DAT*-IRES-cre driver line. DA release probability, as assessed using the ratio of evoked $[DA]_o$ from a four pulse, 100 Hz stimulation to evoked $[DA]_o$ from single pulse stimulation, was decreased in acute striatal slices from 1 month-old mice carrying the *ATG7*cKO$^{DAT\text{-IRES-cre}}$ genotype (see Figure 5.5). However, there was no such decrease in DA release probability in *ATG7*cKO$^{TH\text{-IRES-cre}}$ mice using the same measure (Figure 6.4). A multitude of factors can influence DA release probability, and may account for this discrepancy. For example, changes in the probability of DA release may arise due to changes in the size of the synaptic vesicle pool, which may differ between the *DAT*-IRES-

cre and the *TH*-IRES-cre expression systems. Similarly, DA release probability can be altered by changes in ionic conductances, changes in receptors for acetycholine, substance P or endogenous opioids, as well as changes in structural factors such as the number of axon branch points (Branco and Staras 2009; Pan and Ryan 2012). In any case, reduced caudate-putamen DA release probability did not account for any of the phenotypes observed in *ATG7*cKO$^{DAT\text{-IRES-cre}}$ and *ATG7*cKO$^{TH\text{-IRES-cre}}$ mice, which had increased evoked $[DA]_o$, the opposite of what would be expected from reduced DA release probability.

6.4.3 Limitations of examining dopamine neurotransmission using the *TH*-IRES-cre system

The *TH*-IRES-cre system used in this chapter has several limitations. TH is expressed in non-dopaminergic tissues throughout the body, including the locus coeruleus, a noradrenergic brainstem ganglion, and the adrenal medulla, which is responsible for synthesising circulating adrenaline and noradrenaline (Lindeberg *et al.* 2004). The locus coeruleus projects to the VTA, where it elicits burst firing of nucleus accumbens projection neurons (Jones and Moore 1977; Lategan *et al.* 1990; Grenhoff *et al.* 1993). The locus coeruleus has multiple other projections that may impact DA neurotransmission, and a critical role in the reticular activating system, which mediates arousal (Threlfell *et al.* 2012). It is unclear what effect impaired macroautophagy would have in the locus coeruleus, and therefore what broader effects it may have on DA neurotransmission. Likewise, it is not known what effects on circulating adrenaline and noradrenaline would be perpetrated by macroautophagy inhibition in the adrenal medulla.

One of the key discrepancies between *ATG7*cKO$^{DAT\text{-IRES-cre}}$ and *ATG7*cKO$^{TH\text{-IRES-cre}}$ mice is that the former are hyperlocomotor (Threlfell *et al.* 2012), whereas *ATG7*cKO$^{TH\text{-IRES-cre}}$ are hypolocomotor (Ahmed *et al.* 2012). This difference could be explained by changes in arousal in *ATG7*cKO$^{TH\text{-IRES-cre}}$ mice mediated by the effects of impaired macroautophagy on the locus coeruleus. An alternative or supplementary explanation could be deleterious effects of macroautophagy impairment on the adrenal medulla in *ATG7*cKO$^{TH\text{-IRES-cre}}$ mice, and subsequent changes to circulating catecholamines.

Further limitations are specific to the experiments described in this chapter. In the present study, DA neuron number was not examined. A previous study by Friedman *et al.* (Friedman *et al.* 2012) in the same *ATG7*cKO$^{TH\text{-IRES-cre}}$ line demonstrated that SNc neuron number was unchanged at 4 months, and the DA content in the mice studied in this chapter was also unchanged, suggesting DA neuron number is unlikely to differ between genotypes. Additionally, older age groups and the effect of h*SNCA* were not examined in this chapter, which limits its comparability to Chapter 5.

6.4.4 Chapter summary

A summary of the data described in this chapter is provided in Table 6.2. In general, the data in this chapter agree with the data in Chapter 5, that impaired macroautophagy in DA neurons enhances DA neurotransmission. The concordance of these two data sets suggests that this may be a universal phenomenon, and lends support to the idea that enhanced DA neurotransmission caused the improvements in motor performance observed in mice with the *ATG7*cKO$^{DAT\text{-IRES-cre}}$ genotype in Chapter 4.

Chapter 7: Discussion

7 Discussion

7.1 Overview

In this thesis, mouse models were used to study the effect of macroautophagy impairment in DA neurons in conjunction with overexpression of human α-synuclein. Data regarding the effect of impaired macroautophagy on DA neurotransmission were, to a large extent, confirmed in a second transgenic model. A summary of the most important findings from these mouse models is provided in Table 7.1 (below), separated according to the original aims of the thesis. This chapter contains general conclusions, potential future experiments, along with possible explanations and ramifications of the data described in this thesis.

Table 7.1. Summary of the effects of ATG7cKO and hSNCA genotypes in experimental mice

Chapter and aim:	**Effect of gene on features of Parkinson's disease:**	***ATG7*cKO**	**h*SNCA***
Chapter 3: histological characterisation	SNc DA neuron number	Reduced	No effect
	VTA DA neuron number	No effect	No effect
	Caudate-putamen dopamine content	Reduced	Increased at 1 month
	Nucleus accumbens dopamine content	No effect	No effect
	Lewy bodies	None	None
	P62 inclusions	Present	None
	Ubiquitin inclusions	Present	None
Chapter 4: behavioural characterisation	Locomotor activity	Increased	No effect
	Rotarod performance	Improved at 20 to 24 months	No effect
	Stride swing speed	Increased	No effect
	Gait cadence	Increased	No effect
Chapters 5 and 6: dopamine neurotransmission	Evoked $[DA]_o$	Increased when no DA neuron loss	Decreased at 20 to 24 months
	Dopamine reuptake	Slowed	Slowed in NAc
	Paired-pulse depression	Reduced	Increased

7.2 Impaired macroautophagy in dopamine neurons has divergent effects on parkinsonian phenotypes, worsening neuropathology but improving behavioural measures

Perhaps the most significant finding from this thesis is that impairment of macroautophagy in DA neurons has two divergent effects, worsening parkinsonian neuropathology but

improving parkinsonian behaviour. The *ATG7*cKO$^{DAT\text{-IRES-cre}}$ genotype was associated with loss of SNc DA neurons, reductions in striatal DA, and accumulation of P62 and ubiquitin in surviving DA neurons. All of these are key neuropathological features found in PD, and are consistent with previous similar studies (Inoue *et al.* 2012; Friedman *et al.* 2012; Ahmed *et al.* 2012). In general, parkinsonian behavioural phenotypes, such as reduced locomotor activity, bradykinesia and impaired rotarod performance would be expected to result from the extensive nigral cell loss observed in *ATG7*cKO$^{DAT\text{-IRES-cre}}$ mice. Paradoxically, however, mice with the *ATG7*cKO$^{DAT\text{-IRES-cre}}$ genotype were hyperlocomotor, hyperkinetic and demonstrated improved rotarod performance in old-age. These behavioural findings are consistent with a hyperdopaminergic state, and therefore DA neurotransmission was investigated in order to determine if there was a neurochemical difference that could explain the behavioural findings. *ATG7*cKO using both *DAT*-IRES-cre and *TH*-IRES-cre driver lines was associated with an increase in peak evoked $[DA]_o$ in regions without cell loss, consistent with a previous study by Hernandez *et al.* (2012). Additionally, DA reuptake and PPD were reduced, both factors likely to enhance DA availability. Taken in aggregate, these data suggest that impairment of macroautophagy has deleterious effects, particularly at the soma, while at the same time having synaptic effects that increase the availability of DA, mediating improvements in behavioural parameters (Figure 7.1).

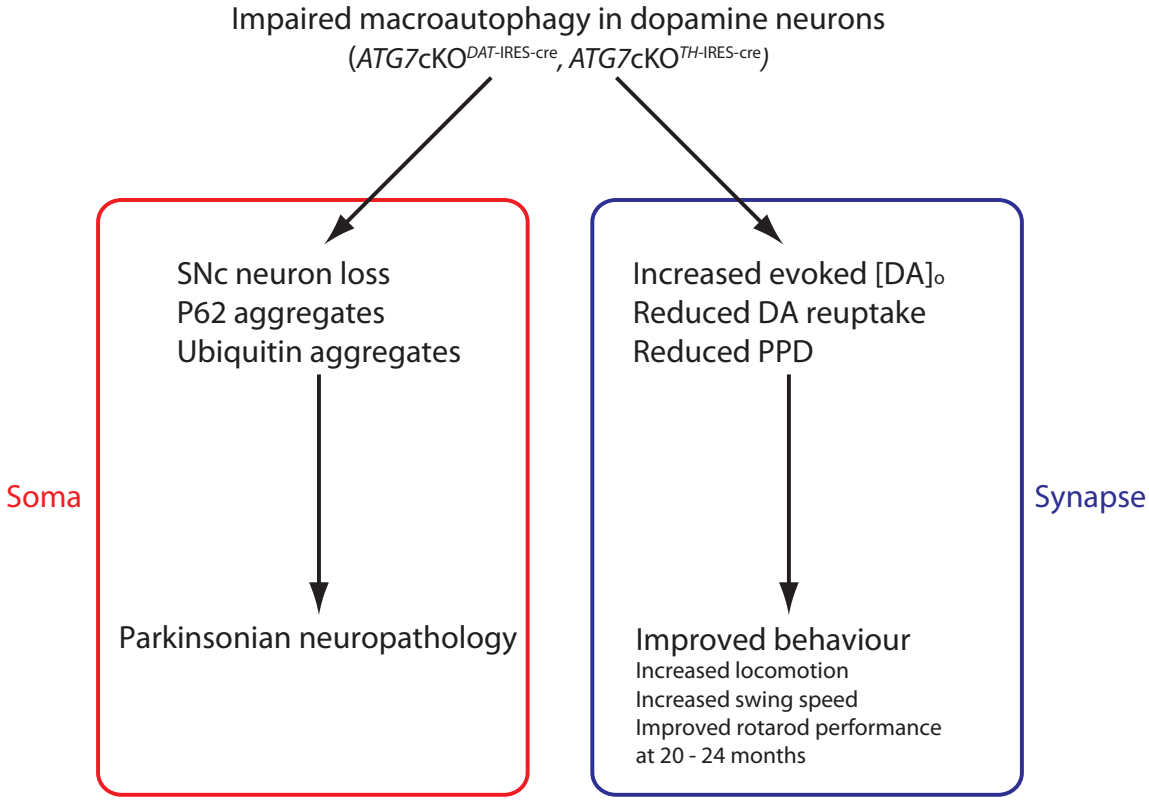


Figure 7.1. Divergent effects of impaired macroautophagy in dopamine neurons on parkinsonian phenotypes: a suggested framework.
Separate somatic and synaptic effects of macroautophagy impairment cause divergent neuropathological and behavioural phenotypes. $[DA]_o$, extracellular dopamine; DA, dopamine; DAT, dopamine active transporter; IRES, internal ribosome entry site; PPD, paired-pulse depression; SNc, substantia nigra pars compacta; TH, tyrosine hydroxylase.

Future studies should aim to determine the mechanisms by which impaired macroautophagy mediates enhanced DA neurotransmission. It may be possible to separate the molecular pathways that cause protein accumulation when macroautophagy is impaired from those that facilitate DA release and reuptake. This would provide new targets for therapeutic intervention in PD. It would also inform on dopaminergic pathways which underlie basic attributes of human behaviour, as well as other disease states such as addiction, schizophrenia and Huntington's disease.

7.3 Why don't h*SNCA*:*ATG7*cKO$^{DAT\text{-IRES-cre}}$ mice form Lewy bodies?

Lewy bodies are one of the key pathological features of PD. The lack of Lewy bodies in aged h*SNCA*:*ATG7*cKO$^{DAT\text{-IRES-cre}}$ mice is informative as it suggests three potentially overlapping possibilities. Firstly, that the presence of endogenous mouse α-synuclein inhibits the formation of Lewy bodies. Secondly, that some other factor in mice precludes Lewy body formation. Thirdly, that impairment of macroautophagy is not essential to the formation of Lewy bodies, as α-synuclein can be cleared via other mechanisms.

Further experiments, probably best conducted in endogenous α-synuclein knockout mice, could investigate the necessity of different neuronal mechanisms for clearance of α-synuclein, and the formation of the neuropathological features of PD, such as Lewy bodies. For example, mice could be generated without the necessary machinery for the functioning of the UPS in DA neurons, such as a proteasomal subunit, using a similar strategy to the *DAT*-IRES-cre system described in this thesis. The addition of an inducible element, for example a tamoxifen-responsive cre element, may serve to abrogate any developmental toxicity associated with impairment of the UPS (Kühn *et al.* 1995). Similarly, proteins essential for CMA, such as LAMP2A, could be knocked out in DA neurons using the same techniques described in this thesis. It may be that impairment of multiple mechanisms of α-synuclein clearance is necessary for Lewy body formation. This could be achieved experimentally by using a cre-based technique to impair one clearance mechanism, and a flippase-based genetic alteration to impair another (Dymecki 1996; Rodríguez *et al.* 2000). Alternatively, or additionally, chemical modifiers of clearance mechanisms, such as bafilomycin, which impairs macroautophagy, could be administered by direct injection. Using such techniques it may be possible to determine which α-synuclein clearance

mechanisms predominate *in vivo*, and those that may account for the development of PD pathology and thus target these for therapeutic development.

7.4 Lack of pathological and motor phenotypes associated with the h*SNCA* gene

One of the findings throughout this thesis has been an absence of association between the h*SNCA* transgene and any overt behavioural or neuropathological phenotypes. In part, this demonstrates the difficulty of establishing any toxicity associated with α-synuclein overexpression in mice, and underscores the potential for mismatches between human disease and animal models. Part of this absence of effect may be attributable to the presence of endogenous mouse α-synuclein, which has been shown to reduce the toxicity of human α-synuclein (Cabin *et al.* 2005; Fares *et al.* 2016). This thesis contributes to the body of literature that suggests that endogenous mouse α-synuclein impairs the toxicity of human α-synuclein, as the same h*SNCA* BAC transgene used in this thesis has been shown to cause SNc neuron loss when expressed in mice lacking endogenous α-synuclein (Cabin *et al.* 2005; Fares *et al.* 2016). Small changes in DA neurotransmission were associated with the h*SNCA* transgene. Specifically, it was found that there was a reduction in DA content in the caudate-putamen in 20 to 24 month-old mice, reduced evoked $[DA]_o$ at 20 to 24 months, slowed DA reuptake in the nucleus accumbens, and there were minor increases in PPD in association with the h*SNCA* gene. The sample sizes used in the behavioural studies in this thesis may not have been large enough to detect any effects of these small changes in DA and its neurotransmission. These late phenotypes may be consistent with delayed neurotoxicity, due to the presence of endogenous mouse α-synuclein. It is possible that mice aged for a more prolonged period may develop more severe neurodegeneration associated with the h*SNCA* gene. The small effect sizes associated with the h*SNCA*

transgene comparison with the *ATG7*cKO$^{DAT\text{-IRES-cre}}$ genotype highlight the differences between overexpressing a non-essential gene (*SNCA*), and knocking out an essential gene (*ATG7*). In future, the use of humanised mouse models may provide greater insight into PD than models utilising mouse α-synuclein. To this end, the Wade-Martins laboratory has developed a number of mouse lines expressing human α-synuclein at different levels on a mouse α-synuclein knockout background, which are in various stages of characterisation.

7.5 Absence of interactions between h*SNCA*:*ATG7*cKO$^{DAT\text{-IRES-cre}}$ and h*SNCA*

It is important to note that in the experiments described in this thesis, there were no interactions detected between the *ATG7*cKO$^{DAT\text{-IRES-cre}}$ and the h*SNCA* genotypes. This suggests that impaired macroautophagy does not directly impact on the level or toxicity of α-synuclein *in vivo*. Experiments by other members of the Wade-Martins laboratory reinforce the concept that there is no interaction between impaired macroautophagy and human α-synuclein. PLA experiments, which detect α-synuclein oligomers, demonstrated no evidence of a change in α-synuclein oligomerisation in h*SNCA*:*ATG7*cKO$^{DAT\text{-IRES-cre}}$ mice (N. Bengoa-Vergniory, in preparation). Similarly, no change in α-synuclein protein level, as assessed by Western blotting, was found in h*SNCA*:*ATG7*cKO$^{DAT\text{-IRES-cre}}$ mice compared to hSNCA mice at 1 month of age (S. Vingill, in preparation). Mirroring the absence of a biochemical interaction, there were no interactions found in regards to behavioural or DA neurotransmission phenotypes. It remains possible, even likely, that there is some interaction between impaired macroautophagy in DA neurons and human α-synuclein in this mouse line, but such interactions remain undetected by the experimental techniques used to date. A more in-depth exploration may yield interactions between impaired macroautophagy and α-synuclein, in regards to areas such as mitochondrial

dysfunction, prion-like spread of α-synuclein, post-translational modification of α-synuclein, or neuronal calcium handling.

7.6 Macroautophagy may be a novel direct or indirect regulator of the dopamine transporter

This thesis has presented evidence that impairment of macroautophagy in DA neurons causes slower DA reuptake. The mechanisms underlying this observation have not been addressed in this thesis. Several possibilities present themselves. Firstly, impairment of macroautophagy may alter DAT protein levels. Secondly, impairment of macroautophagy may alter post-translational modification of DAT. Post-translational modifications such as phosphorylation, glycosylation and ubiquitination all serve to alter DAT activity (Johnson *et al.* 2005; Miranda *et al.* 2007). Thirdly, impairment of macroautophagy may sequester DAT away from the synaptic membrane, preventing its regular reuptake activity. Preliminary data assessing DAT levels by Western blot from 1 month-old mice carrying the *ATG7*cKO$^{DAT\text{-IRES-cre}}$ genotype suggests that the first possibility, a reduction in protein levels, may be the primary mechanism causing reduced DAT availability (S. Vingill, in preparation).

A reduction in DAT protein levels in *ATG7*cKO$^{DAT\text{-IRES-cre}}$ mice could be attributable to toxicity to the dendritic arbor causing loss of DA terminals. However, loss of DA terminals would also reduce evoked $[DA]_o$, which was not observed. This suggests that reductions in DAT protein levels are mediated by some other mechanism, for example increased degradation or reduced expression. One method to more definitively separate the effects of neurodegeneration from the effect of macroautophagy on DA reuptake would be to utilise

a cell line that expresses human DAT. The cell line could be treated with chemical or genetic modifiers of macroautophagy, and DA uptake determined using radiolabelled DA. If the cell line incorporated a fluorescent tag (Eriksen *et al.* 2009), the localisation of DAT could be visualised, providing further information on DAT processing.

Indirect evidence suggesting that impairment of macroautophagy reduces DAT availability is supplied in two other papers, from Niu *et al.* (2016) and Hung and colleagues (2014). The Niu et al. study showed that *ATG7*cKO$^{TH\text{-cre}}$ mice were less susceptible to MPTP intoxication. In the study by Hung *et al*. acute administration of *ATG7* siRNA into the SNc reduced the toxicity of MPP+, the toxic metabolite of MPTP. Entry of MPP+ into DA neurons is mediated by DAT, and therefore a reduction in DAT availability would reduce MPTP toxicity. Studies conducted in DAT knockout mice have shown that, without DAT, MPP+ toxicity is absent (Bezard *et al.* 1999). Therefore, the absence of MPTP toxicity in *ATG7*cKO mice is indirect evidence of reduced DAT availability.

During the course of this thesis it became clear that the regulation of DAT is relatively poorly understood, and that individual regulators of DAT have been investigated on a largely *ad hoc* basis. More systematic investigation of DAT regulation could prove informative, for example using siRNA libraries to screen for DA reuptake phenotypes in a cell line, and followed by more in-depth studies in transgenic mice. A well-considered siRNA study determining molecules that regulate autophagy could provide the template for such an investigation (Lipinski *et al.* 2010).

7.7 Impaired macroautophagy in dopamine neurons is associated with improved motor function: implications for clinical trials

An improvement in motor performance associated with impaired macroautophagy in DA neurons has implications for PD trials. Clinical trials are currently underway using nilotinib, a stimulator of macroautophagy, to treat PD (Pagan *et al.* 2016). The data in this thesis suggest that although stimulating macroautophagy may be beneficial to long-term neuronal survival, it may also worsen motor performance, at least in the short-term. This is a factor that may need to be considered in the design and interpretation of data from PD clinical trials, which typically rely heavily on scores of motor function to determine efficacy (and approval) of experimental drugs (Connolly and Lang 2014). Other measures may need to be used to judge drug effectiveness in the case of macroautophagy stimulators, such as PD biomarkers, or positron emission tomography (PET) scans that identify DA neurons. The use of such non-clinical measures needs to be chosen carefully on the basis of the underlying biology, because, for example, PET scans that depend on DAT availability may not be appropriate, as evidence from this thesis suggests that changes in autophagic state may influence DAT availability (Whone *et al.* 2003)

Appendix: midbrain dopamine neuron counts

In this appendix, dopamine neuron counts as assessed by TH stereology are presented for each genotype in each age group. Two-way ANOVAs have been performed within each group to determine any differences in neuron number associated with genotype.

Appendix Table 1. Substantia nigra dopamine neuron counts with gene effects analysed using two-way ANOVA in each age group

Age (months)	Genotype	Neuron number (SEM)	*ATG7*cKO$^{DAT\text{-IRES-cre}}$ x *hSNCA*		*ATG7*cKO$^{DAT\text{-IRES-cre}}$		h*SNCA*	
			F	**P value**	***F***	**P value**	***F***	**P value**
1	Control	2082 (184)						
	h*SNCA*	2180 (193)						
	*ATG7*cKO$^{DAT\text{-IRES-cre}}$	2041 (131)						
	h*SNCA*:*ATG7*cKO$^{DAT\text{-IRES-cre}}$	1970 (246)	$F_{(1,15)}$=0.190	0.67	$F_{(1, 15)}$=0.412	0.52	$F_{(1, 15)}$= 0.004	0.94
6	Control	1867 (303)						
	h*SNCA*	1796 (214)						
	*ATG7*cKO$^{DAT\text{-IRES-cre}}$	1279 (87)						
	h*SNCA*:*ATG7*cKO$^{DAT\text{-IRES-cre}}$	1266 (110)	$F_{(1,12)}$=0.022	0.89	$F_{(1, 12)}$=7.955	0.02	$F_{(1, 12)}$=0.046	0.83
20 to 24	Control	1446 (231)						
	h*SNCA*	1611 (226)						
	*ATG7*cKO$^{DAT\text{-IRES-cre}}$	944 (198)						
	h*SNCA*:*ATG7*cKO$^{DAT\text{-IRES-cre}}$	780 (151)	$F_{(1, 17)}$=0.674	0.42	$F_{(1, 17)}$=11.07	<0.01	$F_{(1, 17)}$=0.000	0.99

Appendix Table 2. Ventral tegmental area dopamine neuron counts with gene effects analysed using two-way ANOVA in each age group								
Age (months)	**Genotype**	**Neuron number (SEM)**	***ATG7*cKO$^{DAT\text{-IRES-cre}}$ x *hSNCA***		***ATG7*cKO$^{DAT\text{-IRES-cre}}$**		**h*SNCA***	
			F	**P value**	***F***	**P value**	***F***	**P value**
1	Control	2688 (226)						
	h*SNCA*	3023 (219)						
	*ATG7*cKO$^{DAT\text{-IRES-cre}}$	3006 (219)						
	h*SNCA*:*ATG7*cKO$^{DAT\text{-IRES-cre}}$	3095 (285)	$F_{(1, 15)}$= 0.257	0.62	$F_{(1, 15)}$=0.643	0.44	$F_{(1, 15)}$= 0.760	0.3970
6	Control	1798 (177)						
	h*SNCA*	2159 (241)						
	*ATG7*cKO$^{DAT\text{-IRES-cre}}$	1860 (265)						
	h*SNCA*:*ATG7*cKO$^{DAT\text{-IRES-cre}}$	2139 (241)	$F_{(1,12)}$=0.031	0.86	$F_{(1, 12)}$=0.008	0.93	$F_{(1, 12)}$=1.88	0.1952
20 to 24	Control	2028 (302)						
	h*SNCA*	2111 (322)						
	*ATG7*cKO$^{DAT\text{-IRES-cre}}$	1570 (285)						
	h*SNCA*:*ATG7*cKO$^{DAT\text{-IRES-cre}}$	1793 (314)	$F_{(1,17)}$=0.052	0.82	$F_{(1, 17)}$=1.57	0.23	$F_{(1,17)}$=0.246	0.6263

References

Aasly JO, Vilarino Guell C, Dachsel JC, Webber PJ, West AB, Haugarvoll K, Johansen KK, JG, Payami H, Kachergus JM, Lincoln SJ, Felic A, Wider C, Soto Ortolaza AI, Cobb SA Ross OA, Farrer MJ. Novel pathogenic LRRK2 p.Asn1437His substitution in familial Pa disease. *Movement Disorders* 2010;**25**:2156–63.

Abbas N, Lucking CB, Ricard S, Dürr A, Bonifati V, De Michele G, Bouley S, Vaughan JR, Marconi R, Broussolle E, Brefel-Courbon C, Harhangi BS, Oostra, AB, Fabrizio E, Bohı L, Wood NW, Filla A *et al.* A wide variety of mutations in the parkin gene are responsib autosomal recessive parkinsonism in Europe. *Human Molecular Genetics* 1999;**8**:567–74

Abeliovich A, Schmitz Y, Farinas I, Choi-Lundberg D, Ho WH, Castillo PE, Shinsky N, Verc Armanini M, Ryan A, Hynes M, Phillips H, Sulzer D, Rosenthal A. Mice lacking alpha-s display functional deficits in the nigrostriatal dopamine system. *Neuron* 2000;**25**:239–52

Adams-Carr KL, Bestwick JP, Shribman S, Lees A, Schrag A, Noyce AJ. Constipation preced Parkinson's disease: a systematic review and meta-analysis. *Journal of Neurology, Neuro Psychiatry* 2016;**87**:710–6.

Ahlberg J, Glaumann H. Uptake--microautophagy--and degradation of exogenous proteins by liver lysosomes. Effects of pH, ATP, and inhibitors of proteolysis. *Experimental and mo pathology* 1985;**42**:78–88.

Ahlberg J, Marzella L, Glaumann H. Uptake and degradation of proteins by isolated rat liver l Suggestion of a microautophagic pathway of proteolysis. *Laboratory investigation; a jou technical methods and pathology* 1982;**47**:523–32.

Ahmed I, Liang Y, Schools S, Dawson VL, Dawson TM, Savitt JM. Development and charac new Parkinson's disease model resulting from impaired autophagy. *Journal of Neuroscie* 2012;**32**:16503–9.

Al-Wandi A, Ninkina N, Millership S, Williamson SJM, Jones PA, Buchman VL. Absence of affects dopamine metabolism and synaptic markers in the striatum of aging mice. *Neuro Aging* 2010;**31**:796–804.

Alegre-Abarrategui J, Christian H, Lufino MMP, Mutihac R, Venda LL, Ansorge O, Wade-M LRRK2 regulates autophagic activity and localizes to specific membrane microdomains human genomic reporter cellular model. *Human Molecular Genetics* 2009;**18**:4022–34.

Alvarado-Bolanos A, Cervantes-Arriaga A, Rodriguez-Violante M, Llorens-Arenas R, Calder Millan-Cepeda R, Leal-Ortega R, Estrada-Bellmann I, Zuniga-Ramirez C. Impact of Neu Symptoms on the Quality of Life of Subjects with Parkinson's Disease. *Journal of Parki* 2015;**5**:541–8.

Ando M, Funayama M, Li Y, Kashihara K, Murakami Y, Ishizu N, Toyoda C, Noguchi K, Ha Nakano N, Sasaki R, Kokubo Y, Kuzuhara S, Ogaki K, Yamashita C, Yoshino H, Hatano H, Hattori N. VPS35 mutation in Japanese patients with typical Parkinson's disease. *Mov Disorders* 2012;**27**:1413–7.

Anglade P, Vyas S, Javoy-Agid F, Herrero MT, Michel PP, Marquez J, Mouatt-Prigent A, Ru EC, Agid Y. Apoptosis and autophagy in nigral neurons of patients with Parkinson's dise *and Histopathology* 1997;**12**:25–32.

Annesi G, Savettieri G, Pugliese P, D'Amelio M, Tarantino P, Ragonese P, La Bella V, Picco Annesi F, Fierro B, Piccoli F, Arabia G, Caracciolo M, Cirò Candiano IC, Quattrone A. and parkinsonism-dementia-amyotrophic lateral sclerosis complex. *Annals of Neurology*

Anwar S, Peters O, Millership S, Ninkina N, Doig N, Connor-Robson N, Threlfell S, Kooner G, Deacon RM, Bannerman DM, Bolam JP, Chandra SS, Cragg SJ, Wade-Martins R, Buchman VL. Functional Alterations to the Nigrostriatal System in Mice Lacking All Three Members of the Synuclein Family. *Journal of Neuroscience* 2011;**31**:7264–74.

Appel Cresswell S, Vilarino Guell C, Encarnacion M, Sherman H, Yu I, Shah B, Weir D, Thompson C, Szu Tu C, Trinh J, Aasly JO, Rajput A, Rajput AH, Jon Stoessl A, Farrer MJ. Alpha-synuclein p.H50Q, a novel pathogenic mutation for Parkinson's disease. *Movement Disorders* 2013;**28**:811–3.

Arai N, Misugi K, Goshima Y, Misu Y. Evaluation of a 1-methyl-4-phenyl-1,2,3,6-tetrahydropyridine (MPTP)-treated C57 black mouse model for parkinsonism. *Brain Research* 1990;**515**:57–63.

Araki K, Yagi N, Nakatani R, Sekiguchi H, So M, Yagi H, Ohta N, Nagai Y, Goto Y, Mochizuki H. A small-angle X-ray scattering study of alpha-synuclein from human red blood cells. *Scientific Reports* 2016;**6**, DOI: 10.1038/srep30473.

Ashburn A, Stack E, Pickering RM, Ward CD. A community-dwelling sample of people with Parkinson's disease: characteristics of fallers and non-fallers. *Age and Ageing* 2001;**30**:47–52.

Ayton S, George JL, Adlard PA, Bush AI, Cherny RA, Finkelstein DI. The effect of dopamine on MPTP-induced rotarod disability. *Neuroscience Letters* 2013;**543**:105–9.

Bai X, Wey MC-Y, Fernandez E, Hart MJ, Gelfond J, Bokov AF, Rani S, Strong R. Rapamycin improves motor function, reduces 4-hydroxynonenal adducted protein in brain, and attenuates synaptic injury in a mouse model of synucleinopathy. *Pathobiology of Aging & Age-related Diseases* 2015;**5**:28743.

Baiguera C, Alghisi M, Pinna A, Bellucci A, De Luca MA, Frau L, Morelli M, Ingrassia R, Benarese M, Porrini V, Pellitteri M, Bertini G, Fabene PF, Sigala S, Spillantini M-G, Liou H-C, Spano PF, Pizzi M. Late-onset Parkinsonism in NFκB/c-Rel-deficient mice. *Brain* 2012;**135**:2750–65.

Balsinde J, Balboa MA. Cellular regulation and proposed biological functions of group VIA calcium-independent phospholipase A2 in activated cells. *Cellular signalling* 2005;**17**:1052–62.

Bandyopadhyay U, Kaushik S, Varticovski L, Cuervo AM. The chaperone-mediated autophagy receptor organizes in dynamic protein complexes at the lysosomal membrane. *Molecular and Cellular Biology* 2008;**28**:5747–63.

Bartels T, Choi JG, Selkoe DJ. alpha-Synuclein occurs physiologically as a helically folded tetramer that resists aggregation. *Nature* 2011;**477**:107–10.

Bäckman CM, Malik N, Zhang Y, Shan L, Grinberg A, Hoffer BJ, Westphal H, Tomac AC. Characterization of a mouse strain expressing Cre recombinase from the 3′ untranslated region of the dopamine transporter locus. *Genesis* 2006;**44**:383–90.

Beilina A, Cookson MR. Genes associated with Parkinson's disease: regulation of autophagy and beyond. *Journal of Neurochemistry* 2016;**139**:91–107.

Beilina A, Rudenko IN, Kaganovich A, Civiero L, Chau H, Kalia SK, Kalia LV, Lobbestael E, Chia R, Ndukwe K, Ding J, Nalls MA, Olszewski M, Hauser DN, Kumaran R, Lozano AM, Baekelandt V, Greene LE, Taymans J-M *et al.* Unbiased screen for interactors of leucine-rich repeat kinase 2 supports a common pathway for sporadic and familial Parkinson disease. *Proceedings of the National Academy of Sciences* 2014;**111**:2626–31.

Benedetti MD, Maraganore DM, Bower JH, McDonnell SK, Peterson BJ, Ahlskog JE, Schaid DJ, Rocca WA. Hysterectomy, menopause, and estrogen use preceding Parkinson's disease: An exploratory case-control study. *Movement Disorders* 2001;**16**:830–7.

Benoit-Marand M, Borrelli E, Gonon F. Inhibition of Dopamine Release Via Presynaptic D2 Receptors: Time Course and Functional Characteristics In Vivo. *Journal of Neuroscience* 2001;**21**:9134–41.

Bento CF, Renna M, Ghislat G, Puri C, Ashkenazi A, Vicinanza M, Menzies FM, Rubinsztein DC. Mammalian Autophagy: How Does It Work? *Annual review of biochemistry* 2016;**85**:685–713.

Berger K, Breteler MM, Helmer C, Inzitari D, Fratiglioni L, Trenkwalder C, Hofman A, Launer LJ. Prognosis with Parkinson's disease in europe: A collaborative study of population-based cohorts. Neurologic Diseases in the Elderly Research Group. *Neurology* 2000;**54**:S24–7.

Bernheimer H, Birkmayer W, Hornykiewicz O, Jellinger K, Seitelberger F. Brain dopamine and the syndromes of Parkinson and Huntington. Clinical, morphological and neurochemical correlations. *Journal of the neurological sciences* 1973;**20**:415–55.

Betarbet R, Sherer TB, MacKenzie G, Garcia-Osuna M, Panov AV, Greenamyre JT. Chronic systemic pesticide exposure reproduces features of Parkinson's disease. *Nature Neuroscience* 2000;**3**:1301–6.

Betin VMS, Singleton BK, Parsons SF, Anstee DJ, Lane JD. Autophagy facilitates organelle clearance during differentiation of human erythroblasts. *Autophagy* 2013;**9**:881–93.

Betz UAK, Voßhenrich CAJ, Rajewsky K, Müller W. Bypass of lethality with mosaic mice generated by Cre–loxP-mediated recombination. *Current Biology* 1996;**6**:1307–16.

Bevan MD, Magill PJ, Terman D, Bolam JP, Wilson CJ. Move to the rhythm: oscillations in the subthalamic nucleus–external globus pallidus network. *Trends in Neurosciences* 2002;**25**:525–31.

Bezard E, Gross CE, Fournier MC, Dovero S, Bloch B, Jaber M. Absence of MPTP-induced neuronal death in mice lacking the dopamine transporter. *Experimental Neurology* 1999;**155**:268–73.

Bianco Lo C, Ridet JL, Schneider BL, Déglon N, Aebischer P. α-synucleinopathy and selective dopaminergic neuron loss in a rat lentiviral-based model of Parkinson's disease. *Proceedings of the National Academy of Sciences* 2002;**99**:10813–8.

Biazik J, Ylä-Anttila P, Vihinen H, Jokitalo E, Eskelinen E-L. Ultrastructural relationship of the phagophore with surrounding organelles. *Autophagy* 2015;**11**:439–51.

Biere AL, Wood SJ, Wypych J, Steavenson S, Jiang Y, Anafi D, Jacobsen FW, Jarosinski MA, Wu GM, Louis JC, Martin F, Narhi LO, Citron M. Parkinson's disease-associated alpha-synuclein is more fibrillogenic than beta- and gamma-synuclein and cannot cross-seed its homologs. *Journal of Biological Chemistry* 2000;**275**:34574–9.

Bisaglia M, Mammi S, Bubacco L. Structural insights on physiological functions and pathological effects of alpha-synuclein. *FASEB Journal* 2009;**23**:329–40.

Boileau I, Warsh JJ, Guttman M, Saint Cyr JA, McCluskey T, Rusjan P, Houle S, Wilson AA, Meyer JH, Kish SJ. Elevated serotonin transporter binding in depressed patients with Parkinson's disease: a preliminary PET study with [11C]DASB. *Movement Disorders* 2008;**23**:1776–80.

Bonifati V, Rizzu P, van Baren MJ, Schaap O, Breedveld GJ, Krieger E, Dekker MCJ, Squitieri F, Ibanez P, Joosse M, van Dongen JW, Vanacore N, van Swieten JC, Brice A, Meco G, van Duijn CM, Ben A Oostra, Heutink P. Mutations in the *DJ-1* Gene Associated with Autosomal Recessive Early-Onset Parkinsonism. *Science* 2003;**299**:256–9.

Bosboom J, Stoffers D, Wolters EC. Cognitive dysfunction and dementia in Parkinson's disease. *Journal of Neural Transmission* 2004.

Boya P, Reggiori F, Codogno P. Emerging regulation and functions of autophagy. *Nature Cell Biology* 2013;**15**:713–20.

Braak H, Bohl JR, Müller CM, Rüb U, de Vos RAI, Del Tredici K. Stanley Fahn Lecture 2005: The staging procedure for the inclusion body pathology associated with sporadic Parkinson's disease reconsidered. *Movement Disorders* 2006;**21**:2042–51.

Braak H, Del Tredici K. *Neuroanatomy and Pathology of Sporadic Parkinson's Disease*. Berlin: Springer, 2008.

Braak H, Rüb U, Jansen Steur ENH, Del Tredici K, de Vos RAI. Cognitive status correlates with neuropathologic stage in Parkinson disease. *Neurology* 2005;**64**:1404–10.

Branco T, Staras K. The probability of neurotransmitter release: variability and feedback control at single synapses. *Nature Reviews Neuroscience* 2009;**10**:373–83.

Braungart E, Gerlach M, Riederer P, Baumeister R, Hoener MC. Caenorhabditis elegans MPP+ Model of Parkinson's Disease for High-Throughput Drug Screenings. *Neurodegenerative Diseases* 2004;**1**:175–83.

Brimblecombe KR, Cragg SJ. Ni2+ affects dopamine uptake which limits suitability as inhibitor of T-type voltage-gated Ca^{2+} channels. *ACS chemical neuroscience* 2014, DOI: 10.1021/cn500274g.

Buchman VL, Hunter HJA, Pinõn LGP, Thompson J, Privalova EM, Ninkina NN, Davies AM. Persyn, a Member of the Synuclein Family, Has a Distinct Pattern of Expression in the Developing Nervous System. *Journal of Neuroscience* 1998;**18**:9335–41.

Burré J, Sharma M, Südhof TC. α-Synuclein assembles into higher-order multimers upon membrane binding to promote SNARE complex formation. *Proceedings of the National Academy of Sciences* 2014;**111**:E4274–83.

Burré J, Vivona S, Diao J, Sharma M, Brunger AT, Südhof TC. Properties of native brain alpha-synuclein. *Nature* 2013;**498**:E4–6–discussionE6–7.

Cabin DE, Gispert-Sanchez S, Murphy D, Auburger G, Myers RR, Nussbaum RL. Exacerbated synucleinopathy in mice expressing A53T SNCA on a Snca null background. *Neurobiology of Aging* 2005;**26**:25–35.

Can A, Dao DT, Terrillion CE, Piantadosi SC, Bhat S, Gould TD. The tail suspension test. *Journal of visualized experiments : JoVE* 2012:e3769–9.

Cang C, Aranda K, Seo Y-J, Gasnier B, Ren D. TMEM175 Is an Organelle K + Channel Regulating Lysosomal Function. *Cell* 2015;**162**:1101–12.

Carter DA, Fibiger HC. Ascending projections of presumed dopamine-containing neurons in the ventral tegmentum of the rat as demonstrated by horseradish peroxidase. *Neuroscience* 1977;**2**:569–76.

Caslake R, Moore JN, Gordon JC, Harris CE, Counsell C. Changes in diagnosis with follow-up in an incident cohort of patients with parkinsonism. *Journal of Neurology, Neurosurgery & Psychiatry* 2008;**79**:1202–7.

Cárdenas C, Miller RA, Smith I, Bui T, Molgó J, Müller M, Vais H, Cheung K-H, Yang J, Parker I, Thompson CB, Birnbaum MJ, Hallows KR, Foskett JK. Essential Regulation of Cell Bioenergetics by Constitutive InsP3 Receptor Ca2+ Transfer to Mitochondria. *Cell* 2010;**142**:270–83.

Chan CS, Guzman JN, Ilijic E, Mercer JN, Rick C, Tkatch T, Meredith GE, Surmeier DJ. 'Rejuvenation' protects neurons in mouse models of Parkinson's disease. *Nature* 2007;**447**:1081–6.

Chan G, White CC, Winn PA, Cimpean M, Replogle JM, Glick LR, Cuerdon NE, Ryan KJ, Johnson KA, Schneider JA, Bennett DA, Chibnik LB, Sperling RA, De Jager PL, Bradshaw EM. Trans-pQTL study identifies immune crosstalk between Parkinson and Alzheimer loci. *Neurology Genetics* 2016;**2**:e90.

Chandra S, Gallardo G, Fernández-Chacón R, Schlüter OM, Südhof TC. α-Synuclein Cooperates with CSPα in Preventing Neurodegeneration. *Cell* 2005;**123**:383–96.

Chen BT, Moran KA, Avshalumov MV, Rice ME. Limited regulation of somatodendritic dopamine release by voltage-sensitive Ca2+ channels contrasted with strong regulation of axonal dopamine release. *Journal of Neurochemistry* 2006;**96**:645–55.

Chen D, Pang S, Feng X, Huang W, Hawley RG, Yan B. Genetic analysis of the ATG7 gene promoter in sporadic Parkinson's disease. *Neuroscience Letters* 2013;**534**:193–8.

Chen H, Zhao EJ, Zhang W, Lu Y, Liu R, Huang X, Ciesielski-Jones AJ, Justice MA, Cousins DS, Peddada S. Meta-analyses on prevalence of selected Parkinson's nonmotor symptoms before and after diagnosis. *Translational Neurodegeneration* 2015;**4**:1.

Chiang HL, Terlecky SR, Plant CP, Dice JF. A role for a 70-kilodalton heat shock protein in lysosomal degradation of intracellular proteins. *Science* 1989;**246**:382–5.

Chu Y, Dodiya H, Aebischer P, Olanow CW, Kordower JH. Alterations in lysosomal and proteasomal markers in Parkinson's disease: relationship to alpha-synuclein inclusions. *Neurobiology of Disease* 2009;**35**:385–98.

Chung CY. Cell type-specific gene expression of midbrain dopaminergic neurons reveals molecules involved in their vulnerability and protection. *Human Molecular Genetics* 2005;**14**:1709–25.

Chung KK, Zhang Y, Lim KL, Tanaka Y, Huang H, Gao J, Ross CA, Dawson VL, Dawson TM. Parkin ubiquitinates the alpha-synuclein-interacting protein, synphilin-1: implications for Lewy-body formation in Parkinson disease. *Nature Medicine* 2001;**7**:1144–50.

Clarke CE, Zobkiw RM, Gullaksen E. Quality of life and care in Parkinson's disease. *The British Journal of Clinical Practice* 1995;**49**:288–93.

Cleveland DW, Hwo S-Y, Kirschner MW. Purification of tau, a microtubule-associated protein that induces assembly of microtubules from purified tubulin. *Journal of Molecular Biology* 1977;**116**:207–25.

Colotla VA, Flores E, Oscos A, Meneses A, Tapia R. Effects of MPTP on locomotor activity in mice. *Neurotoxicology and Teratology* 1990;**12**:405–7.

Connolly BS, Lang AE. Pharmacological treatment of Parkinson disease: a review. *JAMA* 2014;**311**:1670–83.

Connor-Robson N, Peters OM, Millership S, Ninkina N, Buchman VL. Combinational losses of synucleins reveal their differential requirements for compensating age-dependent alterations in motor behavior and dopamine metabolism. *Neurobiology of Aging* 2016;**46**:107–12.

Conway KA, Harper JD, Lansbury PT. Accelerated in vitro fibril formation by a mutant alpha-synuclein linked to early-onset Parkinson disease. *Nature Medicine* 1998;**4**:1318–20.

Cornejo-Olivas MR, Torres L, Mata IF, Mazzetti P, Rivas D, Cosentino C, Inca-Martinez M, Cuba JM, Zabetian CP, Leverenz JB. A Peruvian family with a novel PARK2 mutation: Clinical and pathological characteristics. *Parkinsonism and Related Disorders* 2015;**21**:444–8.

Costa J, Lunet N, Santos C, Santos J, Vaz-Carneiro A. Caffeine exposure and the risk of Parkinson's disease: a systematic review and meta-analysis of observational studies. *Journal of Alzheimer's Disease* 2010;**20 Suppl 1**:S221–38.

Cragg SJ, Hille CJ, Greenfield SA. Dopamine release and uptake dynamics within nonhuman primate striatum in vitro. *Journal of Neuroscience* 2000;**20**:8209–17.

Cragg SJ. Variable dopamine release probability and short-term plasticity between functional domains of the primate striatum. *Journal of Neuroscience* 2003;**23**:4378–85.

Crews L, Spencer B, Desplats P, Patrick C, Paulino A, Rockenstein E, Hansen L, Adame A, Galasko D, Masliah E. Selective molecular alterations in the autophagy pathway in patients with Lewy body disease and in models of alpha-synucleinopathy. Ikezu T (ed.). *PLoS ONE* 2010;**5**:e9313.

Cryan JF, Mombereau C, Vassout A. The tail suspension test as a model for assessing antidepressant activity: Review of pharmacological and genetic studies in mice. *Neuroscience & Biobehavioral Reviews* 2005;**29**:571–625.

Cuervo AM, Stefanis L, Fredenburg R, Lansbury PT, Sulzer D. Impaired Degradation of Mutant α-Synuclein by Chaperone-Mediated Autophagy. *Science* 2004;**305**:1292–5.

Dan I, Watanabe NM, Kusumi A. The Ste20 group kinases as regulators of MAP kinase cascades. *Trends in Cell Biology* 2001;**11**:220–30.

Daniel JA, Galbraith S, Iacovitti L, Abdipranoto A, Vissel B. Functional heterogeneity at dopamine release sites. *Journal of Neuroscience* 2009;**29**:14670–80.

Dauer W, Kholodilov N, Vila M, Trillat A-C, Goodchild R, Larsen KE, Staal R, Tieu K, Schmitz Y, Yuan CA, Rocha M, Jackson-Lewis V, Hersch S, Sulzer D, Przedborski S, Burke R, Hen R. Resistance of alpha -synuclein null mice to the parkinsonian neurotoxin MPTP. *Proceedings of the National Academy of Sciences* 2002;**99**:14524–9.

Davis C. *SPSS for Applied Sciences*. CSIRO PUBLISHING, 2013.

Dawson TM, Ko HS, Dawson VL. Genetic animal models of Parkinson's disease. *Neuron* 2010;**66**:646–61.

de Rijk MC, Breteler MM, Graveland GA, Ott A, Grobbee DE, van der Meché FG, Hofman A. Prevalence of Parkinson's disease in the elderly: the Rotterdam Study. *Neurology* 1995;**45**:2143–6.

Deacon RMJ, Bannerman DM, Kirby BP, Croucher A, Rawlins JNP. Effects of cytotoxic hippocampal lesions in mice on a cognitive test battery. *Behavioural Brain Research* 2002;**133**:57–68.

Deacon RMJ, Rawlins JNP. T-maze alternation in the rodent. *Nature Protocols* 2006;**1**:7–12.

Deacon RMJ. Measuring the strength of mice. *Journal of Visualized Experiments* 2013a, DOI: 10.3791/2610.

Deacon RMJ. Measuring motor coordination in mice. *Journal of Visualized Experiments* 2013b:e2609.

Decressac M, Mattsson B, Weikop P, Lundblad M, Jakobsson J, Björklund A. TFEB-mediated autophagy rescues midbrain dopamine neurons from alpha-synuclein toxicity. *Proceedings of the National Academy of Sciences* 2013;**110**:E1817–26.

Dehay B, Bove J, Rodriguez-Muela N, Perier C, Recasens A, Boya P, Vila M. Pathogenic lysosomal depletion in Parkinson's disease. *Journal of Neuroscience* 2010;**30**:12535–44.

Dehay B, Ramirez A, Martinez-Vicente M, Perier C, Canron M-H, Doudnikoff E, Vital A, Vila M, Klein C, Bezard E. Loss of P-type ATPase ATP13A2/PARK9 function induces general lysosomal deficiency and leads to Parkinson disease neurodegeneration. *Proceedings of the National Academy of Sciences* 2012;**109**:9611–6.

Delfs JM, Schreiber L, Kelley AE. Microinjection of cocaine into the nucleus accumbens elicits locomotor activation in the rat. *Journal of Neuroscience* 1990;**10**:303.

DeLong MR, Wichmann T. Circuits and Circuit Disorders of the Basal Ganglia. *Archives of Neurology* 2007;**64**:20–4.

DeMaagd G, Philip A. Parkinson's Disease and Its Management: Part 1: Disease Entity, Risk Factors, Pathophysiology, Clinical Presentation, and Diagnosis. *P & T : a peer-reviewed journal for formulary management* 2015;**40**:504–32.

Desplats P, Lee H-J, Bae E-J, Patrick C, Rockenstein E, Crews L, Spencer B, Masliah E, Lee S-J. Inclusion formation and neuronal cell death through neuron-to-neuron transmission of alpha-synuclein. *Proceedings of the National Academy of Sciences* 2009;**106**:13010–5.

Dettmer U, Newman AJ, Luth ES, Bartels T, Selkoe D. In Vivo Cross-linking Reveals Principally Oligomeric Forms of alpha-Synuclein and beta-Synuclein in Neurons and Non-neural Cells. *Journal of Biological Chemistry* 2013;**288**:6371–85.

Dexter DT, Carter CJ, Wells FR, Javoy-Agid F, Agid Y, Lees A, Jenner P, Marsden CD. Basal Lipid Peroxidation in Substantia Nigra Is Increased in Parkinson's Disease. *Journal of Neurochemistry* 1989;**52**:381–9.

Diao J, Burré J, Vivona S, Cipriano DJ, Sharma M, Kyoung M, Südhof TC, Brunger AT. Native alpha-synuclein induces clustering of synaptic-vesicle mimics via binding to phospholipids and synaptobrevin-2/VAMP2. *eLife* 2013;**2**:e00592.

Dice JF, Chiang HL, Spencer EP, Backer JM. Regulation of catabolism of microinjected ribonuclease A. Identification of residues 7-11 as the essential pentapeptide. *Journal of Biological Chemistry* 1986;**261**:6853–9.

Dice JF. Peptide sequences that target cytosolic proteins for lysosomal proteolysis. *Trends in biochemical sciences* 1990;**15**:305–9.

Dodel RC, Singer M, Köhne-Volland R, Szucs T, Rathay B, Scholz E, Oertel WH. The economic impact of Parkinson's disease. An estimation based on a 3-month prospective analysis. *PharmacoEconomics* 1998;**14**:299–312.

Dorsey ER, Constantinescu R, Thompson JP, Biglan KM, Holloway RG, Kieburtz K, Marshall FJ, Ravina BM, Schifitto G, Siderowf A, Tanner CM. Projected number of people with Parkinson disease in the most populous nations, 2005 through 2030. *Neurology* 2007;**68**:384–6.

Dusonchet J, Kochubey O, Stafa K, Young SMJ, Zufferey R, Moore DJ, Schneider BL, Aebischer P. A rat model of progressive nigral neurodegeneration induced by the Parkinson's disease-associated G2019S mutation in LRRK2. *Journal of Neuroscience* 2011;**31**:907–12.

Dymecki SM. Flp recombinase promotes site-specific DNA recombination in embryonic stem cells and transgenic mice. *Proceedings of the National Academy of Sciences* 1996;**93**:6191–6.

Ebrahimi-Fakhari D, Cantuti-Castelvetri I, Fan Z, Rockenstein E, Masliah E, Hyman BT, McLean PJ, Unni VK. Distinct Roles *In Vivo* for the Ubiquitin–Proteasome System and the Autophagy–Lysosomal Pathway in the Degradation of α-Synuclein. *Journal of Neuroscience* 2011;**31**:14508–20.

Ehringer H, Hornykiewicz O. Verteilung Von Noradrenalin Und Dopamin (3-Hydroxytyramin) Im Gehirn Des Menschen Und Ihr Verhalten Bei Erkrankungen Des Extrapyramidalen Systems. *Klinische Wochenschrift* 1960;**38**:1236–9.

Ellison SLR, Farrant TJ, Barwick V. *Practical Statistics for the Analytical Scientist*. Royal Society of Chemistry, 2009.

Emre M. Dementia associated with Parkinson's disease. *The Lancet Neurology* 2003;**2**:229–37.

Eriksen J, Rasmussen SGF, Rasmussen TN, Vaegter CB, Cha JH, Zou M-F, Newman AH, Gether U. Visualization of dopamine transporter trafficking in live neurons by use of fluorescent cocaine analogs. *Journal of Neuroscience* 2009;**29**:6794–808.

Exner N, Treske B, Paquet D, Holmström K, Schiesling C, Gispert S, Carballo-Carbajal I, Berg D, Hoepken H-H, Gasser T, Krüger R, Winklhofer KF, Vogel F, Reichert AS, Auburger G, Kahle PJ, Schmid B, Haass C. Loss-of-Function of Human PINK1 Results in Mitochondrial Pathology and Can Be Rescued by Parkin. *Journal of Neuroscience* 2007;**27**:12413–8.

Fahn S, Oakes D, Shoulson I, Kieburtz K, Rudolph A, Lang A, Olanow CW, Tanner C, Marek K. Levodopa and the progression of Parkinson's disease. *New England Journal of Medicine* 2004;**351**:2498–508.

Fares M-B, Maco B, Oueslati A, Rockenstein E, Ninkina N, Buchman VL, Masliah E, Lashuel HA. Induction of de novo α-synuclein fibrillization in a neuronal model for Parkinson's disease. *Proceedings of the National Academy of Sciences* 2016;**113**:E912–21.

Farrer M, Chan P, Chen R, Tan L, Lincoln S, Hernandez D, Forno L, Gwinn Hardy K, Petrucelli L, Hussey J, Singleton A, Tanner C, Hardy J, Langston JW. Lewy bodies and parkinsonism in families with parkin mutations. *Annals of Neurology* 2001;**50**:293–300.

Fauvet B, Mbefo MK, Fares M-B, Desobry C, Michael S, Ardah MT, Tsika E, Coune P, Prudent M, Lion N, Eliezer D, Moore DJ, Schneider B, Aebischer P, El-Agnaf OM, Masliah E, Lashuel HA. α-Synuclein in central nervous system and from erythrocytes, mammalian cells, and Escherichia coli exists predominantly as disordered monomer. *The Journal of Biological Chemistry* 2012;**287**:15345–64.

Feany MB, Bender WW. A Drosophila model of Parkinson's disease. *Nature* 2000;**404**:394–8.

Feir-Walsh BJ, Toothaker LE. An Empirical Comparison of the Anova F-Test, Normal Scores Test and Kruskal-Wallis Test Under Violation of Assumptions. *Educational and Psychological Measurement* 2016;**34**:789–99.

Feng Y, Backues SK, Baba M, Heo J-M, Harper JW, Klionsky DJ. Phosphorylation of Atg9 regulates movement to the phagophore assembly site and the rate of autophagosome formation. *Autophagy* 2016;**12**:648–58.

Ferrer I, Martinez A, Blanco R, Dalfó E, Carmona M. Neuropathology of sporadic Parkinson disease before the appearance of parkinsonism: preclinical Parkinson disease. *Journal of Neural Transmission* 2011;**118**:821–39.

Findley L, Aujla M, Bain PG, Baker M, Beech C, Bowman C, Holmes J, Kingdom WK, MacMahon DG, Peto V, Playfer JR. Direct economic impact of Parkinson's disease: a research survey in the United Kingdom. *Movement Disorders* 2003;**18**:1139–45.

Findley LJ, Gresty MA, Halmagyi GM. Tremor, the cogwheel phenomenon and clonus in Parkinson's disease. *Journal of Neurology, Neurosurgery & Psychiatry* 1981;**44**:534–46.

Fleming SM, Tetreault NA, Mulligan CK, Hutson CB, Masliah E, Chesselet M-F. Olfactory deficits in mice overexpressing human wildtype α-synuclein. *European Journal of Neuroscience* 2008;**28**:247–56.

Fountaine TM, Venda LL, Warrick N, Christian HC, Brundin P, Channon KM, Wade-Martins R. The effect of alpha-synuclein knockdown on MPP+ toxicity in models of human neurons. *European Journal of Neuroscience* 2008;**28**:2459–73.

Fountaine TM, Wade-Martins R. RNA interference-mediated knockdown of α-synuclein protects human dopaminergic neuroblastoma cells from MPP+ toxicity and reduces dopamine transport. *Journal of Neuroscience Research* 2007;**85**:351–63.

Frey U, Schroeder H, Matthies HR. Dopaminergic antagonists prevent long-term maintenance of posttetanic LTP in the CA1 region of rat hippocampal slices. *Brain Research* 1990;**522**:69–75.

Friedman LG, Lachenmayer ML, Wang J, He L, Poulose SM, Komatsu M, Holstein GR, Yue Z. Disrupted autophagy leads to dopaminergic axon and dendrite degeneration and promotes presynaptic accumulation of alpha-synuclein and LRRK2 in the brain. *Journal of Neuroscience* 2012;**32**:7585–93.

Fuchs J, Nilsson C, Kachergus J, Munz M, Larsson EM, Schule B, Langston JW, Middleton FA, Ross OA, Hulihan M, Gasser T, Farrer MJ. Phenotypic variation in a large Swedish pedigree due to SNCA duplication and triplication. *Neurology* 2007;**68**:916–22.

Fukuoka S-I, Ishiguro K, Yanagihara K, Tanabe A, Egashira Y, Sanada H, Shibata K. Identification and Expression of a cDNA Encoding Human α-Amino-β-carboxymuconate-ε-semialdehyde Decarboxylase (ACMSD). *Journal of Biological Chemistry* 2002;**277**:35162–7.

Garcia-Reitböck P, Anichtchik O, Bellucci A, Iovino M, Ballini C, Fineberg E, Ghetti B, Corte Della L, Spano P, Tofaris GK, Goedert M, Spillantini M-G. SNARE protein redistribution and synaptic failure in a transgenic mouse model of Parkinson's disease. *Brain* 2010;**133**:2032–44.

Gautier CA, Kitada T, Shen J. Loss of PINK1 causes mitochondrial functional defects and increased sensitivity to oxidative stress. *Proceedings of the National Academy of Sciences* 2008;**105**:11364–9.

Geisler S, Holmström KM, Skujat D, Fiesel FC, Rothfuss OC, Kahle PJ, Springer W. PINK1/Parkin-mediated mitophagy is dependent on VDAC1 and p62/SQSTM1. *Nature Cell Biology* 2010;**12**:119–31.

Gelman DM, Noaín D, Avale ME, Otero V, Low MJ, Rubinstein M. Transgenic mice engineered to target Cre/loxP-mediated DNA recombination into catecholaminergic neurons. *Genesis* 2003;**36**:196–202.

Giros B, Jaber M, Jones SR, Wightman RM, Caron MG. Hyperlocomotion and indifference to cocaine and amphetamine in mice lacking the dopamine transporter. *Nature* 1996;**379**:606–12.

Gitler AD, Bevis BJ, Shorter J, Strathearn KE, Hamamichi S, Su LJ, Caldwell KA, Caldwell GA, Rochet J-C, McCaffery JM, Barlowe C, Lindquist S. The Parkinson's disease protein alpha-synuclein disrupts cellular Rab homeostasis. *Proceedings of the National Academy of Sciences* 2008;**105**:145–50.

Goldberg MS, Fleming SM, Palacino JJ, Cepeda C, Lam HA, Bhatnagar A, Meloni EG, Wu NP, Ackerson LC, Klapstein GJ, Gajendiran M, Roth BL, Chesselet MF, Maidment NT, Levine MS, Shen J. Parkin-deficient mice exhibit nigrostriatal deficits but not loss of dopaminergic neurons. *Journal of Biological Chemistry* 2003;**278**:43628–35.

Goldberg MS, Pisani A, Haburcak M, Vortherms TA, Kitada T, Costa C, Tong Y, Martella G, Tscherter A, Martins A, Bernardi G, Roth BL, Pothos EN, Calabresi P, Shen J. Nigrostriatal dopaminergic deficits and hypokinesia caused by inactivation of the familial Parkinsonism-linked gene DJ-1. *Neuron* 2005;**45**:489–96.

Gouider-Khouja N, Larnaout A, Amouri R, Sfar S, Belal S, Ben Hamida C, Ben Hamida M, Hattori N, Mizuno Y, Hentati F. Autosomal recessive parkinsonism linked to parkin gene in a Tunisian family. Clinical, genetic and pathological study. *Parkinsonism and Related Disorders* 2003;**9**:247–51.

Gómez-Isla T, Irizarry MC, Mariash A, Cheung B, Soto O, Schrump S, Sondel J, Kotilinek L, Day J, Schwarzschild MA, Cha J-HJ, Newell K, Miller DW, Uéda K, Young AB, Hyman BT, Ashe KH. Motor dysfunction and gliosis with preserved dopaminergic markers in human alpha-synuclein A30P transgenic mice. *Neurobiology of Aging* 2003;**24**:245–58.

Grace AA, Bunney BS. The control of firing pattern in nigral dopamine neurons: burst firing. *Journal of Neuroscience* 1984;**4**:2877–90.

Graybiel AM, Ohta K, Roffler-Tarlov S. Patterns of cell and fiber vulnerability in the mesostriatal system of the mutant mouse weaver. I. Gradients and compartments. *Journal of Neuroscience* 1990;**10**:720–33.

Grenhoff J, Nisell M, Ferré S, Aston-Jones G, Svensson TH. Noradrenergic modulation of midbrain dopamine cell firing elicited by stimulation of the locus coeruleus in the rat. *Journal of neural transmission General section* 1993;**93**:11–25.

Grünblatt E, Mandel S, Jacob-Hirsch J, Zeligson S, Amariglo N, Rechavi G, Li J, Ravid R, Roggendorf W, Riederer P, Youdim MBH. Gene expression profiling of parkinsonian substantia nigra pars compacta; alterations in ubiquitin-proteasome, heat shock protein, iron and oxidative stress regulated proteins, cell adhesion/cellular matrix and vesicle trafficking genes. *Journal of Neural Transmission* 2004;**111**:1543–73.

Grünewald A, Arns B, Seibler P, Rakovic A, Münchau A, Ramirez A, Sue CM, Klein C. ATP13A2 mutations impair mitochondrial function in fibroblasts from patients with Kufor-Rakeb syndrome. *Neurobiology of Aging* 2012;**33**:1843.e1–1843.e7.

Gu M, Cooper JM, Taanman JW, Schapira AH. Mitochondrial DNA transmission of the mitochondrial defect in Parkinson's disease. *Annals of Neurology* 1998;**44**:177–86.

Gudala K, Kanukula R, Bansal D. Reduced Risk of Parkinson's Disease in Users of Calcium Channel Blockers: A Meta-Analysis. *International Journal of Chronic Diseases* 2015;**2015**:697404–7.

Gusdon AM, Zhu J, Van Houten B, Chu CT. ATP13A2 regulates mitochondrial bioenergetics through macroautophagy. *Neurobiology of Disease* 2012;**45**:962–72.

Guzman JN, Sanchez-Padilla J, Wokosin D, Kondapalli J, Ilijic E, Schumacker PT, Surmeier DJ. Oxidant stress evoked by pacemaking in dopaminergic neurons is attenuated by DJ-1. *Nature* 2010;**468**:696–700.

Haaxma CA, Bloem BR, Borm GF, Oyen WJG, Leenders KL, Eshuis S, Booij J, Dluzen DE, Horstink MWIM. Gender differences in Parkinson's disease. *Journal of Neurology, Neurosurgery & Psychiatry* 2007;**78**:819–24.

Hall H, Jewett M, Landeck N, Nilsson N, Schagerlöf U, Leanza G, Kirik D. Characterization of Cognitive Deficits in Rats Overexpressing Human Alpha-Synuclein in the Ventral Tegmental Area and Medial Septum Using Recombinant Adeno-Associated Viral Vectors. Kahle PJ (ed.). *PLoS ONE* 2013;**8**:e64844.

Hamasaki M, Furuta N, Matsuda A, Nezu A, Yamamoto A, Fujita N, Oomori H, Noda T, Haraguchi T, Hiraoka Y, Amano A, Yoshimori T. Autophagosomes form at ER-mitochondria contact sites. *Nature* 2013a;**495**:389–93.

Hamasaki M, Shibutani ST, Yoshimori T. Up-to-date membrane biogenesis in the autophagosome formation. *Current Opinion in Cell Biology* 2013b;**25**:455–60.

Hansen C, Angot E, Bergström A-L, Steiner JA, Pieri L, Paul G, Outeiro TF, Melki R, Kallunki P, Fog K, Li J-Y, Brundin P. α-Synuclein propagates from mouse brain to grafted dopaminergic neurons and seeds aggregation in cultured human cells. *The Journal of Clinical Investigation* 2011;**121**:715–25.

Hansen C, Björklund T, Petit GH, Lundblad M, Murmu RP, Brundin P, Li J-Y. A novel α-synuclein-GFP mouse model displays progressive motor impairment, olfactory dysfunction and accumulation of α-synuclein-GFP. *Neurobiology of Disease* 2013;**56**:145–55.

Hara T, Nakamura K, Matsui M, Yamamoto A, Nakahara Y, Suzuki-Migishima R, Yokoyama M, Mishima K, Saito I, Okano H, Mizushima N. Suppression of basal autophagy in neural cells causes neurodegenerative disease in mice. *Nature* 2006;**441**:885–9.

Harris H, Rubinsztein DC. Control of autophagy as a therapy for neurodegenerative disease. *Nature Reviews Neurology* 2012;**8**:108–17.

Hashimoto M, Rockenstein E, Mante M, Mallory M, Masliah E. beta-Synuclein inhibits alpha-synuclein aggregation: a possible role as an anti-parkinsonian factor. *Neuron* 2001;**32**:213–23.

Hatami A, Chesselet M-F. Transgenic rodent models to study alpha-synuclein pathogenesis, with a focus on cognitive deficits. *Current topics in behavioral neurosciences* 2015;**22**:303–30.

Hauser DN, Primiani CT, Langston RG, Kumaran R, Cookson MR. The Polg Mutator Phenotype Does Not Cause Dopaminergic Neurodegeneration in DJ-1-Deficient Mice. *eNeuro* 2015;**2**, DOI: 10.1523/ENEURO.0075-14.2015.

Hayashi S, Wakabayashi K, Ishikawa A, Nagai H, Saito M, Maruyama M, Takahashi T, Ozawa T, Tsuji S, Takahashi H. An autopsy case of autosomal-recessive juvenile parkinsonism with a homozygous exon 4 deletion in the parkin gene. *Movement Disorders* 2000;**15**:884–8.

He Q, Koprich JB, Wang Y, Yu W-B, Xiao B-G, Brotchie JM, Wang J. Treatment with Trehalose Prevents Behavioral and Neurochemical Deficits Produced in an AAV alpha-Synuclein Rat Model of Parkinson's Disease. *Molecular Neurobiology* 2016;**53**:2258–68.

Hebron ML, Lonskaya I, Moussa CEH. Nilotinib reverses loss of dopamine neurons and improves motor behavior via autophagic degradation of α-synuclein in Parkinson's disease models. *Human Molecular Genetics* 2013;**22**:3315–28.

Hely MA, Reid WGJ, Adena MA, Halliday GM, Morris JGL. The Sydney multicenter study of Parkinson's disease: the inevitability of dementia at 20 years. *Movement Disorders* 2008;**23**:837–44.

Hernandez D, Torres CA, Setlik W, Cebrián C, Mosharov EV, Tang G, Cheng H-C, Kholodilov N, Yarygina O, Burke RE, Gershon M, Sulzer D. Regulation of presynaptic neurotransmission by macroautophagy. *Neuron* 2012;**74**:277–84.

Hernandez DG, Reed X, Singleton AB. Genetics in Parkinson disease: Mendelian versus non-Mendelian inheritance. *Journal of Neurochemistry* 2016;**139 Suppl 1**:59–74.

Hernán MA, Takkouche B, Caamaño Isorna F, Gestal Otero JJ. A meta-analysis of coffee drinking, cigarette smoking, and the risk of Parkinson's disease. *Annals of Neurology* 2002;**52**:276–84.

Hierro A, Rojas AL, Rojas R, Murthy N, Effantin G, Kajava AV, Steven AC, Bonifacino JS, Hurley JH. Functional architecture of the retromer cargo-recognition complex. *Nature* 2007;**449**:1063–7.

Hirsch E, Graybiel AM, Agid YA. Melanized dopaminergic neurons are differentially susceptible to degeneration in Parkinson's disease. *Nature* 1988;**334**:345–8.

Holtzman E, Freeman AR, Kashner LA. Stimulation-Dependent Alterations in Peroxidase Uptake at Lobster Neuromuscular Junctions. *Science* 1971;**173**:733–6.

Hong WC, Amara SG. Differential targeting of the dopamine transporter to recycling or degradative pathways during amphetamine- or PKC-regulated endocytosis in dopamine neurons. *FASEB Journal* 2013;**27**:2995–3007.

Hosokawa N, Sasaki T, Iemura S-I, Natsume T, Hara T, Mizushima N. Atg101, a novel mammalian autophagy protein interacting with Atg13. *Autophagy* 2009;**5**:973–9.

Hsu LJ, Sagara Y, Arroyo A, Rockenstein E, Sisk A, Mallory M, Wong J, Takenouchi T, Hashimoto M, Masliah E. α-Synuclein Promotes Mitochondrial Deficit and Oxidative Stress. *The American Journal of Pathology* 2000;**157**:401–10.

Hughes AJ, Daniel SE, Lees AJ. Improved accuracy of clinical diagnosis of Lewy body Parkinson's disease. *Neurology* 2001;**57**:1497–9.

Hung K-C, Huang H-J, Lin M-W, Lei Y-P, Lin AM-Y. Roles of autophagy in MPP+-induced neurotoxicity *in vivo*: the involvement of mitochondria and α-synuclein sggregation. *PLoS ONE* 2014;**9**:e91074.

Hunn BHM, Cragg SJ, Bolam JP, Spillantini M-G, Wade-Martins R. Impaired intracellular trafficking defines early Parkinson's disease. *Trends in Neurosciences* 2015;**38**:178–88.

Hyland BI, Reynolds JNJ, Hay J, Perk CG, Miller R. Firing modes of midbrain dopamine cells in the freely moving rat. *Neuroscience* 2002;**114**:475–92.

Ichimura Y, Kirisako T, Takao T, Satomi Y, Shimonishi Y, Ishihara N, Mizushima N, Tanida I, Kominami E, Ohsumi M, Noda T, Ohsumi Y. A ubiquitin-like system mediates protein lipidation. *Nature* 2000;**408**:488–92.

Ichinose H, Ohye T, Takahashi E-I, Seki N, Hori T-A, Segawa M, Nomura Y, Endo K, Tanaka H, Tsuji S, Fujita K, Nagatsu T. Hereditary progressive dystonia with marked diurnal fluctuation caused by mutations in the GTP cyclohydrolase I gene. *Nature Genetics* 1994;**8**:236–42.

Inoue K, Rispoli J, Kaphzan H, Klann E, Chen EI, Kim J, Komatsu M, Abeliovich A. Macroautophagy deficiency mediates age-dependent neurodegeneration through a phospho-tau pathway. *Molecular Neurodegeneration* 2012;**7**:48.

Itakura E, Mizushima N. Characterization of autophagosome formation site by a hierarchical analysis of mammalian Atg proteins. *Autophagy* 2010;**6**:764–76.

Iwai A, Masliah E, Yoshimoto M, Ge N, Flanagan L, Rohan de Silva HA, Kittel A, Saitoh T. The precursor protein of non-Aβ component of Alzheimer's disease amyloid is a presynaptic protein of the central nervous system. *Neuron* 1995;**14**:467–75.

Jackson-Lewis V, Przedborski S. Protocol for the MPTP mouse model of Parkinson's disease. *Nature Protocols* 2007;**2**:141–51.

Jafari S, Etminan M, Aminzadeh F, Samii A. Head injury and risk of Parkinson disease: a systematic review and meta-analysis. *Movement Disorders* 2013;**28**:1222–9.

Jakes R, Spillantini M-G, Goedert M. Identification of two distinct synucleins from human brain. 2001;**345**:27–32.

Janezic S, Threlfell S, Dodson PD, Dowie MJ, Taylor TN, Potgieter D, Parkkinen L, Senior SL, Anwar S, Ryan B, Deltheil T, Kosillo P, Cioroch M, Wagner K, Ansorge O, Bannerman DM, Bolam JP, Magill PJ, Cragg SJ *et al.* Deficits in dopaminergic transmission precede neuron loss and dysfunction in a new Parkinson model. *Proceedings of the National Academy of Sciences* 2013;**110**:E4016–25.

Jankovic J. Parkinson's disease: clinical features and diagnosis. *Journal of Neurology, Neurosurgery & Psychiatry* 2008;**79**:368–76.

Javier Blesa SP. Parkinson's disease: animal models and dopaminergic cell vulnerability. *Frontiers in Neuroanatomy* 2014;**8**:117.

Javitch JA, D'Amato RJ, Strittmatter SM, Snyder SH. Parkinsonism-inducing neurotoxin, N-methyl-4-phenyl-1,2,3,6 -tetrahydropyridine: uptake of the metabolite N-methyl-4-phenylpyridine by dopamine neurons explains selective toxicity. *Proceedings of the National Academy of Sciences* 1985;**82**:2173–7.

Johnson LA, Furman CA, Zhang M, Guptaroy B, Gnegy ME. Rapid delivery of the dopamine transporter to the plasmalemmal membrane upon amphetamine stimulation. *Neuropharmacology* 2005;**49**:750–8.

Johnson SJ, Wade-Martins R. A BACwards glance at neurodegeneration: molecular insights into disease from LRRK2, SNCA and MAPT BAC-transgenic mice. *Biochemical Society Transactions* 2011;**39**:862–7.

Jones BE, Moore RY. Ascending projections of the locus coeruleus in the rat. II. Autoradiographic study. *Brain Research* 1977;**127**:23–53.

Jones BJ, Roberts DJ. The quantitative measurement of motor inco-ordination in naive mice using an accelerating rotarod. *Journal of Pharmacy and Pharmacology* 1968;**20**:302–4.

Jones SR, Gainetdinov RR, Jaber M, Giros B, Wightman RM, Caron MG. Profound neuronal plasticity in response to inactivation of the dopamine transporter. *Proceedings of the National Academy of Sciences* 1998;**95**:4029–34.

Jung CH, Jun CB, Ro S-H, Kim Y-M, Otto NM, Cao J, Kundu M, Kim D-H. ULK-Atg13-FIP200 complexes mediate mTOR signaling to the autophagy machinery. *Molecular Biology of the Cell* 2009;**20**:1992–2003.

Kachergus J, Mata IF, Hulihan M, Taylor JP, Lincoln S, Aasly J, Gibson JM, Ross OA, Lynch T, Wiley J, Payami H, Nutt J, Maraganore DM, Czyzewski K, Styczynska M, Wszolek ZK, Farrer MJ, Toft M. Identification of a Novel LRRK2 Mutation Linked to Autosomal Dominant Parkinsonism: Evidence of a Common Founder across European Populations. *The American Journal of Human Genetics* 2005;**76**:672–80.

Kahle PJ, Neumann M, Ozmen L, Müller V, Jacobsen H, Schindzielorz A, Okochi M, Leimer U, van der Putten H, Probst A, Kremmer E, Kretzschmar HA, Haass C. Subcellular Localization of Wild-Type and Parkinson's Disease-Associated Mutant α-Synuclein in Human and Transgenic Mouse Brain. *Journal of Neuroscience* 2000;**20**:6365–73.

Kaisho T, Ishikawa J, Oritani K, Inazawa J, Tomizawa H, Muraoka O, Ochi T, Hirano T. BST-1, a surface molecule of bone marrow stromal cell lines that facilitates pre-B-cell growth. *Proceedings of the National Academy of Sciences* 1994;**91**:5325–9.

Karuppagounder SS, Brahmachari S, Lee Y, Dawson VL, Dawson TM, Ko HS. The c-Abl inhibitor, nilotinib, protects dopaminergic neurons in a preclinical animal model of Parkinson's disease. *Scientific Reports* 2014;**4**:4874.

Kastenmayer RJ, Fain MA, Perdue KA. A retrospective study of idiopathic ulcerative dermatitis in mice with a C57BL/6 background. *Journal of the American Association for Laboratory Animal Science : JAALAS* 2006;**45**:8–12.

Kelly PH, Seviour PW, Iversen SD. Amphetamine and apomorphine responses in the rat following 6-OHDA lesions of the nucleus accumbens septi and corpus striatum. *Brain Research* 1975;**94**:507–22.

Keppel G, Wickens TD. *Design and Analysis: a Researcher's Handbook*. Prentice Hall, 2004.

Kéry M, Hatfield JS. Normality of Raw Data in General Linear Models: the Most Widespread Myth in Statistics. *Bulletin of the Ecological Society of America* 2003;**84**:92–4.

Kieburtz K, Wunderle KB. Parkinson's disease: Evidence for environmental risk factors. *Movement Disorders* 2013;**28**:8–13.

Kim E, Cho K-O, Rothschild A, Sheng M. Heteromultimerization and NMDA Receptor-Clustering Activity of Chapsyn-110, a Member of the PSD-95 Family of Proteins. *Neuron* 1996;**17**:103–13.

Kinghorn KJ, Castillo-Quan JI, Bartolome F, Angelova PR, Li L, Pope S, Cochemé HM, Khan S, Asghari S, Bhatia KP, Hardy J, Abramov AY, Partridge L. Loss of PLA2G6 leads to elevated mitochondrial lipid peroxidation and mitochondrial dysfunction. *Brain* 2015;**138**:1801–16.

Kirik D, Rosenblad C, Burger C, Lundberg C, Johansen TE, Muzyczka N, Mandel RJ, Björklund A. Parkinson-Like Neurodegeneration Induced by Targeted Overexpression of α-Synuclein in the Nigrostriatal System. *Journal of Neuroscience* 2002;**22**:2780–91.

Kirisako T, Ichimura Y, Okada H, Kabeya Y, Mizushima N, Yoshimori T, Ohsumi M, Takao T, Noda T, Ohsumi Y. The reversible modification regulates the membrane-binding state of Apg8/Aut7 essential for autophagy and the cytoplasm to vacuole targeting pathway. *Journal of Cell Biology* 2000;**151**:263–76.

Kirk R. *Experimental Design: Procedures for the Behavioral Sciences*. Thousand Oaks, California, 2013.

Kitada T, Asakawa S, Hattori N, Matsumine H, Yamamura Y, Minoshima S, Yokochi M, Mizuno Y, Shimizu N. Mutations in the parkin gene cause autosomal recessive juvenile parkinsonism. *Nature* 1998;**392**:605–8.

Klein C, Westenberger A. Genetics of Parkinson's disease. *Cold Spring Harbor Perspectives in Medicine* 2012;**2**:a008888–8.

Klein RL, King MA, Hamby ME, Meyer EM. Dopaminergic cell loss induced by human A30P alpha-synuclein gene transfer to the rat substantia nigra. *Human Gene Therapy* 2002;**13**:605–12.

Klionsky DJ, Cuervo AM, Dunn WAJ, Levine B, van der Klei I, Seglen PO. How shall I eat thee? *Autophagy* 2007;**3**:413–6.

Koga H, Martinez-Vicente M, Macian F, Verkhusha VV, Cuervo AM. A photoconvertible fluorescent reporter to track chaperone-mediated autophagy. *Nature Communications* 2011;**2**:386.

Komatsu M, Waguri S, Chiba T, Murata S, Iwata J-I, Tanida I, Ueno T, Koike M, Uchiyama Y, Kominami E, Tanaka K. Loss of autophagy in the central nervous system causes neurodegeneration in mice. *Nature* 2006;**441**:880–4.

Komatsu M, Waguri S, Ueno T, Iwata J, Murata S, Tanida I, Ezaki J, Mizushima N, Ohsumi Y, Uchiyama Y, Kominami E, Tanaka K, Chiba T. Impairment of starvation-induced and constitutive autophagy in Atg7-deficient mice. *Journal of Cell Biology* 2005;**169**:425–34.

Korczyn AD, Brunt ER, Larsen JP, Nagy Z, Poewe WH, Ruggieri S. A 3-year randomized trial of ropinirole and bromocriptine in early Parkinson's disease. The 053 Study Group. *Neurology* 1999;**53**:364–70.

Kordower JH, Chu Y, Hauser RA, Freeman TB, Olanow CW. Lewy body-like pathology in long-term embryonic nigral transplants in Parkinson's disease. *Nature Medicine* 2008a;**14**:504–6.

Kordower JH, Chu Y, Hauser RA, Olanow CW, Freeman TB. Transplanted dopaminergic neurons develop PD pathologic changes: A second case report. *Movement Disorders* 2008b;**23**:2303–6.

Kordower JH, Emborg ME, Bloch J, Ma SY, Chu Y, Leventhal L, McBride J, Chen EY, Palfi S, Roitberg BZ, Brown WD, Holden JE, Pyzalski R, Taylor MD, Carvey P, Ling Z, Trono D, Hantraye P, Déglon N *et al.* Neurodegeneration prevented by lentiviral vector delivery of GDNF in primate models of Parkinson's disease. *Science* 2000;**290**:767–73.

Kordower JH, Freeman TB, Snow BJ, Vingerhoets FJG, Mufson EJ, Sanberg PR, Hauser RA, Smith DA, Nauert GM, Perl DP, Olanow CW. Neuropathological Evidence of Graft Survival and Striatal Reinnervation after the Transplantation of Fetal Mesencephalic Tissue in a Patient with Parkinson's Disease. *New England Journal of Medicine* 1995;**332**:1118–24.

Kowall NW, Hantraye P, Brouillet E, Beal MF, McKee AC, Ferrante RJ. MPTP induces alpha-synuclein aggregation in the substantia nigra of baboons. *NeuroReport* 2000;**11**:211.

Koyano F, Okatsu K, Kosako H, Tamura Y, Go E, Kimura M, Kimura Y, Tsuchiya H, Yoshihara H, Hirokawa T, Endo T, Fon EA, Trempe J-F, Saeki Y, Tanaka K, Matsuda N. Ubiquitin is phosphorylated by PINK1 to activate parkin. *Nature* 2014;**510**:162–6.

Krüger R, Kuhn W, Müller T, Woitalla D, Graeber M, Kosel S, Przuntek H, Epplen JT, Schols L, Riess O. Ala30Pro mutation in the gene encoding alpha-synuclein in Parkinson's disease. *Nature Genetics* 1998;**18**:106–8.

Kuma A, Hatano M, Matsui M, Yamamoto A, Nakaya H, Yoshimori T, Ohsumi Y, Tokuhisa T, Mizushima N. The role of autophagy during the early neonatal starvation period. *Nature* 2004;**432**:1032–6.

Kuo Y-M, Li Z, Jiao Y, Gaborit N, Pani AK, Orrison BM, Bruneau BG, Giasson BI, Smeyne RJ, Gershon MD, Nussbaum RL. Extensive enteric nervous system abnormalities in mice transgenic for artificial chromosomes containing Parkinson disease-associated α-synuclein gene mutations precede central nervous system changes. *Human Molecular Genetics* 2010;**19**:1633–50.

Kuzuhara S, Mori H, Izumiyama N, Yoshimura M, Ihara Y. Lewy bodies are ubiquitinated. A light and electron microscopic immunocytochemical study. *Acta Neuropathologica* 1988;**75**:345–53.

Kühn R, Schwenk F, Aguet M, Rajewsky K. Inducible gene targeting in mice. *Science* 1995;**269**:1427–9.

Lammel S, Steinberg EE, Földy C, Wall NR, Beier K, Luo L, Malenka RC. Diversity of transgenic mouse models for selective targeting of midbrain dopamine neurons. *Neuron* 2015;**85**:429–38.

Langston JW, Forno LS, Rebert CS, Irwin I. Selective nigral toxicity after systemic administration of 1-methyl-4-phenyl-1,2,5,6-tetrahydropyrine (MPTP) in the squirrel monkey. *Brain Research* 1984;**292**:390–4.

Langston JW, Forno LS, Tetrud J, Reeves AG, Kaplan JA, Karluk D. Evidence of active nerve cell degeneration in the substantia nigra of humans years after 1-methyl-4-phenyl-1,2,3,6-tetrahydropyridine exposure. *Annals of Neurology* 1999;**46**:598–605.

Lashuel HA, Petre BM, Wall J, Simon M, Nowak RJ, Walz T, Lansbury PTJ. Alpha-synuclein, especially the Parkinson's disease-associated mutants, forms pore-like annular and tubular protofibrils. *Journal of Molecular Biology* 2002;**322**:1089–102.

Lategan AJ, Marien MR, Colpaert FC. Effects of locus coeruleus lesions on the release of endogenous dopamine in the rat nucleus accumbens and caudate nucleus as determined by intracerebral microdialysis. *Brain Research* 1990;**523**:134–8.

Lee H-J, Cho E-D, Lee KW, Kim J-H, Cho S-G, Lee S-J. Autophagic failure promotes the exocytosis and intercellular transfer of α-synuclein. *Experimental & Molecular Medicine* 2013;**45**:e22.

Lee MK, Stirling W, Xu Y, Xu X, Qui D, Mandir AS, Dawson TM, Copeland NG, Jenkins NA, Price DL. Human alpha-synuclein-harboring familial Parkinson's disease-linked Ala-53 --> Thr mutation causes neurodegenerative disease with alpha-synuclein aggregation in transgenic mice. *Proceedings of the National Academy of Sciences* 2002;**99**:8968–73.

Lee P-C, Bordelon Y, Bronstein J, Ritz B. Traumatic brain injury, paraquat exposure, and their relationship to Parkinson disease. *Neurology* 2012;**79**:2061–6.

Lees AJ, Hardy J, Revesz T. Parkinson's disease. *The Lancet* 2009;**373**:2055–66.

Lesage S, Anheim M, Letournel F, Bousset L, Honoré A, Rozas N, Pieri L, Madiona K, Dürr A, Melki R, Verny C, Brice A. G51D α-synuclein mutation causes a novel Parkinsonian–pyramidal syndrome. *Annals of Neurology* 2013;**73**:459–71.

Lesage S, Condroyer C, Klebe S, Honoré A, Tison F, Brefel-Courbon C, Dürr A, Brice A, French Parkinson's Disease Genetics Study Group. Identification of VPS35 mutations replicated in French families with Parkinson disease. *Neurology* 2012;**78**:1449–50.

Lesage S, Ibanez P, Lohmann E, Pollak P, Tison F, Tazir M, Leutenegger AL, Guimaraes J, Bonnet AM, Agid Y, Dürr A, Brice A. G2019S LRRK2 mutation in French and North African families with Parkinson's disease. *Annals of Neurology* 2005;**58**:784–7.

Lewy FH. Paralysis agitans. I. Pathologische Anatomie. *Handbuch der Neurologie* 1912;**3**:920–58.

Li J-Y, Englund E, Holton JL, Soulet D, Hagell P, Lees AJ, Lashley T, Quinn NP, Rehncrona S, Björklund A, Widner H, Revesz T, Lindvall O, Brundin P. Lewy bodies in grafted neurons in subjects with Parkinson's disease suggest host-to-graft disease propagation. *Nature Medicine* 2008;**14**:501–3.

Li S, Cullen WK, Anwyl R, Rowan MJ. Dopamine-dependent facilitation of LTP induction in hippocampal CA1 by exposure to spatial novelty. *Nature Neuroscience* 2003;**6**:526–31.

Li X, Patel JC, Wang J, Avshalumov MV, Nicholson C, Buxbaum JD, Elder GA, Rice ME, Yue Z. Enhanced striatal dopamine transmission and motor performance with LRRK2 overexpression in mice is eliminated by familial Parkinson's disease mutation G2019S. *Journal of Neuroscience* 2010;**30**:1788–97.

Li ZS, Pham TD, Tamir H, Chen JJ, Gershon MD. Enteric dopaminergic neurons: definition, developmental lineage, and effects of extrinsic denervation. *Journal of Neuroscience* 2004;**24**:1330–9.

Lindeberg J, Usoskin D, Bengtsson H, Gustafsson A, Kylberg A, Söderström S, Ebendal T. Transgenic expression of Cre recombinase from the tyrosine hydroxylase locus. *Genesis* 2004;**40**:67–73.

Lindersson E, Beedholm R, Højrup P, Moos T, Gai W, Hendil KB, Jensen PH. Proteasomal inhibition by alpha-synuclein filaments and oligomers. *Journal of Biological Chemistry* 2004;**279**:12924–34.

Lipinski MM, Hoffman G, Ng A, Zhou W, Py BF, Hsu E, Liu X, Eisenberg J, Liu J, Blenis J, Xavier RJ, Yuan J. A genome-wide siRNA screen reveals multiple mTORC1 independent signaling pathways regulating autophagy under normal nutritional conditions. *Developmental Cell* 2010;**18**:1041–52.

Liscovitch N, French L. Differential co-expression between α-synuclein and IFN-γ signaling genes across development and in parkinson's Disease. *PLoS ONE* 2014;**9**:e115029.

Lister RG. The use of a plus-maze to measure anxiety in the mouse. *Psychopharmacology* 1987;**92**:180–5.

Liu J, Wang Y, Song L, Zeng L, Yi W, Liu T, Chen H, Wang M, Ju Z, Cong Y-S. A critical role of DDRGK1 in endoplasmic reticulum homoeostasis via regulation of IRE1α stability. *Nature Communications* 2017;**8**:ncomms14186.

Liu R, Guo X, Park Y, Huang X, Sinha R, Freedman ND, Hollenbeck AR, Blair A, Chen H. Caffeine intake, smoking, and risk of Parkinson disease in men and women. *American Journal of Epidemiology* 2012;**175**:1200–7.

Llopis SP, de Celis SVR, Schwartz JC, Wolff NC, Tran TAT, Zou L, Xie XJ, Corey DR, Brugarolas J. Regulation of TFEB and V-ATPases by mTORC1. *The EMBO Journal* 2011;**30**:3242–58.

Loder MK, Melikian HE. The dopamine transporter constitutively internalizes and recycles in a protein kinase C-regulated manner in stably transfected PC12 cell lines. *Journal of Biological Chemistry* 2003;**278**:22168–74.

Lucking CB, Dürr A, Bonifati V, Vaughan J, De Michele G, Gasser T, Harhangi BS, Meco G, Denefle P, Wood NW, Agid Y, Brice A. Association between early-onset Parkinson's disease and mutations in the parkin gene. *New England Journal of Medicine* 2000;**342**:1560–7.

Luk KC, Kehm V, Carroll J, Bin Zhang, O'Brien P, Trojanowski JQ, Lee VMY. Pathological α-synuclein transmission initiates parkinson-like neurodegeneration in nontransgenic mice. *Science* 2012a;**338**:949–53.

Luk KC, Kehm VM, Bin Zhang, O'Brien P, Trojanowski JQ, Lee VMY. Intracerebral inoculation of pathological α-synuclein initiates a rapidly progressive neurodegenerative α-synucleinopathy in mice. *Journal of Experimental Medicine* 2012b;**209**:jem.20112457–986.

MacLeod DA, Rhinn H, Kuwahara T, Zolin A, Di Paolo G, McCabe BD, Marder KS, Honig LS, Clark LN, Small SA, Abeliovich A. RAB7L1 interacts with LRRK2 to modify intraneuronal protein sorting and Parkinson's disease risk. *Neuron* 2013;**77**:425–39.

Manzoni C, Mamais A, Dihanich S, Abeti R, Soutar MPM, Plun-Favreau H, Giunti P, Tooze SA, Bandopadhyay R, Lewis PA. Inhibition of LRRK2 kinase activity stimulates macroautophagy. *Biochimica et Biophysica Acta (BBA) - Molecular Cell Research* 2013;**1833**:2900–10.

Marques ARA, Gabriel TL, Aten J, van Roomen CPAA, Ottenhoff R, Claessen N, Alfonso P, Irún P, Giraldo P, Aerts JMFG, van Eijk M. Gpnmb Is a potential marker for the visceral pathology in Niemann-Pick type C disease. *PLoS ONE* 2016;**11**:e0147208.

Martinez-Vicente M, Talloczy Z, Kaushik S, Massey AC, Mazzulli J, Mosharov EV, Hodara R, Fredenburg R, Wu D-C, Follenzi A, Dauer W, Przedborski S, Ischiropoulos H, Lansbury PT, Sulzer D, Cuervo AM. Dopamine-modified α-synuclein blocks chaperone-mediated autophagy. *The Journal of Clinical Investigation* 2008;**118**:777–88.

Masliah E, Rockenstein E, Veinbergs I, Mallory M, Hashimoto M, Takeda A, Sagara Y, Sisk A, Mucke L. Dopaminergic loss and inclusion body formation in α-synuclein mice: implications for neurodegenerative disorders. *Science* 2000;**287**:1265–9.

Matsuda N, Sato S, Shiba K, Okatsu K, Saisho K, Gautier CA, Sou Y-S, Saiki S, Kawajiri S, Sato F, Kimura M, Komatsu M, Hattori N, Tanaka K. PINK1 stabilized by mitochondrial depolarization recruits Parkin to damaged mitochondria and activates latent Parkin for mitophagy. *Journal of Cell Biology* 2010;**189**:211–21.

Matsuda S, Miura E, Matsuda K, Kakegawa W, Kohda K, Watanabe M, Yuzaki M. Accumulation of AMPA receptors in autophagosomes in neuronal axons lacking adaptor protein AP-4. *Neuron* 2008;**57**:730–45.

Matsui H, Gavinio R, Takahashi R. Medaka Fish Parkinson's Disease Model. *Experimental Neurobiology* 2012;**21**:94–100.

Matsuoka Y, Vila M, Lincoln S, McCormack A, Picciano M, LaFrancois J, Yu X, Dickson D, Langston WJ, McGowan E, Farrer M, Hardy J, Duff K, Przedborski S, Di Monte DA. Lack of nigral pathology in transgenic mice expressing human alpha-synuclein driven by the tyrosine hydroxylase promoter. *Neurobiology of Disease* 2001;**8**:535–9.

Mattay VS, Tessitore A, Callicott JH, Bertolino A, Goldberg TE, Chase TN, Hyde TM, Weinberger DR. Dopaminergic modulation of cortical function in patients with Parkinson's disease. *Annals of Neurology* 2002;**51**:156–64.

Mazzulli JR, Xu Y-H, Sun Y, Knight AL, McLean PJ, Caldwell GA, Sidransky E, Grabowski GA, Krainc D. Gaucher disease glucocerebrosidase and a-synuclein form a bidirectional pathogenic loop in synucleinopathies. *Cell* 2011;**146**:37–52.

McAlpine F, Williamson LE, Tooze SA, Chan EYW. Regulation of nutrient-sensitive autophagy by uncoordinated 51-like kinases 1 and 2. *Autophagy* 2013, DOI: 10.4161/auto.23066.

McDonald JH. *Handbook of Biological Statistics*. Sparky House Publishing Baltimore, MD, 2009.

McNaught KSP, Jenner P. Proteasomal function is impaired in substantia nigra in Parkinson's disease. *Neuroscience Letters* 2001;**297**:191–4.

McNaught KSP, Shashidharan P, Perl DP, Jenner P, Olanow CW. Aggresome-related biogenesis of Lewy bodies. *European Journal of Neuroscience* 2002;**16**:2136–48.

Melikian HE, Buckley KM. Membrane Trafficking Regulates the Activity of the Human Dopamine Transporter. *Journal of Neuroscience* 1999;**19**:7699–710.

Metzger S, Walter C, Riess O, Roos RAC, Nielsen JE, Craufurd D, Nguyen HP, Hu RIE. The V471A Polymorphism in Autophagy-Related Gene ATG7 Modifies Age at Onset Specifically in Italian Huntington Disease Patients. *PLoS ONE* 2013;**8**:e68951.

Migdalska Richards A, Schapira AHV. The relationship between glucocerebrosidase mutations and Parkinson disease. *Journal of Neurochemistry* 2016;**139**:77–90.

Miki Y, Tanji K, Mori F, Utsumi J, Sasaki H, Kakita A, Takahashi H, Wakabayashi K. Alteration of Upstream Autophagy-Related Proteins (ULK1, ULK2, Beclin1, VPS34 and AMBRA1) in Lewy Body Disease. *Brain Pathology* 2016;**26**:359–70.

Millership S, Ninkina N, Guschina IA, Norton J, Brambilla R, Oort PJ, Adams SH, Dennis RJ, Voshol PJ, Rochford JJ, Buchman VL. Increased lipolysis and altered lipid homeostasis protect γ-synuclein–null mutant mice from diet-induced obesity. *Proceedings of the National Academy of Sciences* 2012;**109**:20943–8.

Miocinovic S, Somayajula S, Chitnis S, Vitek JL. History, applications, and mechanisms of deep brain stimulation. *JAMA Neurology* 2013;**70**:163–71.

Miranda M, Dionne KR, Sorkina T, Sorkin A. Three ubiquitin conjugation sites in the amino terminus of the dopamine transporter mediate protein kinase C-dependent endocytosis of the transporter. *Molecular Biology of the Cell* 2007;**18**:313–23.

Mittal S, Bjørnevik K, Im DS, Flierl A, Dong X, Locascio JJ, Abo KM, Long E, Jin M, Xu B, Xiang YK, Rochet J-C, Engeland A, Rizzu P, Heutink P, Bartels T, Selkoe DJ, Caldarone BJ, Glicksman MA *et al.* β2-Adrenoreceptor is a regulator of the α-synuclein gene driving risk of Parkinson's disease. *Science* 2017;**357**:891–8.

Mizushima N, Noda T, Ohsumi Y. Apg16p is required for the function of the Apg12p–Apg5p conjugate in the yeast autophagy pathway. *The EMBO Journal* 1999;**18**:3888–96.

Mizushima N, Noda T, Yoshimori T, Tanaka Y, Ishii T, George MD, Klionsky DJ, Ohsumi M, Ohsumi Y. A protein conjugation system essential for autophagy. *Nature* 1998;**395**:395–8.

Montgomery EB, Baker KB, Lyons K, Koller WC. Abnormal performance on the PD test battery by asymptomatic first-degree relatives. *Neurology* 1999;**52**:757–62.

Moore DJ, Zhang L, Troncoso J, Lee MK, Hattori N, Mizuno Y, Dawson TM, Dawson VL. Association of DJ-1 and parkin mediated by pathogenic DJ-1 mutations and oxidative stress. *Human Molecular Genetics* 2005;**14**:71–84.

Moreau K, Ravikumar B, Renna M, Puri C, Rubinsztein DC. Autophagosome Precursor Maturation Requires Homotypic Fusion. *Cell* 2011;**146**:303–17.

Mori F, Tanji K, Yoshimoto M, Takahashi H, Wakabayashi K. Immunohistochemical comparison of α- and β-synuclein in adult rat central nervous system. *Brain Research* 2002;**941**:118–26.

Mori H, Kondo T, Yokochi M, Matsumine H, Nakagawa-Hattori Y, Miyake T, Suda K, Mizuno Y. Pathologic and biochemical studies of juvenile parkinsonism linked to chromosome 6q. *Neurology* 1998;**51**:890–2.

Morscher RJ, Grünert SC, Bürer C, Burda P, Suormala T, Fowler B, Baumgartner MR. A single mutation in MCCC1 or MCCC2 as a potential cause of positive screening for 3-methylcrotonyl-CoA carboxylase deficiency. *Molecular Genetics and Metabolism* 2012;**105**:602–6.

Mougenot A-L, Nicot S, Bencsik A, Morignat E, Verchère J, Lakhdar L, Legastelois S, Baron T. Prion-like acceleration of a synucleinopathy in a transgenic mouse model. *Neurobiology of Aging* 2012;**33**:2225–8.

Muhammad A, Flores I, Zhang H, Yu R, Staniszewski A, Planel E, Herman M, Ho L, Kreber R, Honig LS, Ganetzky B, Duff K, Arancio O, Small SA. Retromer deficiency observed in Alzheimer's disease causes hippocampal dysfunction, neurodegeneration, and Abeta accumulation. *Proceedings of the National Academy of Sciences* 2008;**105**:7327–32.

Munhoz RP, Werneck LC, Teive HAG. The differential diagnoses of parkinsonism: findings from a cohort of 1528 patients and a 10 years comparison in tertiary movement disorders clinics. *Clinical neurology and neurosurgery* 2010;**112**:431–5.

Murphy KE, Gysbers AM, Abbott SK, Tayebi N, Kim WS, Sidransky E, Cooper A, Garner B, Halliday GM. Reduced glucocerebrosidase is associated with increased α-synuclein in sporadic Parkinson's disease. *Brain* 2014;**137**:834–48.

Nagelkerke A, Sieuwerts AM, Bussink J, Sweep FCGJ, Look MP, Foekens JA, Martens JWM, Span PN. LAMP3 is involved in tamoxifen resistance in breast cancer cells through the modulation of autophagy. *Endocrine-Related Cancer* 2014;**21**:101–12.

Nair U, Jotwani A, Geng J, Gammoh N, Richerson D, Yen W-L, Griffith J, Nag S, Wang K, Moss T, Baba M, McNew JA, Jiang X, Reggiori F, Melia TJ, Klionsky DJ. SNARE proteins are required for macroautophagy. *Cell* 2011;**146**:290–302.

Nakatsu F, Messa M, Nández R, Czapla H, Zou Y, Strittmatter SM, Pietro De Camilli. Sac2/INPP5F is an inositol 4-phosphatase that functions in the endocytic pathway. *Journal of Cell Biology* 2015;**209**:85–95.

Nalls MA, Pankratz N, Lill CM, Do CB, Hernandez DG, Saad M, DeStefano AL, Kara E, Bras J, Sharma M, Schulte C, Keller MF, Arepalli S, Letson C, Edsall C, Stefansson H, Liu X, Pliner H, Lee JH *et al.* Large-scale meta-analysis of genome-wide association data identifies six new risk loci for Parkinson's disease. *Nature Genetics* 2014;**46**:989–93.

Narendra DP, Jin SM, Tanaka A, Suen D-F, Gautier CA, Shen J, Cookson MR, Youle RJ. PINK1 is selectively stabilized on impaired mitochondria to activate Parkin. *PLOS Biology* 2010;**8**:e1000298.

Nemani VM, Lu W, Berge V, Nakamura K, Onoa B, Lee MK, Chaudhry FA, Nicoll RA, Edwards RH. Increased expression of alpha-synuclein reduces neurotransmitter release by inhibiting synaptic vesicle reclustering after endocytosis. *Neuron* 2010;**65**:66–79.

Nieto M, Gil-Bea FJ, Dalfó E, Cuadrado M, Cabodevilla F, Sánchez B, Catena S, Sesma T, Ribé E, Ferrer I, Ramírez MJ, Gómez-Isla T. Increased sensitivity to MPTP in human α-synuclein A30P transgenic mice. *Neurobiology of Aging* 2006;**27**:848–56.

Ninkina N, Peters O, Millership S, Salem H, van der Putten H, Buchman VL. Gamma-synucleinopathy: neurodegeneration associated with overexpression of the mouse protein. *Human Molecular Genetics* 2009;**18**:1779–94.

Ninkina N, Peters OM, Connor-Robson N, Lytkina O, Sharfeddin E, Buchman VL. Contrasting Effects of α-Synuclein and γ-Synuclein on the Phenotype of Cysteine String Protein α (CSPα) Null Mutant Mice Suggest Distinct Function of these Proteins in Neuronal Synapses. *Journal of Biological Chemistry* 2012;**287**:44471–7.

Ninkina NN, Alimova-Kost MV, Paterson JW, Delaney L, Cohen BB, Imreh S, Gnuchev NV, Davies AM, Buchman VL. Organization, expression and polymorphism of the human persyn gene. *Human Molecular Genetics* 1998;**7**:1417–24.

Nishida Y, Arakawa S, Fujitani K, Yamaguchi H, Mizuta T, Kanaseki T, Komatsu M, Otsu K, Tsujimoto Y, Shimizu S. Discovery of Atg5/Atg7-independent alternative macroautophagy. *Nature* 2009;**461**:654–8.

Niu X-Y, Huang H-J, Zhang J-B, Zhang C, Chen W-G, Sun C-Y, Ding Y-Q, Liao M. Deletion of autophagy-related gene 7 in dopaminergic neurons prevents their loss induced by MPTP. *Neuroscience* 2016;**339 IS -**:22–31.

Novarino G, El-Fishawy P, Kayserili H, Meguid NA, Scott EM, Schroth J, Silhavy JL, Kara M, Khalil RO, Ben-Omran T, Ercan-Sencicek AG, Hashish AF, Sanders SJ, Gupta AR, Hashem HS, Matern D, Gabriel S, Sweetman L, Rahimi Y *et al.* Mutations in *BCKD*-kinase lead to a potentially treatable form of autism with epilepsy. *Science* 2012;**338**:394–7.

Olerup O, Smith CI, Björkander J, Hammarström L. Shared HLA class II-associated genetic susceptibility and resistance, related to the HLA-DQB1 gene, in IgA deficiency and common variable immunodeficiency. *Proceedings of the National Academy of Sciences* 1992;**89**:10653–7.

Oliveras-Salvá M, Van der Perren A, Casadei N, Stroobants S, Nuber S, D'Hooge R, Van den Haute C, Baekelandt V. rAAV2/7 vector-mediated overexpression of alpha-synuclein in mouse substantia nigra induces protein aggregation and progressive dose-dependent neurodegeneration. *Molecular Neurodegeneration* 2013;**8**:44.

Olzmann JA, Li L, Chudaev MV, Chen J, Perez FA, Palmiter RD, Chin L-S. Parkin-mediated K63-linked polyubiquitination targets misfolded DJ-1 to aggresomes via binding to HDAC6. *Journal of Cell Biology* 2007;**178**:1025–38.

Ozelius LJ, Senthil G, Saunders-Pullman R, Ohmann E, Deligtisch A, Tagliati M, Hunt AL, Klein C, Henick B, Hailpern SM, Lipton RB, Soto-Valencia J, Risch N, Bressman SB. LRRK2 G2019S as a cause of Parkinson's disease in Ashkenazi Jews. *New England Journal of Medicine* 2009;**354**:424–5.

Pagan F, Hebron M, Valadez EH, Torres-Yaghi Y, Huang X, Mills RR, Wilmarth BM, Howard H, Dunn C, Carlson A, Lawler A, Rogers SL, Falconer RA, Ahn J, Li Z, Moussa C. Nilotinib effects in Parkinson's disease and Dementia with Lewy bodies. *Journal of Parkinson's Disease* 2016;**6**:503–17.

Paisan-Ruiz C, Jain S, Evans EW, Gilks WP, Simon J, van der Brug M, Lopez de Munain A, Aparicio S, Gil AM, Khan N, Johnson J, Martinez JR, Nicholl D, Carrera IM, Pena AS, de Silva R, Lees A, Marti-Masso JF, Perez-Tur J *et al.* Cloning of the gene containing mutations that cause PARK8-linked Parkinson's disease. *Neuron* 2004;**44**:595–600.

Pakkenberg H, Brody H. The number of nerve cells in the substantia nigra in paralysis agitans. *Acta Neuropathologica* 1965;**5**:320–4.

Pan P-Y, Ryan TA. Calbindin controls release probability in ventral tegmental area dopamine neurons. *Nature Neuroscience* 2012;**15**:813–5.

Panaretou C, Doming J, Cockcroft S, Waterfield MD. Characterization of p150, an adaptor protein for the human phosphatidylinositol (PtdIns) 3-kinase. Substrate presentation by phosphatidylinositol transfer protein to the p150·PtdIns 3-kinase complex. *Journal of Biological Chemistry* 1997;**272**:2477–85.

Pankiv S, Clausen TH, Lamark T, Brech A, Bruun J-A, Outzen H, Øvervatn A, Bjørkøy G, Johansen T. p62/SQSTM1 binds directly to Atg8/LC3 to facilitate degradation of ubiquitinated protein aggregates by autophagy. *Journal of Biological Chemistry* 2007;**282**:24131–45.

Parihar MS, Parihar A, Fujita M, Hashimoto M, Ghafourifar P. Mitochondrial association of alpha-synuclein causes oxidative stress. *Cellular and Molecular Life Sciences* 2008;**65**:1272–84.

Park J, Lee SB, Lee S, Kim Y, Song S, Kim S, Bae E, Kim J, Shong M, Kim J-M, Chung J. Mitochondrial dysfunction in Drosophila PINK1 mutants is complemented by parkin. *Nature* 2006;**441**:1157–61.

Parkinson J. *An Essay on the Shaking Palsy*. London: Sherwood Neely and Jones, 1817.

Parkinson Study Group. Phase II safety, tolerability, and dose selection study of isradipine as a potential disease-modifying intervention in early Parkinson's disease (STEADY-PD). *Movement Disorders* 2013;**28**:1823–31.

Parkkinen L, O'Sullivan SS, Collins C, Petrie A, Holton JL, Revesz T, Lees AJ. Disentangling the Relationship between Lewy Bodies and Nigral Neuronal Loss in Parkinson's Disease. *Journal of Parkinson's Disease* 2011;**1**:277–86.

Pascual A, Hidalgo-Figueroa M, Piruat JI, Pintado CO, Gómez-Díaz R, López-Barneo J. Absolute requirement of GDNF for adult catecholaminergic neuron survival. *Nature Neuroscience* 2008;**11**:755–61.

Patel JC, Rossignol E, Rice ME, Machold RP. Opposing regulation of dopaminergic activity and exploratory motor behavior by forebrain and brainstem cholinergic circuits. *Nature Communications* 2012;**3**:1172.

Paxinos G, Franklin KBJ. *The Mouse Brain in Stereotaxic Coordinates*. Academic Press, 2008.

PD MED Collaborative Group. Long-term effectiveness of dopamine agonists and monoamine oxidase B inhibitors compared with levodopa as initial treatment for Parkinson's disease (PD MED): a large, open-label, pragmatic randomised trial. *The Lancet* 2014;**384**:1196–205.

Pearson ES. The Analysis of Variance in Cases of Non-Normal Variation. *Biometrika* 1931;**23**:114.

Pedro JMB-S, Niso-Santano M, Gómez-Sánchez R, Pizarro-Estrella E, Aiastui-Pujana A, Gorostidi A, Climent V, de Maturana RL, Sanchez-Pernaute R, de Munain AL, Fuentes JM, González-Polo RA. The LRRK2 G2019S mutant exacerbates basal autophagy through activation of the MEK/ERK pathway. *Cellular and Molecular Life Sciences* 2013;**70**:121–36.

Pellow S, File SE. Anxiolytic and anxiogenic drug effects on exploratory activity in an elevated plus-maze: A novel test of anxiety in the rat. *Pharmacology Biochemistry and Behavior* 1986;**24**:525–9.

Periquet M, Fulga T, Myllykangas L, Schlossmacher MG, Feany MB. Aggregated α-synuclein mediates dopaminergic neurotoxicity *in vivo*. *Journal of Neuroscience* 2007;**27**:3338–46.

Peters OM, Shelkovnikova T, Highley JR, Cooper Knock J, Hortobágyi T, Troakes C, Ninkina N, Buchman VL. Gamma-synuclein pathology in amyotrophic lateral sclerosis. *Annals of Clinical and Translational Neurology* 2015;**2**:29–37.

Pezzoli G, Cereda E. Exposure to pesticides or solvents and risk of Parkinson disease. *Neurology* 2013;**80**:2035–41.

Pijnenburg AJJ, van Rossum JM. Stimulation of locomotor activity following injection of dopamine into the nucleus accumbens. *Journal of Pharmacy and Pharmacology* 1973;**25**:1003–5.

Politis M, Wu K, Loane C, Turkheimer FE, Molloy S, Brooks DJ, Piccini P. Depressive symptoms in PD correlate with higher 5-HTT binding in raphe and limbic structures. *Neurology* 2010;**75**:1920–7.

Polymeropoulos MH, Lavedan C, Leroy E, Ide SE, Dehejia A, Dutra A, Pike B, Root H, Rubenstein J, Boyer R, Stenroos ES, Chandrasekharappa S, Athanassiadou A, Papapetropoulos T, Johnson WG, Lazzarini AM, Duvoisin RC, Di Iorio G, Golbe LI *et al.* Mutation in the α-synuclein gene identified in families with Parkinson's disease. *Science* 1997;**276**:2045–7.

Ponsen MM, Stoffers D, Booij J, van Eck-Smit BLF, Wolters EC, Berendse HW. Idiopathic hyposmia as a preclinical sign of Parkinson's disease. *Annals of Neurology* 2004;**56**:173–81.

Poole AC, Thomas RE, Andrews LA, McBride HM, Whitworth AJ, Pallanck LJ. The PINK1/Parkin pathway regulates mitochondrial morphology. *Proceedings of the National Academy of Sciences* 2008;**105**:1638–43.

Postuma RB, Lang AE, Munhoz RP, Charland K, Pelletier A, Moscovich M, Filla L, Zanatta D, Romenets SR, Altman R, Chuang R, Shah B. Caffeine for treatment of Parkinson disease: a randomized controlled trial. *Neurology* 2012;**79**:651–8.

Pramstaller PP, Schlossmacher MG, Jacques TS, Scaravilli F, Eskelson C, Pepivani I, Hedrich K, Adel S, Gonzales McNeal M, Hilker R, Kramer PL, Klein C. Lewy body Parkinson's disease in a large pedigree with 77 Parkin mutation carriers. *Annals of Neurology* 2005;**58**:411–22.

Priault M, Salin B, Schaeffer J, Vallette FM, di Rago J-P, Martinou J-C. Impairing the bioenergetic status and the biogenesis of mitochondria triggers mitophagy in yeast. *Cell death and differentiation* 2005;**12**:1613–21.

Pringsheim T, Jette N, Frolkis A, Steeves TDL. The prevalence of Parkinson's disease: A systematic review and meta-analysis. *Movement Disorders* 2014;**29**:1583–90.

Proukakis C, Dudzik CG, Brier T, MacKay DS, Cooper JM, Millhauser GL, Houlden H, Schapira AH. A novel α-synuclein missense mutation in Parkinson disease. *Neurology* 2013;**80**:1062–4.

Przedbroski S, Leviver M, Jiang H, Ferreira M, Jackson-Lewis V, Donaldson D, Togasaki DM. Dose-dependent lesions of the dopaminergic nigrostriatal pathway induced by instrastriatal injection of 6-hydroxydopamine. *Neuroscience* 1995;**67**:631–47.

Ramirez A, Heimbach A, Gründemann J, Stiller B, Hampshire D, Cid LP, Goebel I, Mubaidin AF, Wriekat A-L, Roeper J, Al-Din A, Hillmer AM, Karsak M, Liss B, Woods CG, Behrens MI, Kubisch C. Hereditary parkinsonism with dementia is caused by mutations in ATP13A2, encoding a lysosomal type 5 P-type ATPase. *Nature Genetics* 2006;**38**:1184–91.

Ramonet D, Daher JPL, Lin BM, Stafa K, Kim J, Banerjee R, Westerlund M, Pletnikova O, Glauser L, Yang L, Liu Y, Swing DA, Beal MF, Troncoso JC, McCaffery JM, Jenkins NA, Copeland NG, Galter D, Thomas B *et al.* Dopaminergic neuronal loss, reduced neurite complexity and autophagic abnormalities in transgenic mice expressing G2019S mutant LRRK2. Cai H (ed.). *PLoS ONE* 2011;**6**:e18568.

Rascol O, Brooks DJ, Korczyn AD, De Deyn PP, Clarke CE, Lang AE. A five-year study of the incidence of dyskinesia in patients with Early Parkinson's disease who were treated with ropinirole or levodopa. *New England Journal of Medicine* 2000;**342**:1484–91.

Reddy JV, Seaman MN. Vps26p, a component of retromer, directs the interactions of Vps35p in endosome-to-Golgi retrieval. *Molecular Biology of the Cell* 2001;**12**:3242–56.

Reeve A, Simcox E, Turnbull D. Ageing and Parkinson's disease: why is advancing age the biggest risk factor? *Ageing research reviews* 2014;**14**:19–30.

Reggiori F, Ungermann C. Autophagosome maturation and fusion. *Journal of Molecular Biology* 2017;**429**:486–96.

Rice ME, Cragg SJ. Nicotine amplifies reward-related dopamine signals in striatum. *Nature Neuroscience* 2004;**7**:583–4.

Ripoll N, David DJP, Dailly E, Hascoët M, Bourin M. Antidepressant-like effects in various mice strains in the tail suspension test. *Behavioural Brain Research* 2003;**143**:193–200.

Ritz B, Ascherio A, Checkoway H, Marder KS, Nelson LM, Rocca WA, Ross GW, Strickland D, Van Den Eeden SK, Gorell J. Pooled analysis of tobacco use and risk of Parkinson disease. *Archives of Neurology* 2007;**64**:990–7.

Ritz B, Rhodes SL, Qian L, Schernhammer E, Olsen JH, Friis S. L-type calcium channel blockers and Parkinson disease in Denmark. *Annals of Neurology* 2010;**67**:600–6.

Roberts P, Moshitch-Moshkovitz S, Kvam E, O'Toole E, Winey M, Goldfarb DS. Piecemeal microautophagy of nucleus in Saccharomyces cerevisiae. *Molecular Biology of the Cell* 2003;**14**:129–41.

Roberts RF, Wade-Martins R, Alegre-Abarrategui J. Direct visualization of alpha-synuclein oligomers reveals previously undetected pathology in Parkinson's disease brain. *Brain* 2015;**138**:1642–57.

Robertson DC, Schmidt O, Ninkina N, Jones PA, Sharkey J, Buchman VL. Developmental loss and resistance to MPTP toxicity of dopaminergic neurones in substantia nigra pars compacta of gamma-synuclein, alpha-synuclein and double alpha/gamma-synuclein null mutant mice. *Journal of Neurochemistry* 2004;**89**:1126–36.

Rocca WA, Bower JH, Maraganore DM, Ahlskog JE, Grossardt BR, de Andrade M, Melton LJ. Increased risk of parkinsonism in women who underwent oophorectomy before menopause. *Neurology* 2008;**70**:200–9.

Rodríguez CI, Buchholz F, Galloway J, Sequerra R, Kasper J, Ayala R, Stewart AF, Dymecki SM. High-efficiency deleter mice show that FLPe is an alternative to Cre-loxP. *Nature Genetics* 2000;**25**:139–40.

Rowland AM, Richmond JE, Olsen JG, Hall DH, Bamber BA. Presynaptic terminals independently regulate synaptic clustering and autophagy of $GABA_A$ receptors in Caenorhabditis elegans. *Journal of Neuroscience* 2006;**26**:1711–20.

Rudow G, O'Brien R, Savonenko AV, Resnick SM, Zonderman AB, Pletnikova O, Marsh L, Dawson TM, Crain BJ, West MJ, Troncoso JC. Morphometry of the human substantia nigra in ageing and Parkinson's disease. *Acta Neuropathologica* 2008;**115**:461–70.

Saggu H, Cooksey J, Dexter D, Wells FR, Lees A, Jenner P, Marsden CD. A selective increase in particulate superoxide dismutase activity in Parkinsonian substantia nigra. *Journal of Neurochemistry* 1989;**53**:692–7.

Saha AR, Ninkina NN, Hanger DP, Anderton BH, Davies AM, Buchman VL. Induction of neuronal death by α-synuclein. *European Journal of Neuroscience* 2000;**12**:3073–7.

Sakai M, Araki N, Ogawa K. Lysosomal movements during heterophagy and autophagy: with special reference to nematolysosome and wrapping lysosome. *Microscopy Research and Technique* 1989;**12**:101–31.

Sanderson DJ, Bannerman DM. The role of habituation in hippocampus-dependent spatial working memory tasks: evidence from GluA1 AMPA receptor subunit knockout mice. Lubec G (ed.). *Hippocampus* 2012;**22**:981–94.

Sarkar S, Davies JE, Huang Z, Tunnacliffe A, Rubinsztein DC. Trehalose, a novel mTOR-independent autophagy enhancer, accelerates the clearance of mutant huntingtin and alpha-synuclein. *Journal of Biological Chemistry* 2007;**282**:5641–52.

Sasaki S, Shirata A, Yamane K, Iwata M. Parkin-positive autosomal recessive juvenile Parkinsonism with alpha-synuclein-positive inclusions. *Neurology* 2004;**63**:678–82.

Scatton B, Simon H, Le Moal M, Bischoff S. Origin of dopaminergic innervation of the rat hippocampal formation. *Neuroscience Letters* 1980;**18**:125–31.

Schank JR, Liles LC, Weinshenker D. Norepinephrine signaling through beta-adrenergic receptors is critical for expression of cocaine-induced anxiety. *Biological Psychiatry* 2008;**63**:1007–12.

Schapansky J, Nardozzi JD, Felizia F, LaVoie MJ. Membrane recruitment of endogenous LRRK2 precedes its potent regulation of autophagy. *Human Molecular Genetics* 2014;**23**:4201–14.

Schapira AHV, Cooper JM, Dexter D, Clark JB, Jenner P, Marsden CD. Mitochondrial complex I deficiency in Parkinson's disease. *Journal of Neurochemistry* 1990;**54**:823–7.

Schneppenheim J, Hüttl S, Mentrup T, Lüllmann-Rauch R, Rothaug M, Engelke M, Dittmann K, Dressel R, Araki M, Araki K, Wienands J, Fluhrer R, Saftig P, Schröder B. The intramembrane proteases signal Peptide peptidase-like 2a and 2b have distinct functions in vivo. *Molecular and Cellular Biology* 2014;**34**:1398–411.

Schott BH, Niehaus L, Wittmann BC, Schütze H. Ageing and early-stage Parkinson's disease affect separable neural mechanisms of mesolimbic reward processing. *Brain* 2007.

Schultheis PJ, Fleming SM, Clippinger AK, Lewis J, Tsunemi T, Giasson B, Dickson DW, Mazzulli JR, Bardgett ME, Haik KL, Ekhator O, Chava AK, Howard J, Gannon M, Hoffman E, Chen Y, Prasad V, Linn SC, Tamargo RJ *et al.* Atp13a2-deficient mice exhibit neuronal ceroid lipofuscinosis, limited α-synuclein accumulation and age-dependent sensorimotor deficits. *Human Molecular Genetics* 2013;**22**:2067–82.

Senior SL, Ninkina N, Deacon R, Bannerman D, Buchman VL, Cragg SJ, Wade-Martins R. Increased striatal dopamine release and hyperdopaminergic-like behaviour in mice lacking both alpha-synuclein and gamma-synuclein. *European Journal of Neuroscience* 2008;**27**:947–57.

Settembre C, Di Malta C, Polito VA, Arencibia MG, Vetrini F, Erdin S, Erdin SU, Huynh T, Medina D, Colella P, Sardiello M, Rubinsztein DC, Ballabio A. TFEB links autophagy to lysosomal biogenesis. *Science* 2011;**332**:1429–33.

Settembre C, Zoncu R, Medina DL, Vetrini F, Erdin S, Erdin S, Huynh T, Ferron M, Karsenty G, Vellard MC, Facchinetti V, Sabatini DM, Ballabio A. A lysosome-to-nucleus signalling mechanism senses and regulates the lysosome via mTOR and TFEB. *The EMBO Journal* 2012;**31**:1095–108.

Shapiro SS, Wilk MB. An Analysis of Variance Test for Normality (Complete Samples). *Biometrika* 1965;**52**:591.

Sherer TB, Kim J-H, Betarbet R, Greenamyre JT. Subcutaneous rotenone exposure causes highly selective dopaminergic degeneration and α-synuclein aggregation. *Experimental Neurology* 2003;**179**:9–16.

Shimura H, Hattori N, Kubo S, Yoshikawa M, Kitada T, Matsumine H, Asakawa S, Minoshima S, Yamamura Y, Shimizu N, Mizuno Y. Immunohistochemical and subcellular localization of Parkin protein: absence of protein in autosomal recessive juvenile parkinsonism patients. *Annals of Neurology* 1999;**45**:668–72.

Shimura H, Schlossmacher MG, Hattori N, Frosch MP, Trockenbacher A, Schneider R, Mizuno Y, Kosik KS, Selkoe DJ. Ubiquitination of a new form of α-synuclein by parkin from human brain: implications for Parkinson's disease. *Science* 2001;**293**:263–9.

Shojaee S, Sina F, Banihosseini SS, Kazemi MH, Kalhor R, Shahidi G-A, Fakhrai-Rad H, Ronaghi M, Elahi E. Genome-wide linkage analysis of a Parkinsonian-pyramidal syndrome pedigree by 500 K SNP arrays. *The American Journal of Human Genetics* 2008;**82**:1375–84.

Sidransky E, Nalls MA, Aasly JO, Aharon-Peretz J, Annesi G, Barbosa ER, Bar-Shira A, Berg D, Bras J, Brice A, Chen CM, Clark LN, Condroyer C, De Marco EV, Dürr A, Eblan MJ, Fahn S, Farrer MJ, Fung HC *et al.* Multicenter analysis of glucocerebrosidase mutations in Parkinson's disease. *New England Journal of Medicine* 2009;**361**:1651–61.

Simon KC, Gao X, Chen H, Schwarzschild MA, Ascherio A. Calcium channel blocker use and risk of Parkinson's disease. *Movement Disorders* 2010;**25**:1818–22.

Simuni T, Borushko E, Avram MJ, Miskevics S, Martel A, Zadikoff C, Videnovic A, Weaver FM, Williams K, Surmeier DJ. Tolerability of isradipine in early Parkinson's disease: a pilot dose escalation study. *Movement Disorders* 2010;**25**:2863–6.

Singleton AB, Farrer M, Johnson J, Singleton A, Hague S, Kachergus J, Hulihan M, Peuralinna T, Dutra A, Nussbaum R, Lincoln S, Crawley A, Hanson M, Maraganore D, Adler C, Cookson MR, Muenter M, Baptista M, Miller D *et al.* α-Synuclein locus triplication causes Parkinson's disease. *Science* 2003;**302**:841–1.

Sloan M, Alegre-Abarrategui J, Potgieter D, Kaufmann A-K, Exley R, Deltheil T, Threlfell S, Connor-Robson N, Brimblecombe K, Wallings R, Cioroch M, Bannerman DM, Bolam JP, Magill PJ, Cragg SJ, Dodson PD, Wade-Martins R. LRRK2 BAC transgenic rats develop progressive, L-DOPA-responsive motor impairment, and deficits in dopamine circuit function. *Human Molecular Genetics* 2016;**25**:951–63.

Smith PK, Krohn RI, Hermanson GT, Mallia AK, Gartner FH, Provenzano MD, Fujimoto EK, Goeke NM, Olson BJ, Klenk DC. Measurement of protein using bicinchoninic acid. *Analytical Biochemistry* 1985;**150**:76–85.

Snyder H, Mensah K, Theisler C, Lee J, Matouschek A, Wolozin B. Aggregated and monomeric alpha-synuclein bind to the S6' proteasomal protein and inhibit proteasomal function. *Journal of Biological Chemistry* 2003;**278**:11753–9.

Soper JH, Roy S, Stieber A, Lee E, Wilson RB, Trojanowski JQ, Burd CG, Lee VMY. Alpha-synuclein-induced aggregation of cytoplasmic vesicles in Saccharomyces cerevisiae. *Molecular Biology of the Cell* 2008;**19**:1093–103.

Spencer B, Potkar R, Trejo M, Rockenstein E, Patrick C, Gindi R, Adame A, Wyss-Coray T, Masliah E. Beclin 1 gene transfer activates autophagy and ameliorates the neurodegenerative pathology in alpha-synuclein models of Parkinson's and Lewy body diseases. *Journal of Neuroscience* 2009;**29**:13578–88.

Spillantini M-G, Schmidt ML, Lee VMY, Trojanowski JQ, Jakes R, Goedert M. α-Synuclein in Lewy bodies. *Nature* 1997;**388**:839–40.

Spillantini MG, Divane A, Goedert M. Assignment of human alpha-synuclein (SNCA) and beta-synuclein (SNCB) genes to chromosomes 4q21 and 5q35. *Genomics* 1995;**27**:379–81.

Stefanis L, Larsen KE, Rideout HJ, Sulzer D, Greene LA. Expression of A53T mutant but not wild-type α-synuclein in PC12 cells induces alterations of the ubiquitin-dependent degradation system, loss of dopamine release, and autophagic cell death. *Journal of Neuroscience* 2001;**21**:9549–60.

Steru L, Chermat R, Thierry B, Simon P. The tail suspension test: A new method for screening antidepressants in mice. *Psychopharmacology* 1985;**85**:367–70.

Sun Q, Fan W, Chen K, Ding X, Chen S, Zhong Q. Identification of Barkor as a mammalian autophagy-specific factor for Beclin 1 and class III phosphatidylinositol 3-kinase. *Proceedings of the National Academy of Sciences* 2008;**105**:19211–6.

Sung Y-H, Eliezer D. Residual structure, backbone dynamics, and interactions within the synuclein family. *Journal of Molecular Biology* 2007;**372**:689–707.

Taira T, Saito Y, Niki T, Ariga SMMI, Takahashi K, Ariga H. DJ-1 has a role in antioxidative stress to prevent cell death. *EMBO reports* 2004;**5**:213–8.

Tang G, Gudsnuk K, Kuo S-H, Cotrina ML, Rosoklija G, Sosunov A, Sonders MS, Kanter E, Castagna C, Yamamoto A, Yue Z, Arancio O, Peterson BS, Champagne F, Dwork AJ, Goldman J, Sulzer D. Loss of mTOR-Dependent Macroautophagy Causes Autistic-like Synaptic Pruning Deficits. *Neuron* **83**:1131–43.

Tanik SA, Schultheiss CE, Volpicelli-Daley LA, Brunden KR, Lee VMY. Lewy body-like α-synuclein aggregates resist degradation and impair macroautophagy. *The Journal of Biological Chemistry* 2013;**288**:15194–210.

Taylor KSM, Cook JA, Counsell CE. Heterogeneity in male to female risk for Parkinson's disease. *Journal of Neurology, Neurosurgery & Psychiatry* 2007;**78**:905–6.

Taylor TN, Greene JG, Miller GW. Behavioral phenotyping of mouse models of Parkinson's disease. *Behavioural Brain Research* 2010;**211**:1–10.

Taylor TN, Potgieter D, Anwar S, Senior SL, Janezic S, Threlfell S, Ryan B, Parkkinen L, Deltheil T, Cioroch M, Livieratos A, Oliver PL, Jennings KA, Davies KE, Ansorge O, Bannerman DM, Cragg SJ, Wade-Martins R. Region-specific deficits in dopamine, but not norepinephrine, signaling in a novel A30P alpha-synuclein BAC transgenic mouse. *Neurobiology of Disease* 2014;**62**:193–207.

Terlecky SR, Dice JF. Polypeptide import and degradation by isolated lysosomes. *Journal of Biological Chemistry* 1993;**268**:23490–5.

Terman D, Rubin JE, Yew AC, Wilson CJ. Activity Patterns in a Model for the Subthalamopallidal Network of the Basal Ganglia. *Journal of Neuroscience* 2002;**22**:2963–76.

Thiruchelvam M, Richfield EK, Baggs RB, Tank AW, Cory-Slechta DA. The nigrostriatal dopaminergic system as a preferential target of repeated exposures to combined paraquat and maneb: implications for Parkinson's disease. *Journal of Neuroscience* 2000;**20**:9207–14.

Threlfell S, Lalic T, Platt NJ, Jennings KA, Deisseroth K, Cragg SJ. Striatal dopamine release is triggered by synchronized activity in cholinergic interneurons. *Neuron* 2012;**75**:58–64.

Totterdell S, Hanger D, Meredith GE. The ultrastructural distribution of alpha-synuclein-like protein in normal mouse brain. *Brain Research* 2004;**1004**:61–72.

Usenovic M, Tresse E, Mazzulli JR, Taylor JP, Krainc D. Deficiency of ATP13A2 leads to lysosomal dysfunction, α-synuclein accumulation, and neurotoxicity. *Journal of Neuroscience* 2012;**32**:4240–6.

Valente EM, Abou-Sleiman PM, Caputo V, Muqit MMK, Harvey K, Gispert S, Ali Z, Del Turco D, Bentivoglio AR, Healy DG, Albanese A, Nussbaum R, González-Maldonado R, Deller T, Salvi S, Pietro Cortelli, Gilks WP, Latchman DS, Harvey RJ *et al.* Hereditary early-onset Parkinson's disease caused by mutations in *PINK1*. *Science* 2004;**304**:1158–60.

van de Warrenburg BP, Lammens M, Lucking CB, Denefle P, Wesseling P, Booij J, Praamstra P, Quinn N, Brice A, Horstink MW. Clinical and pathologic abnormalities in a family with parkinsonism and parkin gene mutations. *Neurology* 2001;**56**:555–7.

van der Putten H, Wiederhold K-H, Probst A, Barbieri S, Mistl C, Danner S, Kauffmann S, Hofele K, Spooren WPJM, Ruegg MA, Lin S, Caroni P, Sommer B, Tolnay M, Bilbe G. Neuropathology in mice expressing human α-synuclein. *Journal of Neuroscience* 2000;**20**:6021–9.

Vargas KJ, Schrod N, Davis T, Fernandez-Busnadiego R, Taguchi YV, Laugks U, Lucic V, Chandra SS. Synucleins Have Multiple Effects on Presynaptic Architecture. *Cell Reports* 2017;**18**:161–73.

Velikkakath AKG, Nishimura T, Oita E, Ishihara N, Mizushima N. Mammalian Atg2 proteins are essential for autophagosome formation and important for regulation of size and distribution of lipid droplets. *Molecular Biology of the Cell* 2012;**23**:896–909.

Verwey M, Grant A, Meti N, Adye-White L, Torres-Berrío A, Rioux V, Lévesque M, Charron F, Flores C. Mesocortical Dopamine Phenotypes in Mice Lacking the Sonic Hedgehog Receptor Cdon. *eNeuro* 2016;**3**:ENEURO.0009–16.2016.

Vila M, Vukosavic S, Jackson-Lewis V, Neystat M, Jakowec M, Przedborski S. α-Synuclein up-regulation in substantia nigra dopaminergic neurons following administration of the parkinsonian toxin MPTP. *Journal of Neurochemistry* 2000;**74**:721–9.

Vilarino-Gueell C, Wider C, Ross OA, Dachsel JC, Kachergus JM, Lincoln SJ, Soto Ortolaza AI, Cobb SA, Wilhoite GJ, Bacon JA, Behrouz B, Melrose HL, Hentati E, Puschmann A, Evans DM, Conibear E, Wasserman WW, Aasly JO, Burkhard PR *et al.* VPS35 Mutations in Parkinson Disease. *American Journal of Human Genetics* 2011;**89**:162–7.

Vingill S, Brockelt D, Lancelin C, Tatenhorst L, Dontcheva G, Preisinger C, Domeyer NS, Joseph S, Mitkovski M, Goebbels S, Nave KA, Schulz JB, Marquardt T, Lingor P, Stegmüller J. Loss of FBXO7 (PARK15) results in reduced proteasome activity and models a parkinsonism-like phenotype in mice. *The EMBO Journal* 2016;**35**:2008–25.

Vives-Bauza C, Zhou C, Huang Y, Cui M, de Vries RLA, Kim J, May J, Tocilescu MA, Liu W, Ko HS, Magrané J, Moore DJ, Dawson VL, Grailhe R, Dawson TM, Li C, Tieu K, Przedborski S. PINK1-dependent recruitment of Parkin to mitochondria in mitophagy. *Proceedings of the National Academy of Sciences* 2010;**107**:378–83.

Vogiatzi T, Xilouri M, Vekrellis K, Stefanis L. Wild type alpha-synuclein is degraded by chaperone-mediated autophagy and macroautophagy in neuronal cells. *Journal of Biological Chemistry* 2008;**283**:23542–56.

Vyas I, Heikkila RE, Nicklas WJ. Studies on the neurotoxicity of 1-methyl-4-phenyl-1,2,3,6-tetrahydropyridine: inhibition of NAD-linked substrate oxidation by its metabolite, 1-methyl-4-phenylpyridinium. *Journal of Neurochemistry* 1986;**46**:1501–7.

Walf AA, Frye CA. The use of the elevated plus maze as an assay of anxiety-related behavior in rodents. *Nature Protocols* 2007;**2**:322–8.

Wang L, Das U, Scott DA, Tang Y, McLean PJ, Roy S. α-Synuclein multimers cluster synaptic vesicles and attenuate recycling. *Current Biology* 2014;**24**:2319–26.

Webb JL, Ravikumar B, Atkins J, Skepper JN, Rubinsztein DC. Alpha-synuclein is degraded by both autophagy and the proteasome. *Journal of Biological Chemistry* 2003;**278**:25009–13.

Wei Y, Pattingre S, Sinha S, Bassik M, Levine B. JNK1-mediated phosphorylation of Bcl-2 regulates starvation-induced autophagy. *Molecular Cell* 2008;**30**:678–88.

Whone AL, Watts RL, Stoessl AJ, Davis M, Reske S, Nahmias C, Lang AE, Rascol O, Ribeiro MJ, Remy P, Poewe WH, Hauser RA, Brooks DJ. Slower progression of Parkinson's disease with ropinirole versus levodopa: The REAL-PET study. *Annals of Neurology* 2003;**54**:93–101.

Winner B, Jappelli R, Maji SK, Desplats PA, Boyer L, Aigner S, Hetzer C, Loher T, Vilar M, Campioni S, Tzitzilonis C, Soragni A, Jessberger S, Mira H, Consiglio A, Pham E, Masliah E, Gage FH, Riek R. In vivo demonstration that alpha-synuclein oligomers are toxic. *Proceedings of the National Academy of Sciences* 2011;**108**:4194–9.

Winslow AR, Chen C-W, Corrochano S, Acevedo-Arozena A, Gordon DE, Peden AA, Lichtenberg M, Menzies FM, Ravikumar B, Imarisio S, Brown S, O'Kane CJ, Rubinsztein DC. α-Synuclein impairs macroautophagy: implications for Parkinson's disease. 2010;**190**:1023–37.

Wolf A, Bauer B, Abner EL, Ashkenazy-Frolinger T, Hartz AMS. A Comprehensive Behavioral Test Battery to Assess Learning and Memory in 129S6/Tg2576 Mice. Reddy H (ed.). *PLoS ONE* 2016;**11**:e0147733.

Wooten GF, Currie LJ, Bovbjerg VE, Lee JK, Patrie J. Are men at greater risk for Parkinson's disease than women? *Journal of Neurology, Neurosurgery & Psychiatry* 2004;**75**:637–9.

Wu Y, Cheng S, Zhao H, Zou W, Yoshina S, Mitani S, Zhang H, Wang X. PI3P phosphatase activity is required for autophagosome maturation and autolysosome formation. *EMBO reports* 2014;**15**:973–81.

Xiong H, Wang D, Chen L, Choo YS, Ma H, Tang C, Xia K, Jiang W, Ronai Z, Zhuang X, Zhang Z. Parkin, PINK1, and DJ-1 form a ubiquitin E3 ligase complex promoting unfolded protein degradation. *The Journal of Clinical Investigation* 2009;**119**:650–60.

Yamada M, Iwatsubo T, Mizuno Y, Mochizuki H. Overexpression of α-synuclein in rat substantia nigra results in loss of dopaminergic neurons, phosphorylation of α-synuclein and activation of caspase-9: resemblance to pathogenetic changes in Parkinson's disease. *Journal of Neurochemistry* 2004;**91**:451–61.

Yamada T, McGeer PL, Baimbridge KG, McGeer EG. Relative sparing in Parkinson's disease of substantia nigra dopamine neurons containing calbindin-D28K. *Brain Research* 1990;**526**:303–7.

Yamakado H, Moriwaki Y, Yamasaki N, Miyakawa T, Kurisu J, Uemura K, Inoue H, Takahashi M, Takahashi R. α-Synuclein BAC transgenic mice as a model for Parkinson's disease manifested decreased anxiety-like behavior and hyperlocomotion. *Neuroscience Research* 2012;**73**:173–7.

Yamamura Y, Kuzuhara S, Kondo K, Yanagi T, Uchida M, Matsumine H, Mizuno Y. Clinical, pathologic and genetic studies on autosomal recessive early-onset parkinsonism with diurnal fluctuation. *Parkinsonism and Related Disorders* 1998;**4**:65–72.

Yousefi S, Perozzo R, Schmid I, Ziemiecki A, Schaffner T, Scapozza L, Brunner T, Simon H-U. Calpain-mediated cleavage of Atg5 switches autophagy to apoptosis. *Nature Cell Biology* 2006;**8**:1124–32.

Yue Z, Jin S, Yang C, Levine AJ, Heintz N. Beclin 1, an autophagy gene essential for early embryonic development, is a haploinsufficient tumor suppressor. *Proceedings of the National Academy of Sciences* 2003;**100**:15077–82.

Zarranz JJ, Alegre J, Gómez Esteban JC, Lezcano E, Ros R, Ampuero I, Vidal L, Hoenicka J, Rodriguez O, Atarés B, Llorens V, Tortosa EG, del Ser T, Muñoz DG, de Yebenes JG. The new mutation, E46K, of α-synuclein causes parkinson and Lewy body dementia. *Annals of Neurology* 2004;**55**:164–73.

Zatloukal K, Stumptner C, Fuchsbichler A, Heid H, Schnoelzer M, Kenner L, Kleinert R, Prinz M, Aguzzi A, Denk H. p62 is a common component of cytoplasmic inclusions in protein aggregation diseases. *The American Journal of Pathology* 2002;**160**:255–63.

Zhang J, Perry G, Smith MA, Robertson D, Olson SJ, Graham DG, Montine TJ. Parkinson's disease is associated with oxidative damage to cytoplasmic DNA and RNA in substantia nigra neurons. *The American Journal of Pathology* 1999;**154**:1423–9.

Zhang L, Shimoji M, Thomas B, Moore DJ, Yu S-W, Marupudi NI, Torp R, Torgner IA, Ottersen OP, Dawson TM, Dawson VL. Mitochondrial localization of the Parkinson's disease related protein DJ-1: implications for pathogenesis. *Human Molecular Genetics* 2005;**14**:2063–73.

Zhuang X, Masson J, Gingrich JA, Rayport S, Hen R. Targeted gene expression in dopamine and serotonin neurons of the mouse brain. *Journal of Neuroscience Methods* 2005;**143**:27–32.

Zimprich A, Benet-Pagès A, Struhal W, Graf E, Eck SH, Offman MN, Haubenberger D, Spielberger S, Schulte EC, Lichtner P, Rossle SC, Klopp N, Wolf E, Seppi K, Pirker W, Presslauer S, Mollenhauer B, Katzenschlager R, Foki T *et al.* A mutation in VPS35, encoding a subunit of the retromer complex, causes late-onset Parkinson disease. *American Journal of Human Genetics* 2011;**89**:168–75.

Zimprich A, Biskup S, Leitner P, Lichtner P, Farrer M, Lincoln S, Kachergus J, Hulihan M, Uitti RJ, Calne DB, Stoessl AJ, Pfeiffer RF, Patenge N, Carbajal IC, Vieregge P, Asmus F, M ller-Myhsok B, Dickson DW, Meitinger T *et al.* Mutations in LRRK2 cause autosomal-dominant parkinsonism with pleomorphic pathology. *Neuron* 2004;**44**:601–7.

Appendix: midbrain dopamine neuron counts

In this appendix, dopamine neuron counts as assessed by TH stereology are presented for each genotype in each age group. Two-way ANOVAs have been performed within each group to determine any differences in neuron number associated with genotype.

Appendix Table 1. Substantia nigra dopamine neuron counts with gene effects analysed using two-way ANOVA in each age group

Age (months)	Genotype	Neuron number (SEM)	*ATG7*cKO$^{DAT\text{-IRES-cre}}$ x *hSNCA*		*ATG7*cKO$^{DAT\text{-IRES-cre}}$		h*SNCA*	
			F	**P value**	***F***	**P value**	***F***	**P value**
1	Control	2082 (184)						
	h*SNCA*	2180 (193)						
	*ATG7*cKO$^{DAT\text{-IRES-cre}}$	2041 (131)						
	h*SNCA*:*ATG7*cKO$^{DAT\text{-IRES-cre}}$	1970 (246)	$F_{(1,15)}$=0.190	0.67	$F_{(1, 15)}$=0.412	0.52	$F_{(1, 15)}$= 0.004	0.94
6	Control	1867 (303)						
	h*SNCA*	1796 (214)						
	*ATG7*cKO$^{DAT\text{-IRES-cre}}$	1279 (87)						
	h*SNCA*:*ATG7*cKO$^{DAT\text{-IRES-cre}}$	1266 (110)	$F_{(1,12)}$=0.022	0.89	$F_{(1, 12)}$=7.955	0.02	$F_{(1, 12)}$=0.046	0.83
20 to 24	Control	1446 (231)						
	h*SNCA*	1611 (226)						
	*ATG7*cKO$^{DAT\text{-IRES-cre}}$	944 (198)						
	h*SNCA*:*ATG7*cKO$^{DAT\text{-IRES-cre}}$	780 (151)	$F_{(1, 17)}$=0.674	0.42	$F_{(1, 17)}$=11.07	<0.01	$F_{(1, 17)}$=0.000	0.99

Appendix Table 2. Ventral tegmental area dopamine neuron counts with gene effects analysed using two-way ANOVA in each age group								
Age (months)	**Genotype**	**Neuron number (SEM)**	***ATG7*cKO$^{DAT\text{-IRES-cre}}$ x *hSNCA***		***ATG7*cKO$^{DAT\text{-IRES-cre}}$**		**h*SNCA***	
			F	**P value**	***F***	**P value**	***F***	**P value**
1	Control	2688 (226)						
	h*SNCA*	3023 (219)						
	*ATG7*cKO$^{DAT\text{-IRES-cre}}$	3006 (219)						
	h*SNCA*:*ATG7*cKO$^{DAT\text{-IRES-cre}}$	3095 (285)	$F_{(1, 15)}$= 0.257	0.62	$F_{(1, 15)}$=0.643	0.44	$F_{(1, 15)}$= 0.760	0.3970
6	Control	1798 (177)						
	h*SNCA*	2159 (241)						
	*ATG7*cKO$^{DAT\text{-IRES-cre}}$	1860 (265)						
	h*SNCA*:*ATG7*cKO$^{DAT\text{-IRES-cre}}$	2139 (241)	$F_{(1,12)}$=0.031	0.86	$F_{(1, 12)}$=0.008	0.93	$F_{(1, 12)}$=1.88	0.1952
20 to 24	Control	2028 (302)						
	h*SNCA*	2111 (322)						
	*ATG7*cKO$^{DAT\text{-IRES-cre}}$	1570 (285)						
	h*SNCA*:*ATG7*cKO$^{DAT\text{-IRES-cre}}$	1793 (314)	$F_{(1,17)}$=0.052	0.82	$F_{(1, 17)}$=1.57	0.23	$F_{(1,17)}$=0.246	0.6263

References

Aasly JO, Vilarino Guell C, Dachsel JC, Webber PJ, West AB, Haugarvoll K, Johansen KK, Toft M, Nutt JG, Payami H, Kachergus JM, Lincoln SJ, Felic A, Wider C, Soto Ortolaza AI, Cobb SA, White LR, Ross OA, Farrer MJ. Novel pathogenic LRRK2 p.Asn1437His substitution in familial Parkinson's disease. *Movement Disorders* 2010;**25**:2156–63.

Abbas N, Lucking CB, Ricard S, Dürr A, Bonifati V, De Michele G, Bouley S, Vaughan JR, Gasser T, Marconi R, Broussolle E, Brefel-Courbon C, Harhangi BS, Oostra, AB, Fabrizio E, Bohme GA, Pradier L, Wood NW, Filla A *et al.* A wide variety of mutations in the parkin gene are responsible for autosomal recessive parkinsonism in Europe. *Human Molecular Genetics* 1999;**8**:567–74.

Abeliovich A, Schmitz Y, Farinas I, Choi-Lundberg D, Ho WH, Castillo PE, Shinsky N, Verdugo J, Armanini M, Ryan A, Hynes M, Phillips H, Sulzer D, Rosenthal A. Mice lacking alpha-synuclein display functional deficits in the nigrostriatal dopamine system. *Neuron* 2000;**25**:239–52.

Adams-Carr KL, Bestwick JP, Shribman S, Lees A, Schrag A, Noyce AJ. Constipation preceding Parkinson's disease: a systematic review and meta-analysis. *Journal of Neurology, Neurosurgery & Psychiatry* 2016;**87**:710–6.

Ahlberg J, Glaumann H. Uptake--microautophagy--and degradation of exogenous proteins by isolated rat liver lysosomes. Effects of pH, ATP, and inhibitors of proteolysis. *Experimental and molecular pathology* 1985;**42**:78–88.

Ahlberg J, Marzella L, Glaumann H. Uptake and degradation of proteins by isolated rat liver lysosomes. Suggestion of a microautophagic pathway of proteolysis. *Laboratory investigation; a journal of technical methods and pathology* 1982;**47**:523–32.

Ahmed I, Liang Y, Schools S, Dawson VL, Dawson TM, Savitt JM. Development and characterization of a new Parkinson's disease model resulting from impaired autophagy. *Journal of Neuroscience* 2012;**32**:16503–9.

Al-Wandi A, Ninkina N, Millership S, Williamson SJM, Jones PA, Buchman VL. Absence of α-synuclein affects dopamine metabolism and synaptic markers in the striatum of aging mice. *Neurobiology of Aging* 2010;**31**:796–804.

Alegre-Abarrategui J, Christian H, Lufino MMP, Mutihac R, Venda LL, Ansorge O, Wade-Martins R. LRRK2 regulates autophagic activity and localizes to specific membrane microdomains in a novel human genomic reporter cellular model. *Human Molecular Genetics* 2009;**18**:4022–34.

Alvarado-Bolanos A, Cervantes-Arriaga A, Rodriguez-Violante M, Llorens-Arenas R, Calderon-Fajardo H, Millan-Cepeda R, Leal-Ortega R, Estrada-Bellmann I, Zuniga-Ramirez C. Impact of Neuropsychiatric Symptoms on the Quality of Life of Subjects with Parkinson's Disease. *Journal of Parkinson's Disease* 2015;**5**:541–8.

Ando M, Funayama M, Li Y, Kashihara K, Murakami Y, Ishizu N, Toyoda C, Noguchi K, Hashimoto T, Nakano N, Sasaki R, Kokubo Y, Kuzuhara S, Ogaki K, Yamashita C, Yoshino H, Hatano T, Tomiyama H, Hattori N. VPS35 mutation in Japanese patients with typical Parkinson's disease. *Movement Disorders* 2012;**27**:1413–7.

Anglade P, Vyas S, Javoy-Agid F, Herrero MT, Michel PP, Marquez J, Mouatt-Prigent A, Ruberg M, Hirsch EC, Agid Y. Apoptosis and autophagy in nigral neurons of patients with Parkinson's disease. *Histology and Histopathology* 1997;**12**:25–32.

Annesi G, Savettieri G, Pugliese P, D'Amelio M, Tarantino P, Ragonese P, La Bella V, Piccoli T, Civitelli D, Annesi F, Fierro B, Piccoli F, Arabia G, Caracciolo M, Cirò Candiano IC, Quattrone A. DJ-1 mutations and parkinsonism-dementia-amyotrophic lateral sclerosis complex. *Annals of Neurology* 2005;**58**:803–7.

Anwar S, Peters O, Millership S, Ninkina N, Doig N, Connor-Robson N, Threlfell S, Kooner G, Deacon RM, Bannerman DM, Bolam JP, Chandra SS, Cragg SJ, Wade-Martins R, Buchman VL. Functional Alterations to the Nigrostriatal System in Mice Lacking All Three Members of the Synuclein Family. *Journal of Neuroscience* 2011;**31**:7264–74.

Appel Cresswell S, Vilarino Guell C, Encarnacion M, Sherman H, Yu I, Shah B, Weir D, Thompson C, Szu Tu C, Trinh J, Aasly JO, Rajput A, Rajput AH, Jon Stoessl A, Farrer MJ. Alpha-synuclein p.H50Q, a novel pathogenic mutation for Parkinson's disease. *Movement Disorders* 2013;**28**:811–3.

Arai N, Misugi K, Goshima Y, Misu Y. Evaluation of a 1-methyl-4-phenyl-1,2,3,6-tetrahydropyridine (MPTP)-treated C57 black mouse model for parkinsonism. *Brain Research* 1990;**515**:57–63.

Araki K, Yagi N, Nakatani R, Sekiguchi H, So M, Yagi H, Ohta N, Nagai Y, Goto Y, Mochizuki H. A small-angle X-ray scattering study of alpha-synuclein from human red blood cells. *Scientific Reports* 2016;**6**, DOI: 10.1038/srep30473.

Ashburn A, Stack E, Pickering RM, Ward CD. A community-dwelling sample of people with Parkinson's disease: characteristics of fallers and non-fallers. *Age and Ageing* 2001;**30**:47–52.

Ayton S, George JL, Adlard PA, Bush AI, Cherny RA, Finkelstein DI. The effect of dopamine on MPTP-induced rotarod disability. *Neuroscience Letters* 2013;**543**:105–9.

Bai X, Wey MC-Y, Fernandez E, Hart MJ, Gelfond J, Bokov AF, Rani S, Strong R. Rapamycin improves motor function, reduces 4-hydroxynonenal adducted protein in brain, and attenuates synaptic injury in a mouse model of synucleinopathy. *Pathobiology of Aging & Age-related Diseases* 2015;**5**:28743.

Baiguera C, Alghisi M, Pinna A, Bellucci A, De Luca MA, Frau L, Morelli M, Ingrassia R, Benarese M, Porrini V, Pellitteri M, Bertini G, Fabene PF, Sigala S, Spillantini M-G, Liou H-C, Spano PF, Pizzi M. Late-onset Parkinsonism in NFκB/c-Rel-deficient mice. *Brain* 2012;**135**:2750–65.

Balsinde J, Balboa MA. Cellular regulation and proposed biological functions of group VIA calcium-independent phospholipase A2 in activated cells. *Cellular signalling* 2005;**17**:1052–62.

Bandyopadhyay U, Kaushik S, Varticovski L, Cuervo AM. The chaperone-mediated autophagy receptor organizes in dynamic protein complexes at the lysosomal membrane. *Molecular and Cellular Biology* 2008;**28**:5747–63.

Bartels T, Choi JG, Selkoe DJ. alpha-Synuclein occurs physiologically as a helically folded tetramer that resists aggregation. *Nature* 2011;**477**:107–10.

Bäckman CM, Malik N, Zhang Y, Shan L, Grinberg A, Hoffer BJ, Westphal H, Tomac AC. Characterization of a mouse strain expressing Cre recombinase from the 3′ untranslated region of the dopamine transporter locus. *Genesis* 2006;**44**:383–90.

Beilina A, Cookson MR. Genes associated with Parkinson's disease: regulation of autophagy and beyond. *Journal of Neurochemistry* 2016;**139**:91–107.

Beilina A, Rudenko IN, Kaganovich A, Civiero L, Chau H, Kalia SK, Kalia LV, Lobbestael E, Chia R, Ndukwe K, Ding J, Nalls MA, Olszewski M, Hauser DN, Kumaran R, Lozano AM, Baekelandt V, Greene LE, Taymans J-M *et al.* Unbiased screen for interactors of leucine-rich repeat kinase 2 supports a common pathway for sporadic and familial Parkinson disease. *Proceedings of the National Academy of Sciences* 2014;**111**:2626–31.

Benedetti MD, Maraganore DM, Bower JH, McDonnell SK, Peterson BJ, Ahlskog JE, Schaid DJ, Rocca WA. Hysterectomy, menopause, and estrogen use preceding Parkinson's disease: An exploratory case-control study. *Movement Disorders* 2001;**16**:830–7.

Benoit-Marand M, Borrelli E, Gonon F. Inhibition of Dopamine Release Via Presynaptic D2 Receptors: Time Course and Functional Characteristics In Vivo. *Journal of Neuroscience* 2001;**21**:9134–41.

Bento CF, Renna M, Ghislat G, Puri C, Ashkenazi A, Vicinanza M, Menzies FM, Rubinsztein DC. Mammalian Autophagy: How Does It Work? *Annual review of biochemistry* 2016;**85**:685–713.

Berger K, Breteler MM, Helmer C, Inzitari D, Fratiglioni L, Trenkwalder C, Hofman A, Launer LJ. Prognosis with Parkinson's disease in europe: A collaborative study of population-based cohorts. Neurologic Diseases in the Elderly Research Group. *Neurology* 2000;**54**:S24–7.

Bernheimer H, Birkmayer W, Hornykiewicz O, Jellinger K, Seitelberger F. Brain dopamine and the syndromes of Parkinson and Huntington. Clinical, morphological and neurochemical correlations. *Journal of the neurological sciences* 1973;**20**:415–55.

Betarbet R, Sherer TB, MacKenzie G, Garcia-Osuna M, Panov AV, Greenamyre JT. Chronic systemic pesticide exposure reproduces features of Parkinson's disease. *Nature Neuroscience* 2000;**3**:1301–6.

Betin VMS, Singleton BK, Parsons SF, Anstee DJ, Lane JD. Autophagy facilitates organelle clearance during differentiation of human erythroblasts. *Autophagy* 2013;**9**:881–93.

Betz UAK, Voßhenrich CAJ, Rajewsky K, Müller W. Bypass of lethality with mosaic mice generated by Cre–loxP-mediated recombination. *Current Biology* 1996;**6**:1307–16.

Bevan MD, Magill PJ, Terman D, Bolam JP, Wilson CJ. Move to the rhythm: oscillations in the subthalamic nucleus–external globus pallidus network. *Trends in Neurosciences* 2002;**25**:525–31.

Bezard E, Gross CE, Fournier MC, Dovero S, Bloch B, Jaber M. Absence of MPTP-induced neuronal death in mice lacking the dopamine transporter. *Experimental Neurology* 1999;**155**:268–73.

Bianco Lo C, Ridet JL, Schneider BL, Déglon N, Aebischer P. α-synucleinopathy and selective dopaminergic neuron loss in a rat lentiviral-based model of Parkinson's disease. *Proceedings of the National Academy of Sciences* 2002;**99**:10813–8.

Biazik J, Ylä-Anttila P, Vihinen H, Jokitalo E, Eskelinen E-L. Ultrastructural relationship of the phagophore with surrounding organelles. *Autophagy* 2015;**11**:439–51.

Biere AL, Wood SJ, Wypych J, Steavenson S, Jiang Y, Anafi D, Jacobsen FW, Jarosinski MA, Wu GM, Louis JC, Martin F, Narhi LO, Citron M. Parkinson's disease-associated alpha-synuclein is more fibrillogenic than beta- and gamma-synuclein and cannot cross-seed its homologs. *Journal of Biological Chemistry* 2000;**275**:34574–9.

Bisaglia M, Mammi S, Bubacco L. Structural insights on physiological functions and pathological effects of alpha-synuclein. *FASEB Journal* 2009;**23**:329–40.

Boileau I, Warsh JJ, Guttman M, Saint Cyr JA, McCluskey T, Rusjan P, Houle S, Wilson AA, Meyer JH, Kish SJ. Elevated serotonin transporter binding in depressed patients with Parkinson's disease: a preliminary PET study with [11C]DASB. *Movement Disorders* 2008;**23**:1776–80.

Bonifati V, Rizzu P, van Baren MJ, Schaap O, Breedveld GJ, Krieger E, Dekker MCJ, Squitieri F, Ibanez P, Joosse M, van Dongen JW, Vanacore N, van Swieten JC, Brice A, Meco G, van Duijn CM, Ben A Oostra, Heutink P. Mutations in the *DJ-1* Gene Associated with Autosomal Recessive Early-Onset Parkinsonism. *Science* 2003;**299**:256–9.

Bosboom J, Stoffers D, Wolters EC. Cognitive dysfunction and dementia in Parkinson's disease. *Journal of Neural Transmission* 2004.

Boya P, Reggiori F, Codogno P. Emerging regulation and functions of autophagy. *Nature Cell Biology* 2013;**15**:713–20.

Braak H, Bohl JR, Müller CM, Rüb U, de Vos RAI, Del Tredici K. Stanley Fahn Lecture 2005: The staging procedure for the inclusion body pathology associated with sporadic Parkinson's disease reconsidered. *Movement Disorders* 2006;**21**:2042–51.

Braak H, Del Tredici K. *Neuroanatomy and Pathology of Sporadic Parkinson's Disease*. Berlin: Springer, 2008.

Braak H, Rüb U, Jansen Steur ENH, Del Tredici K, de Vos RAI. Cognitive status correlates with neuropathologic stage in Parkinson disease. *Neurology* 2005;**64**:1404–10.

Branco T, Staras K. The probability of neurotransmitter release: variability and feedback control at single synapses. *Nature Reviews Neuroscience* 2009;**10**:373–83.

Braungart E, Gerlach M, Riederer P, Baumeister R, Hoener MC. Caenorhabditis elegans MPP+ Model of Parkinson's Disease for High-Throughput Drug Screenings. *Neurodegenerative Diseases* 2004;**1**:175–83.

Brimblecombe KR, Cragg SJ. Ni2+ affects dopamine uptake which limits suitability as inhibitor of T-type voltage-gated Ca^{2+} channels. *ACS chemical neuroscience* 2014, DOI: 10.1021/cn500274g.

Buchman VL, Hunter HJA, Pinõn LGP, Thompson J, Privalova EM, Ninkina NN, Davies AM. Persyn, a Member of the Synuclein Family, Has a Distinct Pattern of Expression in the Developing Nervous System. *Journal of Neuroscience* 1998;**18**:9335–41.

Burré J, Sharma M, Südhof TC. α-Synuclein assembles into higher-order multimers upon membrane binding to promote SNARE complex formation. *Proceedings of the National Academy of Sciences* 2014;**111**:E4274–83.

Burré J, Vivona S, Diao J, Sharma M, Brunger AT, Südhof TC. Properties of native brain alpha-synuclein. *Nature* 2013;**498**:E4–6–discussionE6–7.

Cabin DE, Gispert-Sanchez S, Murphy D, Auburger G, Myers RR, Nussbaum RL. Exacerbated synucleinopathy in mice expressing A53T SNCA on a Snca null background. *Neurobiology of Aging* 2005;**26**:25–35.

Can A, Dao DT, Terrillion CE, Piantadosi SC, Bhat S, Gould TD. The tail suspension test. *Journal of visualized experiments : JoVE* 2012:e3769–9.

Cang C, Aranda K, Seo Y-J, Gasnier B, Ren D. TMEM175 Is an Organelle K + Channel Regulating Lysosomal Function. *Cell* 2015;**162**:1101–12.

Carter DA, Fibiger HC. Ascending projections of presumed dopamine-containing neurons in the ventral tegmentum of the rat as demonstrated by horseradish peroxidase. *Neuroscience* 1977;**2**:569–76.

Caslake R, Moore JN, Gordon JC, Harris CE, Counsell C. Changes in diagnosis with follow-up in an incident cohort of patients with parkinsonism. *Journal of Neurology, Neurosurgery & Psychiatry* 2008;**79**:1202–7.

Cárdenas C, Miller RA, Smith I, Bui T, Molgó J, Müller M, Vais H, Cheung K-H, Yang J, Parker I, Thompson CB, Birnbaum MJ, Hallows KR, Foskett JK. Essential Regulation of Cell Bioenergetics by Constitutive InsP3 Receptor Ca2+ Transfer to Mitochondria. *Cell* 2010;**142**:270–83.

Chan CS, Guzman JN, Ilijic E, Mercer JN, Rick C, Tkatch T, Meredith GE, Surmeier DJ. 'Rejuvenation' protects neurons in mouse models of Parkinson's disease. *Nature* 2007;**447**:1081–6.

Chan G, White CC, Winn PA, Cimpean M, Replogle JM, Glick LR, Cuerdon NE, Ryan KJ, Johnson KA, Schneider JA, Bennett DA, Chibnik LB, Sperling RA, De Jager PL, Bradshaw EM. Trans-pQTL study identifies immune crosstalk between Parkinson and Alzheimer loci. *Neurology Genetics* 2016;**2**:e90.

Chandra S, Gallardo G, Fernández-Chacón R, Schlüter OM, Südhof TC. α-Synuclein Cooperates with CSPα in Preventing Neurodegeneration. *Cell* 2005;**123**:383–96.

Chen BT, Moran KA, Avshalumov MV, Rice ME. Limited regulation of somatodendritic dopamine release by voltage-sensitive Ca2+ channels contrasted with strong regulation of axonal dopamine release. *Journal of Neurochemistry* 2006;**96**:645–55.

Chen D, Pang S, Feng X, Huang W, Hawley RG, Yan B. Genetic analysis of the ATG7 gene promoter in sporadic Parkinson's disease. *Neuroscience Letters* 2013;**534**:193–8.

Chen H, Zhao EJ, Zhang W, Lu Y, Liu R, Huang X, Ciesielski-Jones AJ, Justice MA, Cousins DS, Peddada S. Meta-analyses on prevalence of selected Parkinson's nonmotor symptoms before and after diagnosis. *Translational Neurodegeneration* 2015;**4**:1.

Chiang HL, Terlecky SR, Plant CP, Dice JF. A role for a 70-kilodalton heat shock protein in lysosomal degradation of intracellular proteins. *Science* 1989;**246**:382–5.

Chu Y, Dodiya H, Aebischer P, Olanow CW, Kordower JH. Alterations in lysosomal and proteasomal markers in Parkinson's disease: relationship to alpha-synuclein inclusions. *Neurobiology of Disease* 2009;**35**:385–98.

Chung CY. Cell type-specific gene expression of midbrain dopaminergic neurons reveals molecules involved in their vulnerability and protection. *Human Molecular Genetics* 2005;**14**:1709–25.

Chung KK, Zhang Y, Lim KL, Tanaka Y, Huang H, Gao J, Ross CA, Dawson VL, Dawson TM. Parkin ubiquitinates the alpha-synuclein-interacting protein, synphilin-1: implications for Lewy-body formation in Parkinson disease. *Nature Medicine* 2001;**7**:1144–50.

Clarke CE, Zobkiw RM, Gullaksen E. Quality of life and care in Parkinson's disease. *The British Journal of Clinical Practice* 1995;**49**:288–93.

Cleveland DW, Hwo S-Y, Kirschner MW. Purification of tau, a microtubule-associated protein that induces assembly of microtubules from purified tubulin. *Journal of Molecular Biology* 1977;**116**:207–25.

Colotla VA, Flores E, Oscos A, Meneses A, Tapia R. Effects of MPTP on locomotor activity in mice. *Neurotoxicology and Teratology* 1990;**12**:405–7.

Connolly BS, Lang AE. Pharmacological treatment of Parkinson disease: a review. *JAMA* 2014;**311**:1670–83.

Connor-Robson N, Peters OM, Millership S, Ninkina N, Buchman VL. Combinational losses of synucleins reveal their differential requirements for compensating age-dependent alterations in motor behavior and dopamine metabolism. *Neurobiology of Aging* 2016;**46**:107–12.

Conway KA, Harper JD, Lansbury PT. Accelerated in vitro fibril formation by a mutant alpha-synuclein linked to early-onset Parkinson disease. *Nature Medicine* 1998;**4**:1318–20.

Cornejo-Olivas MR, Torres L, Mata IF, Mazzetti P, Rivas D, Cosentino C, Inca-Martinez M, Cuba JM, Zabetian CP, Leverenz JB. A Peruvian family with a novel PARK2 mutation: Clinical and pathological characteristics. *Parkinsonism and Related Disorders* 2015;**21**:444–8.

Costa J, Lunet N, Santos C, Santos J, Vaz-Carneiro A. Caffeine exposure and the risk of Parkinson's disease: a systematic review and meta-analysis of observational studies. *Journal of Alzheimer's Disease* 2010;**20 Suppl 1**:S221–38.

Cragg SJ, Hille CJ, Greenfield SA. Dopamine release and uptake dynamics within nonhuman primate striatum in vitro. *Journal of Neuroscience* 2000;**20**:8209–17.

Cragg SJ. Variable dopamine release probability and short-term plasticity between functional domains of the primate striatum. *Journal of Neuroscience* 2003;**23**:4378–85.

Crews L, Spencer B, Desplats P, Patrick C, Paulino A, Rockenstein E, Hansen L, Adame A, Galasko D, Masliah E. Selective molecular alterations in the autophagy pathway in patients with Lewy body disease and in models of alpha-synucleinopathy. Ikezu T (ed.). *PLoS ONE* 2010;**5**:e9313.

Cryan JF, Mombereau C, Vassout A. The tail suspension test as a model for assessing antidepressant activity: Review of pharmacological and genetic studies in mice. *Neuroscience & Biobehavioral Reviews* 2005;**29**:571–625.

Cuervo AM, Stefanis L, Fredenburg R, Lansbury PT, Sulzer D. Impaired Degradation of Mutant α-Synuclein by Chaperone-Mediated Autophagy. *Science* 2004;**305**:1292–5.

Dan I, Watanabe NM, Kusumi A. The Ste20 group kinases as regulators of MAP kinase cascades. *Trends in Cell Biology* 2001;**11**:220–30.

Daniel JA, Galbraith S, Iacovitti L, Abdipranoto A, Vissel B. Functional heterogeneity at dopamine release sites. *Journal of Neuroscience* 2009;**29**:14670–80.

Dauer W, Kholodilov N, Vila M, Trillat A-C, Goodchild R, Larsen KE, Staal R, Tieu K, Schmitz Y, Yuan CA, Rocha M, Jackson-Lewis V, Hersch S, Sulzer D, Przedborski S, Burke R, Hen R. Resistance of alpha -synuclein null mice to the parkinsonian neurotoxin MPTP. *Proceedings of the National Academy of Sciences* 2002;**99**:14524–9.

Davis C. *SPSS for Applied Sciences*. CSIRO PUBLISHING, 2013.

Dawson TM, Ko HS, Dawson VL. Genetic animal models of Parkinson's disease. *Neuron* 2010;**66**:646–61.

de Rijk MC, Breteler MM, Graveland GA, Ott A, Grobbee DE, van der Meché FG, Hofman A. Prevalence of Parkinson's disease in the elderly: the Rotterdam Study. *Neurology* 1995;**45**:2143–6.

Deacon RMJ, Bannerman DM, Kirby BP, Croucher A, Rawlins JNP. Effects of cytotoxic hippocampal lesions in mice on a cognitive test battery. *Behavioural Brain Research* 2002;**133**:57–68.

Deacon RMJ, Rawlins JNP. T-maze alternation in the rodent. *Nature Protocols* 2006;**1**:7–12.

Deacon RMJ. Measuring the strength of mice. *Journal of Visualized Experiments* 2013a, DOI: 10.3791/2610.

Deacon RMJ. Measuring motor coordination in mice. *Journal of Visualized Experiments* 2013b:e2609.

Decressac M, Mattsson B, Weikop P, Lundblad M, Jakobsson J, Björklund A. TFEB-mediated autophagy rescues midbrain dopamine neurons from alpha-synuclein toxicity. *Proceedings of the National Academy of Sciences* 2013;**110**:E1817–26.

Dehay B, Bove J, Rodriguez-Muela N, Perier C, Recasens A, Boya P, Vila M. Pathogenic lysosomal depletion in Parkinson's disease. *Journal of Neuroscience* 2010;**30**:12535–44.

Dehay B, Ramirez A, Martinez-Vicente M, Perier C, Canron M-H, Doudnikoff E, Vital A, Vila M, Klein C, Bezard E. Loss of P-type ATPase ATP13A2/PARK9 function induces general lysosomal deficiency and leads to Parkinson disease neurodegeneration. *Proceedings of the National Academy of Sciences* 2012;**109**:9611–6.

Delfs JM, Schreiber L, Kelley AE. Microinjection of cocaine into the nucleus accumbens elicits locomotor activation in the rat. *Journal of Neuroscience* 1990;**10**:303.

DeLong MR, Wichmann T. Circuits and Circuit Disorders of the Basal Ganglia. *Archives of Neurology* 2007;**64**:20–4.

DeMaagd G, Philip A. Parkinson's Disease and Its Management: Part 1: Disease Entity, Risk Factors, Pathophysiology, Clinical Presentation, and Diagnosis. *P & T : a peer-reviewed journal for formulary management* 2015;**40**:504–32.

Desplats P, Lee H-J, Bae E-J, Patrick C, Rockenstein E, Crews L, Spencer B, Masliah E, Lee S-J. Inclusion formation and neuronal cell death through neuron-to-neuron transmission of alpha-synuclein. *Proceedings of the National Academy of Sciences* 2009;**106**:13010–5.

Dettmer U, Newman AJ, Luth ES, Bartels T, Selkoe D. In Vivo Cross-linking Reveals Principally Oligomeric Forms of alpha-Synuclein and beta-Synuclein in Neurons and Non-neural Cells. *Journal of Biological Chemistry* 2013;**288**:6371–85.

Dexter DT, Carter CJ, Wells FR, Javoy-Agid F, Agid Y, Lees A, Jenner P, Marsden CD. Basal Lipid Peroxidation in Substantia Nigra Is Increased in Parkinson's Disease. *Journal of Neurochemistry* 1989;**52**:381–9.

Diao J, Burré J, Vivona S, Cipriano DJ, Sharma M, Kyoung M, Südhof TC, Brunger AT. Native alpha-synuclein induces clustering of synaptic-vesicle mimics via binding to phospholipids and synaptobrevin-2/VAMP2. *eLife* 2013;**2**:e00592.

Dice JF, Chiang HL, Spencer EP, Backer JM. Regulation of catabolism of microinjected ribonuclease A. Identification of residues 7-11 as the essential pentapeptide. *Journal of Biological Chemistry* 1986;**261**:6853–9.

Dice JF. Peptide sequences that target cytosolic proteins for lysosomal proteolysis. *Trends in biochemical sciences* 1990;**15**:305–9.

Dodel RC, Singer M, Köhne-Volland R, Szucs T, Rathay B, Scholz E, Oertel WH. The economic impact of Parkinson's disease. An estimation based on a 3-month prospective analysis. *PharmacoEconomics* 1998;**14**:299–312.

Dorsey ER, Constantinescu R, Thompson JP, Biglan KM, Holloway RG, Kieburtz K, Marshall FJ, Ravina BM, Schifitto G, Siderowf A, Tanner CM. Projected number of people with Parkinson disease in the most populous nations, 2005 through 2030. *Neurology* 2007;**68**:384–6.

Dusonchet J, Kochubey O, Stafa K, Young SMJ, Zufferey R, Moore DJ, Schneider BL, Aebischer P. A rat model of progressive nigral neurodegeneration induced by the Parkinson's disease-associated G2019S mutation in LRRK2. *Journal of Neuroscience* 2011;**31**:907–12.

Dymecki SM. Flp recombinase promotes site-specific DNA recombination in embryonic stem cells and transgenic mice. *Proceedings of the National Academy of Sciences* 1996;**93**:6191–6.

Ebrahimi-Fakhari D, Cantuti-Castelvetri I, Fan Z, Rockenstein E, Masliah E, Hyman BT, McLean PJ, Unni VK. Distinct Roles *In Vivo* for the Ubiquitin–Proteasome System and the Autophagy–Lysosomal Pathway in the Degradation of α-Synuclein. *Journal of Neuroscience* 2011;**31**:14508–20.

Ehringer H, Hornykiewicz O. Verteilung Von Noradrenalin Und Dopamin (3-Hydroxytyramin) Im Gehirn Des Menschen Und Ihr Verhalten Bei Erkrankungen Des Extrapyramidalen Systems. *Klinische Wochenschrift* 1960;**38**:1236–9.

Ellison SLR, Farrant TJ, Barwick V. *Practical Statistics for the Analytical Scientist*. Royal Society of Chemistry, 2009.

Emre M. Dementia associated with Parkinson's disease. *The Lancet Neurology* 2003;**2**:229–37.

Eriksen J, Rasmussen SGF, Rasmussen TN, Vaegter CB, Cha JH, Zou M-F, Newman AH, Gether U. Visualization of dopamine transporter trafficking in live neurons by use of fluorescent cocaine analogs. *Journal of Neuroscience* 2009;**29**:6794–808.

Exner N, Treske B, Paquet D, Holmström K, Schiesling C, Gispert S, Carballo-Carbajal I, Berg D, Hoepken H-H, Gasser T, Krüger R, Winklhofer KF, Vogel F, Reichert AS, Auburger G, Kahle PJ, Schmid B, Haass C. Loss-of-Function of Human PINK1 Results in Mitochondrial Pathology and Can Be Rescued by Parkin. *Journal of Neuroscience* 2007;**27**:12413–8.

Fahn S, Oakes D, Shoulson I, Kieburtz K, Rudolph A, Lang A, Olanow CW, Tanner C, Marek K. Levodopa and the progression of Parkinson's disease. *New England Journal of Medicine* 2004;**351**:2498–508.

Fares M-B, Maco B, Oueslati A, Rockenstein E, Ninkina N, Buchman VL, Masliah E, Lashuel HA. Induction of de novo α-synuclein fibrillization in a neuronal model for Parkinson's disease. *Proceedings of the National Academy of Sciences* 2016;**113**:E912–21.

Farrer M, Chan P, Chen R, Tan L, Lincoln S, Hernandez D, Forno L, Gwinn Hardy K, Petrucelli L, Hussey J, Singleton A, Tanner C, Hardy J, Langston JW. Lewy bodies and parkinsonism in families with parkin mutations. *Annals of Neurology* 2001;**50**:293–300.

Fauvet B, Mbefo MK, Fares M-B, Desobry C, Michael S, Ardah MT, Tsika E, Coune P, Prudent M, Lion N, Eliezer D, Moore DJ, Schneider B, Aebischer P, El-Agnaf OM, Masliah E, Lashuel HA. α-Synuclein in central nervous system and from erythrocytes, mammalian cells, and Escherichia coli exists predominantly as disordered monomer. *The Journal of Biological Chemistry* 2012;**287**:15345–64.

Feany MB, Bender WW. A Drosophila model of Parkinson's disease. *Nature* 2000;**404**:394–8.

Feir-Walsh BJ, Toothaker LE. An Empirical Comparison of the Anova F-Test, Normal Scores Test and Kruskal-Wallis Test Under Violation of Assumptions. *Educational and Psychological Measurement* 2016;**34**:789–99.

Feng Y, Backues SK, Baba M, Heo J-M, Harper JW, Klionsky DJ. Phosphorylation of Atg9 regulates movement to the phagophore assembly site and the rate of autophagosome formation. *Autophagy* 2016;**12**:648–58.

Ferrer I, Martinez A, Blanco R, Dalfó E, Carmona M. Neuropathology of sporadic Parkinson disease before the appearance of parkinsonism: preclinical Parkinson disease. *Journal of Neural Transmission* 2011;**118**:821–39.

Findley L, Aujla M, Bain PG, Baker M, Beech C, Bowman C, Holmes J, Kingdom WK, MacMahon DG, Peto V, Playfer JR. Direct economic impact of Parkinson's disease: a research survey in the United Kingdom. *Movement Disorders* 2003;**18**:1139–45.

Findley LJ, Gresty MA, Halmagyi GM. Tremor, the cogwheel phenomenon and clonus in Parkinson's disease. *Journal of Neurology, Neurosurgery & Psychiatry* 1981;**44**:534–46.

Fleming SM, Tetreault NA, Mulligan CK, Hutson CB, Masliah E, Chesselet M-F. Olfactory deficits in mice overexpressing human wildtype α-synuclein. *European Journal of Neuroscience* 2008;**28**:247–56.

Fountaine TM, Venda LL, Warrick N, Christian HC, Brundin P, Channon KM, Wade-Martins R. The effect of alpha-synuclein knockdown on MPP+ toxicity in models of human neurons. *European Journal of Neuroscience* 2008;**28**:2459–73.

Fountaine TM, Wade-Martins R. RNA interference-mediated knockdown of α-synuclein protects human dopaminergic neuroblastoma cells from MPP+ toxicity and reduces dopamine transport. *Journal of Neuroscience Research* 2007;**85**:351–63.

Frey U, Schroeder H, Matthies HR. Dopaminergic antagonists prevent long-term maintenance of posttetanic LTP in the CA1 region of rat hippocampal slices. *Brain Research* 1990;**522**:69–75.

Friedman LG, Lachenmayer ML, Wang J, He L, Poulose SM, Komatsu M, Holstein GR, Yue Z. Disrupted autophagy leads to dopaminergic axon and dendrite degeneration and promotes presynaptic accumulation of alpha-synuclein and LRRK2 in the brain. *Journal of Neuroscience* 2012;**32**:7585–93.

Fuchs J, Nilsson C, Kachergus J, Munz M, Larsson EM, Schule B, Langston JW, Middleton FA, Ross OA, Hulihan M, Gasser T, Farrer MJ. Phenotypic variation in a large Swedish pedigree due to SNCA duplication and triplication. *Neurology* 2007;**68**:916–22.

Fukuoka S-I, Ishiguro K, Yanagihara K, Tanabe A, Egashira Y, Sanada H, Shibata K. Identification and Expression of a cDNA Encoding Human α-Amino-β-carboxymuconate-ε-semialdehyde Decarboxylase (ACMSD). *Journal of Biological Chemistry* 2002;**277**:35162–7.

Garcia-Reitböck P, Anichtchik O, Bellucci A, Iovino M, Ballini C, Fineberg E, Ghetti B, Corte Della L, Spano P, Tofaris GK, Goedert M, Spillantini M-G. SNARE protein redistribution and synaptic failure in a transgenic mouse model of Parkinson's disease. *Brain* 2010;**133**:2032–44.

Gautier CA, Kitada T, Shen J. Loss of PINK1 causes mitochondrial functional defects and increased sensitivity to oxidative stress. *Proceedings of the National Academy of Sciences* 2008;**105**:11364–9.

Geisler S, Holmström KM, Skujat D, Fiesel FC, Rothfuss OC, Kahle PJ, Springer W. PINK1/Parkin-mediated mitophagy is dependent on VDAC1 and p62/SQSTM1. *Nature Cell Biology* 2010;**12**:119–31.

Gelman DM, Noaín D, Avale ME, Otero V, Low MJ, Rubinstein M. Transgenic mice engineered to target Cre/loxP-mediated DNA recombination into catecholaminergic neurons. *Genesis* 2003;**36**:196–202.

Giros B, Jaber M, Jones SR, Wightman RM, Caron MG. Hyperlocomotion and indifference to cocaine and amphetamine in mice lacking the dopamine transporter. *Nature* 1996;**379**:606–12.

Gitler AD, Bevis BJ, Shorter J, Strathearn KE, Hamamichi S, Su LJ, Caldwell KA, Caldwell GA, Rochet J-C, McCaffery JM, Barlowe C, Lindquist S. The Parkinson's disease protein alpha-synuclein disrupts cellular Rab homeostasis. *Proceedings of the National Academy of Sciences* 2008;**105**:145–50.

Goldberg MS, Fleming SM, Palacino JJ, Cepeda C, Lam HA, Bhatnagar A, Meloni EG, Wu NP, Ackerson LC, Klapstein GJ, Gajendiran M, Roth BL, Chesselet MF, Maidment NT, Levine MS, Shen J. Parkin-deficient mice exhibit nigrostriatal deficits but not loss of dopaminergic neurons. *Journal of Biological Chemistry* 2003;**278**:43628–35.

Goldberg MS, Pisani A, Haburcak M, Vortherms TA, Kitada T, Costa C, Tong Y, Martella G, Tscherter A, Martins A, Bernardi G, Roth BL, Pothos EN, Calabresi P, Shen J. Nigrostriatal dopaminergic deficits and hypokinesia caused by inactivation of the familial Parkinsonism-linked gene DJ-1. *Neuron* 2005;**45**:489–96.

Gouider-Khouja N, Larnaout A, Amouri R, Sfar S, Belal S, Ben Hamida C, Ben Hamida M, Hattori N, Mizuno Y, Hentati F. Autosomal recessive parkinsonism linked to parkin gene in a Tunisian family. Clinical, genetic and pathological study. *Parkinsonism and Related Disorders* 2003;**9**:247–51.

Gómez-Isla T, Irizarry MC, Mariash A, Cheung B, Soto O, Schrump S, Sondel J, Kotilinek L, Day J, Schwarzschild MA, Cha J-HJ, Newell K, Miller DW, Uéda K, Young AB, Hyman BT, Ashe KH. Motor dysfunction and gliosis with preserved dopaminergic markers in human alpha-synuclein A30P transgenic mice. *Neurobiology of Aging* 2003;**24**:245–58.

Grace AA, Bunney BS. The control of firing pattern in nigral dopamine neurons: burst firing. *Journal of Neuroscience* 1984;**4**:2877–90.

Graybiel AM, Ohta K, Roffler-Tarlov S. Patterns of cell and fiber vulnerability in the mesostriatal system of the mutant mouse weaver. I. Gradients and compartments. *Journal of Neuroscience* 1990;**10**:720–33.

Grenhoff J, Nisell M, Ferré S, Aston-Jones G, Svensson TH. Noradrenergic modulation of midbrain dopamine cell firing elicited by stimulation of the locus coeruleus in the rat. *Journal of neural transmission General section* 1993;**93**:11–25.

Grünblatt E, Mandel S, Jacob-Hirsch J, Zeligson S, Amariglo N, Rechavi G, Li J, Ravid R, Roggendorf W, Riederer P, Youdim MBH. Gene expression profiling of parkinsonian substantia nigra pars compacta; alterations in ubiquitin-proteasome, heat shock protein, iron and oxidative stress regulated proteins, cell adhesion/cellular matrix and vesicle trafficking genes. *Journal of Neural Transmission* 2004;**111**:1543–73.

Grünewald A, Arns B, Seibler P, Rakovic A, Münchau A, Ramirez A, Sue CM, Klein C. ATP13A2 mutations impair mitochondrial function in fibroblasts from patients with Kufor-Rakeb syndrome. *Neurobiology of Aging* 2012;**33**:1843.e1–1843.e7.

Gu M, Cooper JM, Taanman JW, Schapira AH. Mitochondrial DNA transmission of the mitochondrial defect in Parkinson's disease. *Annals of Neurology* 1998;**44**:177–86.

Gudala K, Kanukula R, Bansal D. Reduced Risk of Parkinson's Disease in Users of Calcium Channel Blockers: A Meta-Analysis. *International Journal of Chronic Diseases* 2015;**2015**:697404–7.

Gusdon AM, Zhu J, Van Houten B, Chu CT. ATP13A2 regulates mitochondrial bioenergetics through macroautophagy. *Neurobiology of Disease* 2012;**45**:962–72.

Guzman JN, Sanchez-Padilla J, Wokosin D, Kondapalli J, Ilijic E, Schumacker PT, Surmeier DJ. Oxidant stress evoked by pacemaking in dopaminergic neurons is attenuated by DJ-1. *Nature* 2010;**468**:696–700.

Haaxma CA, Bloem BR, Borm GF, Oyen WJG, Leenders KL, Eshuis S, Booij J, Dluzen DE, Horstink MWIM. Gender differences in Parkinson's disease. *Journal of Neurology, Neurosurgery & Psychiatry* 2007;**78**:819–24.

Hall H, Jewett M, Landeck N, Nilsson N, Schagerlöf U, Leanza G, Kirik D. Characterization of Cognitive Deficits in Rats Overexpressing Human Alpha-Synuclein in the Ventral Tegmental Area and Medial Septum Using Recombinant Adeno-Associated Viral Vectors. Kahle PJ (ed.). *PLoS ONE* 2013;**8**:e64844.

Hamasaki M, Furuta N, Matsuda A, Nezu A, Yamamoto A, Fujita N, Oomori H, Noda T, Haraguchi T, Hiraoka Y, Amano A, Yoshimori T. Autophagosomes form at ER-mitochondria contact sites. *Nature* 2013a;**495**:389–93.

Hamasaki M, Shibutani ST, Yoshimori T. Up-to-date membrane biogenesis in the autophagosome formation. *Current Opinion in Cell Biology* 2013b;**25**:455–60.

Hansen C, Angot E, Bergström A-L, Steiner JA, Pieri L, Paul G, Outeiro TF, Melki R, Kallunki P, Fog K, Li J-Y, Brundin P. α-Synuclein propagates from mouse brain to grafted dopaminergic neurons and seeds aggregation in cultured human cells. *The Journal of Clinical Investigation* 2011;**121**:715–25.

Hansen C, Björklund T, Petit GH, Lundblad M, Murmu RP, Brundin P, Li J-Y. A novel α-synuclein-GFP mouse model displays progressive motor impairment, olfactory dysfunction and accumulation of α-synuclein-GFP. *Neurobiology of Disease* 2013;**56**:145–55.

Hara T, Nakamura K, Matsui M, Yamamoto A, Nakahara Y, Suzuki-Migishima R, Yokoyama M, Mishima K, Saito I, Okano H, Mizushima N. Suppression of basal autophagy in neural cells causes neurodegenerative disease in mice. *Nature* 2006;**441**:885–9.

Harris H, Rubinsztein DC. Control of autophagy as a therapy for neurodegenerative disease. *Nature Reviews Neurology* 2012;**8**:108–17.

Hashimoto M, Rockenstein E, Mante M, Mallory M, Masliah E. beta-Synuclein inhibits alpha-synuclein aggregation: a possible role as an anti-parkinsonian factor. *Neuron* 2001;**32**:213–23.

Hatami A, Chesselet M-F. Transgenic rodent models to study alpha-synuclein pathogenesis, with a focus on cognitive deficits. *Current topics in behavioral neurosciences* 2015;**22**:303–30.

Hauser DN, Primiani CT, Langston RG, Kumaran R, Cookson MR. The Polg Mutator Phenotype Does Not Cause Dopaminergic Neurodegeneration in DJ-1-Deficient Mice. *eNeuro* 2015;**2**, DOI: 10.1523/ENEURO.0075-14.2015.

Hayashi S, Wakabayashi K, Ishikawa A, Nagai H, Saito M, Maruyama M, Takahashi T, Ozawa T, Tsuji S, Takahashi H. An autopsy case of autosomal-recessive juvenile parkinsonism with a homozygous exon 4 deletion in the parkin gene. *Movement Disorders* 2000;**15**:884–8.

He Q, Koprich JB, Wang Y, Yu W-B, Xiao B-G, Brotchie JM, Wang J. Treatment with Trehalose Prevents Behavioral and Neurochemical Deficits Produced in an AAV alpha-Synuclein Rat Model of Parkinson's Disease. *Molecular Neurobiology* 2016;**53**:2258–68.

Hebron ML, Lonskaya I, Moussa CEH. Nilotinib reverses loss of dopamine neurons and improves motor behavior via autophagic degradation of α-synuclein in Parkinson's disease models. *Human Molecular Genetics* 2013;**22**:3315–28.

Hely MA, Reid WGJ, Adena MA, Halliday GM, Morris JGL. The Sydney multicenter study of Parkinson's disease: the inevitability of dementia at 20 years. *Movement Disorders* 2008;**23**:837–44.

Hernandez D, Torres CA, Setlik W, Cebrián C, Mosharov EV, Tang G, Cheng H-C, Kholodilov N, Yarygina O, Burke RE, Gershon M, Sulzer D. Regulation of presynaptic neurotransmission by macroautophagy. *Neuron* 2012;**74**:277–84.

Hernandez DG, Reed X, Singleton AB. Genetics in Parkinson disease: Mendelian versus non-Mendelian inheritance. *Journal of Neurochemistry* 2016;**139 Suppl 1**:59–74.

Hernán MA, Takkouche B, Caamaño Isorna F, Gestal Otero JJ. A meta-analysis of coffee drinking, cigarette smoking, and the risk of Parkinson's disease. *Annals of Neurology* 2002;**52**:276–84.

Hierro A, Rojas AL, Rojas R, Murthy N, Effantin G, Kajava AV, Steven AC, Bonifacino JS, Hurley JH. Functional architecture of the retromer cargo-recognition complex. *Nature* 2007;**449**:1063–7.

Hirsch E, Graybiel AM, Agid YA. Melanized dopaminergic neurons are differentially susceptible to degeneration in Parkinson's disease. *Nature* 1988;**334**:345–8.

Holtzman E, Freeman AR, Kashner LA. Stimulation-Dependent Alterations in Peroxidase Uptake at Lobster Neuromuscular Junctions. *Science* 1971;**173**:733–6.

Hong WC, Amara SG. Differential targeting of the dopamine transporter to recycling or degradative pathways during amphetamine- or PKC-regulated endocytosis in dopamine neurons. *FASEB Journal* 2013;**27**:2995–3007.

Hosokawa N, Sasaki T, Iemura S-I, Natsume T, Hara T, Mizushima N. Atg101, a novel mammalian autophagy protein interacting with Atg13. *Autophagy* 2009;**5**:973–9.

Hsu LJ, Sagara Y, Arroyo A, Rockenstein E, Sisk A, Mallory M, Wong J, Takenouchi T, Hashimoto M, Masliah E. α-Synuclein Promotes Mitochondrial Deficit and Oxidative Stress. *The American Journal of Pathology* 2000;**157**:401–10.

Hughes AJ, Daniel SE, Lees AJ. Improved accuracy of clinical diagnosis of Lewy body Parkinson's disease. *Neurology* 2001;**57**:1497–9.

Hung K-C, Huang H-J, Lin M-W, Lei Y-P, Lin AM-Y. Roles of autophagy in MPP+-induced neurotoxicity *in vivo*: the involvement of mitochondria and α-synuclein sggregation. *PLoS ONE* 2014;**9**:e91074.

Hunn BHM, Cragg SJ, Bolam JP, Spillantini M-G, Wade-Martins R. Impaired intracellular trafficking defines early Parkinson's disease. *Trends in Neurosciences* 2015;**38**:178–88.

Hyland BI, Reynolds JNJ, Hay J, Perk CG, Miller R. Firing modes of midbrain dopamine cells in the freely moving rat. *Neuroscience* 2002;**114**:475–92.

Ichimura Y, Kirisako T, Takao T, Satomi Y, Shimonishi Y, Ishihara N, Mizushima N, Tanida I, Kominami E, Ohsumi M, Noda T, Ohsumi Y. A ubiquitin-like system mediates protein lipidation. *Nature* 2000;**408**:488–92.

Ichinose H, Ohye T, Takahashi E-I, Seki N, Hori T-A, Segawa M, Nomura Y, Endo K, Tanaka H, Tsuji S, Fujita K, Nagatsu T. Hereditary progressive dystonia with marked diurnal fluctuation caused by mutations in the GTP cyclohydrolase I gene. *Nature Genetics* 1994;**8**:236–42.

Inoue K, Rispoli J, Kaphzan H, Klann E, Chen EI, Kim J, Komatsu M, Abeliovich A. Macroautophagy deficiency mediates age-dependent neurodegeneration through a phospho-tau pathway. *Molecular Neurodegeneration* 2012;**7**:48.

Itakura E, Mizushima N. Characterization of autophagosome formation site by a hierarchical analysis of mammalian Atg proteins. *Autophagy* 2010;**6**:764–76.

Iwai A, Masliah E, Yoshimoto M, Ge N, Flanagan L, Rohan de Silva HA, Kittel A, Saitoh T. The precursor protein of non-Aβ component of Alzheimer's disease amyloid is a presynaptic protein of the central nervous system. *Neuron* 1995;**14**:467–75.

Jackson-Lewis V, Przedborski S. Protocol for the MPTP mouse model of Parkinson's disease. *Nature Protocols* 2007;**2**:141–51.

Jafari S, Etminan M, Aminzadeh F, Samii A. Head injury and risk of Parkinson disease: a systematic review and meta-analysis. *Movement Disorders* 2013;**28**:1222–9.

Jakes R, Spillantini M-G, Goedert M. Identification of two distinct synucleins from human brain. 2001;**345**:27–32.

Janezic S, Threlfell S, Dodson PD, Dowie MJ, Taylor TN, Potgieter D, Parkkinen L, Senior SL, Anwar S, Ryan B, Deltheil T, Kosillo P, Cioroch M, Wagner K, Ansorge O, Bannerman DM, Bolam JP, Magill PJ, Cragg SJ *et al.* Deficits in dopaminergic transmission precede neuron loss and dysfunction in a new Parkinson model. *Proceedings of the National Academy of Sciences* 2013;**110**:E4016–25.

Jankovic J. Parkinson's disease: clinical features and diagnosis. *Journal of Neurology, Neurosurgery & Psychiatry* 2008;**79**:368–76.

Javier Blesa SP. Parkinson's disease: animal models and dopaminergic cell vulnerability. *Frontiers in Neuroanatomy* 2014;**8**:117.

Javitch JA, D'Amato RJ, Strittmatter SM, Snyder SH. Parkinsonism-inducing neurotoxin, N-methyl-4-phenyl-1,2,3,6 -tetrahydropyridine: uptake of the metabolite N-methyl-4-phenylpyridine by dopamine neurons explains selective toxicity. *Proceedings of the National Academy of Sciences* 1985;**82**:2173–7.

Johnson LA, Furman CA, Zhang M, Guptaroy B, Gnegy ME. Rapid delivery of the dopamine transporter to the plasmalemmal membrane upon amphetamine stimulation. *Neuropharmacology* 2005;**49**:750–8.

Johnson SJ, Wade-Martins R. A BACwards glance at neurodegeneration: molecular insights into disease from LRRK2, SNCA and MAPT BAC-transgenic mice. *Biochemical Society Transactions* 2011;**39**:862–7.

Jones BE, Moore RY. Ascending projections of the locus coeruleus in the rat. II. Autoradiographic study. *Brain Research* 1977;**127**:23–53.

Jones BJ, Roberts DJ. The quantitative measurement of motor inco-ordination in naive mice using an accelerating rotarod. *Journal of Pharmacy and Pharmacology* 1968;**20**:302–4.

Jones SR, Gainetdinov RR, Jaber M, Giros B, Wightman RM, Caron MG. Profound neuronal plasticity in response to inactivation of the dopamine transporter. *Proceedings of the National Academy of Sciences* 1998;**95**:4029–34.

Jung CH, Jun CB, Ro S-H, Kim Y-M, Otto NM, Cao J, Kundu M, Kim D-H. ULK-Atg13-FIP200 complexes mediate mTOR signaling to the autophagy machinery. *Molecular Biology of the Cell* 2009;**20**:1992–2003.

Kachergus J, Mata IF, Hulihan M, Taylor JP, Lincoln S, Aasly J, Gibson JM, Ross OA, Lynch T, Wiley J, Payami H, Nutt J, Maraganore DM, Czyzewski K, Styczynska M, Wszolek ZK, Farrer MJ, Toft M. Identification of a Novel LRRK2 Mutation Linked to Autosomal Dominant Parkinsonism: Evidence of a Common Founder across European Populations. *The American Journal of Human Genetics* 2005;**76**:672–80.

Kahle PJ, Neumann M, Ozmen L, Müller V, Jacobsen H, Schindzielorz A, Okochi M, Leimer U, van der Putten H, Probst A, Kremmer E, Kretzschmar HA, Haass C. Subcellular Localization of Wild-Type and Parkinson's Disease-Associated Mutant α-Synuclein in Human and Transgenic Mouse Brain. *Journal of Neuroscience* 2000;**20**:6365–73.

Kaisho T, Ishikawa J, Oritani K, Inazawa J, Tomizawa H, Muraoka O, Ochi T, Hirano T. BST-1, a surface molecule of bone marrow stromal cell lines that facilitates pre-B-cell growth. *Proceedings of the National Academy of Sciences* 1994;**91**:5325–9.

Karuppagounder SS, Brahmachari S, Lee Y, Dawson VL, Dawson TM, Ko HS. The c-Abl inhibitor, nilotinib, protects dopaminergic neurons in a preclinical animal model of Parkinson's disease. *Scientific Reports* 2014;**4**:4874.

Kastenmayer RJ, Fain MA, Perdue KA. A retrospective study of idiopathic ulcerative dermatitis in mice with a C57BL/6 background. *Journal of the American Association for Laboratory Animal Science : JAALAS* 2006;**45**:8–12.

Kelly PH, Seviour PW, Iversen SD. Amphetamine and apomorphine responses in the rat following 6-OHDA lesions of the nucleus accumbens septi and corpus striatum. *Brain Research* 1975;**94**:507–22.

Keppel G, Wickens TD. *Design and Analysis: a Researcher's Handbook*. Prentice Hall, 2004.

Kéry M, Hatfield JS. Normality of Raw Data in General Linear Models: the Most Widespread Myth in Statistics. *Bulletin of the Ecological Society of America* 2003;**84**:92–4.

Kieburtz K, Wunderle KB. Parkinson's disease: Evidence for environmental risk factors. *Movement Disorders* 2013;**28**:8–13.

Kim E, Cho K-O, Rothschild A, Sheng M. Heteromultimerization and NMDA Receptor-Clustering Activity of Chapsyn-110, a Member of the PSD-95 Family of Proteins. *Neuron* 1996;**17**:103–13.

Kinghorn KJ, Castillo-Quan JI, Bartolome F, Angelova PR, Li L, Pope S, Cochemé HM, Khan S, Asghari S, Bhatia KP, Hardy J, Abramov AY, Partridge L. Loss of PLA2G6 leads to elevated mitochondrial lipid peroxidation and mitochondrial dysfunction. *Brain* 2015;**138**:1801–16.

Kirik D, Rosenblad C, Burger C, Lundberg C, Johansen TE, Muzyczka N, Mandel RJ, Björklund A. Parkinson-Like Neurodegeneration Induced by Targeted Overexpression of α-Synuclein in the Nigrostriatal System. *Journal of Neuroscience* 2002;**22**:2780–91.

Kirisako T, Ichimura Y, Okada H, Kabeya Y, Mizushima N, Yoshimori T, Ohsumi M, Takao T, Noda T, Ohsumi Y. The reversible modification regulates the membrane-binding state of Apg8/Aut7 essential for autophagy and the cytoplasm to vacuole targeting pathway. *Journal of Cell Biology* 2000;**151**:263–76.

Kirk R. *Experimental Design: Procedures for the Behavioral Sciences*. Thousand Oaks, California, 2013.

Kitada T, Asakawa S, Hattori N, Matsumine H, Yamamura Y, Minoshima S, Yokochi M, Mizuno Y, Shimizu N. Mutations in the parkin gene cause autosomal recessive juvenile parkinsonism. *Nature* 1998;**392**:605–8.

Klein C, Westenberger A. Genetics of Parkinson's disease. *Cold Spring Harbor Perspectives in Medicine* 2012;**2**:a008888–8.

Klein RL, King MA, Hamby ME, Meyer EM. Dopaminergic cell loss induced by human A30P alpha-synuclein gene transfer to the rat substantia nigra. *Human Gene Therapy* 2002;**13**:605–12.

Klionsky DJ, Cuervo AM, Dunn WAJ, Levine B, van der Klei I, Seglen PO. How shall I eat thee? *Autophagy* 2007;**3**:413–6.

Koga H, Martinez-Vicente M, Macian F, Verkhusha VV, Cuervo AM. A photoconvertible fluorescent reporter to track chaperone-mediated autophagy. *Nature Communications* 2011;**2**:386.

Komatsu M, Waguri S, Chiba T, Murata S, Iwata J-I, Tanida I, Ueno T, Koike M, Uchiyama Y, Kominami E, Tanaka K. Loss of autophagy in the central nervous system causes neurodegeneration in mice. *Nature* 2006;**441**:880–4.

Komatsu M, Waguri S, Ueno T, Iwata J, Murata S, Tanida I, Ezaki J, Mizushima N, Ohsumi Y, Uchiyama Y, Kominami E, Tanaka K, Chiba T. Impairment of starvation-induced and constitutive autophagy in Atg7-deficient mice. *Journal of Cell Biology* 2005;**169**:425–34.

Korczyn AD, Brunt ER, Larsen JP, Nagy Z, Poewe WH, Ruggieri S. A 3-year randomized trial of ropinirole and bromocriptine in early Parkinson's disease. The 053 Study Group. *Neurology* 1999;**53**:364–70.

Kordower JH, Chu Y, Hauser RA, Freeman TB, Olanow CW. Lewy body-like pathology in long-term embryonic nigral transplants in Parkinson's disease. *Nature Medicine* 2008a;**14**:504–6.

Kordower JH, Chu Y, Hauser RA, Olanow CW, Freeman TB. Transplanted dopaminergic neurons develop PD pathologic changes: A second case report. *Movement Disorders* 2008b;**23**:2303–6.

Kordower JH, Emborg ME, Bloch J, Ma SY, Chu Y, Leventhal L, McBride J, Chen EY, Palfi S, Roitberg BZ, Brown WD, Holden JE, Pyzalski R, Taylor MD, Carvey P, Ling Z, Trono D, Hantraye P, Déglon N *et al.* Neurodegeneration prevented by lentiviral vector delivery of GDNF in primate models of Parkinson's disease. *Science* 2000;**290**:767–73.

Kordower JH, Freeman TB, Snow BJ, Vingerhoets FJG, Mufson EJ, Sanberg PR, Hauser RA, Smith DA, Nauert GM, Perl DP, Olanow CW. Neuropathological Evidence of Graft Survival and Striatal Reinnervation after the Transplantation of Fetal Mesencephalic Tissue in a Patient with Parkinson's Disease. *New England Journal of Medicine* 1995;**332**:1118–24.

Kowall NW, Hantraye P, Brouillet E, Beal MF, McKee AC, Ferrante RJ. MPTP induces alpha-synuclein aggregation in the substantia nigra of baboons. *NeuroReport* 2000;**11**:211.

Koyano F, Okatsu K, Kosako H, Tamura Y, Go E, Kimura M, Kimura Y, Tsuchiya H, Yoshihara H, Hirokawa T, Endo T, Fon EA, Trempe J-F, Saeki Y, Tanaka K, Matsuda N. Ubiquitin is phosphorylated by PINK1 to activate parkin. *Nature* 2014;**510**:162–6.

Krüger R, Kuhn W, Müller T, Woitalla D, Graeber M, Kosel S, Przuntek H, Epplen JT, Schols L, Riess O. Ala30Pro mutation in the gene encoding alpha-synuclein in Parkinson's disease. *Nature Genetics* 1998;**18**:106–8.

Kuma A, Hatano M, Matsui M, Yamamoto A, Nakaya H, Yoshimori T, Ohsumi Y, Tokuhisa T, Mizushima N. The role of autophagy during the early neonatal starvation period. *Nature* 2004;**432**:1032–6.

Kuo Y-M, Li Z, Jiao Y, Gaborit N, Pani AK, Orrison BM, Bruneau BG, Giasson BI, Smeyne RJ, Gershon MD, Nussbaum RL. Extensive enteric nervous system abnormalities in mice transgenic for artificial chromosomes containing Parkinson disease-associated α-synuclein gene mutations precede central nervous system changes. *Human Molecular Genetics* 2010;**19**:1633–50.

Kuzuhara S, Mori H, Izumiyama N, Yoshimura M, Ihara Y. Lewy bodies are ubiquitinated. A light and electron microscopic immunocytochemical study. *Acta Neuropathologica* 1988;**75**:345–53.

Kühn R, Schwenk F, Aguet M, Rajewsky K. Inducible gene targeting in mice. *Science* 1995;**269**:1427–9.

Lammel S, Steinberg EE, Földy C, Wall NR, Beier K, Luo L, Malenka RC. Diversity of transgenic mouse models for selective targeting of midbrain dopamine neurons. *Neuron* 2015;**85**:429–38.

Langston JW, Forno LS, Rebert CS, Irwin I. Selective nigral toxicity after systemic administration of 1-methyl-4-phenyl-1,2,5,6-tetrahydropyrine (MPTP) in the squirrel monkey. *Brain Research* 1984;**292**:390–4.

Langston JW, Forno LS, Tetrud J, Reeves AG, Kaplan JA, Karluk D. Evidence of active nerve cell degeneration in the substantia nigra of humans years after 1-methyl-4-phenyl-1,2,3,6-tetrahydropyridine exposure. *Annals of Neurology* 1999;**46**:598–605.

Lashuel HA, Petre BM, Wall J, Simon M, Nowak RJ, Walz T, Lansbury PTJ. Alpha-synuclein, especially the Parkinson's disease-associated mutants, forms pore-like annular and tubular protofibrils. *Journal of Molecular Biology* 2002;**322**:1089–102.

Lategan AJ, Marien MR, Colpaert FC. Effects of locus coeruleus lesions on the release of endogenous dopamine in the rat nucleus accumbens and caudate nucleus as determined by intracerebral microdialysis. *Brain Research* 1990;**523**:134–8.

Lee H-J, Cho E-D, Lee KW, Kim J-H, Cho S-G, Lee S-J. Autophagic failure promotes the exocytosis and intercellular transfer of α-synuclein. *Experimental & Molecular Medicine* 2013;**45**:e22.

Lee MK, Stirling W, Xu Y, Xu X, Qui D, Mandir AS, Dawson TM, Copeland NG, Jenkins NA, Price DL. Human alpha-synuclein-harboring familial Parkinson's disease-linked Ala-53 --> Thr mutation causes neurodegenerative disease with alpha-synuclein aggregation in transgenic mice. *Proceedings of the National Academy of Sciences* 2002;**99**:8968–73.

Lee P-C, Bordelon Y, Bronstein J, Ritz B. Traumatic brain injury, paraquat exposure, and their relationship to Parkinson disease. *Neurology* 2012;**79**:2061–6.

Lees AJ, Hardy J, Revesz T. Parkinson's disease. *The Lancet* 2009;**373**:2055–66.

Lesage S, Anheim M, Letournel F, Bousset L, Honoré A, Rozas N, Pieri L, Madiona K, Dürr A, Melki R, Verny C, Brice A. G51D α-synuclein mutation causes a novel Parkinsonian–pyramidal syndrome. *Annals of Neurology* 2013;**73**:459–71.

Lesage S, Condroyer C, Klebe S, Honoré A, Tison F, Brefel-Courbon C, Dürr A, Brice A, French Parkinson's Disease Genetics Study Group. Identification of VPS35 mutations replicated in French families with Parkinson disease. *Neurology* 2012;**78**:1449–50.

Lesage S, Ibanez P, Lohmann E, Pollak P, Tison F, Tazir M, Leutenegger AL, Guimaraes J, Bonnet AM, Agid Y, Dürr A, Brice A. G2019S LRRK2 mutation in French and North African families with Parkinson's disease. *Annals of Neurology* 2005;**58**:784–7.

Lewy FH. Paralysis agitans. I. Pathologische Anatomie. *Handbuch der Neurologie* 1912;**3**:920–58.

Li J-Y, Englund E, Holton JL, Soulet D, Hagell P, Lees AJ, Lashley T, Quinn NP, Rehncrona S, Björklund A, Widner H, Revesz T, Lindvall O, Brundin P. Lewy bodies in grafted neurons in subjects with Parkinson's disease suggest host-to-graft disease propagation. *Nature Medicine* 2008;**14**:501–3.

Li S, Cullen WK, Anwyl R, Rowan MJ. Dopamine-dependent facilitation of LTP induction in hippocampal CA1 by exposure to spatial novelty. *Nature Neuroscience* 2003;**6**:526–31.

Li X, Patel JC, Wang J, Avshalumov MV, Nicholson C, Buxbaum JD, Elder GA, Rice ME, Yue Z. Enhanced striatal dopamine transmission and motor performance with LRRK2 overexpression in mice is eliminated by familial Parkinson's disease mutation G2019S. *Journal of Neuroscience* 2010;**30**:1788–97.

Li ZS, Pham TD, Tamir H, Chen JJ, Gershon MD. Enteric dopaminergic neurons: definition, developmental lineage, and effects of extrinsic denervation. *Journal of Neuroscience* 2004;**24**:1330–9.

Lindeberg J, Usoskin D, Bengtsson H, Gustafsson A, Kylberg A, Söderström S, Ebendal T. Transgenic expression of Cre recombinase from the tyrosine hydroxylase locus. *Genesis* 2004;**40**:67–73.

Lindersson E, Beedholm R, Højrup P, Moos T, Gai W, Hendil KB, Jensen PH. Proteasomal inhibition by alpha-synuclein filaments and oligomers. *Journal of Biological Chemistry* 2004;**279**:12924–34.

Lipinski MM, Hoffman G, Ng A, Zhou W, Py BF, Hsu E, Liu X, Eisenberg J, Liu J, Blenis J, Xavier RJ, Yuan J. A genome-wide siRNA screen reveals multiple mTORC1 independent signaling pathways regulating autophagy under normal nutritional conditions. *Developmental Cell* 2010;**18**:1041–52.

Liscovitch N, French L. Differential co-expression between α-synuclein and IFN-γ signaling genes across development and in parkinson's Disease. *PLoS ONE* 2014;**9**:e115029.

Lister RG. The use of a plus-maze to measure anxiety in the mouse. *Psychopharmacology* 1987;**92**:180–5.

Liu J, Wang Y, Song L, Zeng L, Yi W, Liu T, Chen H, Wang M, Ju Z, Cong Y-S. A critical role of DDRGK1 in endoplasmic reticulum homoeostasis via regulation of IRE1α stability. *Nature Communications* 2017;**8**:ncomms14186.

Liu R, Guo X, Park Y, Huang X, Sinha R, Freedman ND, Hollenbeck AR, Blair A, Chen H. Caffeine intake, smoking, and risk of Parkinson disease in men and women. *American Journal of Epidemiology* 2012;**175**:1200–7.

Llopis SP, de Celis SVR, Schwartz JC, Wolff NC, Tran TAT, Zou L, Xie XJ, Corey DR, Brugarolas J. Regulation of TFEB and V-ATPases by mTORC1. *The EMBO Journal* 2011;**30**:3242–58.

Loder MK, Melikian HE. The dopamine transporter constitutively internalizes and recycles in a protein kinase C-regulated manner in stably transfected PC12 cell lines. *Journal of Biological Chemistry* 2003;**278**:22168–74.

Lucking CB, Dürr A, Bonifati V, Vaughan J, De Michele G, Gasser T, Harhangi BS, Meco G, Denefle P, Wood NW, Agid Y, Brice A. Association between early-onset Parkinson's disease and mutations in the parkin gene. *New England Journal of Medicine* 2000;**342**:1560–7.

Luk KC, Kehm V, Carroll J, Bin Zhang, O'Brien P, Trojanowski JQ, Lee VMY. Pathological α-synuclein transmission initiates parkinson-like neurodegeneration in nontransgenic mice. *Science* 2012a;**338**:949–53.

Luk KC, Kehm VM, Bin Zhang, O'Brien P, Trojanowski JQ, Lee VMY. Intracerebral inoculation of pathological α-synuclein initiates a rapidly progressive neurodegenerative α-synucleinopathy in mice. *Journal of Experimental Medicine* 2012b;**209**:jem.20112457–986.

MacLeod DA, Rhinn H, Kuwahara T, Zolin A, Di Paolo G, McCabe BD, Marder KS, Honig LS, Clark LN, Small SA, Abeliovich A. RAB7L1 interacts with LRRK2 to modify intraneuronal protein sorting and Parkinson's disease risk. *Neuron* 2013;**77**:425–39.

Manzoni C, Mamais A, Dihanich S, Abeti R, Soutar MPM, Plun-Favreau H, Giunti P, Tooze SA, Bandopadhyay R, Lewis PA. Inhibition of LRRK2 kinase activity stimulates macroautophagy. *Biochimica et Biophysica Acta (BBA) - Molecular Cell Research* 2013;**1833**:2900–10.

Marques ARA, Gabriel TL, Aten J, van Roomen CPAA, Ottenhoff R, Claessen N, Alfonso P, Irún P, Giraldo P, Aerts JMFG, van Eijk M. Gpnmb Is a potential marker for the visceral pathology in Niemann-Pick type C disease. *PLoS ONE* 2016;**11**:e0147208.

Martinez-Vicente M, Talloczy Z, Kaushik S, Massey AC, Mazzulli J, Mosharov EV, Hodara R, Fredenburg R, Wu D-C, Follenzi A, Dauer W, Przedborski S, Ischiropoulos H, Lansbury PT, Sulzer D, Cuervo AM. Dopamine-modified α-synuclein blocks chaperone-mediated autophagy. *The Journal of Clinical Investigation* 2008;**118**:777–88.

Masliah E, Rockenstein E, Veinbergs I, Mallory M, Hashimoto M, Takeda A, Sagara Y, Sisk A, Mucke L. Dopaminergic loss and inclusion body formation in α-synuclein mice: implications for neurodegenerative disorders. *Science* 2000;**287**:1265–9.

Matsuda N, Sato S, Shiba K, Okatsu K, Saisho K, Gautier CA, Sou Y-S, Saiki S, Kawajiri S, Sato F, Kimura M, Komatsu M, Hattori N, Tanaka K. PINK1 stabilized by mitochondrial depolarization recruits Parkin to damaged mitochondria and activates latent Parkin for mitophagy. *Journal of Cell Biology* 2010;**189**:211–21.

Matsuda S, Miura E, Matsuda K, Kakegawa W, Kohda K, Watanabe M, Yuzaki M. Accumulation of AMPA receptors in autophagosomes in neuronal axons lacking adaptor protein AP-4. *Neuron* 2008;**57**:730–45.

Matsui H, Gavinio R, Takahashi R. Medaka Fish Parkinson's Disease Model. *Experimental Neurobiology* 2012;**21**:94–100.

Matsuoka Y, Vila M, Lincoln S, McCormack A, Picciano M, LaFrancois J, Yu X, Dickson D, Langston WJ, McGowan E, Farrer M, Hardy J, Duff K, Przedborski S, Di Monte DA. Lack of nigral pathology in transgenic mice expressing human alpha-synuclein driven by the tyrosine hydroxylase promoter. *Neurobiology of Disease* 2001;**8**:535–9.

Mattay VS, Tessitore A, Callicott JH, Bertolino A, Goldberg TE, Chase TN, Hyde TM, Weinberger DR. Dopaminergic modulation of cortical function in patients with Parkinson's disease. *Annals of Neurology* 2002;**51**:156–64.

Mazzulli JR, Xu Y-H, Sun Y, Knight AL, McLean PJ, Caldwell GA, Sidransky E, Grabowski GA, Krainc D. Gaucher disease glucocerebrosidase and a-synuclein form a bidirectional pathogenic loop in synucleinopathies. *Cell* 2011;**146**:37–52.

McAlpine F, Williamson LE, Tooze SA, Chan EYW. Regulation of nutrient-sensitive autophagy by uncoordinated 51-like kinases 1 and 2. *Autophagy* 2013, DOI: 10.4161/auto.23066.

McDonald JH. *Handbook of Biological Statistics*. Sparky House Publishing Baltimore, MD, 2009.

McNaught KSP, Jenner P. Proteasomal function is impaired in substantia nigra in Parkinson's disease. *Neuroscience Letters* 2001;**297**:191–4.

McNaught KSP, Shashidharan P, Perl DP, Jenner P, Olanow CW. Aggresome-related biogenesis of Lewy bodies. *European Journal of Neuroscience* 2002;**16**:2136–48.

Melikian HE, Buckley KM. Membrane Trafficking Regulates the Activity of the Human Dopamine Transporter. *Journal of Neuroscience* 1999;**19**:7699–710.

Metzger S, Walter C, Riess O, Roos RAC, Nielsen JE, Craufurd D, Nguyen HP, Hu RIE. The V471A Polymorphism in Autophagy-Related Gene ATG7 Modifies Age at Onset Specifically in Italian Huntington Disease Patients. *PLoS ONE* 2013;**8**:e68951.

Migdalska Richards A, Schapira AHV. The relationship between glucocerebrosidase mutations and Parkinson disease. *Journal of Neurochemistry* 2016;**139**:77–90.

Miki Y, Tanji K, Mori F, Utsumi J, Sasaki H, Kakita A, Takahashi H, Wakabayashi K. Alteration of Upstream Autophagy-Related Proteins (ULK1, ULK2, Beclin1, VPS34 and AMBRA1) in Lewy Body Disease. *Brain Pathology* 2016;**26**:359–70.

Millership S, Ninkina N, Guschina IA, Norton J, Brambilla R, Oort PJ, Adams SH, Dennis RJ, Voshol PJ, Rochford JJ, Buchman VL. Increased lipolysis and altered lipid homeostasis protect γ-synuclein–null mutant mice from diet-induced obesity. *Proceedings of the National Academy of Sciences* 2012;**109**:20943–8.

Miocinovic S, Somayajula S, Chitnis S, Vitek JL. History, applications, and mechanisms of deep brain stimulation. *JAMA Neurology* 2013;**70**:163–71.

Miranda M, Dionne KR, Sorkina T, Sorkin A. Three ubiquitin conjugation sites in the amino terminus of the dopamine transporter mediate protein kinase C-dependent endocytosis of the transporter. *Molecular Biology of the Cell* 2007;**18**:313–23.

Mittal S, Bjørnevik K, Im DS, Flierl A, Dong X, Locascio JJ, Abo KM, Long E, Jin M, Xu B, Xiang YK, Rochet J-C, Engeland A, Rizzu P, Heutink P, Bartels T, Selkoe DJ, Caldarone BJ, Glicksman MA *et al.* β2-Adrenoreceptor is a regulator of the α-synuclein gene driving risk of Parkinson's disease. *Science* 2017;**357**:891–8.

Mizushima N, Noda T, Ohsumi Y. Apg16p is required for the function of the Apg12p–Apg5p conjugate in the yeast autophagy pathway. *The EMBO Journal* 1999;**18**:3888–96.

Mizushima N, Noda T, Yoshimori T, Tanaka Y, Ishii T, George MD, Klionsky DJ, Ohsumi M, Ohsumi Y. A protein conjugation system essential for autophagy. *Nature* 1998;**395**:395–8.

Montgomery EB, Baker KB, Lyons K, Koller WC. Abnormal performance on the PD test battery by asymptomatic first-degree relatives. *Neurology* 1999;**52**:757–62.

Moore DJ, Zhang L, Troncoso J, Lee MK, Hattori N, Mizuno Y, Dawson TM, Dawson VL. Association of DJ-1 and parkin mediated by pathogenic DJ-1 mutations and oxidative stress. *Human Molecular Genetics* 2005;**14**:71–84.

Moreau K, Ravikumar B, Renna M, Puri C, Rubinsztein DC. Autophagosome Precursor Maturation Requires Homotypic Fusion. *Cell* 2011;**146**:303–17.

Mori F, Tanji K, Yoshimoto M, Takahashi H, Wakabayashi K. Immunohistochemical comparison of α- and β-synuclein in adult rat central nervous system. *Brain Research* 2002;**941**:118–26.

Mori H, Kondo T, Yokochi M, Matsumine H, Nakagawa-Hattori Y, Miyake T, Suda K, Mizuno Y. Pathologic and biochemical studies of juvenile parkinsonism linked to chromosome 6q. *Neurology* 1998;**51**:890–2.

Morscher RJ, Grünert SC, Bürer C, Burda P, Suormala T, Fowler B, Baumgartner MR. A single mutation in MCCC1 or MCCC2 as a potential cause of positive screening for 3-methylcrotonyl-CoA carboxylase deficiency. *Molecular Genetics and Metabolism* 2012;**105**:602–6.

Mougenot A-L, Nicot S, Bencsik A, Morignat E, Verchère J, Lakhdar L, Legastelois S, Baron T. Prion-like acceleration of a synucleinopathy in a transgenic mouse model. *Neurobiology of Aging* 2012;**33**:2225–8.

Muhammad A, Flores I, Zhang H, Yu R, Staniszewski A, Planel E, Herman M, Ho L, Kreber R, Honig LS, Ganetzky B, Duff K, Arancio O, Small SA. Retromer deficiency observed in Alzheimer's disease causes hippocampal dysfunction, neurodegeneration, and Abeta accumulation. *Proceedings of the National Academy of Sciences* 2008;**105**:7327–32.

Munhoz RP, Werneck LC, Teive HAG. The differential diagnoses of parkinsonism: findings from a cohort of 1528 patients and a 10 years comparison in tertiary movement disorders clinics. *Clinical neurology and neurosurgery* 2010;**112**:431–5.

Murphy KE, Gysbers AM, Abbott SK, Tayebi N, Kim WS, Sidransky E, Cooper A, Garner B, Halliday GM. Reduced glucocerebrosidase is associated with increased α-synuclein in sporadic Parkinson's disease. *Brain* 2014;**137**:834–48.

Nagelkerke A, Sieuwerts AM, Bussink J, Sweep FCGJ, Look MP, Foekens JA, Martens JWM, Span PN. LAMP3 is involved in tamoxifen resistance in breast cancer cells through the modulation of autophagy. *Endocrine-Related Cancer* 2014;**21**:101–12.

Nair U, Jotwani A, Geng J, Gammoh N, Richerson D, Yen W-L, Griffith J, Nag S, Wang K, Moss T, Baba M, McNew JA, Jiang X, Reggiori F, Melia TJ, Klionsky DJ. SNARE proteins are required for macroautophagy. *Cell* 2011;**146**:290–302.

Nakatsu F, Messa M, Nández R, Czapla H, Zou Y, Strittmatter SM, Pietro De Camilli. Sac2/INPP5F is an inositol 4-phosphatase that functions in the endocytic pathway. *Journal of Cell Biology* 2015;**209**:85–95.

Nalls MA, Pankratz N, Lill CM, Do CB, Hernandez DG, Saad M, DeStefano AL, Kara E, Bras J, Sharma M, Schulte C, Keller MF, Arepalli S, Letson C, Edsall C, Stefansson H, Liu X, Pliner H, Lee JH *et al.* Large-scale meta-analysis of genome-wide association data identifies six new risk loci for Parkinson's disease. *Nature Genetics* 2014;**46**:989–93.

Narendra DP, Jin SM, Tanaka A, Suen D-F, Gautier CA, Shen J, Cookson MR, Youle RJ. PINK1 is selectively stabilized on impaired mitochondria to activate Parkin. *PLOS Biology* 2010;**8**:e1000298.

Nemani VM, Lu W, Berge V, Nakamura K, Onoa B, Lee MK, Chaudhry FA, Nicoll RA, Edwards RH. Increased expression of alpha-synuclein reduces neurotransmitter release by inhibiting synaptic vesicle reclustering after endocytosis. *Neuron* 2010;**65**:66–79.

Nieto M, Gil-Bea FJ, Dalfó E, Cuadrado M, Cabodevilla F, Sánchez B, Catena S, Sesma T, Ribé E, Ferrer I, Ramírez MJ, Gómez-Isla T. Increased sensitivity to MPTP in human α-synuclein A30P transgenic mice. *Neurobiology of Aging* 2006;**27**:848–56.

Ninkina N, Peters O, Millership S, Salem H, van der Putten H, Buchman VL. Gamma-synucleinopathy: neurodegeneration associated with overexpression of the mouse protein. *Human Molecular Genetics* 2009;**18**:1779–94.

Ninkina N, Peters OM, Connor-Robson N, Lytkina O, Sharfeddin E, Buchman VL. Contrasting Effects of α-Synuclein and γ-Synuclein on the Phenotype of Cysteine String Protein α (CSPα) Null Mutant Mice Suggest Distinct Function of these Proteins in Neuronal Synapses. *Journal of Biological Chemistry* 2012;**287**:44471–7.

Ninkina NN, Alimova-Kost MV, Paterson JW, Delaney L, Cohen BB, Imreh S, Gnuchev NV, Davies AM, Buchman VL. Organization, expression and polymorphism of the human persyn gene. *Human Molecular Genetics* 1998;**7**:1417–24.

Nishida Y, Arakawa S, Fujitani K, Yamaguchi H, Mizuta T, Kanaseki T, Komatsu M, Otsu K, Tsujimoto Y, Shimizu S. Discovery of Atg5/Atg7-independent alternative macroautophagy. *Nature* 2009;**461**:654–8.

Niu X-Y, Huang H-J, Zhang J-B, Zhang C, Chen W-G, Sun C-Y, Ding Y-Q, Liao M. Deletion of autophagy-related gene 7 in dopaminergic neurons prevents their loss induced by MPTP. *Neuroscience* 2016;**339 IS -**:22–31.

Novarino G, El-Fishawy P, Kayserili H, Meguid NA, Scott EM, Schroth J, Silhavy JL, Kara M, Khalil RO, Ben-Omran T, Ercan-Sencicek AG, Hashish AF, Sanders SJ, Gupta AR, Hashem HS, Matern D, Gabriel S, Sweetman L, Rahimi Y *et al.* Mutations in *BCKD*-kinase lead to a potentially treatable form of autism with epilepsy. *Science* 2012;**338**:394–7.

Olerup O, Smith CI, Björkander J, Hammarström L. Shared HLA class II-associated genetic susceptibility and resistance, related to the HLA-DQB1 gene, in IgA deficiency and common variable immunodeficiency. *Proceedings of the National Academy of Sciences* 1992;**89**:10653–7.

Oliveras-Salvá M, Van der Perren A, Casadei N, Stroobants S, Nuber S, D'Hooge R, Van den Haute C, Baekelandt V. rAAV2/7 vector-mediated overexpression of alpha-synuclein in mouse substantia nigra induces protein aggregation and progressive dose-dependent neurodegeneration. *Molecular Neurodegeneration* 2013;**8**:44.

Olzmann JA, Li L, Chudaev MV, Chen J, Perez FA, Palmiter RD, Chin L-S. Parkin-mediated K63-linked polyubiquitination targets misfolded DJ-1 to aggresomes via binding to HDAC6. *Journal of Cell Biology* 2007;**178**:1025–38.

Ozelius LJ, Senthil G, Saunders-Pullman R, Ohmann E, Deligtisch A, Tagliati M, Hunt AL, Klein C, Henick B, Hailpern SM, Lipton RB, Soto-Valencia J, Risch N, Bressman SB. LRRK2 G2019S as a cause of Parkinson's disease in Ashkenazi Jews. *New England Journal of Medicine* 2009;**354**:424–5.

Pagan F, Hebron M, Valadez EH, Torres-Yaghi Y, Huang X, Mills RR, Wilmarth BM, Howard H, Dunn C, Carlson A, Lawler A, Rogers SL, Falconer RA, Ahn J, Li Z, Moussa C. Nilotinib effects in Parkinson's disease and Dementia with Lewy bodies. *Journal of Parkinson's Disease* 2016;**6**:503–17.

Paisan-Ruiz C, Jain S, Evans EW, Gilks WP, Simon J, van der Brug M, Lopez de Munain A, Aparicio S, Gil AM, Khan N, Johnson J, Martinez JR, Nicholl D, Carrera IM, Pena AS, de Silva R, Lees A, Marti-Masso JF, Perez-Tur J *et al.* Cloning of the gene containing mutations that cause PARK8-linked Parkinson's disease. *Neuron* 2004;**44**:595–600.

Pakkenberg H, Brody H. The number of nerve cells in the substantia nigra in paralysis agitans. *Acta Neuropathologica* 1965;**5**:320–4.

Pan P-Y, Ryan TA. Calbindin controls release probability in ventral tegmental area dopamine neurons. *Nature Neuroscience* 2012;**15**:813–5.

Panaretou C, Doming J, Cockcroft S, Waterfield MD. Characterization of p150, an adaptor protein for the human phosphatidylinositol (PtdIns) 3-kinase. Substrate presentation by phosphatidylinositol transfer protein to the p150·PtdIns 3-kinase complex. *Journal of Biological Chemistry* 1997;**272**:2477–85.

Pankiv S, Clausen TH, Lamark T, Brech A, Bruun J-A, Outzen H, Øvervatn A, Bjørkøy G, Johansen T. p62/SQSTM1 binds directly to Atg8/LC3 to facilitate degradation of ubiquitinated protein aggregates by autophagy. *Journal of Biological Chemistry* 2007;**282**:24131–45.

Parihar MS, Parihar A, Fujita M, Hashimoto M, Ghafourifar P. Mitochondrial association of alpha-synuclein causes oxidative stress. *Cellular and Molecular Life Sciences* 2008;**65**:1272–84.

Park J, Lee SB, Lee S, Kim Y, Song S, Kim S, Bae E, Kim J, Shong M, Kim J-M, Chung J. Mitochondrial dysfunction in Drosophila PINK1 mutants is complemented by parkin. *Nature* 2006;**441**:1157–61.

Parkinson J. *An Essay on the Shaking Palsy*. London: Sherwood Neely and Jones, 1817.

Parkinson Study Group. Phase II safety, tolerability, and dose selection study of isradipine as a potential disease-modifying intervention in early Parkinson's disease (STEADY-PD). *Movement Disorders* 2013;**28**:1823–31.

Parkkinen L, O'Sullivan SS, Collins C, Petrie A, Holton JL, Revesz T, Lees AJ. Disentangling the Relationship between Lewy Bodies and Nigral Neuronal Loss in Parkinson's Disease. *Journal of Parkinson's Disease* 2011;**1**:277–86.

Pascual A, Hidalgo-Figueroa M, Piruat JI, Pintado CO, Gómez-Díaz R, López-Barneo J. Absolute requirement of GDNF for adult catecholaminergic neuron survival. *Nature Neuroscience* 2008;**11**:755–61.

Patel JC, Rossignol E, Rice ME, Machold RP. Opposing regulation of dopaminergic activity and exploratory motor behavior by forebrain and brainstem cholinergic circuits. *Nature Communications* 2012;**3**:1172.

Paxinos G, Franklin KBJ. *The Mouse Brain in Stereotaxic Coordinates*. Academic Press, 2008.

PD MED Collaborative Group. Long-term effectiveness of dopamine agonists and monoamine oxidase B inhibitors compared with levodopa as initial treatment for Parkinson's disease (PD MED): a large, open-label, pragmatic randomised trial. *The Lancet* 2014;**384**:1196–205.

Pearson ES. The Analysis of Variance in Cases of Non-Normal Variation. *Biometrika* 1931;**23**:114.

Pedro JMB-S, Niso-Santano M, Gómez-Sánchez R, Pizarro-Estrella E, Aiastui-Pujana A, Gorostidi A, Climent V, de Maturana RL, Sanchez-Pernaute R, de Munain AL, Fuentes JM, González-Polo RA. The LRRK2 G2019S mutant exacerbates basal autophagy through activation of the MEK/ERK pathway. *Cellular and Molecular Life Sciences* 2013;**70**:121–36.

Pellow S, File SE. Anxiolytic and anxiogenic drug effects on exploratory activity in an elevated plus-maze: A novel test of anxiety in the rat. *Pharmacology Biochemistry and Behavior* 1986;**24**:525–9.

Periquet M, Fulga T, Myllykangas L, Schlossmacher MG, Feany MB. Aggregated α-synuclein mediates dopaminergic neurotoxicity *in vivo*. *Journal of Neuroscience* 2007;**27**:3338–46.

Peters OM, Shelkovnikova T, Highley JR, Cooper Knock J, Hortobágyi T, Troakes C, Ninkina N, Buchman VL. Gamma-synuclein pathology in amyotrophic lateral sclerosis. *Annals of Clinical and Translational Neurology* 2015;**2**:29–37.

Pezzoli G, Cereda E. Exposure to pesticides or solvents and risk of Parkinson disease. *Neurology* 2013;**80**:2035–41.

Pijnenburg AJJ, van Rossum JM. Stimulation of locomotor activity following injection of dopamine into the nucleus accumbens. *Journal of Pharmacy and Pharmacology* 1973;**25**:1003–5.

Politis M, Wu K, Loane C, Turkheimer FE, Molloy S, Brooks DJ, Piccini P. Depressive symptoms in PD correlate with higher 5-HTT binding in raphe and limbic structures. *Neurology* 2010;**75**:1920–7.

Polymeropoulos MH, Lavedan C, Leroy E, Ide SE, Dehejia A, Dutra A, Pike B, Root H, Rubenstein J, Boyer R, Stenroos ES, Chandrasekharappa S, Athanassiadou A, Papapetropoulos T, Johnson WG, Lazzarini AM, Duvoisin RC, Di Iorio G, Golbe LI *et al.* Mutation in the α-synuclein gene identified in families with Parkinson's disease. *Science* 1997;**276**:2045–7.

Ponsen MM, Stoffers D, Booij J, van Eck-Smit BLF, Wolters EC, Berendse HW. Idiopathic hyposmia as a preclinical sign of Parkinson's disease. *Annals of Neurology* 2004;**56**:173–81.

Poole AC, Thomas RE, Andrews LA, McBride HM, Whitworth AJ, Pallanck LJ. The PINK1/Parkin pathway regulates mitochondrial morphology. *Proceedings of the National Academy of Sciences* 2008;**105**:1638–43.

Postuma RB, Lang AE, Munhoz RP, Charland K, Pelletier A, Moscovich M, Filla L, Zanatta D, Romenets SR, Altman R, Chuang R, Shah B. Caffeine for treatment of Parkinson disease: a randomized controlled trial. *Neurology* 2012;**79**:651–8.

Pramstaller PP, Schlossmacher MG, Jacques TS, Scaravilli F, Eskelson C, Pepivani I, Hedrich K, Adel S, Gonzales McNeal M, Hilker R, Kramer PL, Klein C. Lewy body Parkinson's disease in a large pedigree with 77 Parkin mutation carriers. *Annals of Neurology* 2005;**58**:411–22.

Priault M, Salin B, Schaeffer J, Vallette FM, di Rago J-P, Martinou J-C. Impairing the bioenergetic status and the biogenesis of mitochondria triggers mitophagy in yeast. *Cell death and differentiation* 2005;**12**:1613–21.

Pringsheim T, Jette N, Frolkis A, Steeves TDL. The prevalence of Parkinson's disease: A systematic review and meta-analysis. *Movement Disorders* 2014;**29**:1583–90.

Proukakis C, Dudzik CG, Brier T, MacKay DS, Cooper JM, Millhauser GL, Houlden H, Schapira AH. A novel α-synuclein missense mutation in Parkinson disease. *Neurology* 2013;**80**:1062–4.

Przedbroski S, Leviver M, Jiang H, Ferreira M, Jackson-Lewis V, Donaldson D, Togasaki DM. Dose-dependent lesions of the dopaminergic nigrostriatal pathway induced by instrastriatal injection of 6-hydroxydopamine. *Neuroscience* 1995;**67**:631–47.

Ramirez A, Heimbach A, Gründemann J, Stiller B, Hampshire D, Cid LP, Goebel I, Mubaidin AF, Wriekat A-L, Roeper J, Al-Din A, Hillmer AM, Karsak M, Liss B, Woods CG, Behrens MI, Kubisch C. Hereditary parkinsonism with dementia is caused by mutations in ATP13A2, encoding a lysosomal type 5 P-type ATPase. *Nature Genetics* 2006;**38**:1184–91.

Ramonet D, Daher JPL, Lin BM, Stafa K, Kim J, Banerjee R, Westerlund M, Pletnikova O, Glauser L, Yang L, Liu Y, Swing DA, Beal MF, Troncoso JC, McCaffery JM, Jenkins NA, Copeland NG, Galter D, Thomas B *et al.* Dopaminergic neuronal loss, reduced neurite complexity and autophagic abnormalities in transgenic mice expressing G2019S mutant LRRK2. Cai H (ed.). *PLoS ONE* 2011;**6**:e18568.

Rascol O, Brooks DJ, Korczyn AD, De Deyn PP, Clarke CE, Lang AE. A five-year study of the incidence of dyskinesia in patients with Early Parkinson's disease who were treated with ropinirole or levodopa. *New England Journal of Medicine* 2000;**342**:1484–91.

Reddy JV, Seaman MN. Vps26p, a component of retromer, directs the interactions of Vps35p in endosome-to-Golgi retrieval. *Molecular Biology of the Cell* 2001;**12**:3242–56.

Reeve A, Simcox E, Turnbull D. Ageing and Parkinson's disease: why is advancing age the biggest risk factor? *Ageing research reviews* 2014;**14**:19–30.

Reggiori F, Ungermann C. Autophagosome maturation and fusion. *Journal of Molecular Biology* 2017;**429**:486–96.

Rice ME, Cragg SJ. Nicotine amplifies reward-related dopamine signals in striatum. *Nature Neuroscience* 2004;**7**:583–4.

Ripoll N, David DJP, Dailly E, Hascoët M, Bourin M. Antidepressant-like effects in various mice strains in the tail suspension test. *Behavioural Brain Research* 2003;**143**:193–200.

Ritz B, Ascherio A, Checkoway H, Marder KS, Nelson LM, Rocca WA, Ross GW, Strickland D, Van Den Eeden SK, Gorell J. Pooled analysis of tobacco use and risk of Parkinson disease. *Archives of Neurology* 2007;**64**:990–7.

Ritz B, Rhodes SL, Qian L, Schernhammer E, Olsen JH, Friis S. L-type calcium channel blockers and Parkinson disease in Denmark. *Annals of Neurology* 2010;**67**:600–6.

Roberts P, Moshitch-Moshkovitz S, Kvam E, O'Toole E, Winey M, Goldfarb DS. Piecemeal microautophagy of nucleus in Saccharomyces cerevisiae. *Molecular Biology of the Cell* 2003;**14**:129–41.

Roberts RF, Wade-Martins R, Alegre-Abarrategui J. Direct visualization of alpha-synuclein oligomers reveals previously undetected pathology in Parkinson's disease brain. *Brain* 2015;**138**:1642–57.

Robertson DC, Schmidt O, Ninkina N, Jones PA, Sharkey J, Buchman VL. Developmental loss and resistance to MPTP toxicity of dopaminergic neurones in substantia nigra pars compacta of gamma-synuclein, alpha-synuclein and double alpha/gamma-synuclein null mutant mice. *Journal of Neurochemistry* 2004;**89**:1126–36.

Rocca WA, Bower JH, Maraganore DM, Ahlskog JE, Grossardt BR, de Andrade M, Melton LJ. Increased risk of parkinsonism in women who underwent oophorectomy before menopause. *Neurology* 2008;**70**:200–9.

Rodríguez CI, Buchholz F, Galloway J, Sequerra R, Kasper J, Ayala R, Stewart AF, Dymecki SM. High-efficiency deleter mice show that FLPe is an alternative to Cre-loxP. *Nature Genetics* 2000;**25**:139–40.

Rowland AM, Richmond JE, Olsen JG, Hall DH, Bamber BA. Presynaptic terminals independently regulate synaptic clustering and autophagy of $GABA_A$ receptors in Caenorhabditis elegans. *Journal of Neuroscience* 2006;**26**:1711–20.

Rudow G, O'Brien R, Savonenko AV, Resnick SM, Zonderman AB, Pletnikova O, Marsh L, Dawson TM, Crain BJ, West MJ, Troncoso JC. Morphometry of the human substantia nigra in ageing and Parkinson's disease. *Acta Neuropathologica* 2008;**115**:461–70.

Saggu H, Cooksey J, Dexter D, Wells FR, Lees A, Jenner P, Marsden CD. A selective increase in particulate superoxide dismutase activity in Parkinsonian substantia nigra. *Journal of Neurochemistry* 1989;**53**:692–7.

Saha AR, Ninkina NN, Hanger DP, Anderton BH, Davies AM, Buchman VL. Induction of neuronal death by α-synuclein. *European Journal of Neuroscience* 2000;**12**:3073–7.

Sakai M, Araki N, Ogawa K. Lysosomal movements during heterophagy and autophagy: with special reference to nematolysosome and wrapping lysosome. *Microscopy Research and Technique* 1989;**12**:101–31.

Sanderson DJ, Bannerman DM. The role of habituation in hippocampus-dependent spatial working memory tasks: evidence from GluA1 AMPA receptor subunit knockout mice. Lubec G (ed.). *Hippocampus* 2012;**22**:981–94.

Sarkar S, Davies JE, Huang Z, Tunnacliffe A, Rubinsztein DC. Trehalose, a novel mTOR-independent autophagy enhancer, accelerates the clearance of mutant huntingtin and alpha-synuclein. *Journal of Biological Chemistry* 2007;**282**:5641–52.

Sasaki S, Shirata A, Yamane K, Iwata M. Parkin-positive autosomal recessive juvenile Parkinsonism with alpha-synuclein-positive inclusions. *Neurology* 2004;**63**:678–82.

Scatton B, Simon H, Le Moal M, Bischoff S. Origin of dopaminergic innervation of the rat hippocampal formation. *Neuroscience Letters* 1980;**18**:125–31.

Schank JR, Liles LC, Weinshenker D. Norepinephrine signaling through beta-adrenergic receptors is critical for expression of cocaine-induced anxiety. *Biological Psychiatry* 2008;**63**:1007–12.

Schapansky J, Nardozzi JD, Felizia F, LaVoie MJ. Membrane recruitment of endogenous LRRK2 precedes its potent regulation of autophagy. *Human Molecular Genetics* 2014;**23**:4201–14.

Schapira AHV, Cooper JM, Dexter D, Clark JB, Jenner P, Marsden CD. Mitochondrial complex I deficiency in Parkinson's disease. *Journal of Neurochemistry* 1990;**54**:823–7.

Schneppenheim J, Hüttl S, Mentrup T, Lüllmann-Rauch R, Rothaug M, Engelke M, Dittmann K, Dressel R, Araki M, Araki K, Wienands J, Fluhrer R, Saftig P, Schröder B. The intramembrane proteases signal Peptide peptidase-like 2a and 2b have distinct functions in vivo. *Molecular and Cellular Biology* 2014;**34**:1398–411.

Schott BH, Niehaus L, Wittmann BC, Schütze H. Ageing and early-stage Parkinson's disease affect separable neural mechanisms of mesolimbic reward processing. *Brain* 2007.

Schultheis PJ, Fleming SM, Clippinger AK, Lewis J, Tsunemi T, Giasson B, Dickson DW, Mazzulli JR, Bardgett ME, Haik KL, Ekhator O, Chava AK, Howard J, Gannon M, Hoffman E, Chen Y, Prasad V, Linn SC, Tamargo RJ *et al.* Atp13a2-deficient mice exhibit neuronal ceroid lipofuscinosis, limited α-synuclein accumulation and age-dependent sensorimotor deficits. *Human Molecular Genetics* 2013;**22**:2067–82.

Senior SL, Ninkina N, Deacon R, Bannerman D, Buchman VL, Cragg SJ, Wade-Martins R. Increased striatal dopamine release and hyperdopaminergic-like behaviour in mice lacking both alpha-synuclein and gamma-synuclein. *European Journal of Neuroscience* 2008;**27**:947–57.

Settembre C, Di Malta C, Polito VA, Arencibia MG, Vetrini F, Erdin S, Erdin SU, Huynh T, Medina D, Colella P, Sardiello M, Rubinsztein DC, Ballabio A. TFEB links autophagy to lysosomal biogenesis. *Science* 2011;**332**:1429–33.

Settembre C, Zoncu R, Medina DL, Vetrini F, Erdin S, Erdin S, Huynh T, Ferron M, Karsenty G, Vellard MC, Facchinetti V, Sabatini DM, Ballabio A. A lysosome-to-nucleus signalling mechanism senses and regulates the lysosome via mTOR and TFEB. *The EMBO Journal* 2012;**31**:1095–108.

Shapiro SS, Wilk MB. An Analysis of Variance Test for Normality (Complete Samples). *Biometrika* 1965;**52**:591.

Sherer TB, Kim J-H, Betarbet R, Greenamyre JT. Subcutaneous rotenone exposure causes highly selective dopaminergic degeneration and α-synuclein aggregation. *Experimental Neurology* 2003;**179**:9–16.

Shimura H, Hattori N, Kubo S, Yoshikawa M, Kitada T, Matsumine H, Asakawa S, Minoshima S, Yamamura Y, Shimizu N, Mizuno Y. Immunohistochemical and subcellular localization of Parkin protein: absence of protein in autosomal recessive juvenile parkinsonism patients. *Annals of Neurology* 1999;**45**:668–72.

Shimura H, Schlossmacher MG, Hattori N, Frosch MP, Trockenbacher A, Schneider R, Mizuno Y, Kosik KS, Selkoe DJ. Ubiquitination of a new form of α-synuclein by parkin from human brain: implications for Parkinson's disease. *Science* 2001;**293**:263–9.

Shojaee S, Sina F, Banihosseini SS, Kazemi MH, Kalhor R, Shahidi G-A, Fakhrai-Rad H, Ronaghi M, Elahi E. Genome-wide linkage analysis of a Parkinsonian-pyramidal syndrome pedigree by 500 K SNP arrays. *The American Journal of Human Genetics* 2008;**82**:1375–84.

Sidransky E, Nalls MA, Aasly JO, Aharon-Peretz J, Annesi G, Barbosa ER, Bar-Shira A, Berg D, Bras J, Brice A, Chen CM, Clark LN, Condroyer C, De Marco EV, Dürr A, Eblan MJ, Fahn S, Farrer MJ, Fung HC *et al.* Multicenter analysis of glucocerebrosidase mutations in Parkinson's disease. *New England Journal of Medicine* 2009;**361**:1651–61.

Simon KC, Gao X, Chen H, Schwarzschild MA, Ascherio A. Calcium channel blocker use and risk of Parkinson's disease. *Movement Disorders* 2010;**25**:1818–22.

Simuni T, Borushko E, Avram MJ, Miskevics S, Martel A, Zadikoff C, Videnovic A, Weaver FM, Williams K, Surmeier DJ. Tolerability of isradipine in early Parkinson's disease: a pilot dose escalation study. *Movement Disorders* 2010;**25**:2863–6.

Singleton AB, Farrer M, Johnson J, Singleton A, Hague S, Kachergus J, Hulihan M, Peuralinna T, Dutra A, Nussbaum R, Lincoln S, Crawley A, Hanson M, Maraganore D, Adler C, Cookson MR, Muenter M, Baptista M, Miller D *et al.* α-Synuclein locus triplication causes Parkinson's disease. *Science* 2003;**302**:841–1.

Sloan M, Alegre-Abarrategui J, Potgieter D, Kaufmann A-K, Exley R, Deltheil T, Threlfell S, Connor-Robson N, Brimblecombe K, Wallings R, Cioroch M, Bannerman DM, Bolam JP, Magill PJ, Cragg SJ, Dodson PD, Wade-Martins R. LRRK2 BAC transgenic rats develop progressive, L-DOPA-responsive motor impairment, and deficits in dopamine circuit function. *Human Molecular Genetics* 2016;**25**:951–63.

Smith PK, Krohn RI, Hermanson GT, Mallia AK, Gartner FH, Provenzano MD, Fujimoto EK, Goeke NM, Olson BJ, Klenk DC. Measurement of protein using bicinchoninic acid. *Analytical Biochemistry* 1985;**150**:76–85.

Snyder H, Mensah K, Theisler C, Lee J, Matouschek A, Wolozin B. Aggregated and monomeric alpha-synuclein bind to the S6' proteasomal protein and inhibit proteasomal function. *Journal of Biological Chemistry* 2003;**278**:11753–9.

Soper JH, Roy S, Stieber A, Lee E, Wilson RB, Trojanowski JQ, Burd CG, Lee VMY. Alpha-synuclein-induced aggregation of cytoplasmic vesicles in Saccharomyces cerevisiae. *Molecular Biology of the Cell* 2008;**19**:1093–103.

Spencer B, Potkar R, Trejo M, Rockenstein E, Patrick C, Gindi R, Adame A, Wyss-Coray T, Masliah E. Beclin 1 gene transfer activates autophagy and ameliorates the neurodegenerative pathology in alpha-synuclein models of Parkinson's and Lewy body diseases. *Journal of Neuroscience* 2009;**29**:13578–88.

Spillantini M-G, Schmidt ML, Lee VMY, Trojanowski JQ, Jakes R, Goedert M. α-Synuclein in Lewy bodies. *Nature* 1997;**388**:839–40.

Spillantini MG, Divane A, Goedert M. Assignment of human alpha-synuclein (SNCA) and beta-synuclein (SNCB) genes to chromosomes 4q21 and 5q35. *Genomics* 1995;**27**:379–81.

Stefanis L, Larsen KE, Rideout HJ, Sulzer D, Greene LA. Expression of A53T mutant but not wild-type α-synuclein in PC12 cells induces alterations of the ubiquitin-dependent degradation system, loss of dopamine release, and autophagic cell death. *Journal of Neuroscience* 2001;**21**:9549–60.

Steru L, Chermat R, Thierry B, Simon P. The tail suspension test: A new method for screening antidepressants in mice. *Psychopharmacology* 1985;**85**:367–70.

Sun Q, Fan W, Chen K, Ding X, Chen S, Zhong Q. Identification of Barkor as a mammalian autophagy-specific factor for Beclin 1 and class III phosphatidylinositol 3-kinase. *Proceedings of the National Academy of Sciences* 2008;**105**:19211–6.

Sung Y-H, Eliezer D. Residual structure, backbone dynamics, and interactions within the synuclein family. *Journal of Molecular Biology* 2007;**372**:689–707.

Taira T, Saito Y, Niki T, Ariga SMMI, Takahashi K, Ariga H. DJ-1 has a role in antioxidative stress to prevent cell death. *EMBO reports* 2004;**5**:213–8.

Tang G, Gudsnuk K, Kuo S-H, Cotrina ML, Rosoklija G, Sosunov A, Sonders MS, Kanter E, Castagna C, Yamamoto A, Yue Z, Arancio O, Peterson BS, Champagne F, Dwork AJ, Goldman J, Sulzer D. Loss of mTOR-Dependent Macroautophagy Causes Autistic-like Synaptic Pruning Deficits. *Neuron* **83**:1131–43.

Tanik SA, Schultheiss CE, Volpicelli-Daley LA, Brunden KR, Lee VMY. Lewy body-like α-synuclein aggregates resist degradation and impair macroautophagy. *The Journal of Biological Chemistry* 2013;**288**:15194–210.

Taylor KSM, Cook JA, Counsell CE. Heterogeneity in male to female risk for Parkinson's disease. *Journal of Neurology, Neurosurgery & Psychiatry* 2007;**78**:905–6.

Taylor TN, Greene JG, Miller GW. Behavioral phenotyping of mouse models of Parkinson's disease. *Behavioural Brain Research* 2010;**211**:1–10.

Taylor TN, Potgieter D, Anwar S, Senior SL, Janezic S, Threlfell S, Ryan B, Parkkinen L, Deltheil T, Cioroch M, Livieratos A, Oliver PL, Jennings KA, Davies KE, Ansorge O, Bannerman DM, Cragg SJ, Wade-Martins R. Region-specific deficits in dopamine, but not norepinephrine, signaling in a novel A30P alpha-synuclein BAC transgenic mouse. *Neurobiology of Disease* 2014;**62**:193–207.

Terlecky SR, Dice JF. Polypeptide import and degradation by isolated lysosomes. *Journal of Biological Chemistry* 1993;**268**:23490–5.

Terman D, Rubin JE, Yew AC, Wilson CJ. Activity Patterns in a Model for the Subthalamopallidal Network of the Basal Ganglia. *Journal of Neuroscience* 2002;**22**:2963–76.

Thiruchelvam M, Richfield EK, Baggs RB, Tank AW, Cory-Slechta DA. The nigrostriatal dopaminergic system as a preferential target of repeated exposures to combined paraquat and maneb: implications for Parkinson's disease. *Journal of Neuroscience* 2000;**20**:9207–14.

Threlfell S, Lalic T, Platt NJ, Jennings KA, Deisseroth K, Cragg SJ. Striatal dopamine release is triggered by synchronized activity in cholinergic interneurons. *Neuron* 2012;**75**:58–64.

Totterdell S, Hanger D, Meredith GE. The ultrastructural distribution of alpha-synuclein-like protein in normal mouse brain. *Brain Research* 2004;**1004**:61–72.

Usenovic M, Tresse E, Mazzulli JR, Taylor JP, Krainc D. Deficiency of ATP13A2 leads to lysosomal dysfunction, α-synuclein accumulation, and neurotoxicity. *Journal of Neuroscience* 2012;**32**:4240–6.

Valente EM, Abou-Sleiman PM, Caputo V, Muqit MMK, Harvey K, Gispert S, Ali Z, Del Turco D, Bentivoglio AR, Healy DG, Albanese A, Nussbaum R, González-Maldonado R, Deller T, Salvi S, Pietro Cortelli, Gilks WP, Latchman DS, Harvey RJ *et al.* Hereditary early-onset Parkinson's disease caused by mutations in *PINK1*. *Science* 2004;**304**:1158–60.

van de Warrenburg BP, Lammens M, Lucking CB, Denefle P, Wesseling P, Booij J, Praamstra P, Quinn N, Brice A, Horstink MW. Clinical and pathologic abnormalities in a family with parkinsonism and parkin gene mutations. *Neurology* 2001;**56**:555–7.

van der Putten H, Wiederhold K-H, Probst A, Barbieri S, Mistl C, Danner S, Kauffmann S, Hofele K, Spooren WPJM, Ruegg MA, Lin S, Caroni P, Sommer B, Tolnay M, Bilbe G. Neuropathology in mice expressing human α-synuclein. *Journal of Neuroscience* 2000;**20**:6021–9.

Vargas KJ, Schrod N, Davis T, Fernandez-Busnadiego R, Taguchi YV, Laugks U, Lucic V, Chandra SS. Synucleins Have Multiple Effects on Presynaptic Architecture. *Cell Reports* 2017;**18**:161–73.

Velikkakath AKG, Nishimura T, Oita E, Ishihara N, Mizushima N. Mammalian Atg2 proteins are essential for autophagosome formation and important for regulation of size and distribution of lipid droplets. *Molecular Biology of the Cell* 2012;**23**:896–909.

Verwey M, Grant A, Meti N, Adye-White L, Torres-Berrío A, Rioux V, Lévesque M, Charron F, Flores C. Mesocortical Dopamine Phenotypes in Mice Lacking the Sonic Hedgehog Receptor Cdon. *eNeuro* 2016;**3**:ENEURO.0009–16.2016.

Vila M, Vukosavic S, Jackson-Lewis V, Neystat M, Jakowec M, Przedborski S. α-Synuclein up-regulation in substantia nigra dopaminergic neurons following administration of the parkinsonian toxin MPTP. *Journal of Neurochemistry* 2000;**74**:721–9.

Vilarino-Gueell C, Wider C, Ross OA, Dachsel JC, Kachergus JM, Lincoln SJ, Soto Ortolaza AI, Cobb SA, Wilhoite GJ, Bacon JA, Behrouz B, Melrose HL, Hentati E, Puschmann A, Evans DM, Conibear E, Wasserman WW, Aasly JO, Burkhard PR *et al.* VPS35 Mutations in Parkinson Disease. *American Journal of Human Genetics* 2011;**89**:162–7.

Vingill S, Brockelt D, Lancelin C, Tatenhorst L, Dontcheva G, Preisinger C, Domeyer NS, Joseph S, Mitkovski M, Goebbels S, Nave KA, Schulz JB, Marquardt T, Lingor P, Stegmüller J. Loss of FBXO7 (PARK15) results in reduced proteasome activity and models a parkinsonism-like phenotype in mice. *The EMBO Journal* 2016;**35**:2008–25.

Vives-Bauza C, Zhou C, Huang Y, Cui M, de Vries RLA, Kim J, May J, Tocilescu MA, Liu W, Ko HS, Magrané J, Moore DJ, Dawson VL, Grailhe R, Dawson TM, Li C, Tieu K, Przedborski S. PINK1-dependent recruitment of Parkin to mitochondria in mitophagy. *Proceedings of the National Academy of Sciences* 2010;**107**:378–83.

Vogiatzi T, Xilouri M, Vekrellis K, Stefanis L. Wild type alpha-synuclein is degraded by chaperone-mediated autophagy and macroautophagy in neuronal cells. *Journal of Biological Chemistry* 2008;**283**:23542–56.

Vyas I, Heikkila RE, Nicklas WJ. Studies on the neurotoxicity of 1-methyl-4-phenyl-1,2,3,6-tetrahydropyridine: inhibition of NAD-linked substrate oxidation by its metabolite, 1-methyl-4-phenylpyridinium. *Journal of Neurochemistry* 1986;**46**:1501–7.

Walf AA, Frye CA. The use of the elevated plus maze as an assay of anxiety-related behavior in rodents. *Nature Protocols* 2007;**2**:322–8.

Wang L, Das U, Scott DA, Tang Y, McLean PJ, Roy S. α-Synuclein multimers cluster synaptic vesicles and attenuate recycling. *Current Biology* 2014;**24**:2319–26.

Webb JL, Ravikumar B, Atkins J, Skepper JN, Rubinsztein DC. Alpha-synuclein is degraded by both autophagy and the proteasome. *Journal of Biological Chemistry* 2003;**278**:25009–13.

Wei Y, Pattingre S, Sinha S, Bassik M, Levine B. JNK1-mediated phosphorylation of Bcl-2 regulates starvation-induced autophagy. *Molecular Cell* 2008;**30**:678–88.

Whone AL, Watts RL, Stoessl AJ, Davis M, Reske S, Nahmias C, Lang AE, Rascol O, Ribeiro MJ, Remy P, Poewe WH, Hauser RA, Brooks DJ. Slower progression of Parkinson's disease with ropinirole versus levodopa: The REAL-PET study. *Annals of Neurology* 2003;**54**:93–101.

Winner B, Jappelli R, Maji SK, Desplats PA, Boyer L, Aigner S, Hetzer C, Loher T, Vilar M, Campioni S, Tzitzilonis C, Soragni A, Jessberger S, Mira H, Consiglio A, Pham E, Masliah E, Gage FH, Riek R. In vivo demonstration that alpha-synuclein oligomers are toxic. *Proceedings of the National Academy of Sciences* 2011;**108**:4194–9.

Winslow AR, Chen C-W, Corrochano S, Acevedo-Arozena A, Gordon DE, Peden AA, Lichtenberg M, Menzies FM, Ravikumar B, Imarisio S, Brown S, O'Kane CJ, Rubinsztein DC. α-Synuclein impairs macroautophagy: implications for Parkinson's disease. 2010;**190**:1023–37.

Wolf A, Bauer B, Abner EL, Ashkenazy-Frolinger T, Hartz AMS. A Comprehensive Behavioral Test Battery to Assess Learning and Memory in 129S6/Tg2576 Mice. Reddy H (ed.). *PLoS ONE* 2016;**11**:e0147733.

Wooten GF, Currie LJ, Bovbjerg VE, Lee JK, Patrie J. Are men at greater risk for Parkinson's disease than women? *Journal of Neurology, Neurosurgery & Psychiatry* 2004;**75**:637–9.

Wu Y, Cheng S, Zhao H, Zou W, Yoshina S, Mitani S, Zhang H, Wang X. PI3P phosphatase activity is required for autophagosome maturation and autolysosome formation. *EMBO reports* 2014;**15**:973–81.

Xiong H, Wang D, Chen L, Choo YS, Ma H, Tang C, Xia K, Jiang W, Ronai Z, Zhuang X, Zhang Z. Parkin, PINK1, and DJ-1 form a ubiquitin E3 ligase complex promoting unfolded protein degradation. *The Journal of Clinical Investigation* 2009;**119**:650–60.

Yamada M, Iwatsubo T, Mizuno Y, Mochizuki H. Overexpression of α-synuclein in rat substantia nigra results in loss of dopaminergic neurons, phosphorylation of α-synuclein and activation of caspase-9: resemblance to pathogenetic changes in Parkinson's disease. *Journal of Neurochemistry* 2004;**91**:451–61.

Yamada T, McGeer PL, Baimbridge KG, McGeer EG. Relative sparing in Parkinson's disease of substantia nigra dopamine neurons containing calbindin-D28K. *Brain Research* 1990;**526**:303–7.

Yamakado H, Moriwaki Y, Yamasaki N, Miyakawa T, Kurisu J, Uemura K, Inoue H, Takahashi M, Takahashi R. α-Synuclein BAC transgenic mice as a model for Parkinson's disease manifested decreased anxiety-like behavior and hyperlocomotion. *Neuroscience Research* 2012;**73**:173–7.

Yamamura Y, Kuzuhara S, Kondo K, Yanagi T, Uchida M, Matsumine H, Mizuno Y. Clinical, pathologic and genetic studies on autosomal recessive early-onset parkinsonism with diurnal fluctuation. *Parkinsonism and Related Disorders* 1998;**4**:65–72.

Yousefi S, Perozzo R, Schmid I, Ziemiecki A, Schaffner T, Scapozza L, Brunner T, Simon H-U. Calpain-mediated cleavage of Atg5 switches autophagy to apoptosis. *Nature Cell Biology* 2006;**8**:1124–32.

Yue Z, Jin S, Yang C, Levine AJ, Heintz N. Beclin 1, an autophagy gene essential for early embryonic development, is a haploinsufficient tumor suppressor. *Proceedings of the National Academy of Sciences* 2003;**100**:15077–82.

Zarranz JJ, Alegre J, Gómez Esteban JC, Lezcano E, Ros R, Ampuero I, Vidal L, Hoenicka J, Rodriguez O, Atarés B, Llorens V, Tortosa EG, del Ser T, Muñoz DG, de Yebenes JG. The new mutation, E46K, of α-synuclein causes parkinson and Lewy body dementia. *Annals of Neurology* 2004;**55**:164–73.

Zatloukal K, Stumptner C, Fuchsbichler A, Heid H, Schnoelzer M, Kenner L, Kleinert R, Prinz M, Aguzzi A, Denk H. p62 is a common component of cytoplasmic inclusions in protein aggregation diseases. *The American Journal of Pathology* 2002;**160**:255–63.

Zhang J, Perry G, Smith MA, Robertson D, Olson SJ, Graham DG, Montine TJ. Parkinson's disease is associated with oxidative damage to cytoplasmic DNA and RNA in substantia nigra neurons. *The American Journal of Pathology* 1999;**154**:1423–9.

Zhang L, Shimoji M, Thomas B, Moore DJ, Yu S-W, Marupudi NI, Torp R, Torgner IA, Ottersen OP, Dawson TM, Dawson VL. Mitochondrial localization of the Parkinson's disease related protein DJ-1: implications for pathogenesis. *Human Molecular Genetics* 2005;**14**:2063–73.

Zhuang X, Masson J, Gingrich JA, Rayport S, Hen R. Targeted gene expression in dopamine and serotonin neurons of the mouse brain. *Journal of Neuroscience Methods* 2005;**143**:27–32.

Zimprich A, Benet-Pagès A, Struhal W, Graf E, Eck SH, Offman MN, Haubenberger D, Spielberger S, Schulte EC, Lichtner P, Rossle SC, Klopp N, Wolf E, Seppi K, Pirker W, Presslauer S, Mollenhauer B, Katzenschlager R, Foki T *et al.* A mutation in VPS35, encoding a subunit of the retromer complex, causes late-onset Parkinson disease. *American Journal of Human Genetics* 2011;**89**:168–75.

Zimprich A, Biskup S, Leitner P, Lichtner P, Farrer M, Lincoln S, Kachergus J, Hulihan M, Uitti RJ, Calne DB, Stoessl AJ, Pfeiffer RF, Patenge N, Carbajal IC, Vieregge P, Asmus F, M ller-Myhsok B, Dickson DW, Meitinger T *et al.* Mutations in LRRK2 cause autosomal-dominant parkinsonism with pleomorphic pathology. *Neuron* 2004;**44**:601–7.